OCS Study
MMS 93-0042

GRAY WHALE AND PACIFIC WALRUS BENTHIC FEEDING GROUNDS AND SEA FLOOR INTERACTION IN THE CHUKCHI SEA

by

C. Hans Nelson
R. Lawrence Phillips
James McRea, Jr.
John H. Barber, Jr.
Mark W. McLaughlin
John L. Chin

U.S. Geological Survey, Menlo Park, California 94025

TECHNICAL REPORT FOR MINERALS MANAGEMENT SERVICE / IA No. 14157

OCS Study
MMS 93-0042

GRAY WHALE AND PACIFIC WALRUS BENTHIC FEEDING GROUNDS AND SEA FLOOR INTERACTION IN THE CHUKCHI SEA

by

C. Hans Nelson
R. Lawrence Phillips
James McRea, Jr.
John H. Barber, Jr.
Mark W. McLaughlin
John L. Chin

U.S. Geological Survey, Menlo Park, California 94025

TECHNICAL REPORT FOR MINERALS MANAGEMENT SERVICE / IA No. 14157

This study was funded by the Alaska Outer Continental Shelf Region of the Minerals Management Service, U.S. Department of the Interior, Anchorage, Alaska, through Interagency Agreement 14157 with the U.S. Geological Survey.

July, 1994

PROJECT PERSONNEL

Hans Nelson	Co-Chief Investigator, Marine mammal feeding trace specialist
Larry Phillips	Co-Chief Investigator, Chukchi area specialist
Jim McRea	Implementation of image analysis technique
John Barber	Development of image analysis technique and organization of final report
John Chin	Identification of sidescan sonar records bearing marine mammal feeding traces
Mark McLaughlin	Report editing and figure preparation

ABSTRACT

Sidescan sonar has been used to delineate benthic feeding grounds of the Pacific walrus (*Odobenus rosmarus divergens*) and the California gray whale (*Eschrichtius robustus*) on the continental shelf in the northeastern Chukchi Sea. The utilization of image analysis software has enabled us to process approximately 4,800 km of sidescan sonar data, analyze feeding-trace morphology, and quantify the walrus and gray whale feeding effects on the sea floor.

Walrus create feeding furrows along the sea floor that can be mapped with sidescan sonar. A high density of furrows are found throughout 180,000 km^2 of the northeastern Chukchi Sea. The percentage of sea floor disturbed by all young and old walrus furrows ranged between 24 in the south to 36 percent in the north. The highest percentage of traces is associated with the migrating pack ice edge, which walrus follow across the entire Chukchi Sea as they feed. Most furrows observed were between 2 and 6 m long with an average length of 2.46 m that is short because young furrows overlap and destroy traces of older furrows. Because (1) individual feeding pits cannot be resolved on sidescan sonographs, (2) present-feeding-year furrows on sonographs cannot be distinguished from those of past years, and (3) walrus feed selectively on multi-year-class benthic fauna, it is difficult to accurately estimate the annual walrus food supply provided by the Chukchi Sea. The south to north increase in furrow disturbance observed during ice-edge retreat for one-half of the feeding season may however suggest that the minimum annual disturbance is 24 percent and may equal or exceed carrying capacity of the substrate for benthic prey species.

Feeding gray whales create shallow pits that can be resolved and mapped by sidescan sonar. Distribution of these pits matches (1) reported sightings of feeding whales with their associated sediment plumes, and (2) the distribution of whale prey species and corresponding prey substrate types. Limited feeding grounds, delineated by these criteria and observed on sonographs, occur over 29,782 km^2 in Chukchi Sea.

Whale feeding traces in the Chukchi Sea are not abundant and, in general, are limited to the areas where the coastal sand sheet dominates. Within the sands, the percentage of sea floor disturbed averaged 2.62 percent and varied from about 0.5 percent to 20 percent at a site where active feeding whales were observed. Calculations based on average disturbance coupled with energetic models for whale feeding and prey biomass estimates suggest that the Chukchi Sea, with 2.9 percent of the Alaskan feeding range, supplied a minimum of 1-4 percent of the summer food resources for the gray whales in 1984 and 1985. The uneven distribution, low percentage of feeding disturbance, and particularly the small pit size compared to the Bering Sea, may be due to modification of the feeding trace record by the numerous storms which cross the area and the consequent storm wave currents and continuous strong coastal current that rework the bottom sediment.

Mammal feeding activities are a significant geologic process because with walrus disturbance of the seafloor perhaps reaching 24 percent per year, 6.3 billion tons of sediment are resuspended

each year and the entire sea floor is disturbed about every 3 years. Sediment resuspension also may enhance the primary productivity of the prey species by recycling the nutrients in the system and may cause winnowing as well as advection of 252 million tons of mud from the sandy substrate under the Alaska Coastal Current.

Because of the high concentration of prey species in a prime walrus and whale feeding ground that is vulnerable to the development of petroleum and mining for sand, care is required in the exploitation of these resources in the Chukchi Sea.

TABLE OF CONTENTS

INTRODUCTION

Approximately 1 million km^2 in the Bering, Chukchi, and Beaufort seas provide the major foraging grounds for the walrus and gray whales (Scammon, 1874: Zenkovich, 1934; Pike, 1962; Rice and Wolman, 1971; Votrogov and Bogoslovskaya, 1980; Frost and Lowry, 1981; Fay, 1982). Our study covers an important part of the summer feeding grounds in the northeastern Chukchi Sea between Cape Lisburne and Pt. Franklin, near Wainwright, Alaska (figs. 1, 2).

The Pacific walrus (*Odobenus rosmarus divergens*, hereafter called walrus) population of about 234,000 individuals is one of the predominant mammal species of the Bering and Chukchi seas (Fay, 1982; Sease and Chapman, 1988). Extremely successful and omnivorous, this population thrives by migrating with the ice edge as it grows southward to the edge of the Bering shelf during fall and winter and then northward as it recedes to the Pt. Barrow region during spring and summer. The ice edge serves as a moving platform transporting the main walrus community to feed on benthic biomass throughout the Bering and Chukchi sea floor. Stomach contents indicate that walrus feed on most benthic species found in this region. The ice-edge migration results in feeding about one-third of the year each in the Chukchi , northern Bering, and southern Bering Seas.

The California gray whale (*Eschrichtius robustus*, hereafter called gray whale or whale) is perhaps the most resilient and omnivorous of the great whales. Twice hunted to near extinction (Gilmore, 1955), the gray whales have rebounded to near pre-exploitation levels. At present, approximately 21,000 gray whales exist in the eastern Pacific Ocean (Reilly and others, 1980; Herzing and Mate, 1981; Rugh, 1981; Reilly, 1983; Loughlin, 1992). Another stock, the Korean gray whales, which inhabited the western Pacific Ocean, are presumed extinct (Rice and Wolman, 1971) or at least highly depressed (Brownell, 1977). Fossil remains and scanty whaling records verify the existence of an Atlantic stock of gray whales that is also extinct (Mead and Mitchell, 1984).

Each year the gray whales migrate from their winter breeding and calving lagoons in Baja California, Mexico, to their main summer feeding grounds in the Bering and Chukchi seas between Alaska and Siberia (fig. 3). During most of this 6,000-km migration, the whales remain within sight of land (Braham, 1984). The coastal affinity which nearly spelled their doom by allowing easy access for whalers, now allows gray whales to be thoroughly studied.

Gray whales are the only whales that rely predominantly on a benthic food source. When they feed on infaunal organisms, mainly ampeliscid amphipods, they disturb the sediment surface. The disturbance leaves a feeding trace preserved on the sea floor (fig. 4). Similarly, walrus are mainly a benthic feeding mammal that leave mappable traces on the sea floor (fig. 5). We use the sonograph records of feeding traces to outline gray whale and walrus feeding grounds, to understand how they feed and to quantify the importance of the Chukchi Sea feeding area. Because the features of ice gouges (fig. 6), and current-related bedforms from physical process have been identified and mapped before in

this study area (Phillips and others, 1985; Phillips and Colgan, 1987), and compared in detail in the northern Bering Sea (Johnson and others, 1983), there is little potential for confusion of physical features with the biogenic whale and walrus feeding traces.

To interpret the feeding records, we assess (1) distribution and feeding ecology of the gray whales and walrus, (2) distribution and ecology of the prey species, (3) oceanographic setting, (4) nature and extent of the surficial sediment types that are the habitat of the prey species, and, most importantly, (5) types and distribution of feeding traces left in the sea floor by foraging gray whales and walrus. Our ultimate purpose is a more complete understanding of gray whale and walrus feeding patterns and food resources in the Chukchi Sea so that environmentally sound management decisions are possible for this region.

TERMINOLOGY

We use the terms "feeding features" and "feeding traces" to describe the gray whale and walrus feeding disturbances on the sea floor. Other possible candidates for creating similar features are sculpin, rays, and halibut. The pits we are studying, however, - are unlikely, given the demonstrated Since benthic suction is the postulated mode of whale feeding (Hudnall, 1981), "multiple-suction feeding events", "suction events," and "feeding pits" are all acceptable terms. Terms that imply scouring or scooping are inappropriate, as is the term "depression", which implies compaction of the sea floor by the feeding process. The term "furrow" is used for walrus feeding traces because this indicates that some displaced sediment and faunal remains have been transferred to the side of the feeding trace and not simply removed and entirely dispersed into the water column.

For the description of whale pits, the word "elongate" simply implies a length axis much greater than the width axis. The large pits caused by current scour or feeding enlargement of single fresh feeding pits are known as "current-scour-enlarged pits," "current-modified features," or "modified whale feeding pits" because their origin may be both whale- and current-related. The combination of fresh whale feeding pits, partially modified whale pits, and current-scour-enlarged pits (considerably modified pits) is known as "total bottom disturbance. "Bottom disturbance" as used in this report, relates to modification of the sea floor by marine mammal feeding behavior, and does not include features derived entirely from physical processes, such as ice gouges.

METHODS

General Techniques

Data in this study are derived from box cores, grab samples, underwater still photographs, underwater video, and sidescan sonar (Barnes, 1972; Toimil, 1978; Grantz and others, 1982; Phillips and others, 1982, 1983, 1985a, 1985b, 1987a, 1987b, 1987c, 1988; Miley and Barnes, 1986). The association of substrate and benthic communities has been established both qualitatively (Nelson and others, 1981; Johnson and others, 1983) and quantitatively in the

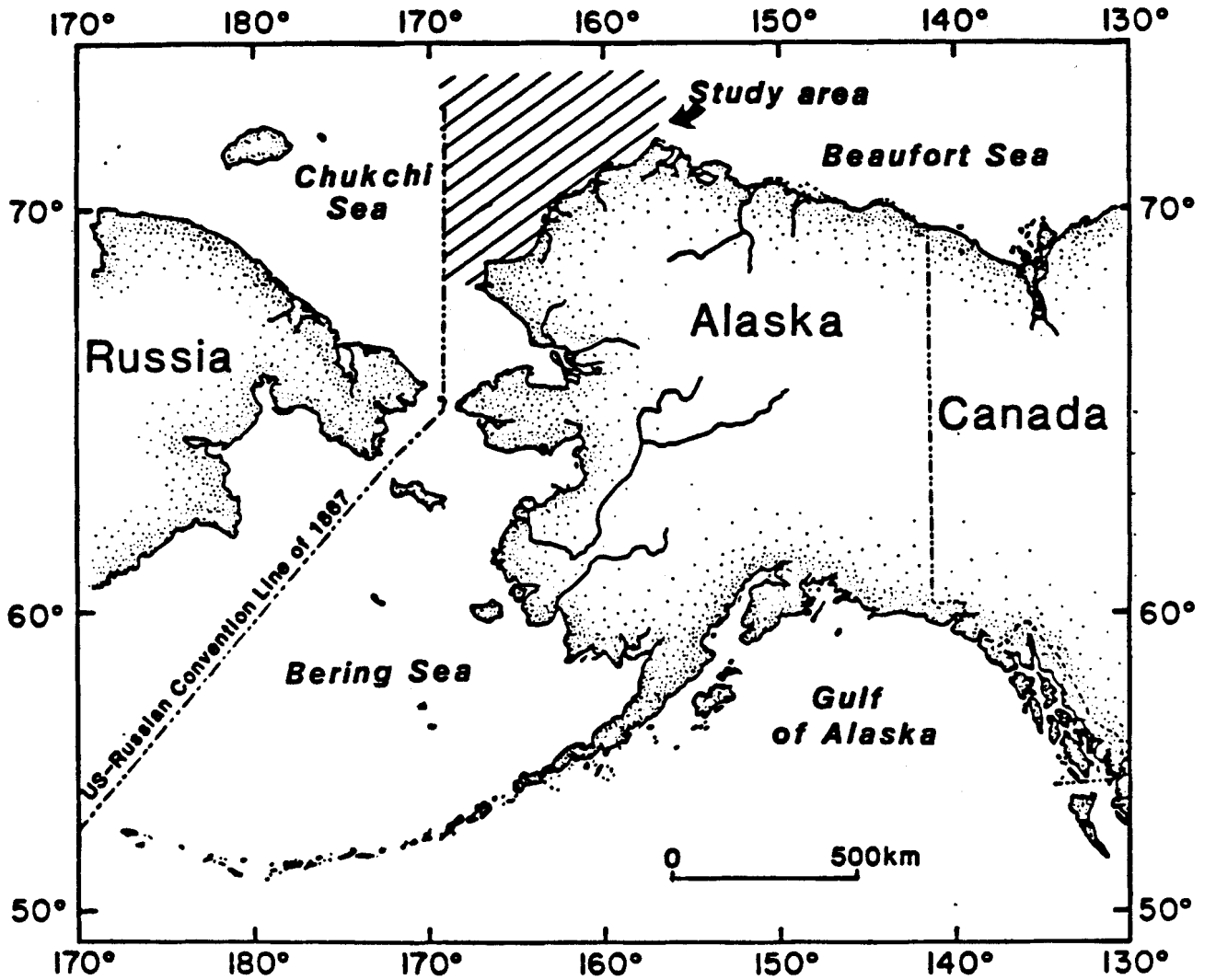

Figure 1. Location of study area in the northeastern Chukchi Sea.

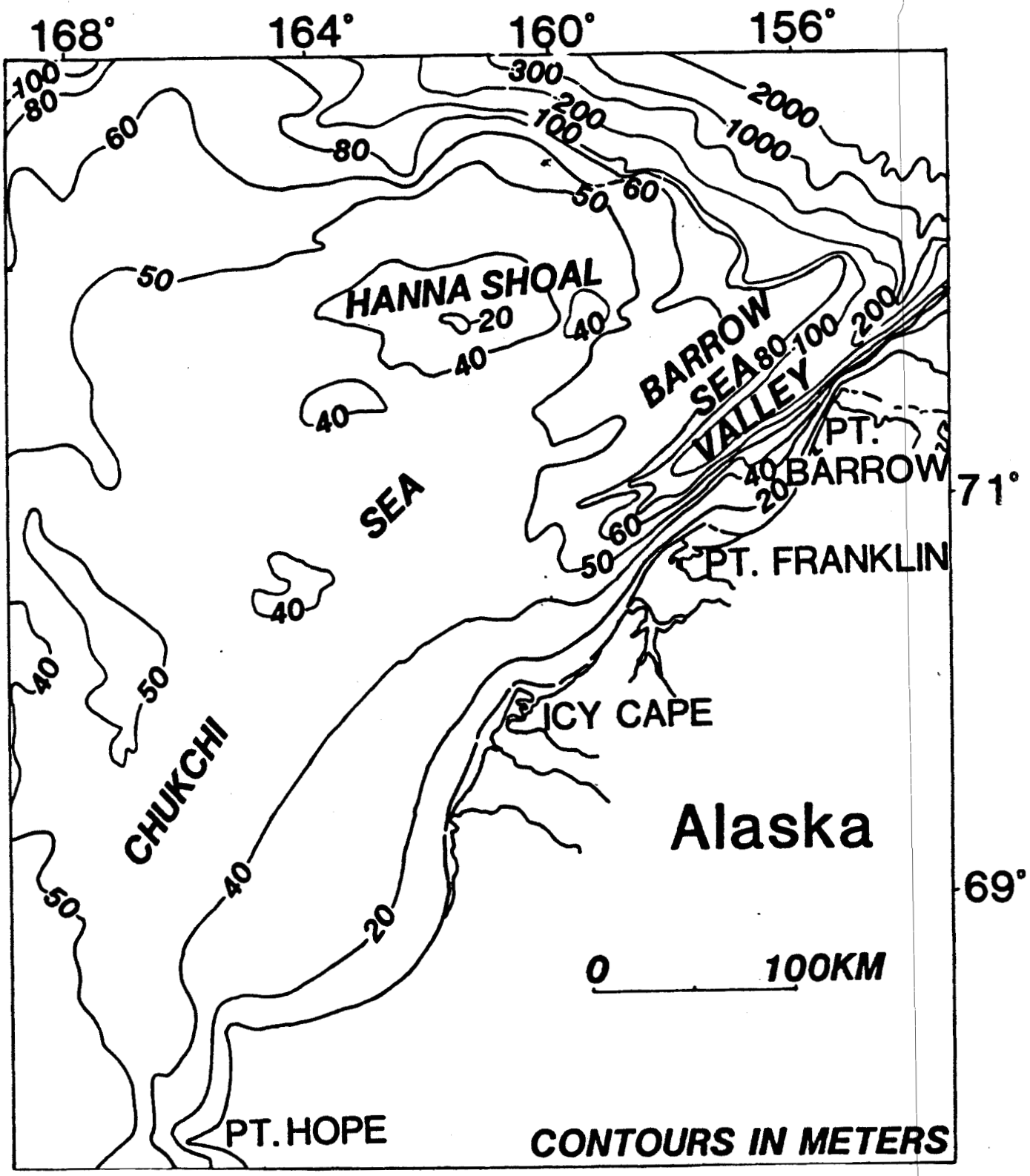

Figure 2. Chukchi Sea bathymetry. Data modified from Hill and others (1984). Contours in meters.

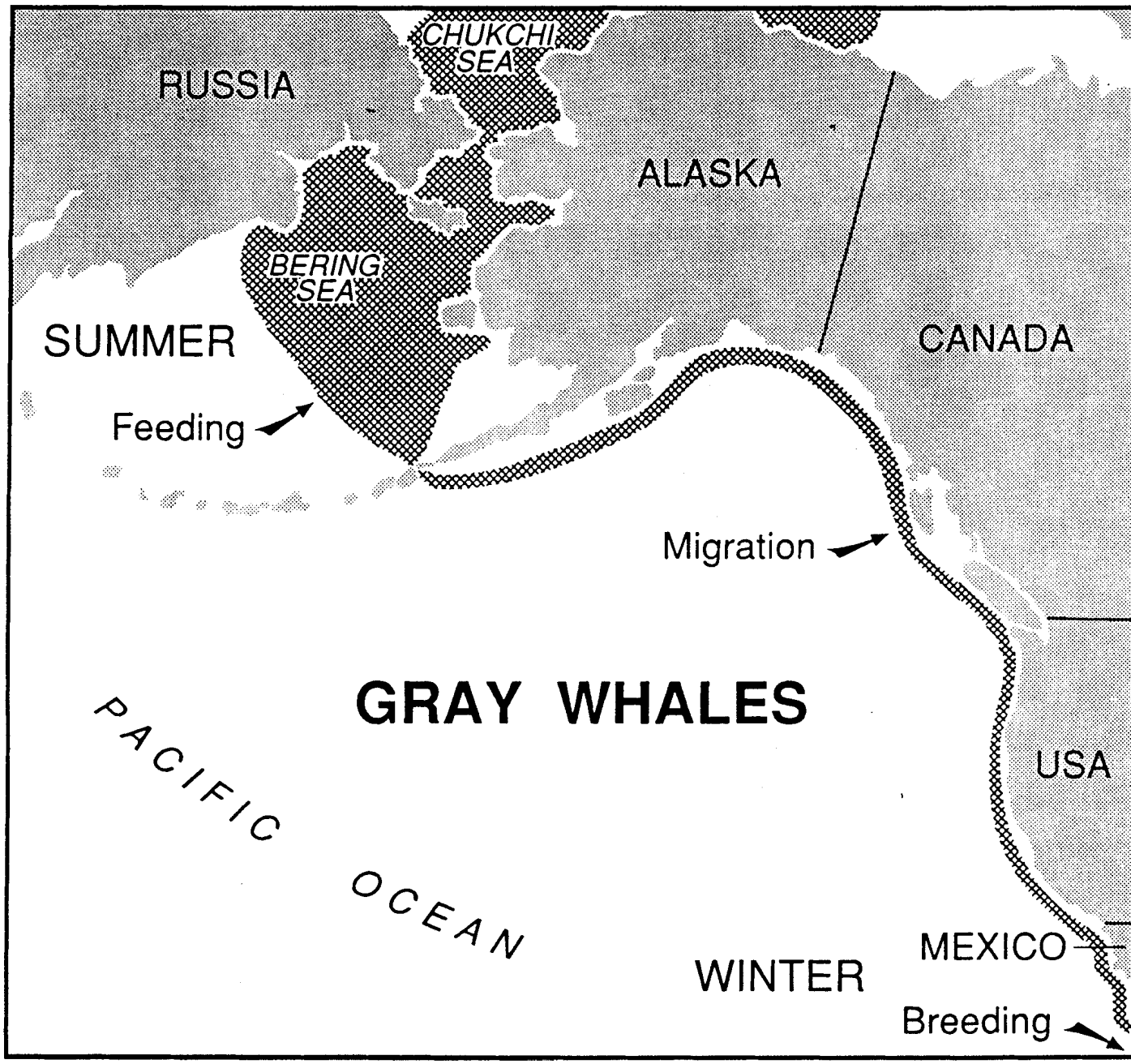

Fig 3. Migration patterns and distribution of the Gray Whale (modified from McIntyre and others, 1983).

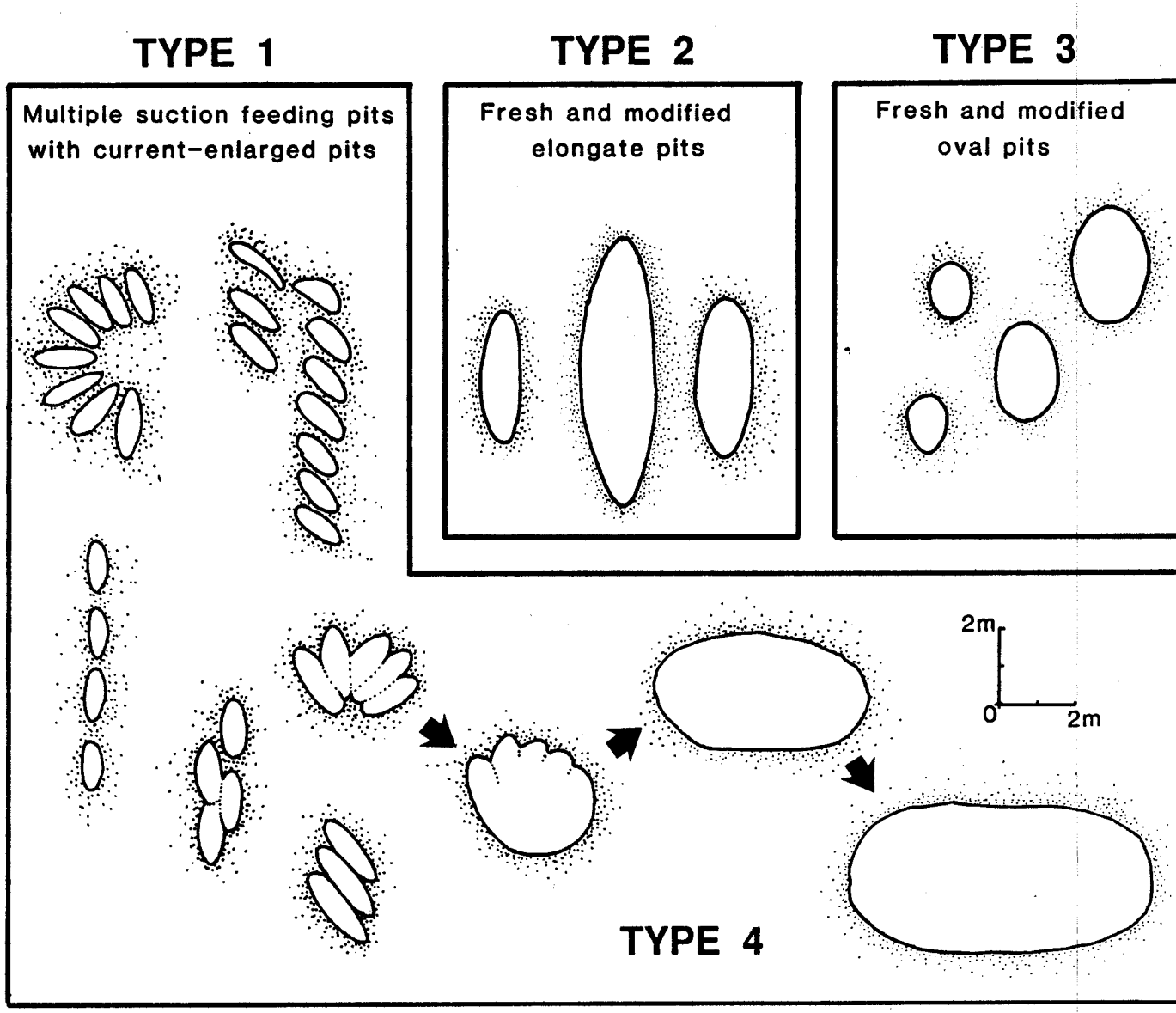

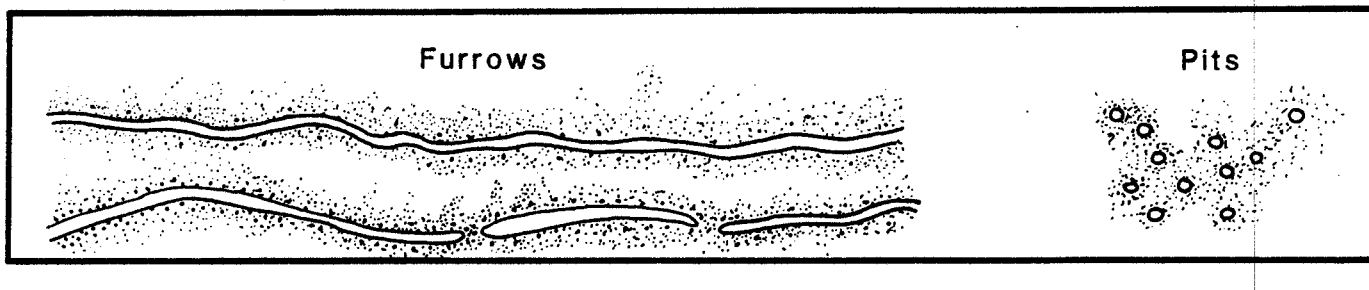

Fig 4. Whale feeding pit types, as defined in the northeastern Bering Sea (modified from Nelson and others, 1987). These sketches are derived from side-scan sonar and scuba diver observations, and are to scale (see Type 4). Types 1, 2, and 3 can all evolve into Type 4 pits through current-scour enlargement and

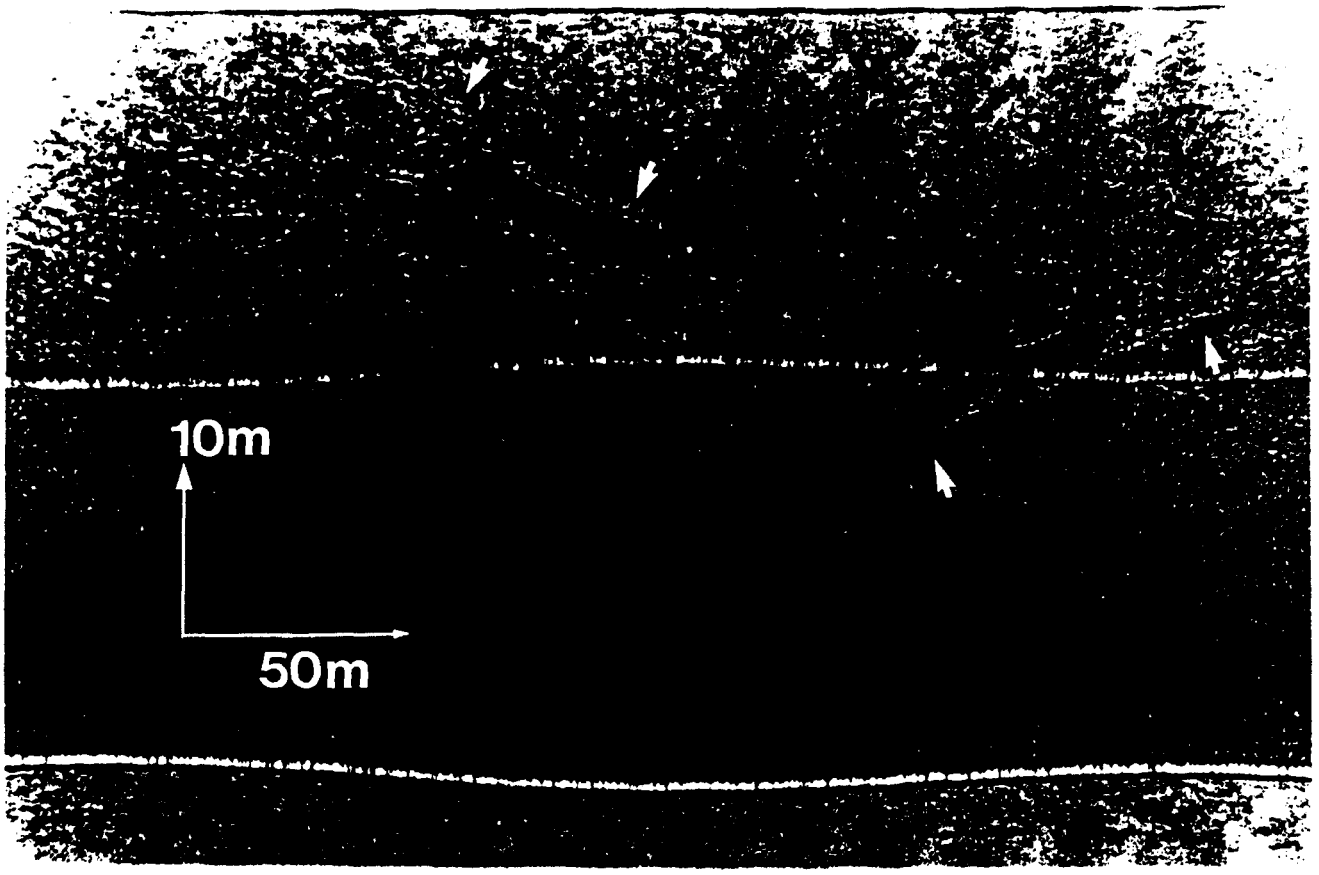

Figure 5. 100-kHz sonograph showing several long, narrow walrus feeding furrows (see arrows) in eastern Chirikov Basin, northeastern Bering Sea (from Nelson and others, 1983).

Figure 6. Sonograph showing two ice gouges, sediment bulldozed by an ice keel, and rippled seafloor. Note crosscutting relationship between the ice gouges. Approximate horizontal scale is 2.5 cm = 10 m. Approximate vertical scale is 4.5 cm = 10 m.

Bering Sea (Stoker, 1978; Nerini and others, 1980; Feder and Jewett, 1981; Oliver and others, 1983a; Thomson, 1984). This same association was demonstrated quantitatively in the northeast Chukchi Sea by Feder and others (1989). A total of 27 sample sites in the Chukchi Sea have been used in the qualitative assessment of the benthic communities (fig. 7) (Appendix 1) whereas 37 stations were used to establish the quantitative association of substrate and benthic communities (fig. 8, Table 1) (Feder and others, 1989). A substrate map (fig. 9) summarizes surface sediment textural data from 228 samples (Barnes, 1972; Phillips and others, 1982, 1984, 1985; and Feder and others, 1989). One box core was obtained in 1988 on the western flank of Hanna Shoal (fig. 10).

Current patterns in the Chukchi Sea have been compiled from a wide variety of current measurement data (fig. 11) (Fleming and Heggarty, 1966; Paquette and Bourke, 1974; Hufford, 1977; Coachman and others, 1975; Sharma, 1979; Wilson and others 1982; Aagaard, 1984; Lewbel and Gallaway, 1984; Hachmeister and Vinelli, 1985). The best observations of gray whale feeding features on the sea floor are accomplished by scuba diving, but this method is limited to short-term and small-area investigations (Nerini and others, 1980; Oliver and others, 1983b; Oliver and Kvitek, 1984). In the early 1980s, gray whale feeding traces were detected on the paper records generated by sidescan sonar, a planographic sea floor mapping device that generates acoustic images of the sea floor analogous to aerial photographs of the land (fig. 12). Recent studies comparing 500 kHz sonographs to diver observations show that small features (<5m long) seen by divers in whale-disturbed substrate could also be detected on sonographs (Oliver and Kvitek, 1984). Sidescan sonar was first used as a regional but accurate bottom-surveying device for assessing sea floor disturbance caused by the feeding activity of marine mammals in the northern Bering Sea (Johnson and Nelson, 1984). Gray whale feeding traces have also been reported from sidescan records taken off the central California coast (Cacchione and others, 1987) and from divers' observations in the fjords of Vancouver Island (Oliver and others, 1984).

In the Chukchi Sea study area (fig. 1) we reviewed 5,993 km of analog sidescan records collected with a 100 kHz and a high-resolution 500 kHz system. The data are from a series of U.S. Geological Survey cruises in the Chukchi Sea on the following research vessels: BURTON ISLAND (1974) (fig. 13), KARLUK (1981, 1982, and 1983) (fig. 14), and the NOAA ships SURVEYOR (1984) (fig. 15), and DISCOVERER (1985) (fig. 16) . The 1974 sidescan sonar records yielded marginal data (that, however, did show ice-gouges, bedforms, or gravel-covered areas) due to "aging" of the wet paper sonographs. Much of the reconnaissance sea-floor surveys were conducted using the 100-kHz system, however switches to the 500-kHz system were enacted when it was possible to observe benthic features. The 100-kHz system under optimum conditions showed both gray whale and walrus feeding traces; the 500-kHz records provided the best data to quantify the feeding traces.

The description of features seen on the sonographs remains somewhat subjective and dependent on weather and instrument conditions at the time of data collection. To minimize distortions, quantitative measurement stations in this report were selected from high-quality records that were taken during calm

seas. Computer processing was undertaken to make anamorphic corrections to the records and to present the feeding traces in their true aspect ratios for quantitative analysis (see computer analysis section).

Lateral resolution of the sidescan system is generally considered to be 1/400 of the lateral-slant range (EG & G, Inc., Environmental Equipment Division, 1982; Klein Associates, Inc., 1982). Thus, at a slant range (or swath width) of 100 m, a feature measuring 25 cm or more can be discerned. The measurement of an object parallel to the trackline is subject to some distortion due to the width of the outgoing beam. In recent studies comparing 500-kHz sonographs with diver observations, most small (<5 m long) features seen by divers were also detected on the sonograph (Oliver and Kvitek, 1984). Depths of whale and walrus feeding pits were determined by diver observation in previous studies in other areas because the relief is too small to be measured accurately from sonographs (Oliver et al., 1983b; Oliver and Kvitek, 1984).

Quantification of Feeding Traces

After examining sidescan records that exhibited whale (fig. 17) and walrus (fig. 18) feeding features, quantification stations were selected from high-quality 500-kHz sonographs at 18 sites for whale features (fig. 19) and 16 sites for walrus features (fig. 20). In each area dimensions and orientation of feeding features were extracted using computer methods outlined in the following section. From these parameters, maximum, minimum, mean, standard deviation, and median sizes were calculated for each of the stations. The percentage of total bottom disturbance was determined by dividing the total pit area (in m^2) at a given station, by the total area surveyed at that station. Using disturbance averages determined at the quantification stations compared with maps of substrate type and faunal distribution (fig. 9), we estimated the total amount of walrus and whale feeding activity in the Chukchi Sea. By using taxa distribution and biomass weights from Feder et al. (1989) together with methods of energetic and sediment resuspension calculations from Johnson and others (1983) and Nelson and others (1987), the potential food resource and sediment resuspension quantities were established for the Chukchi Sea.

Computer Analysis of Sonographs

For the purposes of computer analysis, sidescan sonar records are inspected visually for evidence of feeding features. Areas where feeding is particularly clear or abundant are scaled for range and length with 10-meter bars, drawn on the sonograph (fig. 21). The sonograph is then scanned into the computer using a Microtek MSF-300G Scanner, and Grayscan, an 8-bit grayscale scanning software package. Typically, a 4-x-4-inch area of the record was scanned, approximately the maximum area easily manipulated by the *Image 1.31* program. The memory requirements of a 3.5 x 4 inch image, scanned at 72 DPI and 200 percent Scaling, is approximately 300 kilobytes. Each image is stored on a ds/dd 3.5 inch floppy disk.

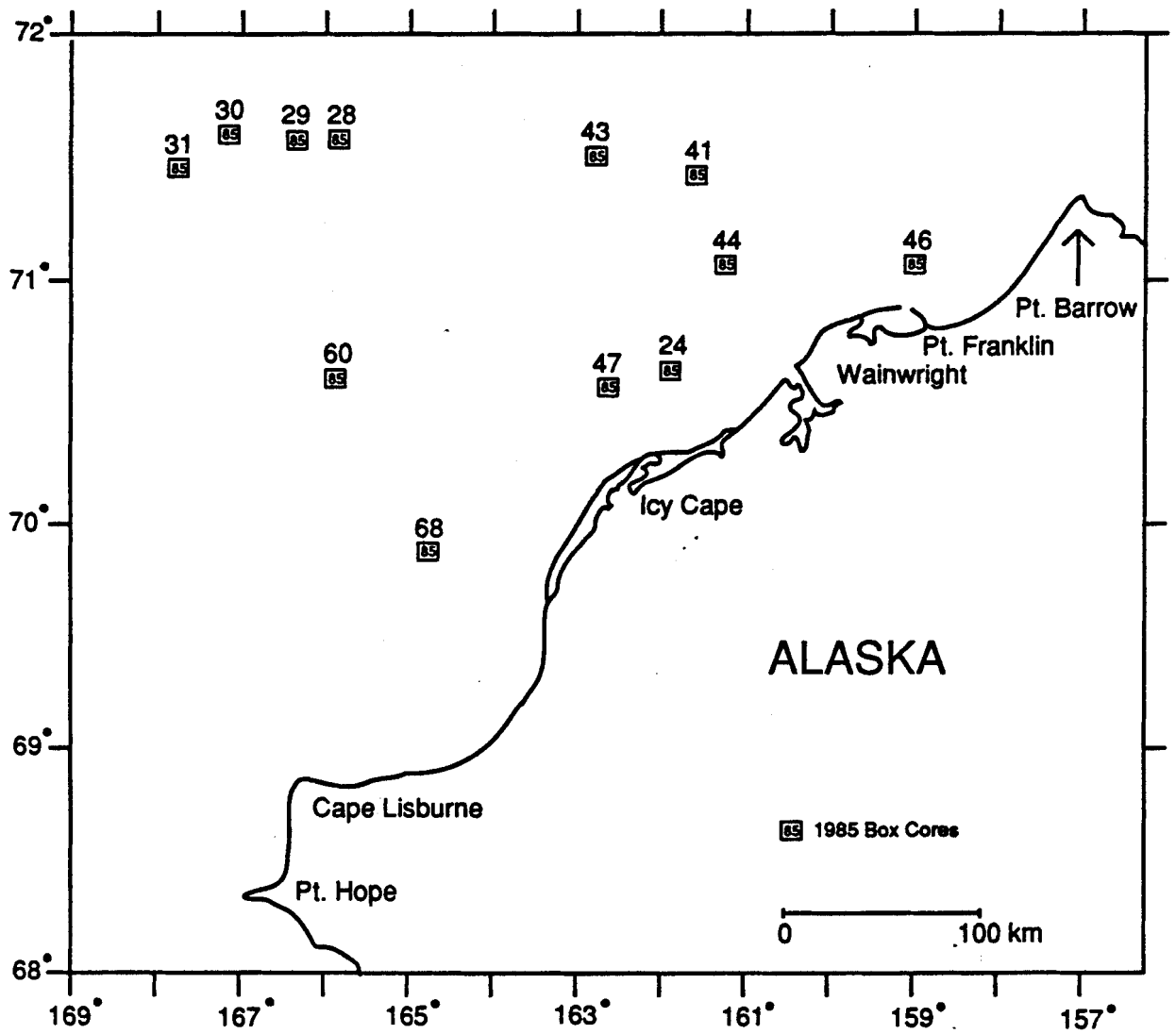

Figure 7. Location of box cores obtained in 1985. Box core descriptions are in Appendix 1.

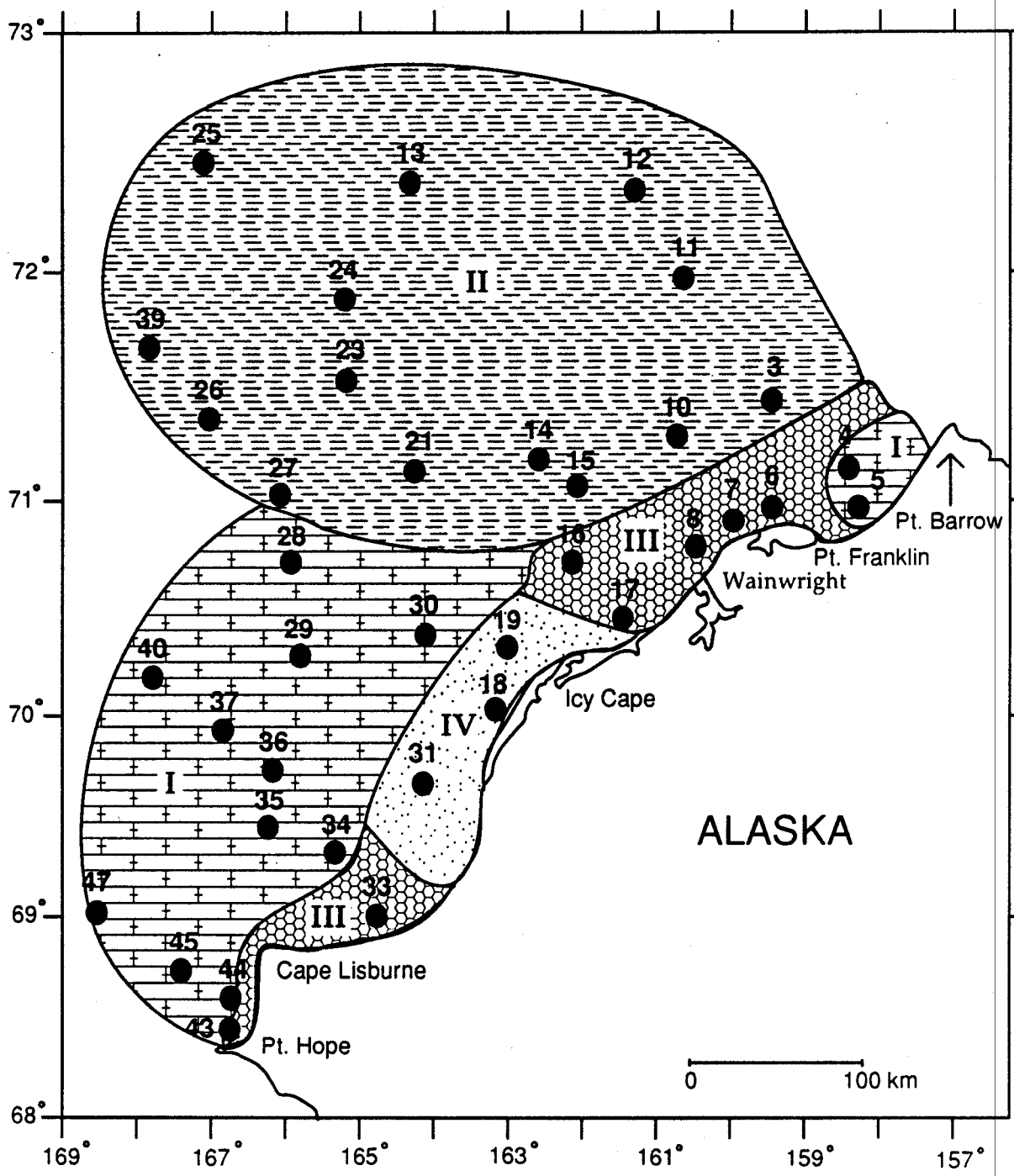

Figure 8. Distribution of macrofaunal communities and sample locations of Feder and others (1989). Four major benthic communities are identified from cluster analysis in the northeastern Chukchi Sea. Group III (see Table 1) contains the greatest variety of amphipods including Ampeliscid amphipods, a major gray whale prey.

Table 1. Benthic station groups and associated dominant taxa.

Group I.

Byblis (amphipod)	Maldane (annelid)
Balanus (barnacle)	Protomedeia (amphipod)
Leitoscoloplos (annelid)	Sternaspis (annelid)
Nucula (protobranch clam)	Thyasira (bivalve)
Echiurus (echiuroid)	Harpinia (amphipod)
Cirratulidae (annelid)	Leucon (cumacean)
Brachydiastylis (cumacean)	Myriochele (annelid)
Barantolla (annelid)	Ampelisca (annelid)

Group II.

Nucula (protobranch clam)	Ostracoda (crustacean)
Maldane (annelid)	Barantolla (annelid)
Lumbrineris (annelid)	Leitoscoloplos (annelid)
Macoma (bivalve)	Harpinia (amphipod)
Byblis (amphipod)	Haploops (amphipod)
Paraphoxus (amphipod)	Ophiura (brittle star)
Cirratulidae (annelid)	

Group III.

Balanus (juv. barnacle)	Cirratulidae (annelid)
Atylus (amphipod)	Grandifoxus (amphipod)
Protomedeia (amphipod)	Ampelisca (amphipod)
Balanus (adult barnacle)	Erichthonius (amphipod)
Ampelisca (amphipod)	Urochordata (tunicate)
Foraminifera	Polydora (annelid)
Ischyrocerus (amphipod)	Pholoe (annelid)
Leitoscoloplos (annelid)	Scoloplos (annelid)

Group IV.

Echinarachnius (sand dollar)	Liocyma (bivalve)
Cyclocardia (cockle)	Amphiophiura (brittle star)
Balanus (juv. barnacle)	Golfingia (sipunculid)
Foraminifera	Melita (amphipod)
Scoloplos (annelid)	Astarte (bivalve)
Spiophanes (annelid)	Chelyosoma (tunicate)
Mysella (bivalve)	Tharyx (annelid)
Glycinde (annelid)	

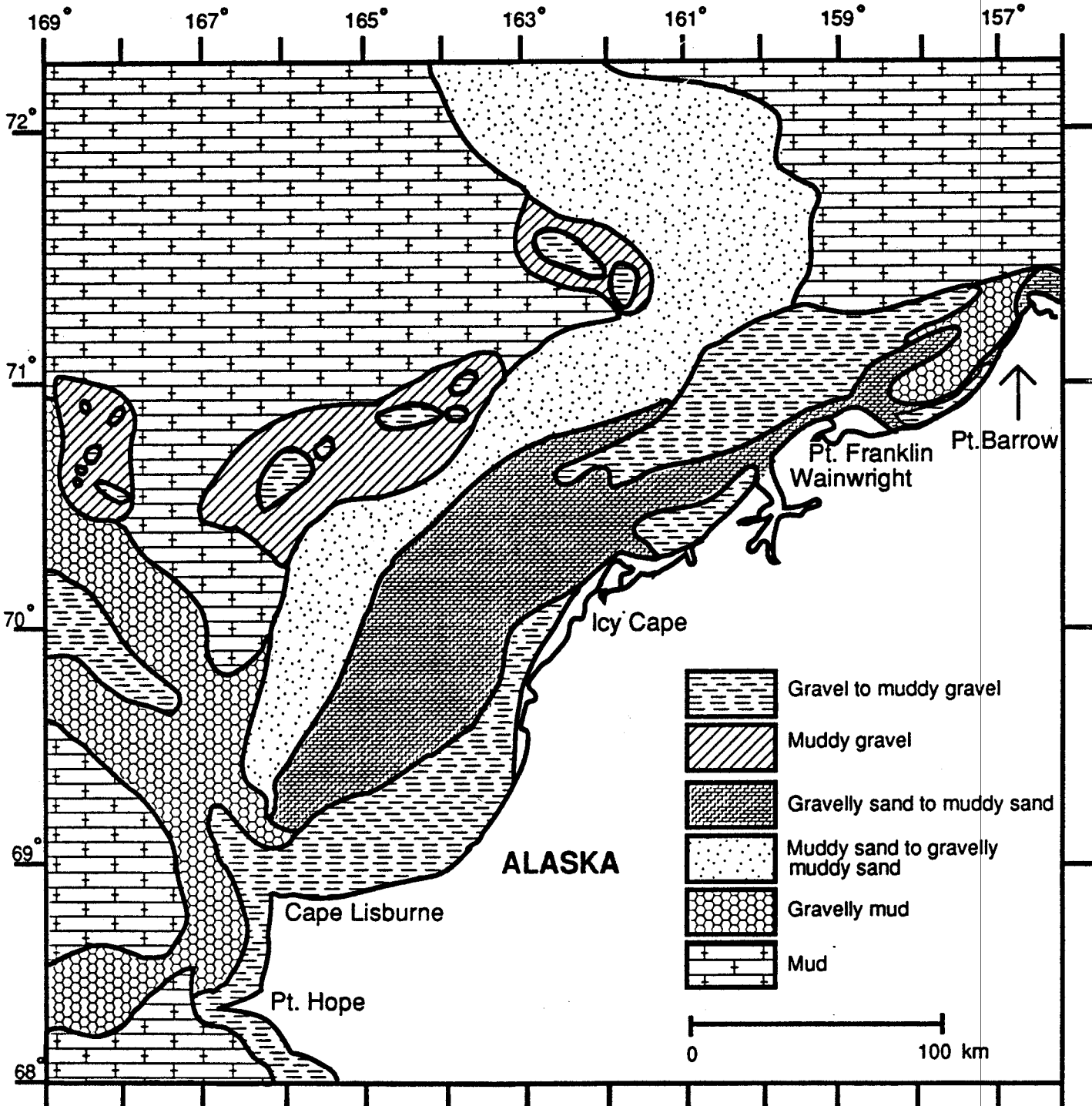

Figure 9. Major surface sediment textures, modified from Feder and others (1989), Naidu,(1987), McManus and others (1969), and sediment samples from Barnes (1974) and this study. Video surveys, camera stations, and sonographs were used to establish the major surface sediment distribution.

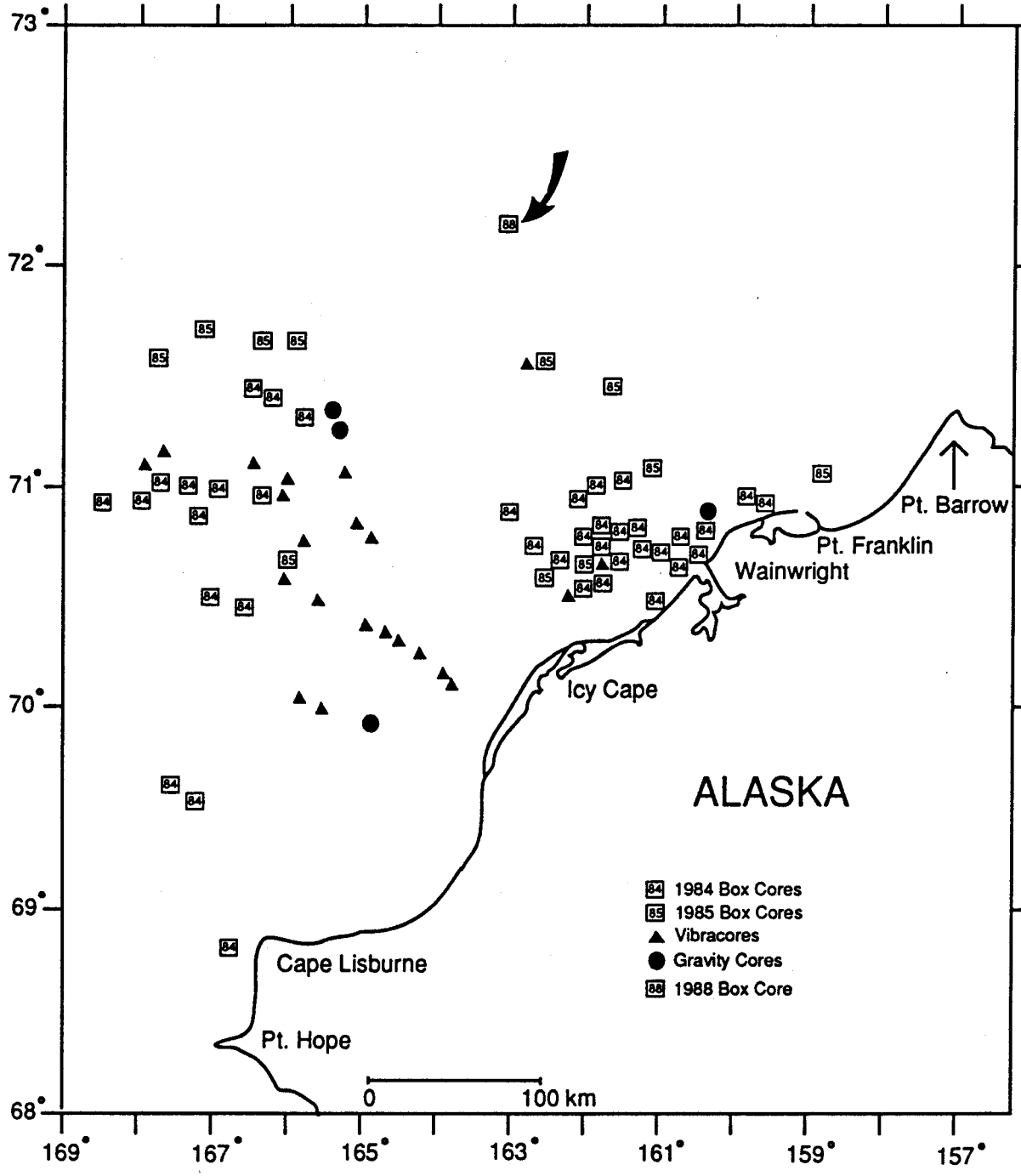

Figure 10. Sample location and type, 1984 (Cruise ID:SI84CS), 1985 (Cruise ID:DI85AR) and 1988 (Cruise ID:PI88AR). Arrow indicates Hanna Shoal box core locations obtained in 1988.

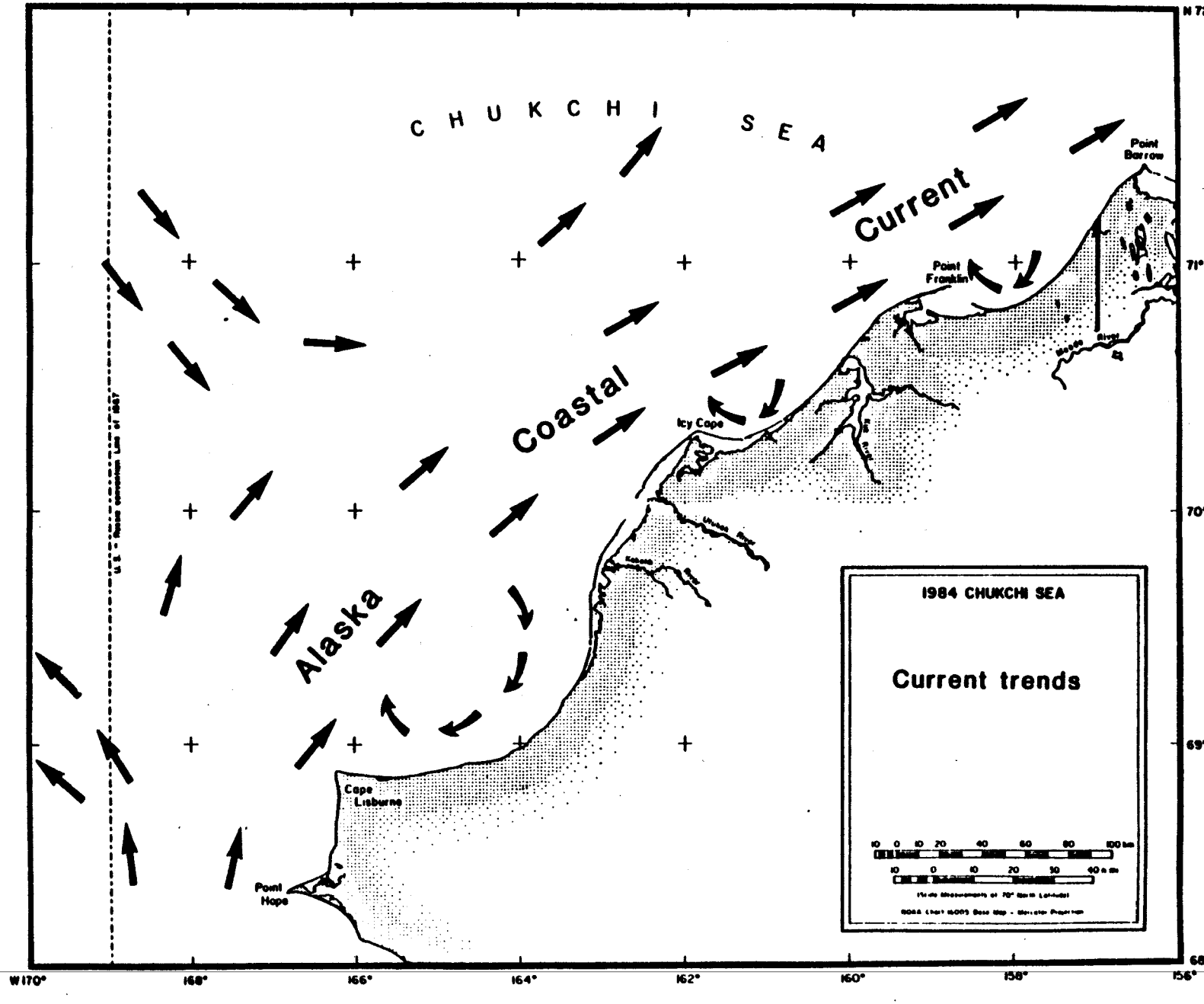

Figure 11. Major currents in the northeastern Chukchi Sea. The Alaskan Coastal Current parallels the coastal region with clockwise rotating currents developing nearshore behind the capes. Current data modifies from Coachman and others (1975).

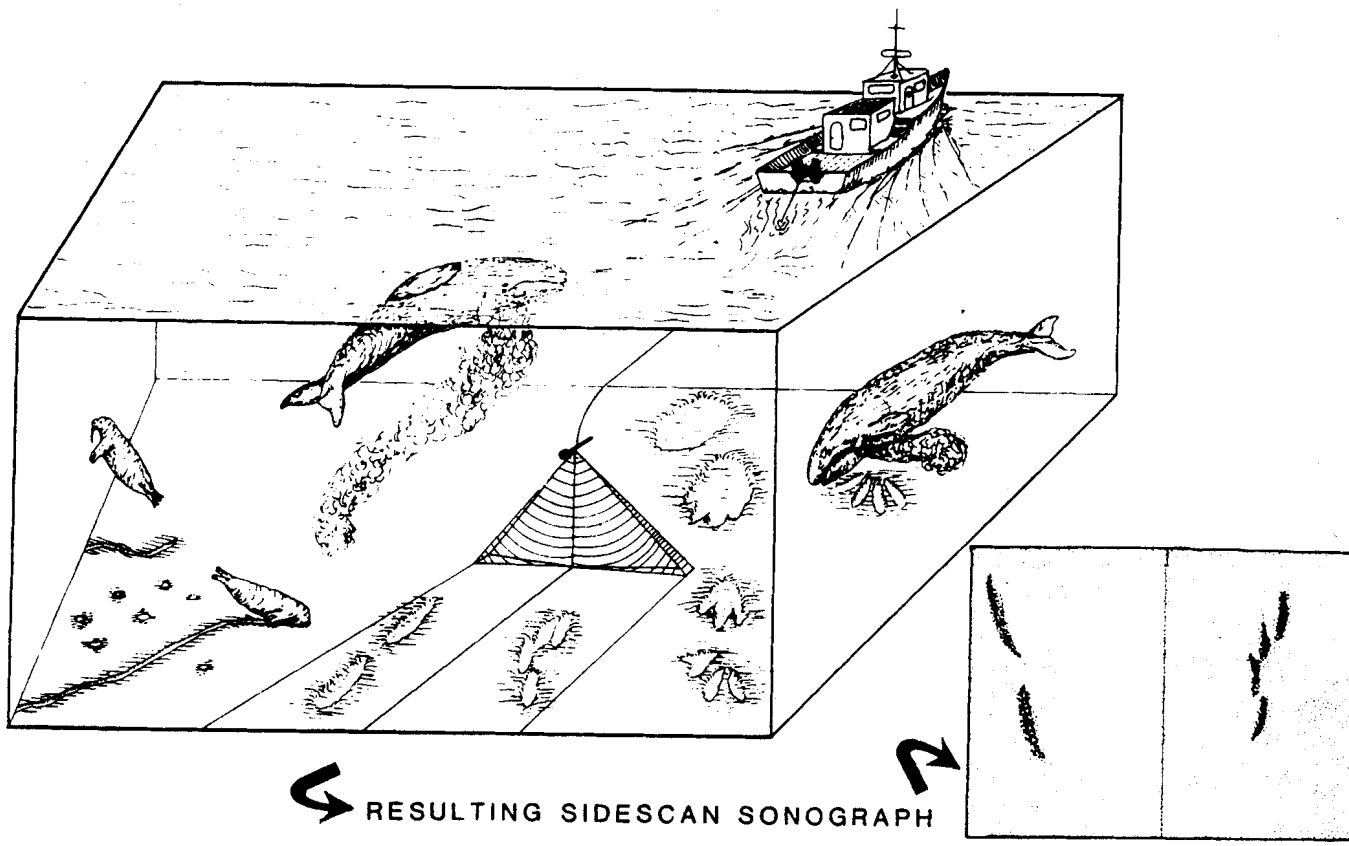

Figure 12. Schematic diagram of side-scan sonar survey technique, showing also gray whale and Pacific walrus feeding behavior and resulting feeding traces.

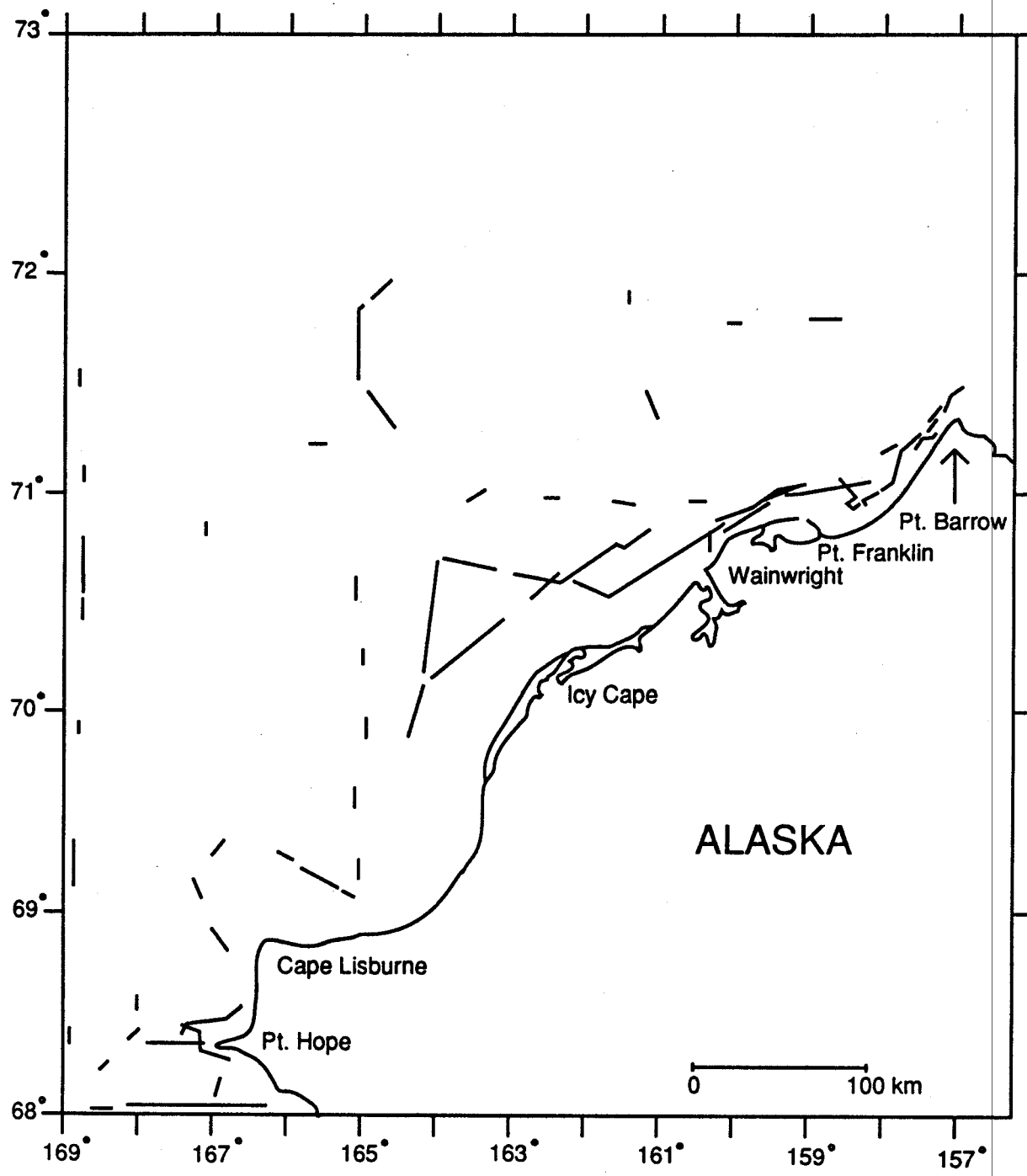

Figure 13. Side-scan sonar (105 kHz) tracklines obtained in 1974 (Cruise ID: BI74AR) in the northeast Chukchi Sea (Toimil, 1978).

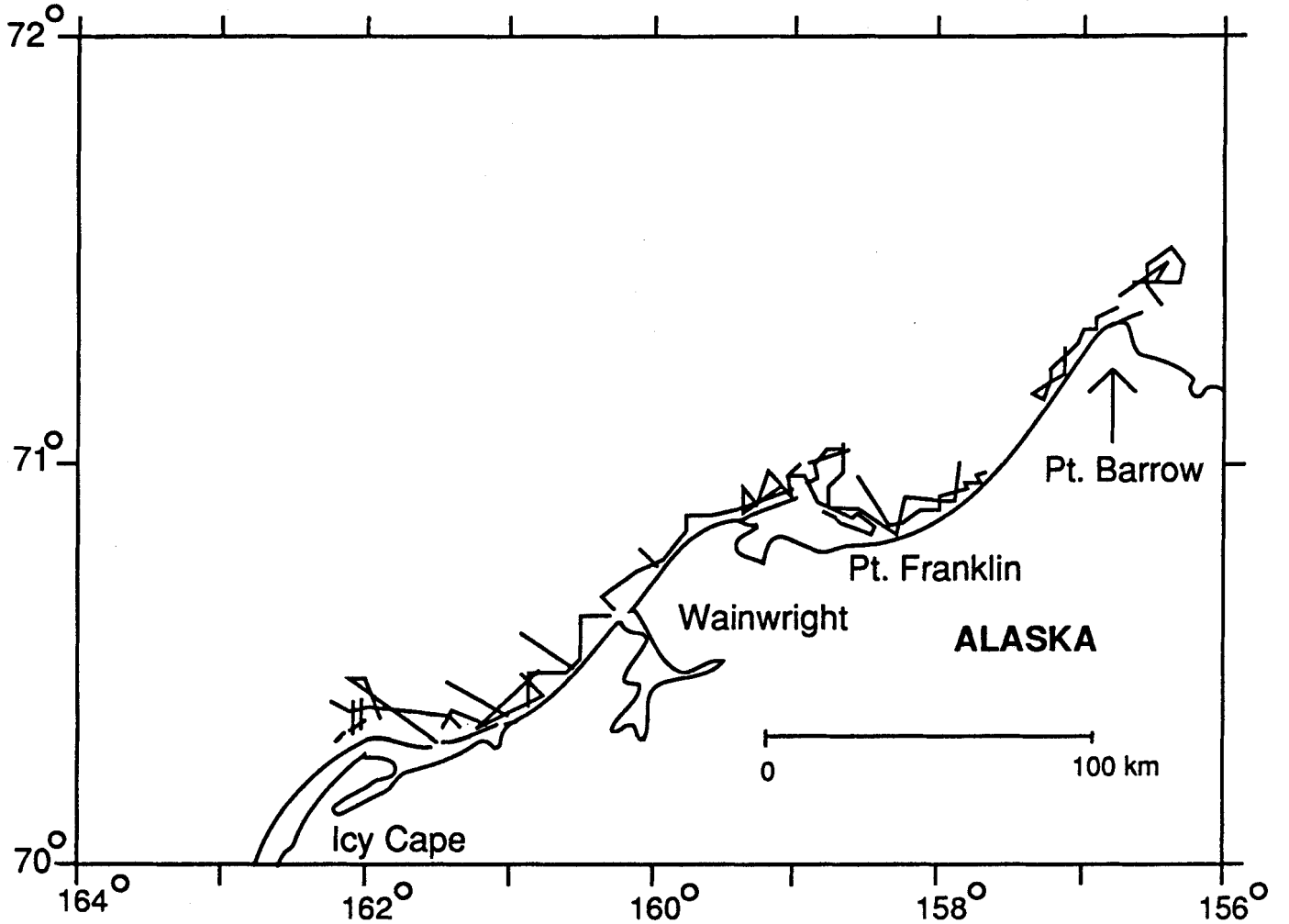

Figure 14. Side-scan sonar (100 kHz) tracklines obtained in 1981 (Cruise ID: K381AR), 1982 (Cruise ID: K282AR), and 1983 (Cruise ID: K383AR) in the northeast Chukchi Sea.

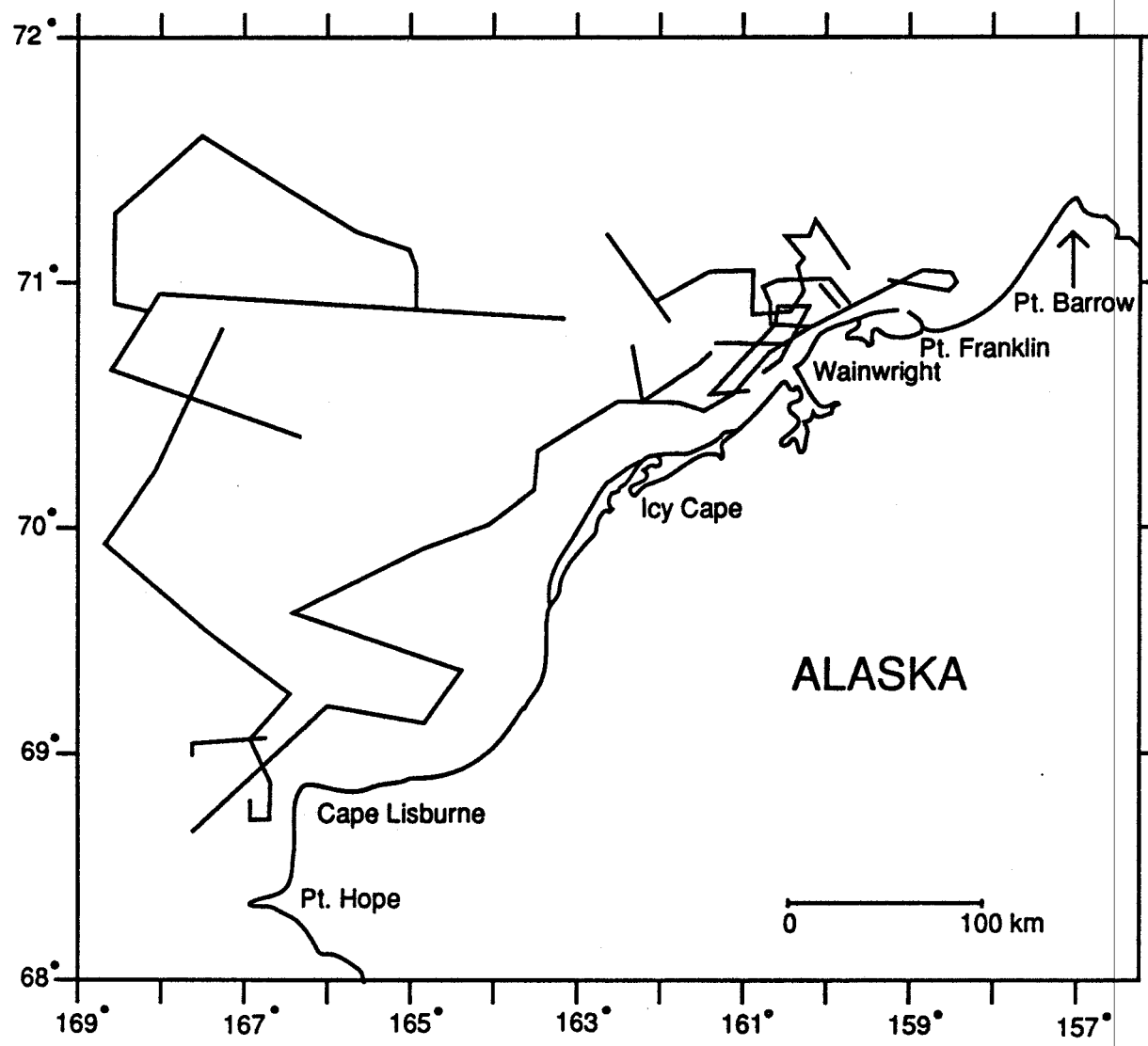

Figure 15. Side-scan sonar (100 and 500 kHz) tracklines obtained August 26 - September 17,1984 (Cruise ID: SI84CS) in the Chukchi Sea.

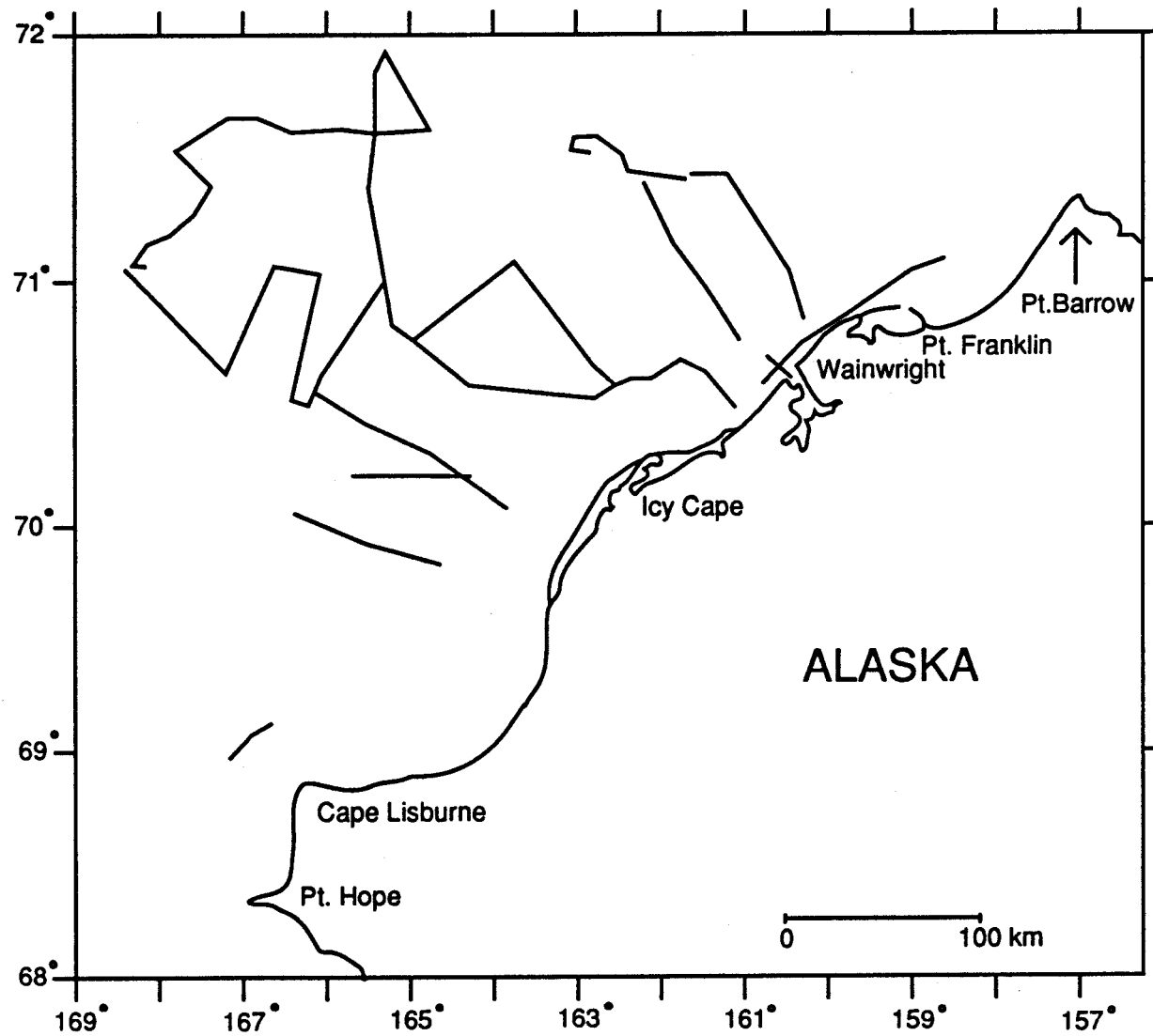

Figure 16. Side-scan sonar (100 and 500 kHz) tracklines obtained September 5 - October 6, 1985 (Cruise ID: DI85AR) in the Chukchi Sea.

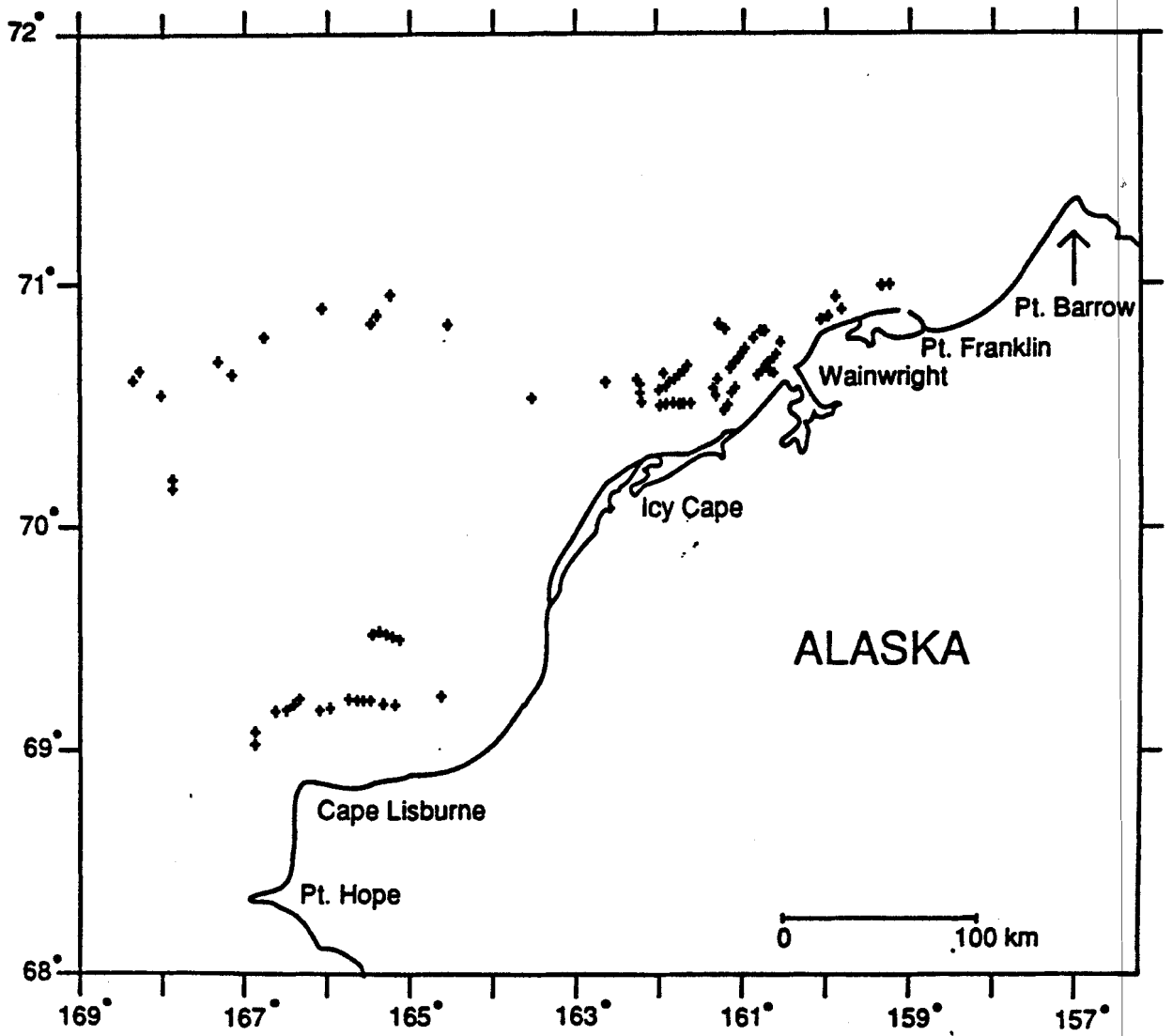

Figure 17. Areas containing feeding traces of gray whales observed in sonographs from 1984 and 1985 in the Chukchi Sea.

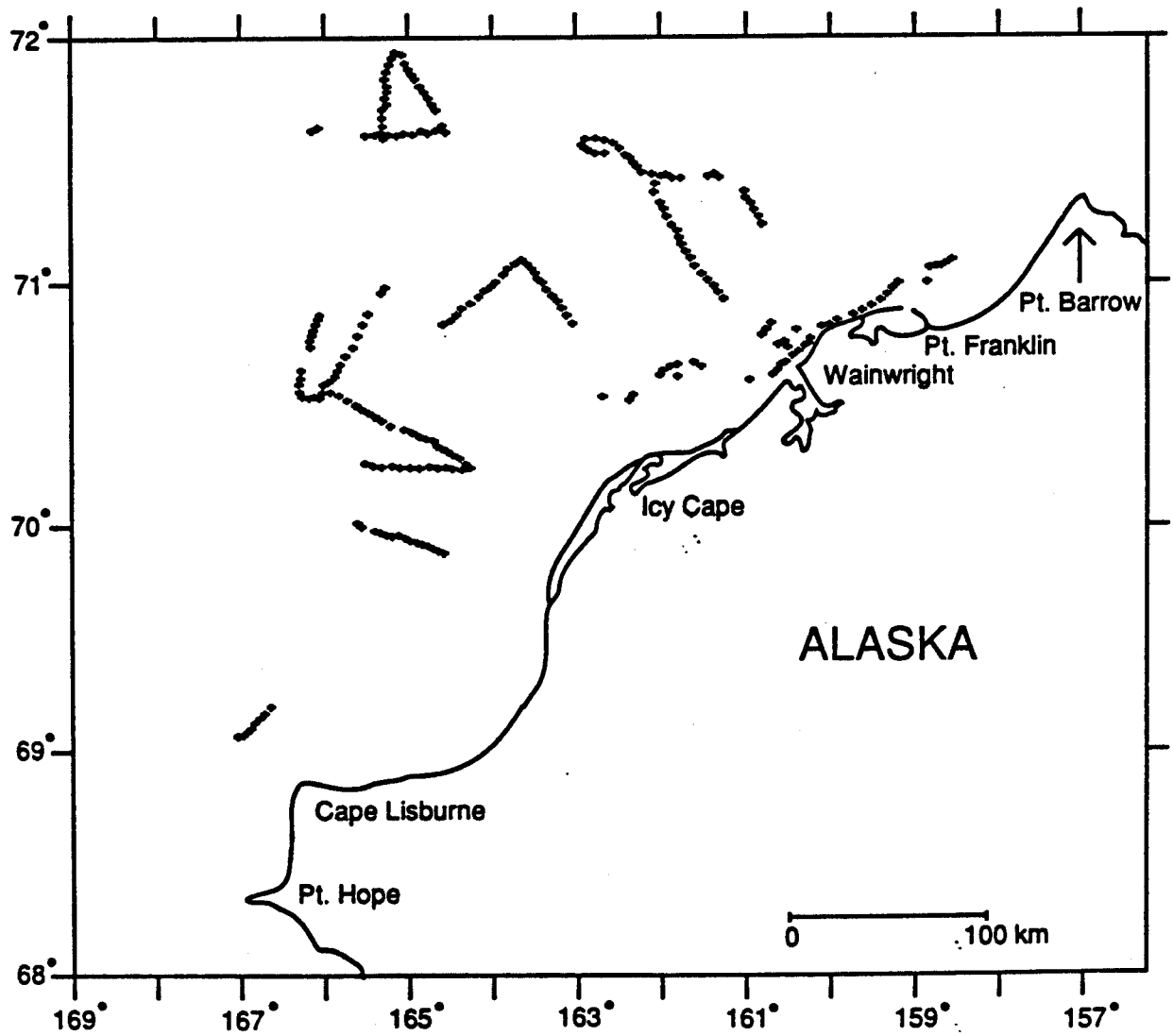

Figure 18. Areas containing feeding traces of walrus observed in sonographs from 1984 and 1985 in the Chukchi Sea.

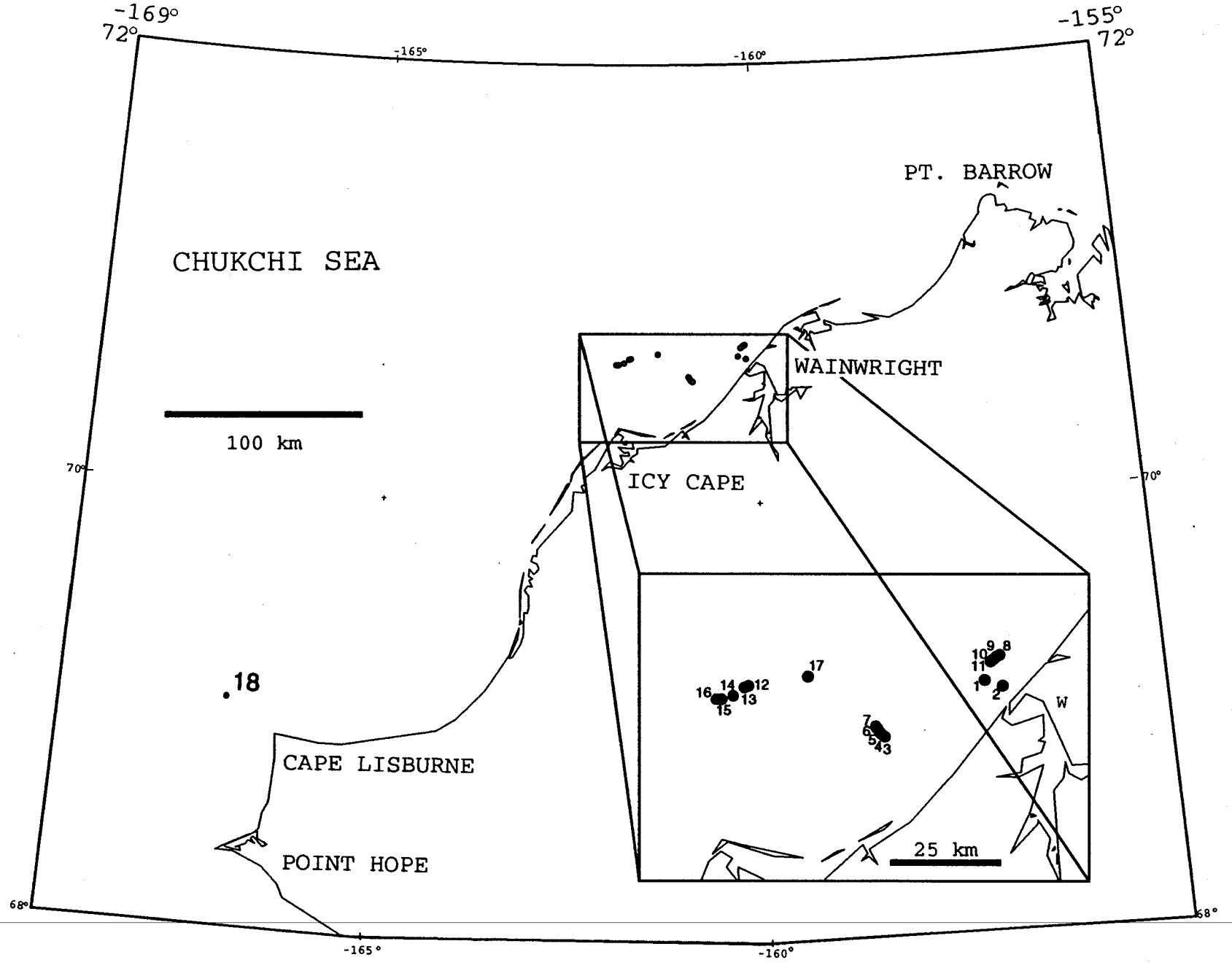

Figure 19. Gray whale feeding trace quantification stations selected from side-scan sonar records collected in the Chukchi Sea.

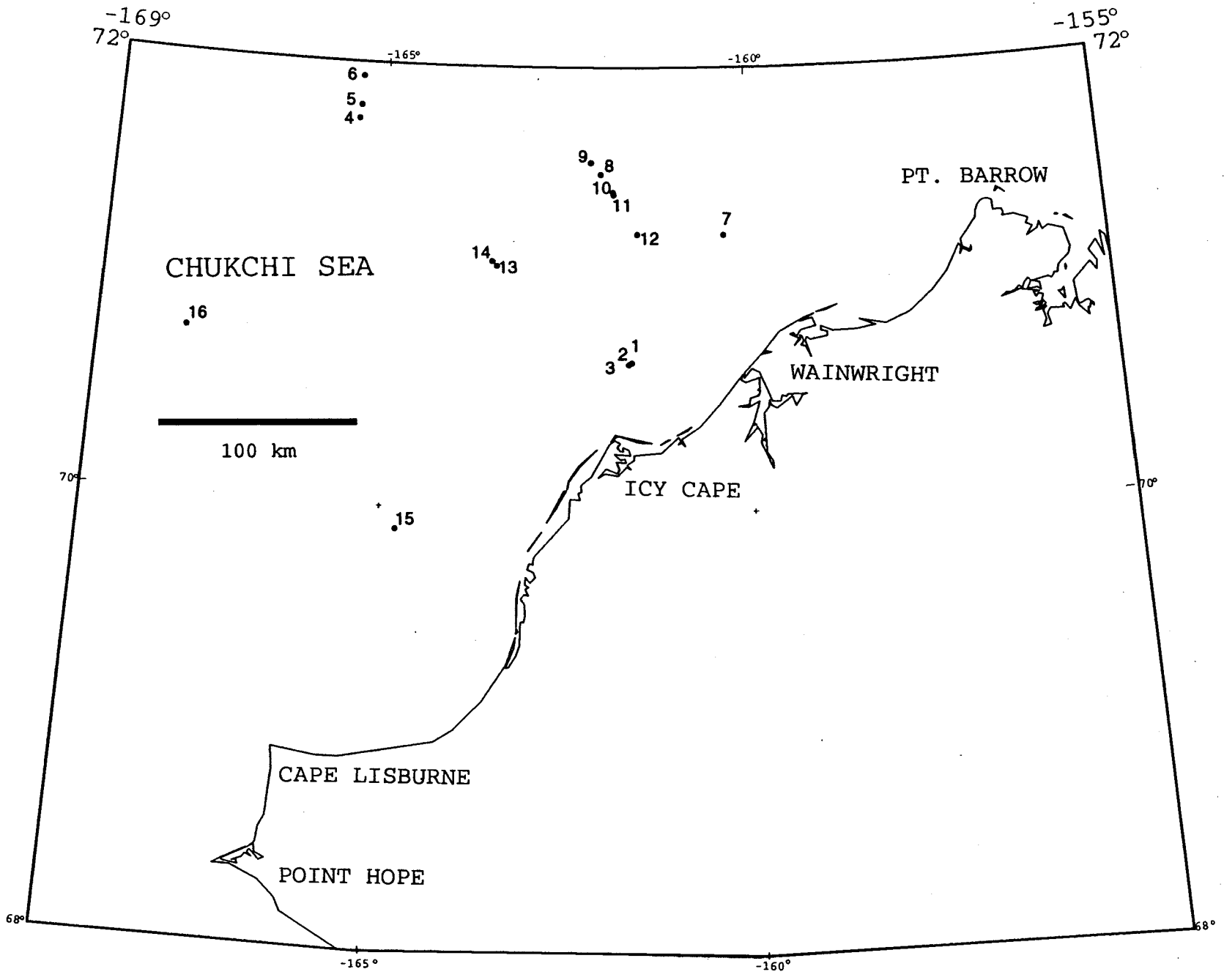

Figure 20. Walrus feeding trace quantification stations selected from side-scan sonar records collectedin the Chukchi Sea.

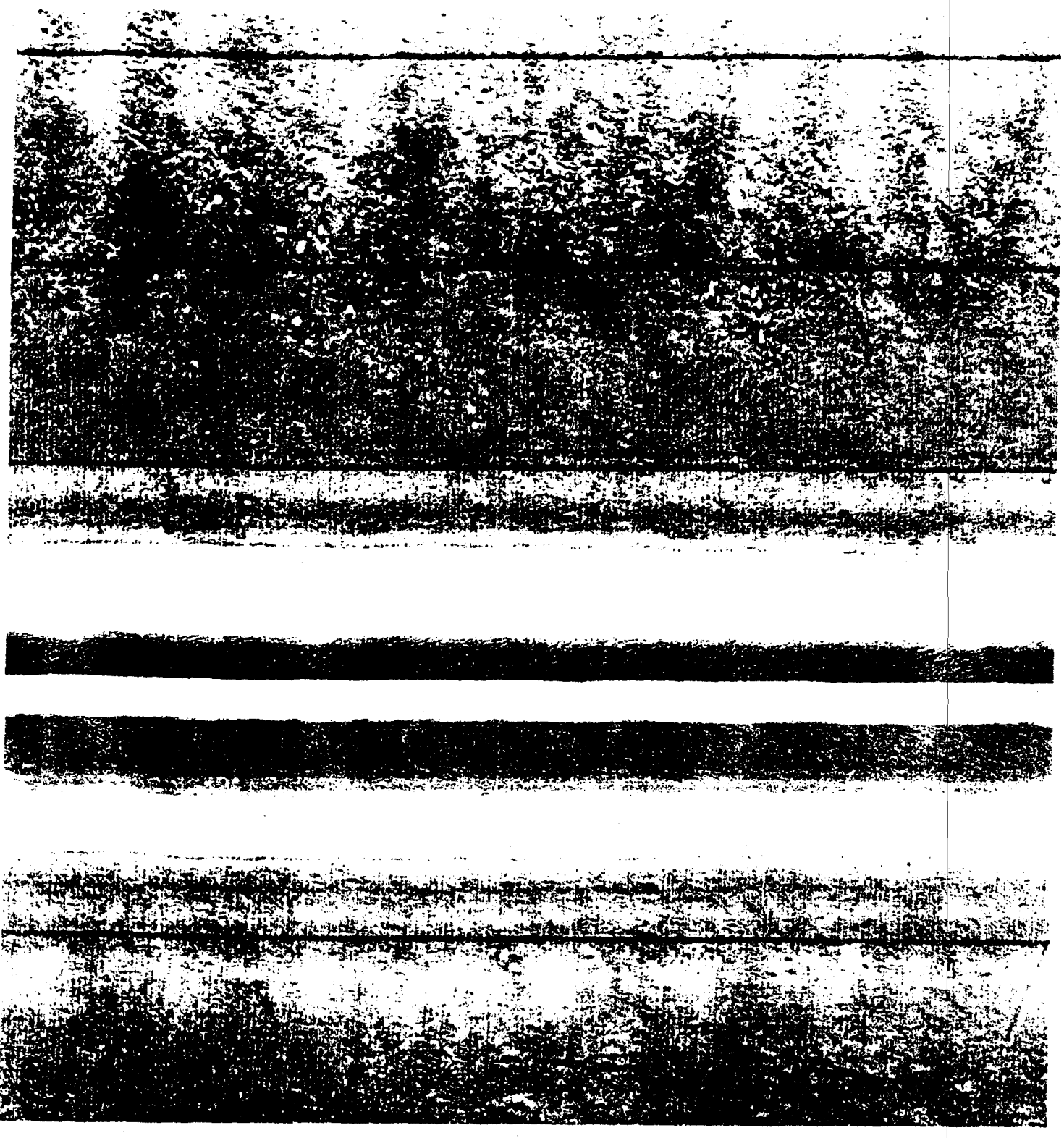

Figure 21. Analog image of original sidescan sonar record at whale pit quantification station 12. Compare with Figure 22. Scale bars are 10 m.

Scanned images are loaded into a Macintosh IIfx computer (fig. 22), and analyzed with *Image 1.31*, image analysis shareware available from the National Institutes of Health, in Bethesda, Maryland (Appendix 2). *Image 1.31* used with 8 bit grayscale[1] supports a palette of 256 shades of gray. Other color palettes are available, but the best support for identification of feeding traces came from a grayscale. In addition to grayscale, the program has an ability to *threshold*, (assign a bright contrasting color to pixels of a specified gray range) for the purposes of analyzing only what is selected by the user. The user must also select the type of measurements to be made. *Image* supports a large number of measurement capabilities. For the purposes of this study, axis length, orientation, labeling, and area were selected. These measurements allow correlation of this study with the Bering Sea study (Johnson and others, 1983), and with studies of the measured gapes of gray whales. Measurements calculated by *Image* are put in tabular format (Table 2) ready for export to another file or a printer, and can be opened in *Macwrite*, *Microsoft Word*, and *Kaleidagraph* (fig. 23).

Image allows scaling in two dimensions, enabling us to normalize data collected at differing ship and recorder/paper speeds. The correction is necessary because along-track scale is not identical to the cross-track scale. By measuring each sonograph, and preparing length and width bar scales at each sample location (fig. 22). *Image* can be used to normalize the two scales (fig. 24). There remains a small amount of slant-range error at the very edges of the sonograph, where a beam spread effect can become noticeable, but the error induced is small, and is minimized by selecting only the central portions of the records for analysis.

Pictures (sonograph images) opened and manipulated in *Image* are saved as altered TIFF [2] files, but the original unaltered file is retained for future studies. One completely analyzed station with original and corrected images, measurements, and rose diagram files can be stored on a 3.5 inch ds/dd floppy disk.

The final analysis of each picture is a multi-step process (fig. 23). The image is scaled, and scanned and saved in a TIFF format onto a disk. The TIFF file is opened in *Image* (fig. 22) where scale correlation and slant range corrections are performed (fig. 24). With selected measurement parameters, minimum particle size and precision set, the features to be analyzed are outlined with the pencil tool in the threshold color. Once all particles have been outlined, analysis of the particles is selected (fig. 26). The *Image* program will determine length, width, area, and orientation for every particle that is above threshold, and prepare the data in a table (Table 2). The table is saved as regional measurements, and the final corrected image is saved as a TIFF file, leaving the original unaltered. Copies of both of these files are kept for reference purposes, to cross check in case irregular measurements are encountered in the data.

---

[1] A color scale which consists of 256 continuous grey tones, with black and white as end-members.

[2] TIFF Stands for 'Tagged Image File Format', and is supposed to represent a high resolution bitmapped standard file format. It is no longer standard, and varies among applications. It supports grey, grayscale, and color images, depending on application. Generally used for saving scanned images, TIFF formats are being constantly adapted and upgraded.

The *Image* program allows the user to determine what levels of gray palette are utilized. For the purposes of selecting particles, the normal mid-value gray scale palette is used. Once all features visible have been mapped, the palette may be shifted towards the white or black ends of the spectrum, and contrast and brightness may be adjusted. Shifting the brightness and gray levels the palette allows the user to see more subtle features which may have otherwise been missed. When asked to print, *Image* will utilize whatever settings are currently in use. In this way, a wider variety of prints can be made, highlighting the features desired. Other grayscale or color palettes may be used, but we used the 8-bit grayscale palette throughout the study to ensure uniformity of coverage.

The analysis of walrus bottom disturbance differs slightly from the analysis of whale bottom disturbance. The reason for the difference lies in the two separate styles of feeding. The pits left by whale feeding are distinct, and the scale of the features makes an overlapping bite wipe out our view of one underneath. Walrus, by comparison, feed by furrowing through the substrate. The furrows may cross and intersect in irregular patterns (fig. 27). To facilitate a quantification, it is necessary to take a smaller area, and look at it in closer detail. A box 5 meters by 10 meters is made, and all the walrus furrows within that box are traced as a linear distance, not outlined as a geometric shape. The measurement tool is selected, and used much like the pencil tool to trace each furrow in the threshold color (fig. 28). *Image* will compile the length of all lines drawn with the measurement tool into a table (Table 3). Similar to the whale analysis, the list of measurements may be exported to another file, or printed (Table 3).

Because of the crosscutting nature of the walrus furrows, the measured lengths do not represent the total length of an individual furrow (as was measured in the Bering Sea), but rather the summed length of furrow segments, which provides an indication of the intensity of feeding in the area. The cumulative length of walrus furrows was computed for all quantitative stations and plotted into histograms (fig. 29). The histograms allowed us to estimate the walrus feeding impact on the Chukchi Sea and to compare similar work done in the Bering Sea (Nelson and others, 1987).

It was not helpful to determine orientations of walrus furrows because they have no net direction, and they often twist and turn across the sediment surface (fig. 27). In contrast, histograms of stations vs orientation for whale pits (Appendix 3) were used to make rose diagrams of the pit orientations (fig. 30). The program to plot the rose diagrams was written in Fortran by David Rubin, (Pers. comm., U.S. Geological Survey, 1991). The data table, used by the program to plot rose diagrams, consists of 36 fields (Table 4). Each field represents the number of measurements made within a 10 degree range (i.e. the first field represents all measurements from 1 to 10 degrees, the second 11 to 20 degrees). The program will self scale the rose plot and deliver an output file which was then enhanced using *Adobe Illustrator* (fig. 30).

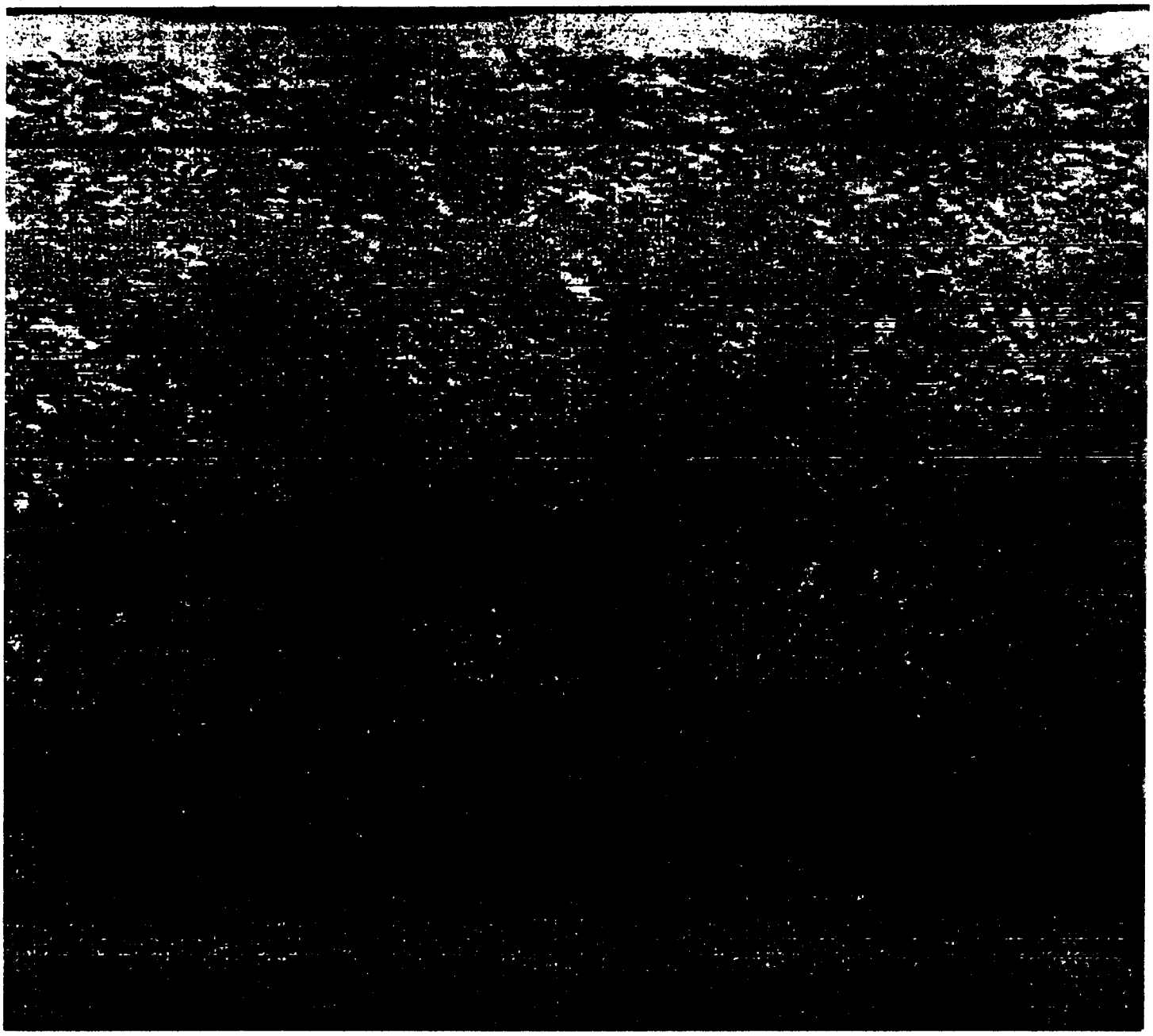

Figure 22. Scanned image of sonograph in Figure 21 (Whale station 12). Scale bars are 10 m.

Table 2. Portion of raw output file from NIH *Image* (version 1.31), showing some measurements extracted from a best-fit ellipse on the identified gray whale feeding pits at whale station 16. First column is length of minor axis, 2nd column is length of major axis, and 3rd column is the angle that the major axis of the best-fit ellipse makes with the horizontal axis of the image. In this study this horizontal axis is always the ship's trackline. The angle value and the ship's trackline azimuth are used to determine pit orientation. Please see Appendix 3 for a complete and corrected data table for whale station 16.

0.247	0.411	114.519
0.287	0.521	45.000
0.202	0.355	107.137
0.259	0.300	76.224
0.257	1.024	158.204
0.242	0.396	39.972
0.315	0.454	177.327
0.243	0.393	25.248
0.204	0.440	149.501
0.536	1.827	6.025
0.435	0.522	100.768
0.255	0.819	13.048
0.309	0.560	142.998
0.339	0.510	50.304
0.275	0.652	171.870
0.174	0.378	139.252
0.272	1.011	171.803
0.238	0.753	156.135
0.232	0.412	77.751
0.303	0.413	39.230
0.288	0.457	177.530
0.353	0.474	111.114
0.317	0.923	18.579
0.220	0.381	97.161
0.171	0.560	174.151
0.130	0.827	174.177
0.201	0.505	38.253
0.182	0.360	116.565
0.409	0.526	126.879
0.300	0.815	21.146
0.354	1.231	6.743
0.217	0.910	165.880
0.224	0.639	22.663

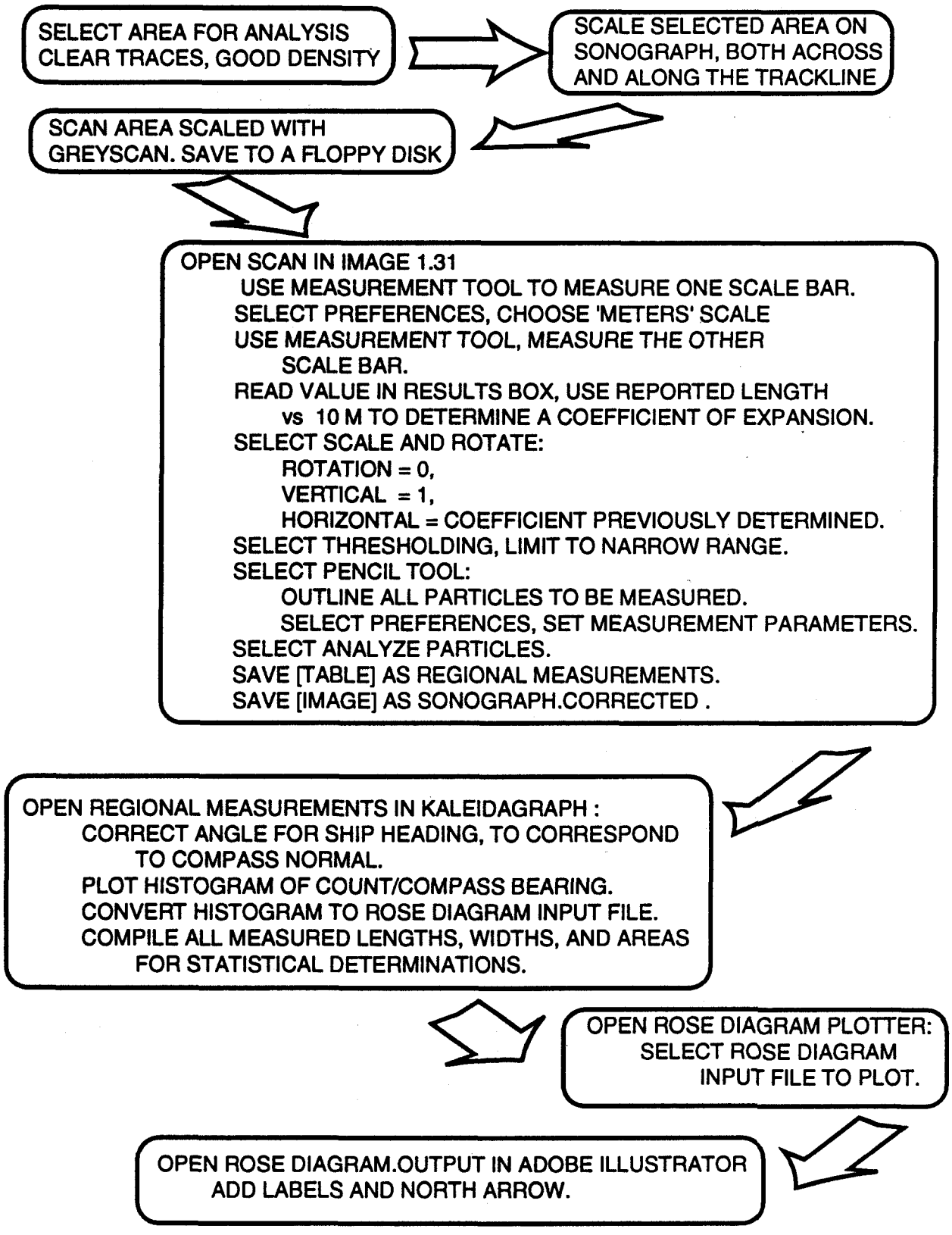

Figure 23. Flow chart for computer analysis of whale and walrus feeding traces.

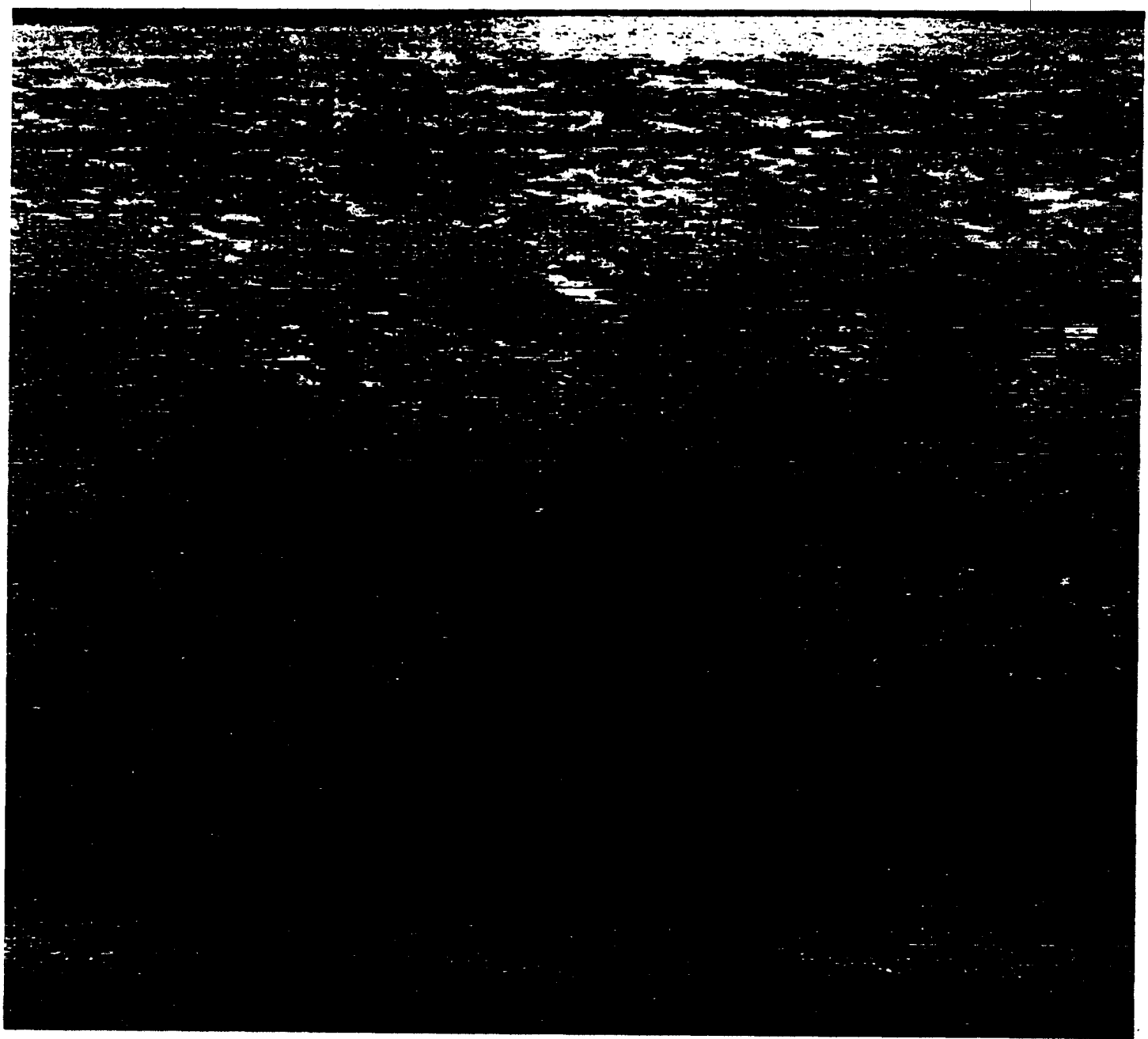

Figure 24. Same image as figure 22, with corrected aspect ratio. Scale bars are 10 m.

Figure 25. No figure. See Figure 26.

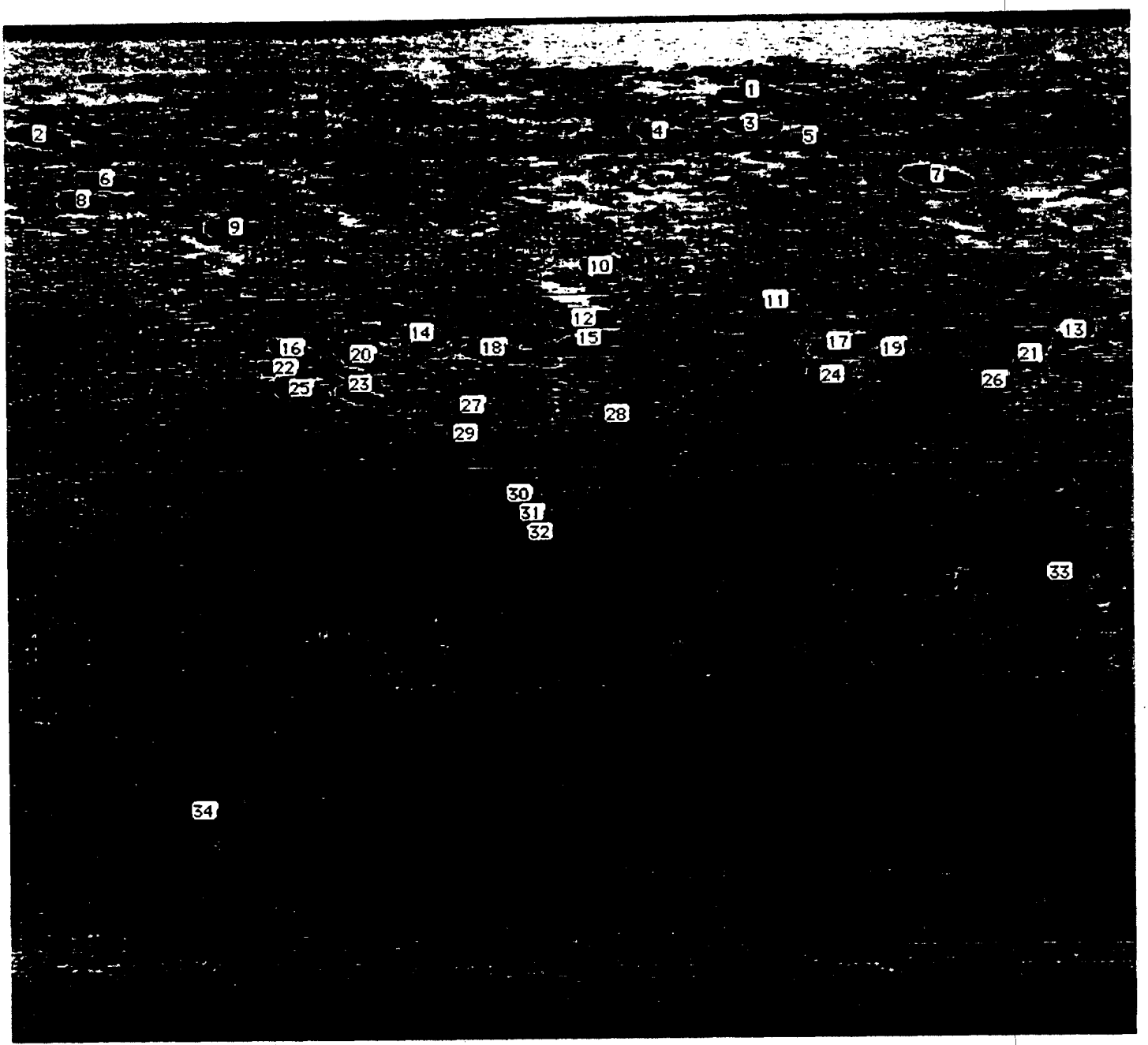

Figure 26. The outline pits have been selected, numbered, and analyzed. Pit parameters have been stored in a text file. Scale bars are 10 m.

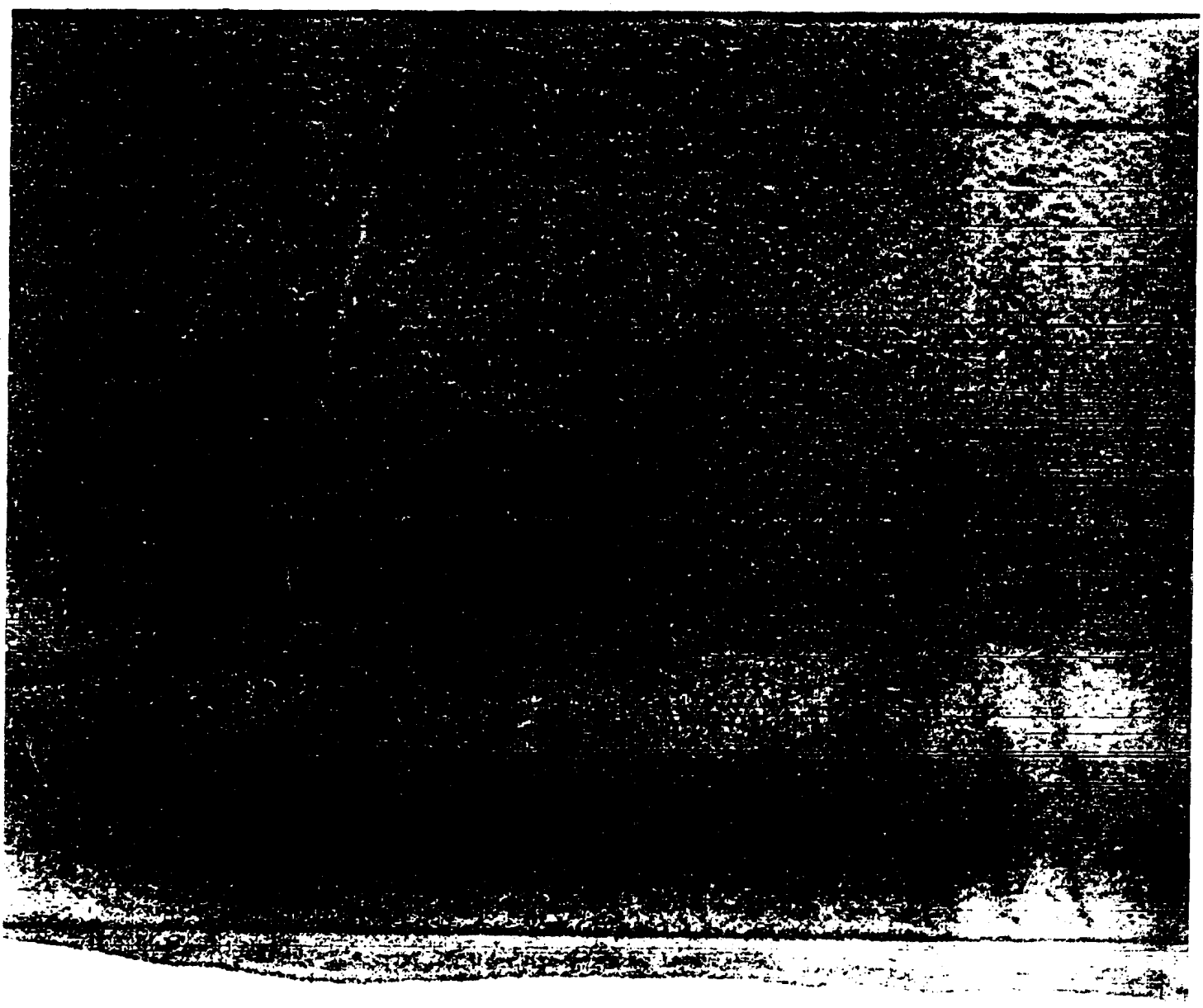

Figure 27. Sidescan record at walrus station 12, showing walrus feeding traces (furrows). Furrows are most distinct in the upper half of the image. Scale bars are 10 m. Note that features are compressed in the along-track direction (left to right). The aspect ratio is corrected in Figure 28.

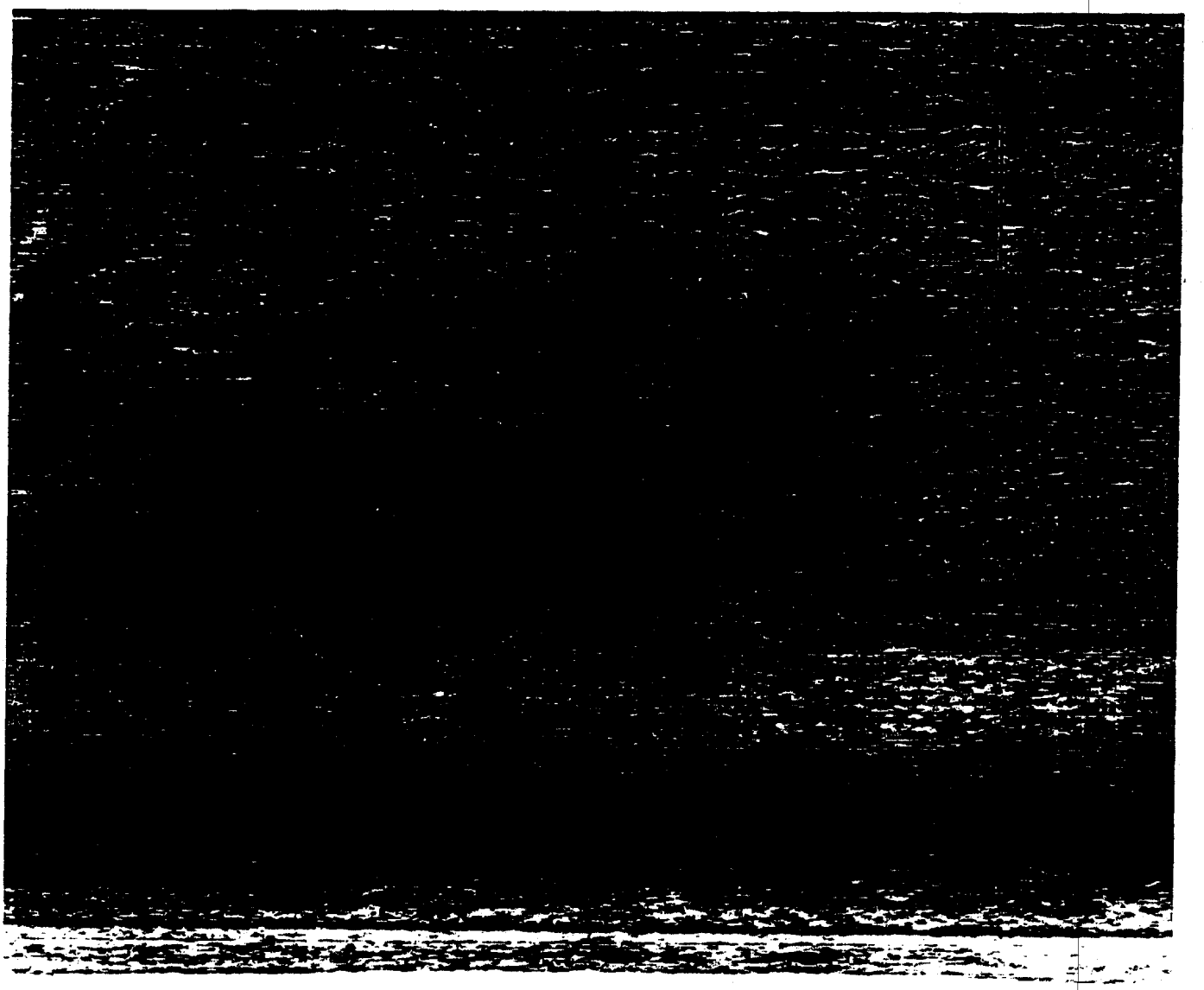

Figure 28. Same image as Figure 27, with corrected aspect ratio, showing 50-m^2-area analyzed.

Table 3. Output file from *Image 1.31*, showing walrus feeding trace length measurements (in meters) at walrus station 12.

2.207
1.170
0.854
1.249
0.844
1.249
0.436
0.930
1.150
0.760
0.726
2.614
2.933
2.094
2.115
1.669
1.719
1.558
0.871
1.370
1.425
0.519
0.699
2.498
2.079
3.594
1.754
1.176
2.551
1.628
0.473
3.321
1.829
0.000
3.311
3.112
1.234
0.790
1.049
0.649
1.570
1.833
1.315
0.846
1.261
1.428
0.976
1.901
1.088
1.428
1.693
0.588

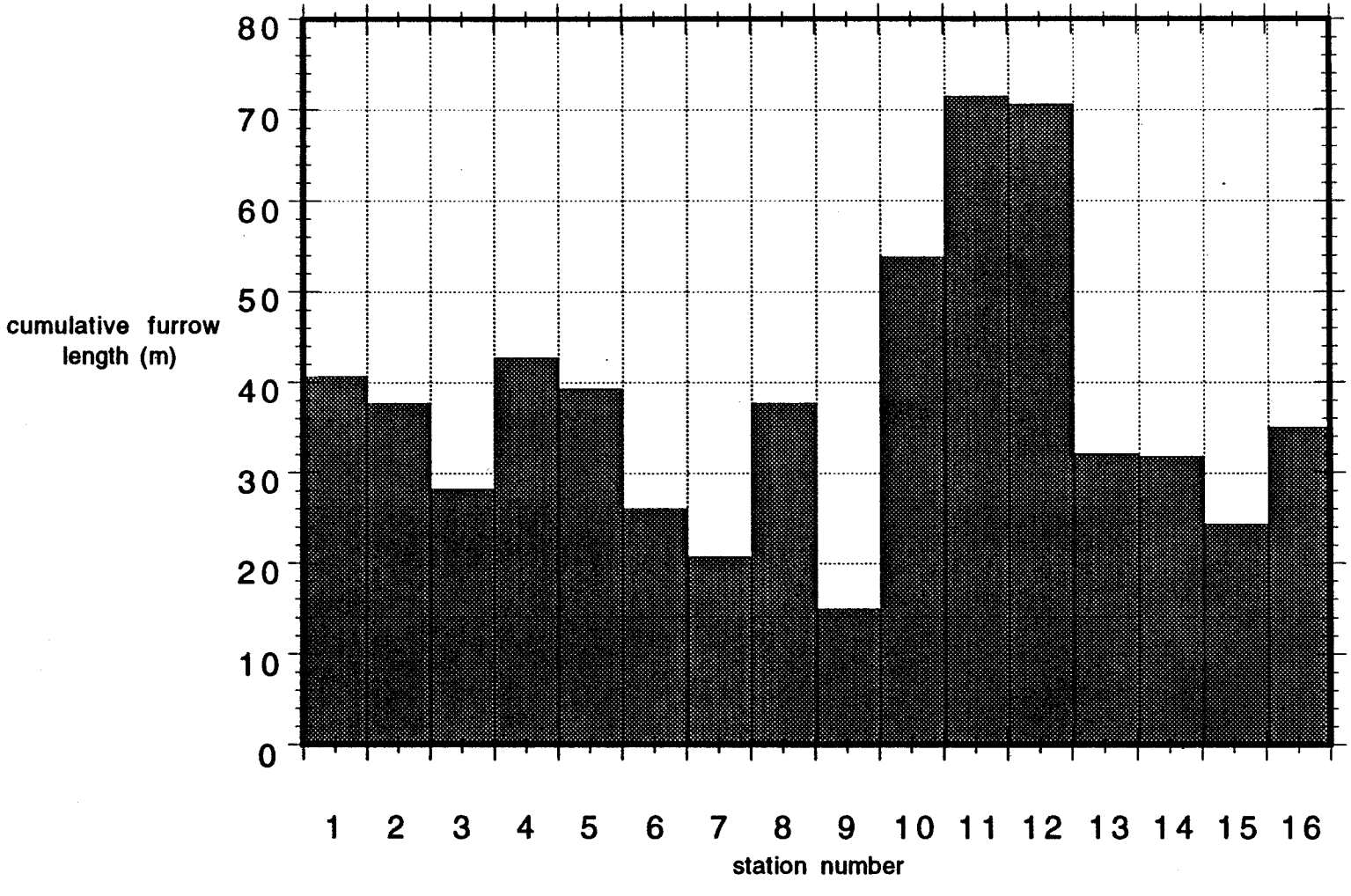

Figure 29. Histogram showing walrus seafloor disturbance (total furrow length) at each of the 16 stations.

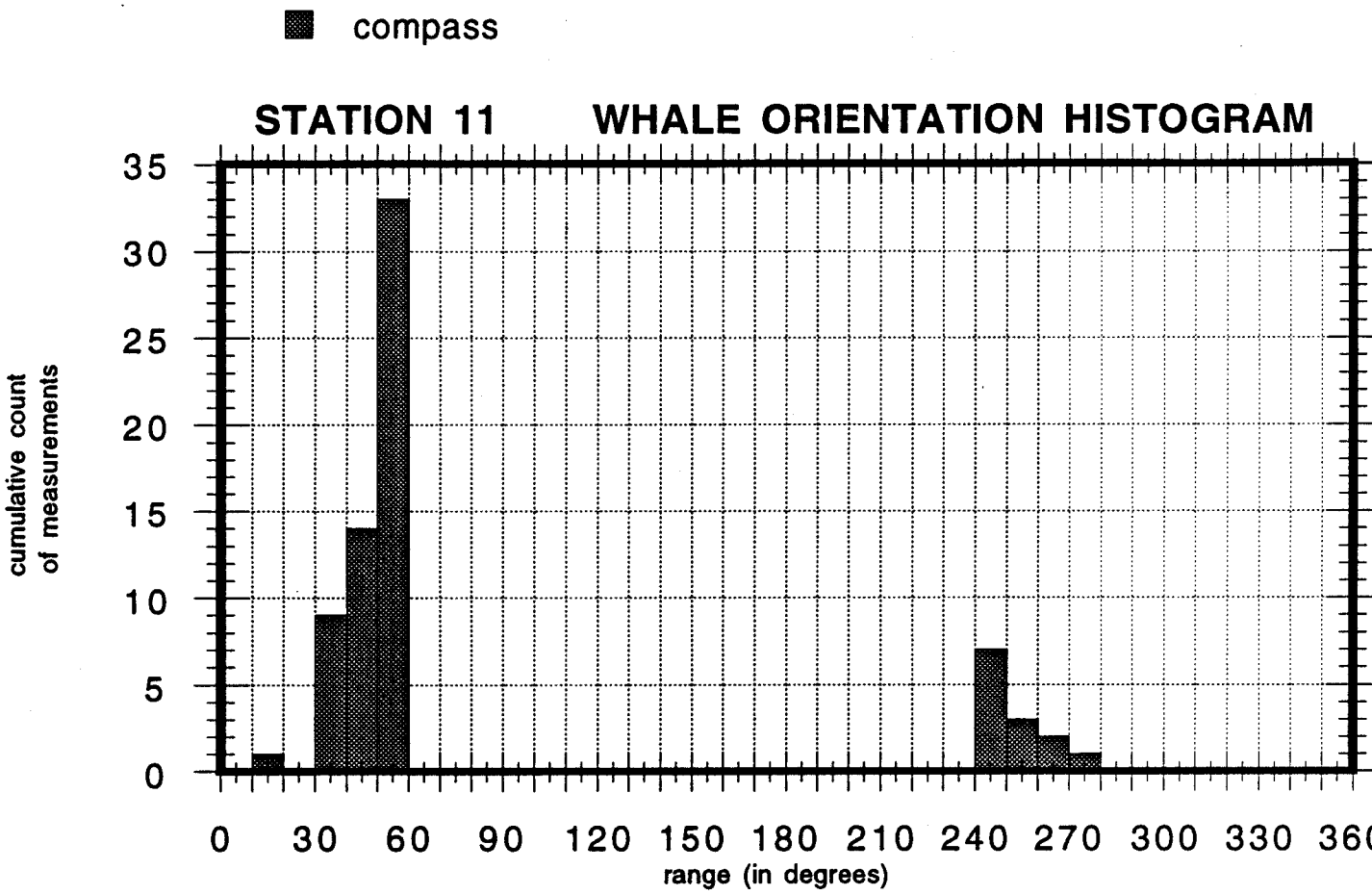

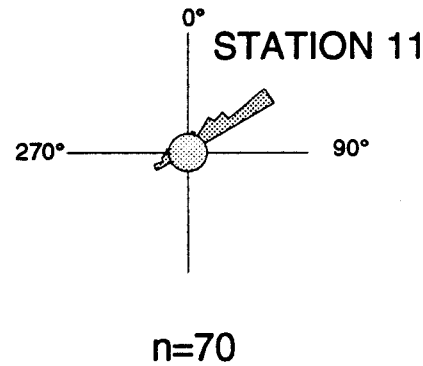

n=70

Figure 30. Histogram and rose diagram showing gray whale feeding pit orientation at station 11.

Table 4. Input data for rose plotter program from whale station 11. The values listed below represent the number of pits with a long-axis azimuth between 0 and 10°, 10 and 20°, and so on. The last value represents orientations between 350 and 0°.

0
1
0
9
14
33
0
0
0
0
0
0
0
0
0
0
0
0
0
0
0
0
0
0
0
7
3
2
1
0
0
0
0
0
0
0
0

The Chukchi Sea is a broad, shallow (<60 m deep) epicontinental sea that is ice-covered for 9 to 10 months per year. Hanna Shoal to the north and the Barrow Sea Valley in the northeastern Chukchi Sea form the major bathymetric features within the study area (fig. 2). Much of the Chukchi Sea floor is relatively flat and shallow, with depths averaging 40 to 50 m depth. Locally enclosed depressions, and local bathymetric highs contribute up to 5 m of relief. On the northern part of the shelf, Hanna Shoal rises to 25 m depth (Hill and others, 1984). North of Hanna Shoal the sea floor slopes north toward the shelf break where at approximately 60 m depth the shelf slope rapidly increases. Along the northeast part of the Chukchi Sea, the Barrow Sea Valley forms a major erosional incision into the sea floor starting west of Point Franklin and trending northeast parallel to shore. The sea floor rapidly drops to over 100 m depth within the sea valley.

During the summer open-water season the ice usually retreats north to near the shelf edge, but during the study period in the offshore regions in 1981 to 1985, the ice rarely moved north of 71° 30' (fig. 31).

Prevailing winds are generally from the northeast (Brower and others, 1977), however, the major storms are reported most frequently from the southwest and west during the open water period in late summer and fall (Wiseman and Rouse, 1980). Storms from the southwest with winds up to 60 knots were common during our period of investigation. Storms, when ice conditions are favorable and sufficient fetch exists, then periodically rework the sea bed to varying water depths across the shallow sea. Storm-generated waves in the Chukchi Sea reached an observed height of 9 m with a period of 9 seconds during a major storm in 1978 (Kalyasin, 1989). Probable maximum wave height that could form in the Chukchi Sea is 14 m (Kalyasin, 1989). Waves of this height can readily rework the sea bed over the entire shelf.

Water Masses

Three water masses have been defined on the northeastern Chukchi Sea. Water masses I and II (fig. 32) consist of water derived from the Alaska coast and the Bering Shelf without significant modification. Water Mass I is Coastal Water and has warm temperatures and lower salinities. Water Mass II is Chukchi Water with warm temperatures connected to the Coastal Water and bottom salinities of 32.0 to 32.2. Water Mass III has generally lower temperatures and slightly higher bottom salinities (Feder and others, 1989). Alaska Coastal Water is formed largely by river runoff along the Alaskan coastline. To the south it fills Norton Sound and hugs the coast in a narrow band from Nome through the Bering Strait along the northern edge of Chirikov Basin (fig. 33). Bering Shelf Water originates in Western Chirikov Basin during winter ice formation and abuts the Alaskan Coastal Water. It covers most of central Chirikov Basin.

Alaskan Coastal Water is the warmest and least saline of the three water masses (Coachman and others, 1975). It shows marked seasonal variations in salinity, particularly in Norton Sound where fluctuations in discharge from the Yukon River influence the

salinity. Temperature varies from less than 2 to 6°C (Drake and others, 1980) and salinity ranges from 14 to 31.5 parts per thousand (Nelson and others, 1981). Bering Shelf Water in the Chirikov Basin has a sharp boundary with Alaskan Coastal Water because it is much colder (0 to 4°C) and more saline (31.5 to 33 parts per thousand) (Coachman and others, 1975; Nelson and others, 1981).

Currents

Surface wind-generated currents, the shore-parallel geostrophic Alaska Coastal Current, and other geostrophic and baroclinic shelf currents erode and transport sediment, modifying the sea floor of the Chukchi Sea. The inshore currents are generated mostly by winds, whereas the offshore region is dominated by northeast- and southwest-directed storm related currents and by the Coastal Current System (fig. 11).

The predominant current system is the Alaska Coastal Current that flows northeastward along the eastern side of the Chukchi Sea, but wind-induced reversals in current direction are common (Mountain and others, 1976; Wilson and others, 1982; Aagaard, 1984; Hachmeister and Vinelli, 1985). Other shelf currents are found further offshore (fig. 11) (Coachman and others, 1975; Wiseman and Rouse, 1980; Feder and others, 1989). The northward flowing Bering Sea Water bifurcates near Point Hope, one part flowing to the northwest around the south side of Herald Shoal and the other forming the Alaska Coastal Current. The Alaska Coastal Current, which can be as narrow as 37 km, approaches the coast near Wainwright and Barrow. Surface velocities of up to 200 cm/s are reported for the Alaska Coastal Current southwest of Point Franklin (Hufford, 1977). Shore-parallel coastal currents with velocities of over 100 cm/s are common along the coast (Wilson and others, 1982; Aagaard, 1984; Feder and others, 1989). Southward-flowing clockwise gyres develop east of the Alaska Coastal Current north of the major promontories off Cape Lisburne, Icy Cape, and Point Franklin (Fleming and Heggarty, 1966; Sharma, 1979, Lewbel and Gallaway, 1984).

Current flow along the coastal region can at times be quite variable, with wind-induced reversals that can persist for several weeks (Aagaard, 1984; Hachmeister and Vinelli, 1985). Evidence of the southwest -directed currents was observed north of Wainwright in 1982 and off Icy Cape in 1985 where southwest -migrating large-scale bedform fields were observed at depths greater than 38 m. At shallower water depths, northeast-migrating large-scale bedform fields were found adjacent to the southwest-oriented bedforms, reflecting rapid sea-bed modification by the northeast-flowing Alaska Coastal Current (see Geologic Setting - section on *Gravel* below.

The tidal range is small, 10 cm or less, but major storm surges (up to 3.5 m) are reported at Barrow (Hunkins, 1965).

Storm Surges

Moderate storms that occur each fall in the northeastern Chukchi Sea result in changes in atmospheric pressure and wind velocity that can cause sea-level setup of 1 meter and fluctuations of bottom-current velocity of as much as 100 percent

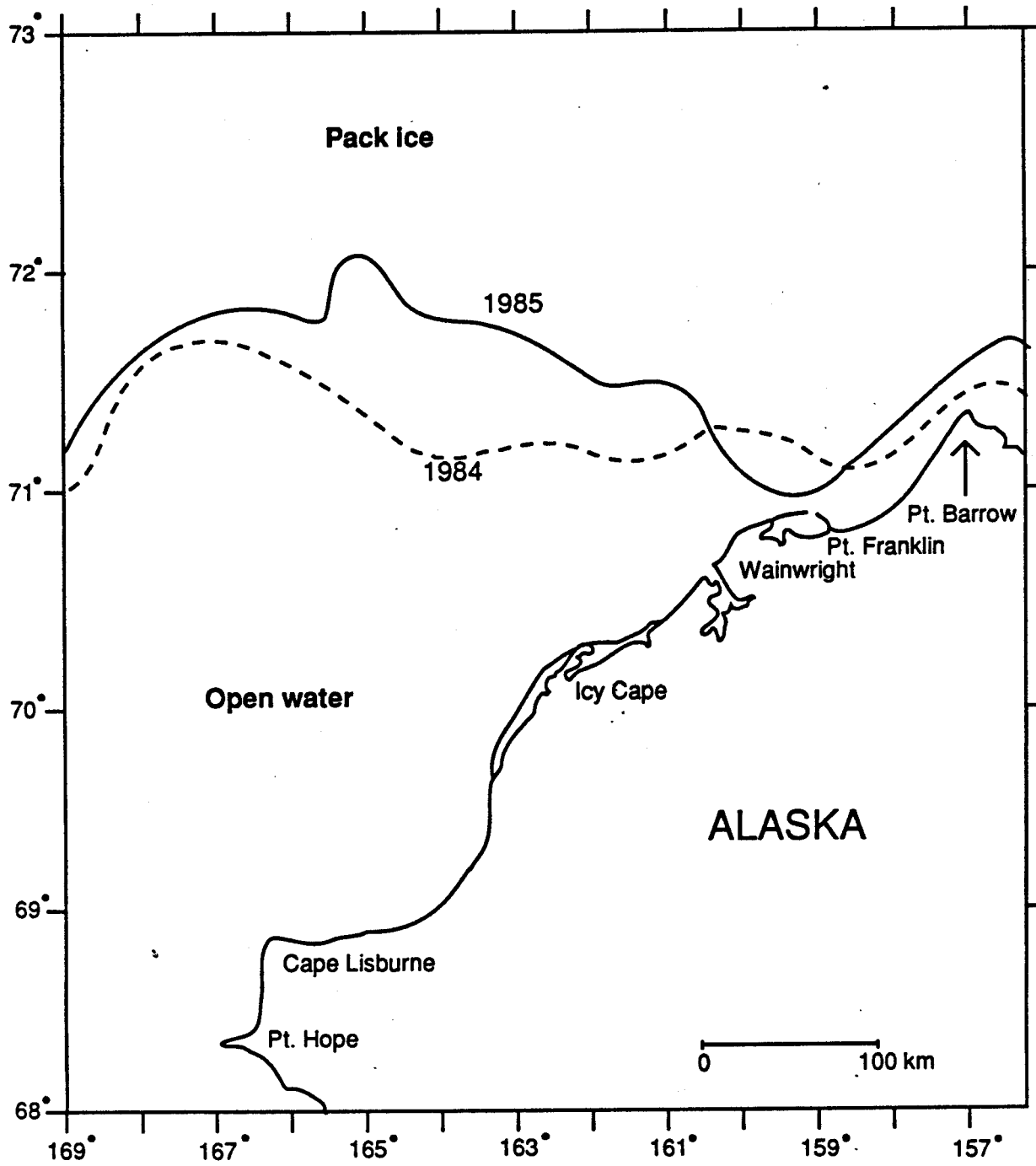

Figure 31. Approximate pack ice edges in the northeastern Chukchi Sea during 1984 and 1985 studies.

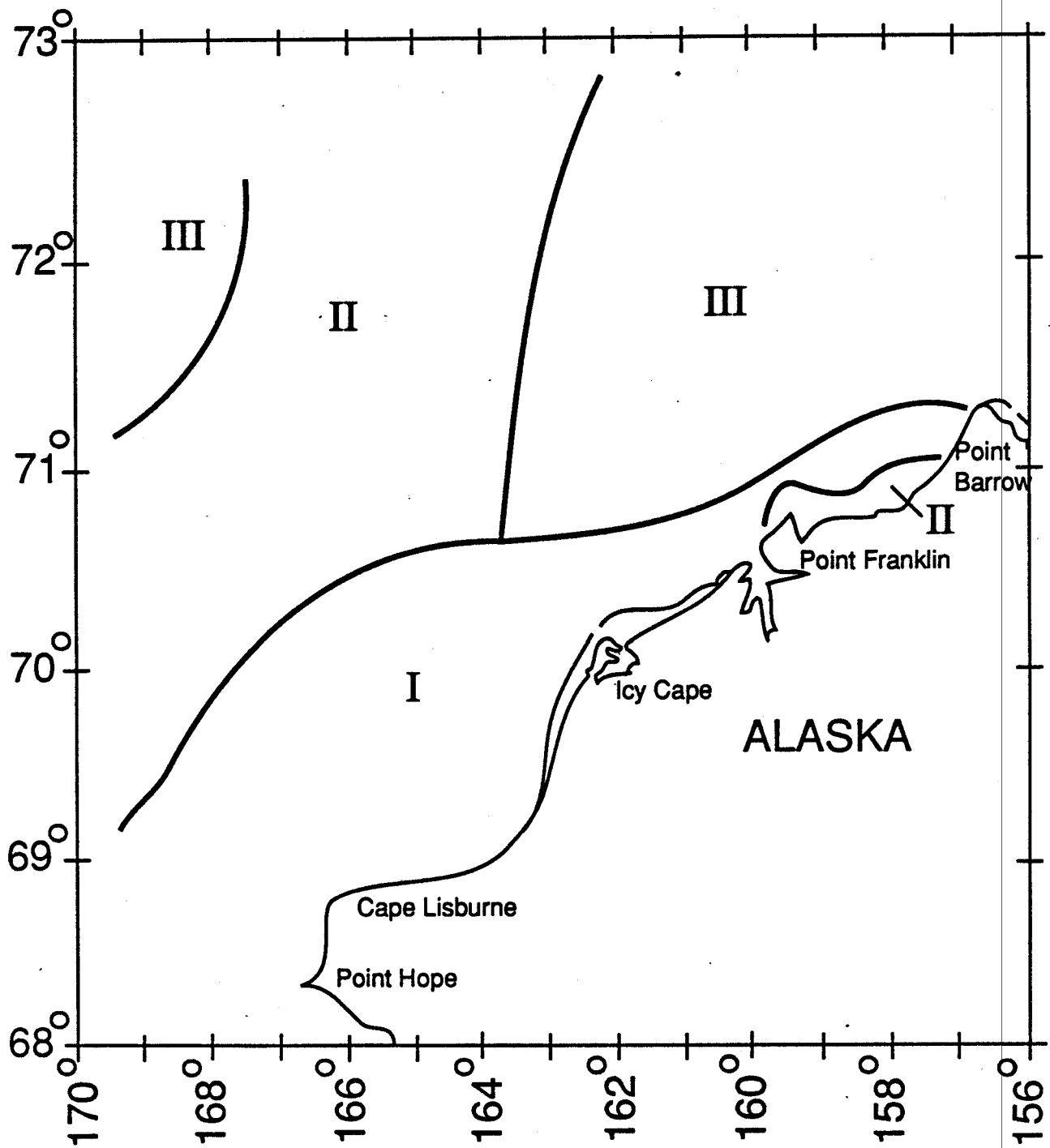

Figure 32. Chart of water mass groupings in the northeastern Chukchi Sea based on surface temperature and salinity cluster analysis (from Feder and others, 1989).

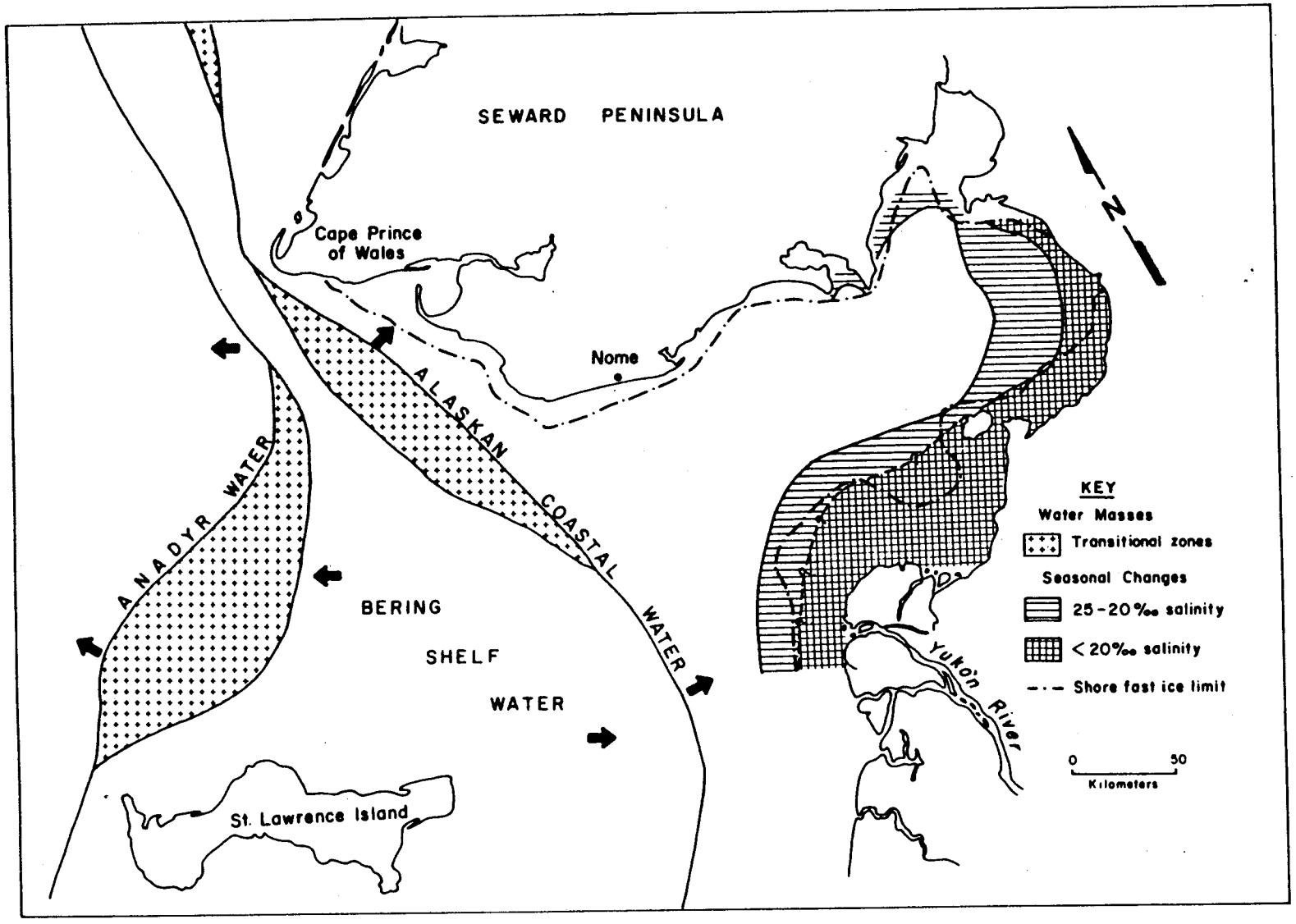

Figure 33. Water masses in the northeastern Bering Sea and southernmost Chukchi Sea (from Nelson and others, 1981).

over periods of a day or more (Coachman and Tripp, 1970; Schumacher and Tripp, 1979; Cacchione and Drake, 1982). Even under moderate storm conditions, wave-surge currents become important at water depths of 20-40 m encountered in the Chukchi Sea. A single storm event can modify the sea-bed, eliminating all traces of ice gouging at depths less than 18 to 20 m, can erode the sea-bed, producing gravel lag deposits, or, in strong storm events, can produce bedforms in gravel across the shelf (Phillips and Colgan, 1989).

Ice Regime

Ice covers the northeastern Chukchi Sea for 9 to 10 months every year with 2 to 4 months of open-water during the summer-fall season. Ice break-up occurs in southern Chukchi Sea in late May or early June and then there is a gradual northern retreat of the ice. During September to October, the Arctic pack ice reaches its maximum northern retreat, near 72 to 73 degrees. The pack ice then advances to the south and by January the entire Chukchi Sea is ice covered (Grantz and others, 1982). Nearshore, fast ice anchored to the shore forms and reaches its maximum development in March and April. Storms and winds from the northeast will move the pack ice to the west resulting in the formation of the persistent Chukchi Polynya along the eastern Chukchi coast usually by January (fig. 34) (Stringer, 1982; Groves and Stringer, 1991; Stringer and Groves, 1991). Generally, the regional pack ice drifts westward, however, currents and storms can readily alter ice drift directions (Stringer, 1978, 1982; Lewbel, 1984).

Sea ice plays an active role in the reworking and transport of sediment on the sea floor in the Chukchi Sea. The Arctic seasonal ice canopy can be divided into three distinct zones. Along the coast and extending from promontory to promontory is the quasi-stable fast-ice zone, that is often of uniform thickness. Immediately seaward of the fast-ice zone, local ice pressure and shear ridges develop in response to the interaction between the stationary fast ice and moving ice further offshore. The ice ridges in this zone are often grounded. However, the formation of the Chukchi Polynya parallel to the coast and the fast-ice boundary and overall westward pack-ice drift may limit ice gouging in this zone in the Chukchi Sea. Further offshore, pack-ice and ice ridges are essentially free to drift guided by winds and currents. Unequal pressure within the yearly ice pack gives rise to numerous pressure ridges of varying heights. Ice keels extend to varying depths beneath the pressure ridges in the ice canopy. When ice keels of sufficient draft are incorporated in the moving ice canopy, they can impinge on sea-floor sediment, forming linear plow marks or gouges. Within the Chukchi Sea, the Barrow Sea Valley allows deep draft ice (pressure ridges that formed in the Arctic Ocean or Beaufort Sea) to move onto the shelf where it grounds on the flanks of the sea valley.

Ice gouging in the Chukchi Sea is found to depths of 69 m on the west side of the Barrow Sea Valley west of Point Barrow (Reimnitz and others, 1984), which suggests that ice of sufficient draft could exist to gouge all depths of the sea bed in the Chukchi Sea. The number of ice-gouge events increases to the north (Toimil, 1978). Ice gouging generally increases with decreasing depths, with the maximum number of gouges found between

20 and 40 m (Barnes and others, 1984). In the Chukchi Sea, however, the ice gouge distribution in relation to depth shows an increasing number of gouges with decreasing depth, but also an increasing number of gouges at 44 to 48 m depth (fig. 35). The apparent increase in ice gouge abundance at 44 to 48 m depth reflects increased preservation potential of the gouges in this depth range. Gouges in deeper water are found mainly on the outer shelf within bathymetric highs covered with gravel. Up to 10 gouges per kilometer of sidescan trackline (an ice gouge in this study represents one ice impact with the sea floor and may contain numerous keels) are found in the gravel fields whereas the regions surrounding the gravel fields contain only one gouge per 5 kilometers of sidescan sonar tracklines on the outer shelf (Phillips and others, 1988) . The gravel is not transported and reworked as rapidly by storm-generated currents as is the mud blanket surrounding the gravel, thus ice gouges in gravel are preserved for longer periods of time.

The ice-gouge trends reflect ice movement from winds or currents moving ice within the Chukchi Sea. Ice-gouge trends summarized from Toimil (1978) show east-west to southeast-northwest oriented gouges in the northern shelf area including Hanna Shoal (fig. 36). These gouge trends probably reflect westward movement of pack ice by the westward-flowing Beaufort Gyre. Southwest-northeast trending gouges parallel the shore along the coast and within the Barrow Sea Valley. These gouges are produced by ice movement to the south as the pack ice advances south during the winter season. East-west trending gouges at Cape Lisburne and the outer shelf may reflect eastward movement of ice by storms from the west or southwest, or they may reflect wind-generated currents derived from the northeast. Ice will generally move 45 degrees to the right of the wind (Thorndike and Colony, 1982). The summer winds in the Chukchi Sea are from the northeast which should move ice to the west or northwest. These directions coincide with the pattern of ice-gouge trends observed in the Chukchi Sea from sidescan sonar records obtained during this study (fig. 37).

The highest gouge intensities are found on the east facing slopes of bathymetric highs and along the steeper slopes of the coastal margins (fig. 38). The bathymetric highs and inshore areas comprise a relatively small portion of the shelf area, yet are subject to higher gouge intensities. Areas lacking or containing low numbers of ice gouges are found between Icy Cape and Cape Lisburne (fig. 38). Toimil (1978) also reports low ice-gouge occurrence or a lack of ice gouging between these capes. Either rapid reworking of the sea bed by currents and filling in of the gouges has occurred or there is a low number of ice grounding events.

Although ice gouging is pervasive on the Chukchi shelf, away from bathymetric highs and near slopes, gouging is rare and gouge relief is low. Furthermore, in water deeper than 48 m, gouge relief is commonly subdued, which suggests that gouging is less important and that waves, currents, and biological activity are the dominant processes reworking the bottom sediment.

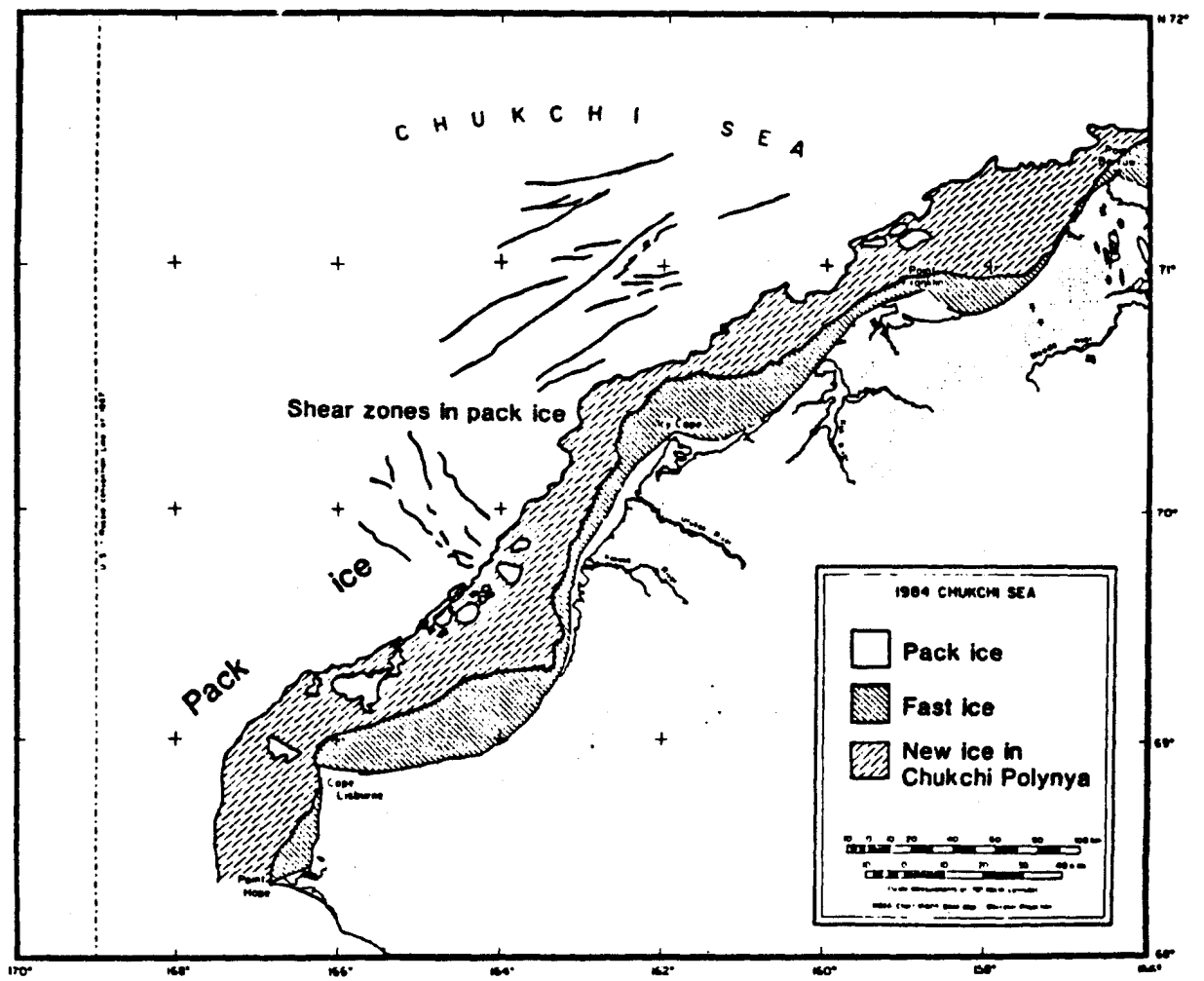

Figure 34. Ice zonation in the northeastern Chukchi Sea during March-April, 1983. The ice field boundaries are from 1983 satellite photos. The maximum extent and development of the shore-fast ice occurs during this period. Storms from the northeast form the Chukchi Polynya separating the fast ice from the offshore pack ice.

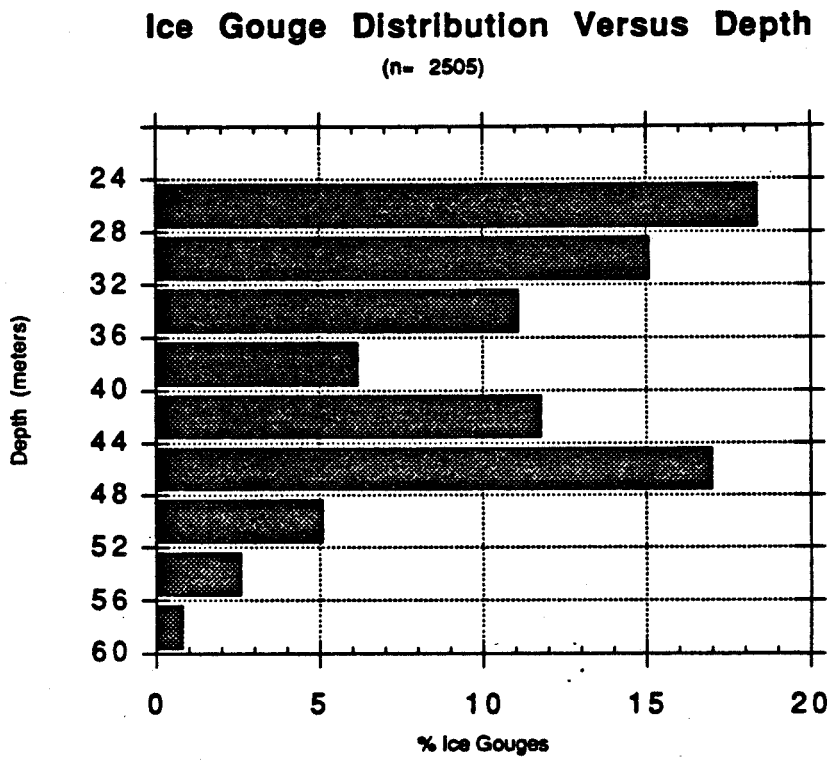

Figure 35. Ice gouge distribution in relation to water depth for the northeastern Chukchi Sea. Ice gouging of the sea floor generally increases with decreasing water depths. The increased gouging between 40 and 48 m depth reflect preservation of ice gouges on the outer shelf gravel fields where the coarse-grained sediment is only periodically transported resulting in preservation of ice gouging for much longer periods of time compared to the muddy sediment surrounding the gravel fields where the gouge traces are rapidly filled.

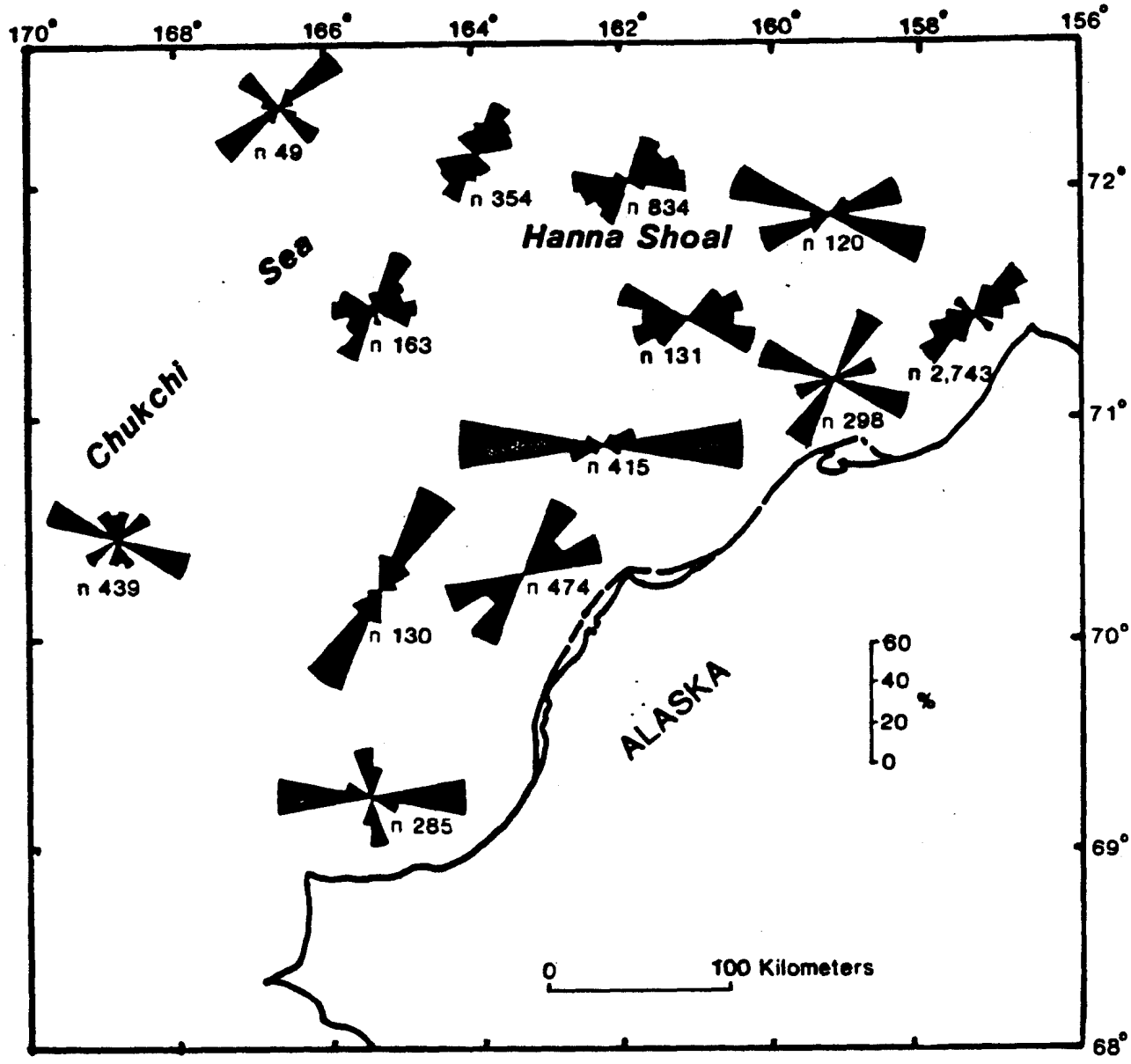

Figure 36. Rose diagram of ice gouge orientations in the northeastern Chukchi Sea. Data summarized from Toimil (1978).

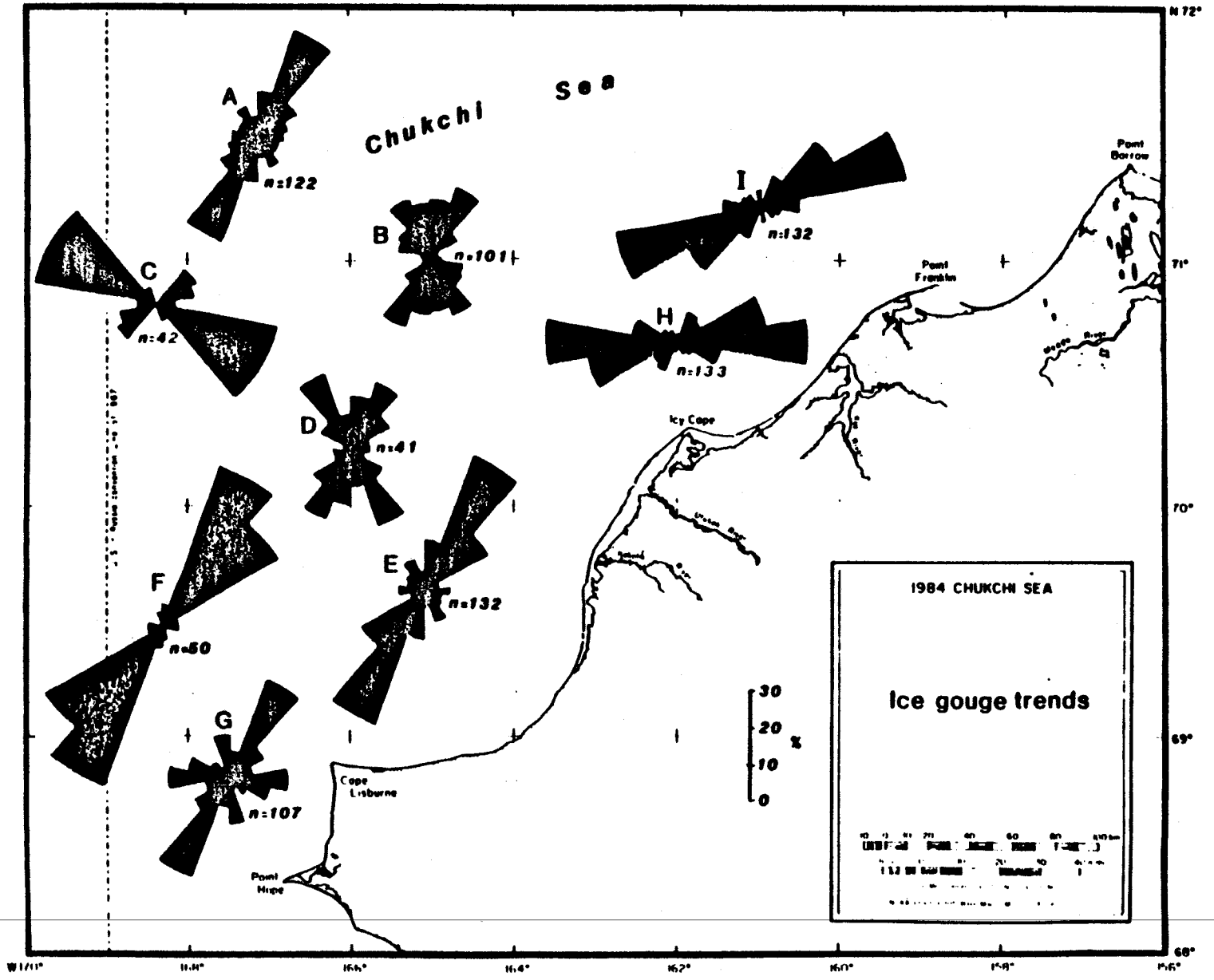

Figure 37. Rose diagram of ice gouge orientations in the northeastern Chukchi Sea from 1984 data.

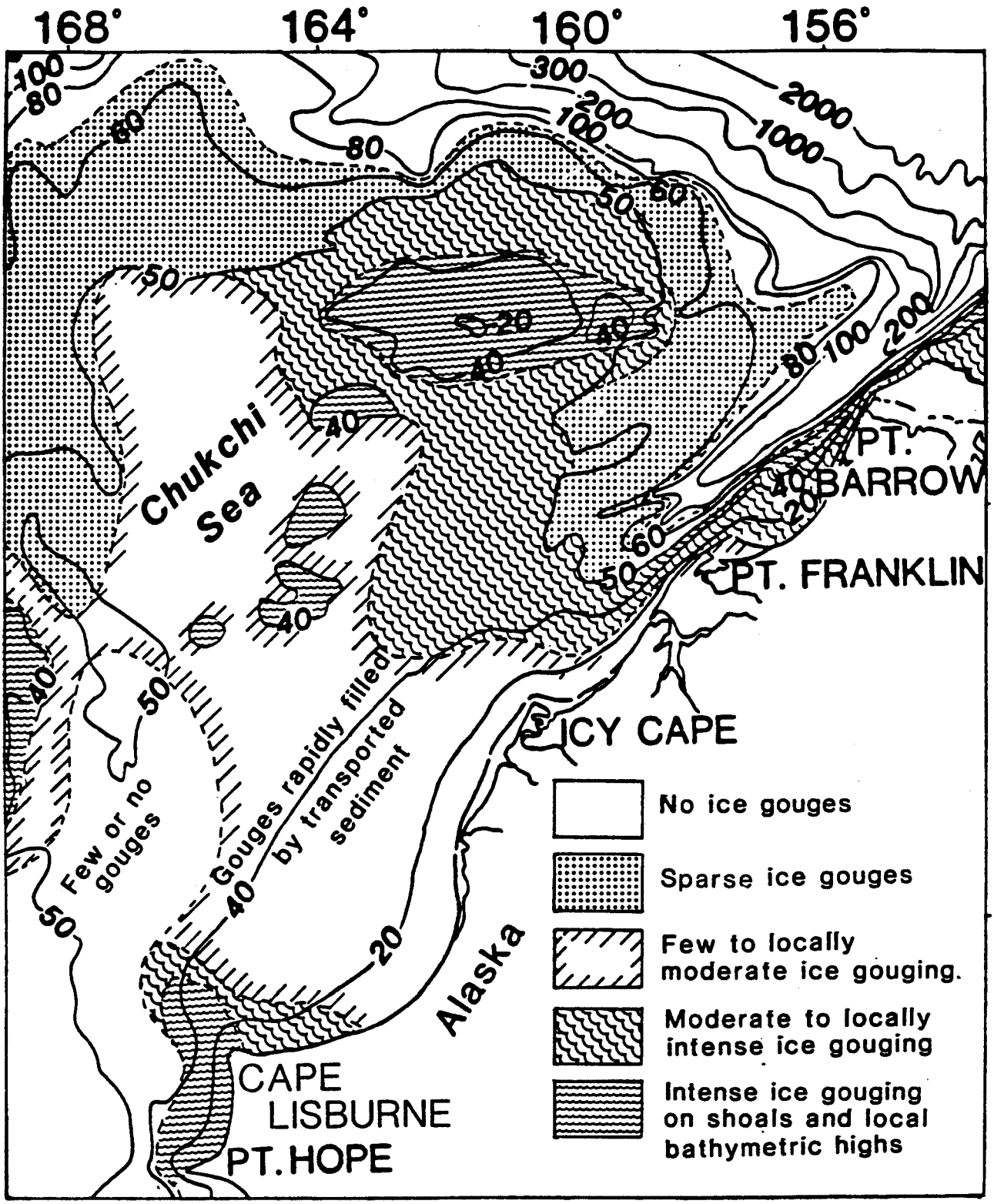

Figure 38. Ice gouge intensity map of the northeastern Chukchi Sea. Modified from data of Toimil (1978) and Grantz and others (1982).

Stratigraphy

For much of the shallow strata in the Chukchi Sea bedrock lies near the sea floor, indicating an erosional history. A thin sediment cover (tens of cm inshore to several m offshore) of marine Holocene transgressive deposits overlies either nonmarine Pleistocene deposits, marine Miocene to Pliocene strata, or gently folded nonmarine Cretaceous consolidated sediment in the central part of the Chukchi Sea (Phillips and Colgan, 1987b). The total Quaternary sediment cover is also thin, between 0.5 and 12 m in thickness.

The oldest strata penetrated by a series of vibracores on the Chukchi Sea shelf consists of late Cretaceous (92 to 95 Ma based on K-Ar ages) nonmarine silt and clay containing organic-rich beds interbedded with vitric to crystalline tephra (figs. 39, 40) (Phillips and others, 1988) . The presence of this overconsolidated Cretaceous strata in the central part of the Chukchi Sea suggests that it has an extensive erosional history with limited sediment deposition. Marine pebbly mud to pebbly sand of probable Miocene-Pliocene(?) age overlies the Cretaceous strata. A nonmarine unit of late Quaternary age (11,000 to 11,300 yr B.P. based on ^{14}C ages from peat) consists of iron-stained sand, gravel, and peat beds containing insects and nonmarine ostracodes. It forms a thin to thick, discontinuous deposit overlying Cretaceous tephra or Miocene-Pliocene strata. A Holocene marine transgressive sequence ranging from 0.5 to 4.4 m in thickness and consisting of a basal gravel lag which changes vertically to sand and mud may overly any of the lower units.

Surface Sediment Distribution

The distribution of relict and modern sea-floor sediment in the northeastern Chukchi Sea is patchy and is dependent upon current patterns and velocity. The surface-sediment distribution has been outlined by Creager and McManus (1967) and summarized by Grantz and others (1982), Lewbel (1984), Naidu (1988), and Feder and others (1989). The most detailed sediment distribution maps for the northeast Chukchi Sea are found in Naidu (1988). We have summarized and simplified the surface-sediment distribution in the Chukchi Sea in order to establish major sea-floor substrate and infaunal areas that relate to feeding grounds for gray whales and walrus. Sonographs, television and camera surveys, bottom sampling, and previously published data were used to define the major textural areas (fig. 9).

The three major surface-sediment areas identified and defined by Feder and others (1989) are: 1) an inner-shelf zone characterized by surficial gravel lag deposits that range from gravel to muddy gravel, and a sand belt that varies from slightly gravelly sand to sand and to muddy sand (classification of Folk (1980)), 2) an outer-shelf region containing scattered surficial deposits of muddy gravel, gravelly mud, or gravelly muddy sand; and 3) a thin to thick mud blanket in the northwest and northern parts of the Chukchi Sea.

Gravel

Storm-generated currents and the Alaska coastal current erode the sea-bed to form extensive gravel bedform patches as well as superficial gravel lag deposits in the northeastern Chukchi Sea. Gravel-covered regions are located on low relief bathymetric highs on the outer shelf, off the major shoals, or where active coastal shelf currents erode the sea bed. Nearshore, from Pt. Hope to south of Icy Cape and between Icy Cape and Pt. Franklin, gravel to muddy gravel characterizes the sea bed (fig. 9) (Naidu, 1988; Phillips and others, 1988). The largest gravel field is located in the head of Barrow Sea Valley starting at depths of 42 m to the south of Icy Cape and extending north at least 165 km to 85 m depth in the coastal-current-dominated inner shelf. Flat-bedded gravel lags, up to 15 cm thick, composed of clasts up to 24 cm, characterize the sea bed (Phillips and others, 1988). Gravelly sand, muddy sandy gravel and muddy gravel ranging from 9 to 32 percent gravel characterize the inner-shelf gravel fields (figs. 41, 42).

Seaward of the coastal-current-dominated inner shelf and up to 240 km from shore (between 29 and 50 m water depth) gravel occurs in scattered small to large patches, as much as 28 km in length, that are separated by mud-floored areas (fig. 9). Muddy gravel containing up to 76 percent gravel characterizes the outer shelf (Phillips and Colgan, 1989). Local bathymetric highs are usually covered with gravel. The outer-shelf gravel deposits can be from 15 cm up to 1.5 m thick based on gravel recovered inboxcores and a vibracore (Phillips and Colgan, 1989). The clasts are somewhat smaller than the inner-shelf gravels, and are up to 11.5 cm. NNE-SSW-trending gravel bedforms, with relief less than 20 cm high and wave lengths of up to 2.5 m are found on most of the outer-shelf gravel fields (fig. 43). One storm event, apparently from the west or northwest during summer open water conditions, may have formed the gravel bedforms in the outer shelf.

Sand

From north of Cape Lisburne to north of Pt. Franklin, slightly gravelly sand to muddy sand forms a northeast-trending textural band seaward of the coastal gravel fields (fig. 43). Underlying the coastal-current-influenced areas, where gravel is not present, there are rare sand banks, actively migrating small-scale bedforms, or sandwave fields composed of 2- and 3-dimensional bedforms (fig. 43). To the west of the active bedforms, the sand grades to muddy sand and gravelly muddy sand forming a band that trends north to Hanna Shoal. In the northeastern flank of this muddy sand belt, gravel bounds the eastern flank along the west side of the Barrow Sea Valley. The sand percent generally decreases to the west from 99 percent in the active bedform fields underlying the coastal current to 50 percent on Hanna Shoal (fig. 44). Grain size analysis of the sand fraction from six samples taken from Icy Cape to north of Point Franklin and from two samples on the western flank of the Barrow Sea Valley gravel field (figs. 45-47) shows that the sand fraction is in the fine sand textural class. The northeasternmost sample exhibited the finest texture. The highest amphipod abundance and

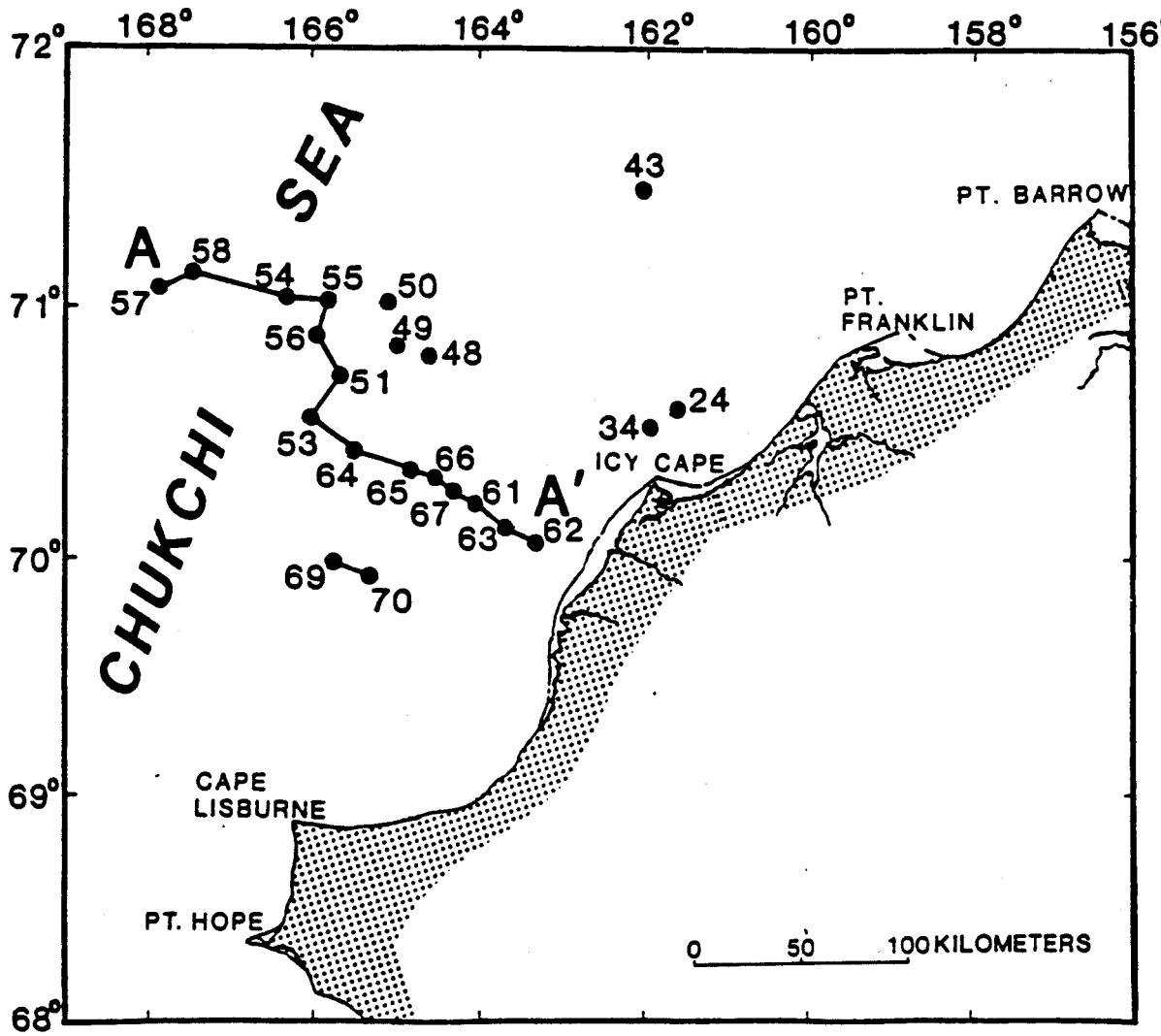

Figure 39. Vibracore locations in the northeastern Chukchi Sea.

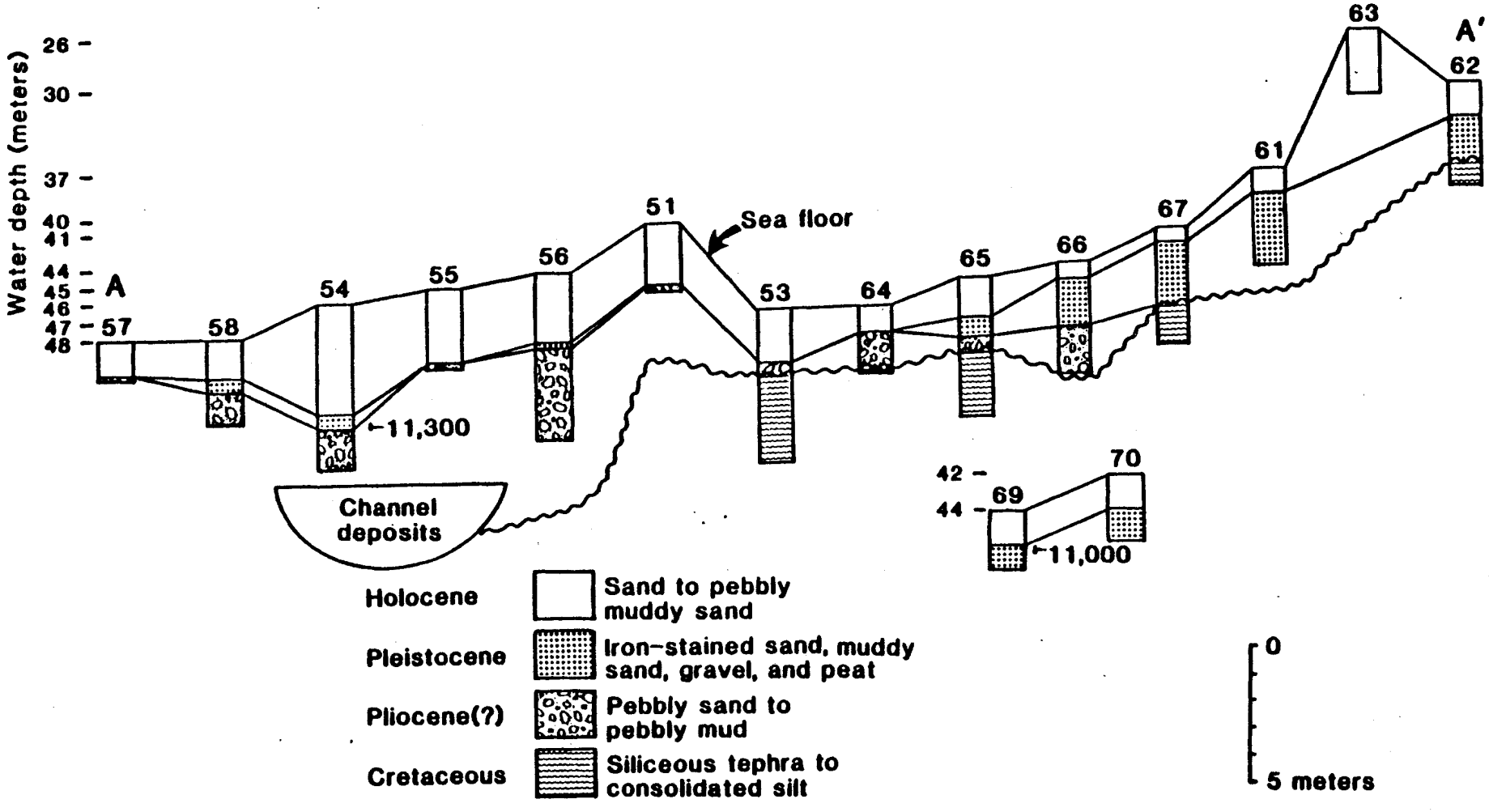

Figure 40. Stratigraphic units identified in vibracores from the northeastern Chukchi Sea. Sea figure 39 for core locations.

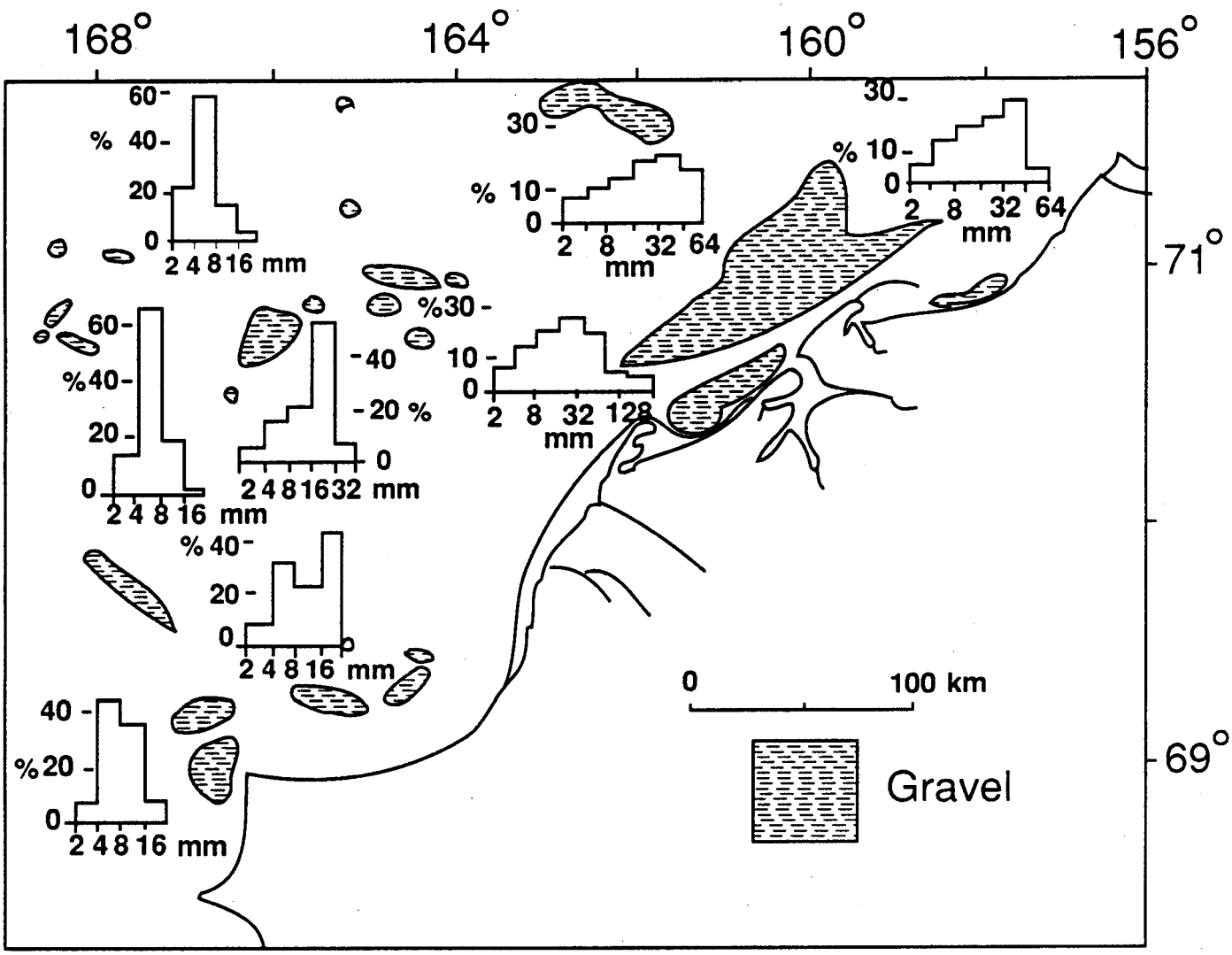

Figure 41. Gravel size distribution in surface sediments for coastal and offshore regions in the northeast Chukchi Sea.

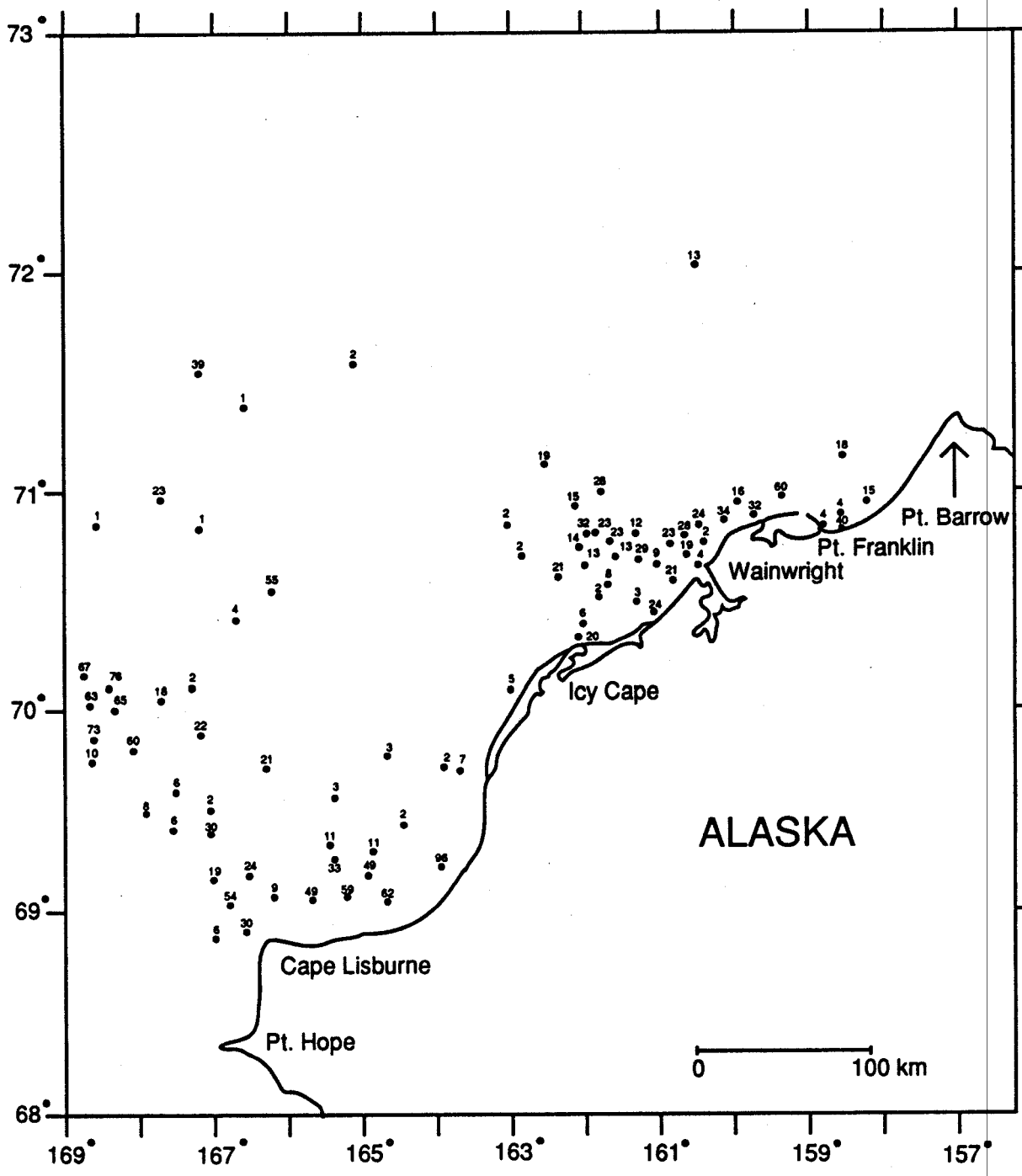

Figure 42. Percent gravel in surface sediments of the Chukchi Sea. Data from Barnes, 1972, Feder and others, 1989, and from our 1981, 1982, 1983, 1984, and 1985 studies in the Chukchi Sea.

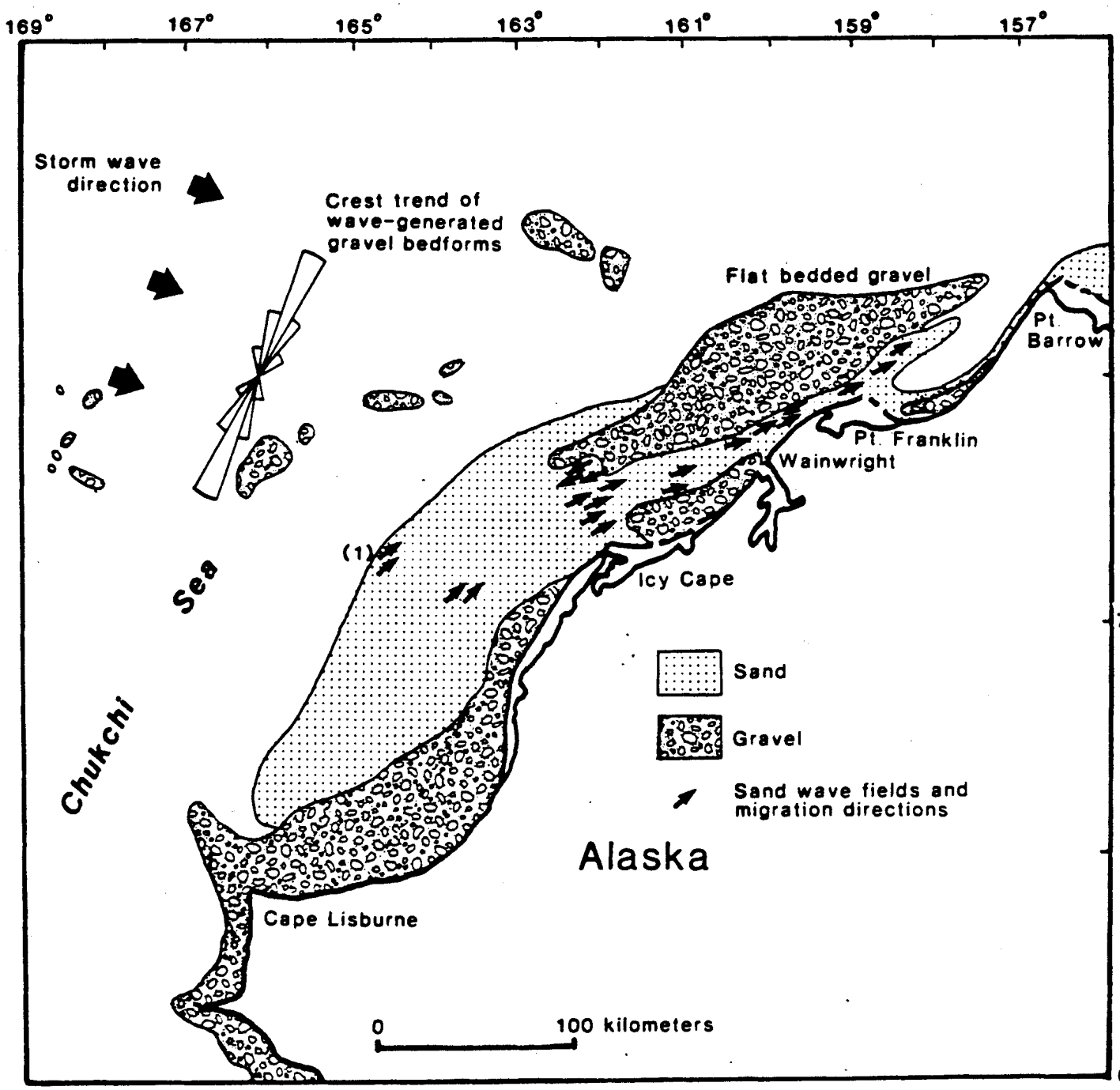

Figure 43. Bedform fields in the northeast Chukchi Sea. Large-scale bedforms exist beneath the northward flowing Alaska Coastal Water increasing in abundance where the currents approach the coast north of Icy Cape, small-scale bedforms (ripples) are observed by camera and Television in areas not containing large-scale bedforms. Reversing, southeast-directed bedforms were found north of Icy Cape and northwest of Wainwright. The offshore gravel fields contain northeast-southwest oriented crests of gravel bedforms probably produced by one storm event from the northwest or west. (1) Data from Toimil (1978).

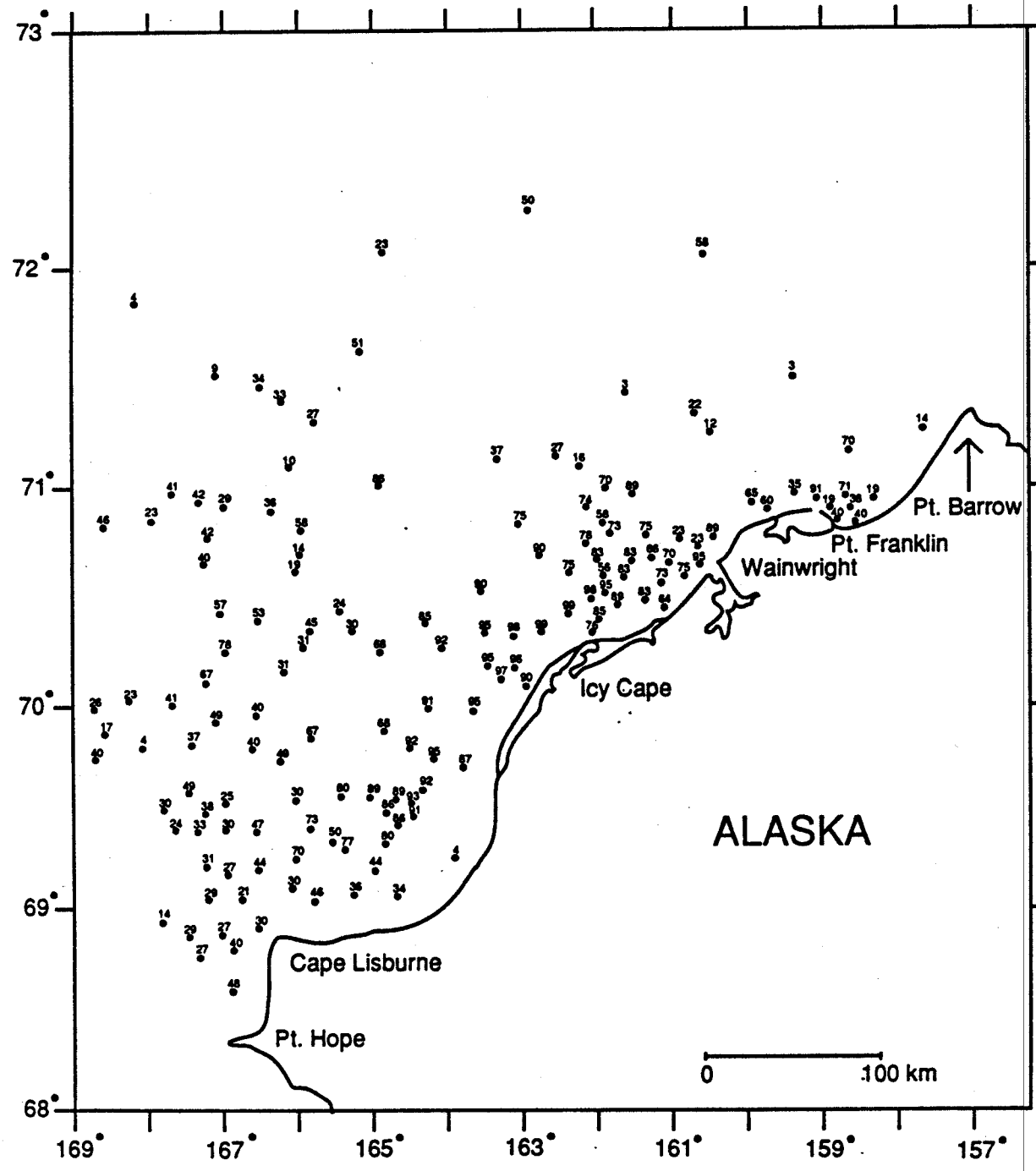

Figure 44. Percent sand fraction in surface sediment from the Chukchi Sea. Data from Barnes (1972), Feder and others (1989), and from our 1981, 1982, 1983, 1984, and 1985 studies in the Chukchi Sea.

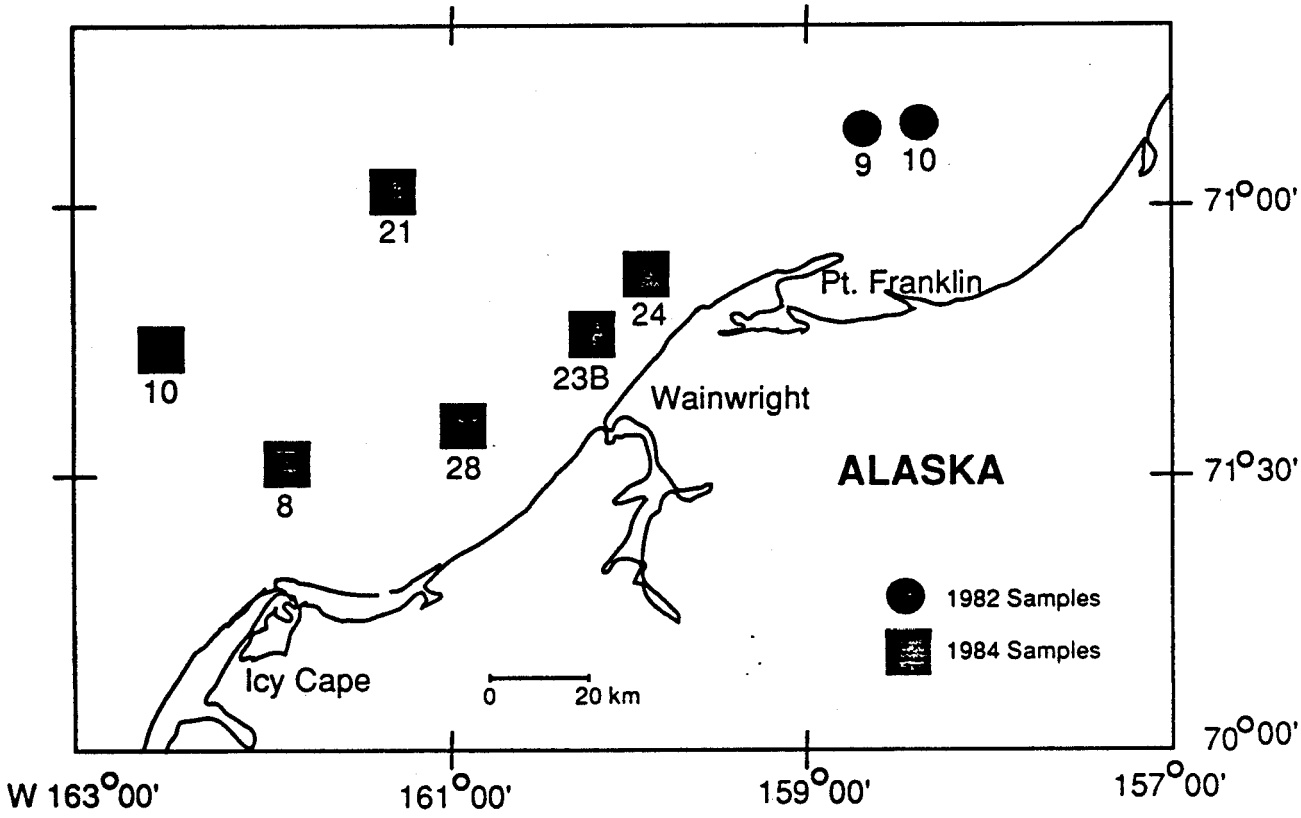

Figure 45. Sample locations for grain size analysis of sand fraction.

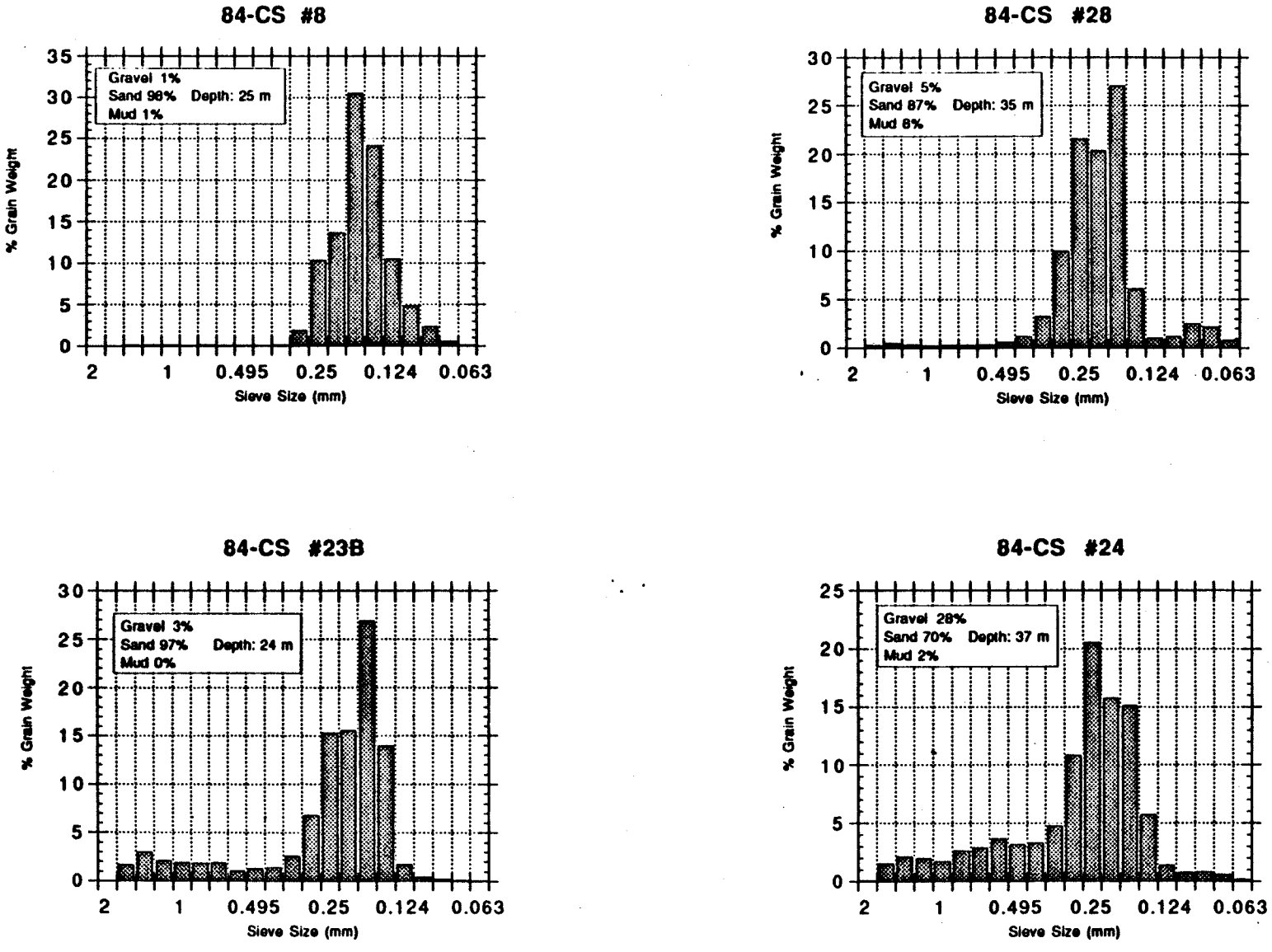

Figure 46. Grain size data. Core 8 from sand wave field north of Icy Cape. Core 28 from rippled sand belt west of Wainwright. Core 23B obtained northwest of Wainwright where gray whales were feeding. Core 24 from the western edge of the coastal sand belt.

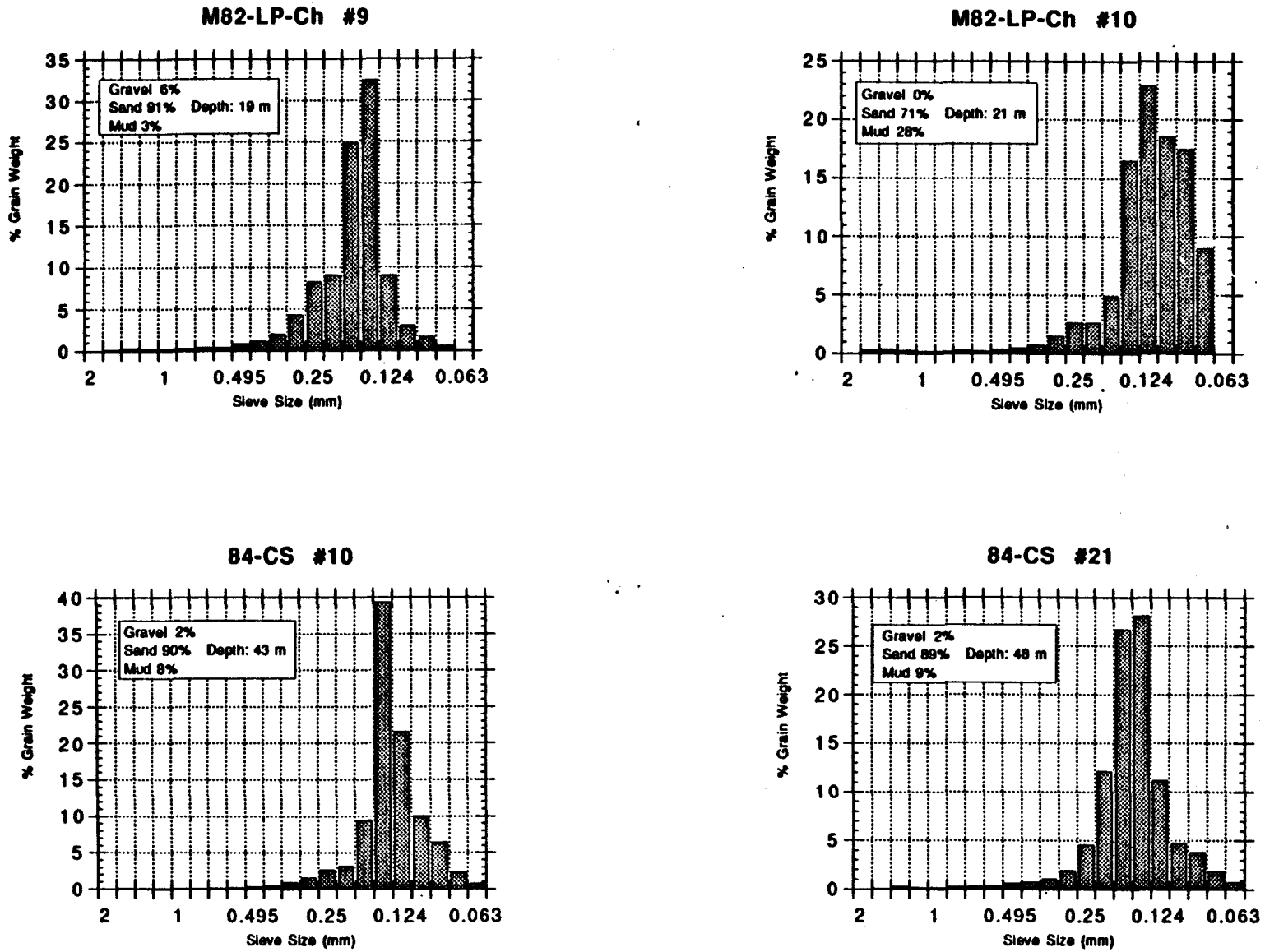

Figure 47. Grain size data. Core 9 from sand wave field north of Point Franklin where gray whales feed. Core 82-10 from northeast flank of sand wave field north of Pt. Franklin. Cores 84-10 and 84-21 obtained in muddy sand west of the gravel field in the Barrow Sea Valley.

feeding by gray whales is observed in the areas where these samples were obtained (figs. 45-49) (Table 1) (Phillips and Colgan 1987a, Feder and others, 1989).

Mud

Sandy mud to slightly gravelly sandy mud is the common texture on the outer shelf of the Chukchi Sea (fig. 8). Up to 4 cm of mud blankets the offshore gravel fields. Away from the gravel fields a 20-to-30 cm-thick mud blanket grades into fine sand. Intense bioturbation (anemone burrows up to 1.5 m in length) has thoroughly mixed the upper sediment beds in the outer shelf. This suggests that sedimentation rates are low and that biological processes dominate over physical processes in the outer shelf regions.

BIOLOGIC SETTING

The northeast Chukchi Sea is an area of locally rich macrobenthic communities of higher diversity and higher density than regions on the outer shelf to the northwest. The productivity levels are lower in the Chukchi Sea than to the south in the Bering Sea (Truett, 1984). In response to the rich benthic food resources, large populations of walrus, bearded seals, and gray whales seasonally inhabit the Chukchi Sea. The dominant benthic organisms in the northeast Chukchi Sea are crustaceans, annelids, mollusks (bivalves) and amphipods, particularly the tube-dwelling ampeliscid amphipods. Siphunculids, clams, sea cucumbers, and sand dollars were also generally dominant in the biomass (Feder and others, 1989). These benthic communities are associated with specific substrate texture that in turn is controlled by general sedimentation processes.

Feder and others (1989), have made the most comprehensive, but still generally limited, quantitative studies of the benthic communities in Chukchi Sea. Using cluster analysis, they recognized four major macrofaunal communities based on substrate texture, sediment water content, and sediment accumulation rates (fig. 9) (Table 1). Group I, located west of Cape Lisburne to Icy Cape on the outer shelf and north of Point Franklin contains a mud-sand-gravel texture with a water content of 20 to 40 percent. The ampeliscid amphipod *Byblis gaemardi* and the barnacle *Balanus crenatus* are the dominant species. Group II occupies the outer-shelf regions north of approximately 71° N latitude. This fauna, associated with a muddy substrate containing 45 to 60 percent water content, is dominated by the tube-dwelling polychaete *Maldane glebefex* and the pelecypod *Nucula bellotte*. Group III is characterized by a sandy substrate with 15 to 20 percent water content. The dominant fauna include *Balanus crenatus* and amphipods (including the large ampeliscid *Ampelisca macrocephala*). Group IV contains a sandy-gravel substrate with less than 20 percent water content. The sand dollar *Echinarachnius parma* and bivalves (the cockle *Cyclocardia rjabininae*) thrive in this environment. Suspension feeders dominate the inner-shelf regions where extensive gravel lag deposits and migrating bedforms exist from Cape Lisburne to north of Point Franklin. They are also abundant in the shallow water areas on Hanna Shoal, whereas

deposit feeders characterize the offshore regions of the northeastern Chukchi Sea (Feder and others, 1989).

Our summary of textural and biological data obtained from serial box cores in 1985 (Appendix 1) generally agrees with the biofacies identified by Feder and others (1989). We recorded some minor variations in the areal distribution of the coastal benthic communities however, based on our analysis of sea floor texture which was done using sonographs, serial box cores, and photographs. Group IV would extend from north of Cape Lisburne, narrow at Icy Cape and continue north beyond Point Franklin following the north-trending belt of sand (fig. 9). Abundant sand dollars (*Echinarachnius parma*) up to 200 per square meter, are usually associated with small- to large-scale bedforms or flat sand surfaces throughout this area (figs. 50-53). Brittle stars (*Ophiura sarsi*) or sea stars inhabit the western (low energy) flank of this facies (fig. 53A). The transition from Group IV to Group III (gravel to sand) communities can be abrupt or gradational (fig. 54). The gravel fields both in the coastal region (figs. 55-57) and in the outer shelf (fig. 58) contain a similar rich benthic community dominated by barnacles and bryozoans. The muddy sea bed in the offshore areas contains either abundant gastropod tracks and trails (fig. 59A) or abundant brittle stars and anemones (figs. 59B, 60).

Areas dominated by the tube-dwelling ampeliscid amphipods show a definite association with the Bering Sea Water to the south in the Chirikov Basin (Nelson and others, 1981) and north of 70° 30' in the inshore region of the northeastern Chukchi Sea where the Bering Sea Water approaches the coast north of Icy Cape (Feder and others, 1989). Grain size in the area from Icy Cape to Point Franklin (figs. 46, 47) is in the fine sand range, which is the preferred substrate for the ampeliscid amphipod's habitat. Feder and others (1989) show high concentrations of amphipod abundance in four stations (fig. 8) (Table 1, see sections 5,6,7, and 17) where we have observed gray whales feeding.

Because of limited sampling around Hanna Shoal, we are not able to establish the distribution of amphipod communities in this region. A box core taken in 1988 on the west flank of Hanna Shoal in muddy fine sand (50 percent sand) contained abundant (>1200 individuals/m^2) tube-dwelling amphipods (fig. 10). Observations of gray whales, both swimming and feeding on Hanna Shoal in 1989 (fig. 48, 49) (Moore and Clarke, 1990) suggest that the amphipod communities may be more extensive. The presence of ice cover over Hanna Shoal, as in 1984 and 1985, may allow the growth of benthic communities which can only be exploited by gray whales when ice retreats north of the shoal, as was the case in 1986.

The amphipod *Ampelisca macrocephala* is the main prey species of the gray whale in Chirikov Basin to the south (Rice and Wolman, 1971) and also most likely in the northeast Chukchi Sea. Ampeliscid amphipods are detritus feeders that build narrow, V-shaped, mucus-lined tubes. When the population of amphipods becomes large, the densely packed tubes coalesce and create extensive mats that stabilize the surface of the sediment. The dense tube mats which are common in the Chirikov Basin are not common in samples taken in the Chukchi Sea. Stoker (1978, 1981) calculated an average total biomass of 533 g/m^2 (his group IA,

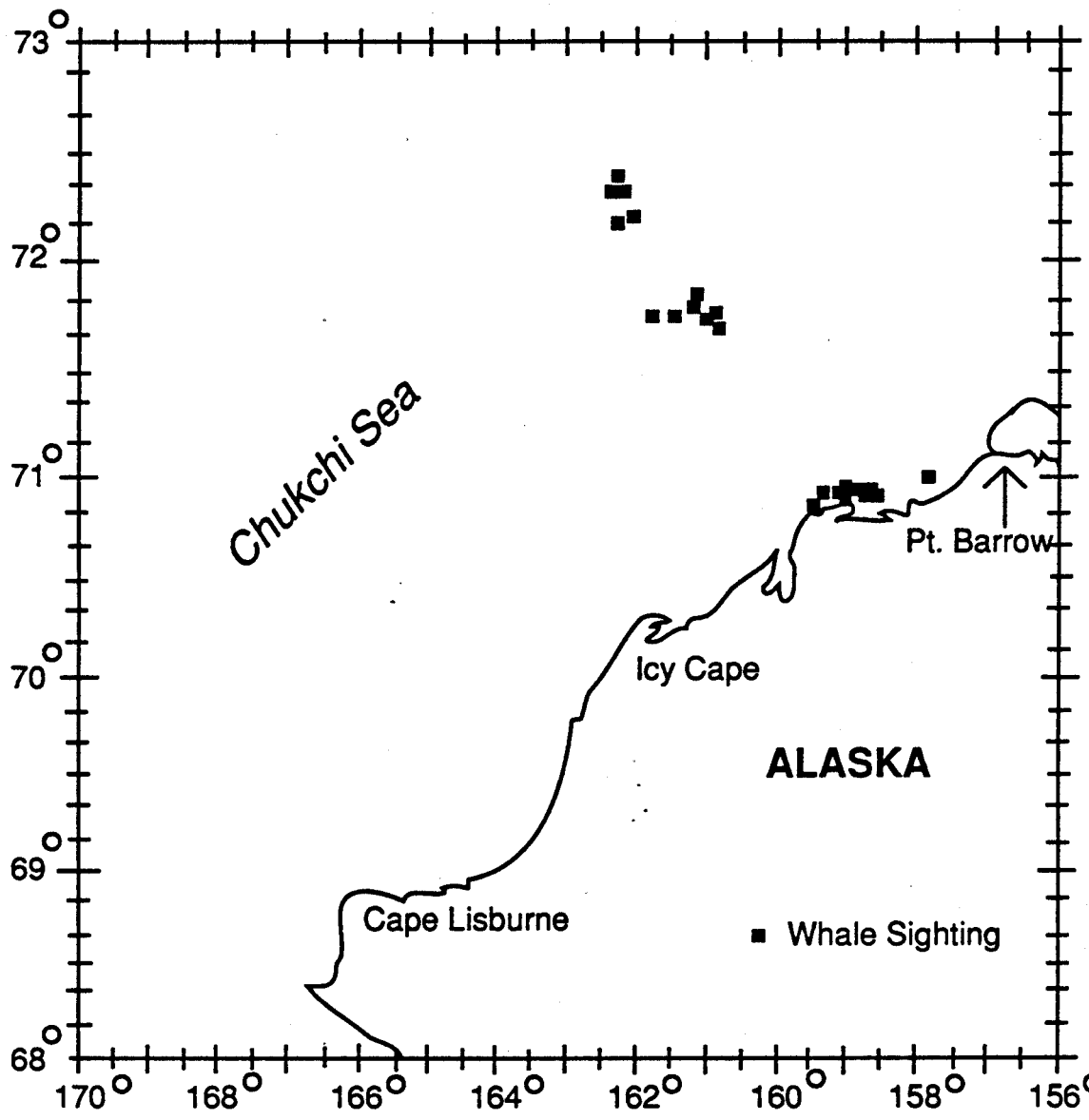

Figure 48. Distribution of sightings of gray whales in the Chukchi Sea from September through October, 1989. Data from Moore and Clarke, 1990.

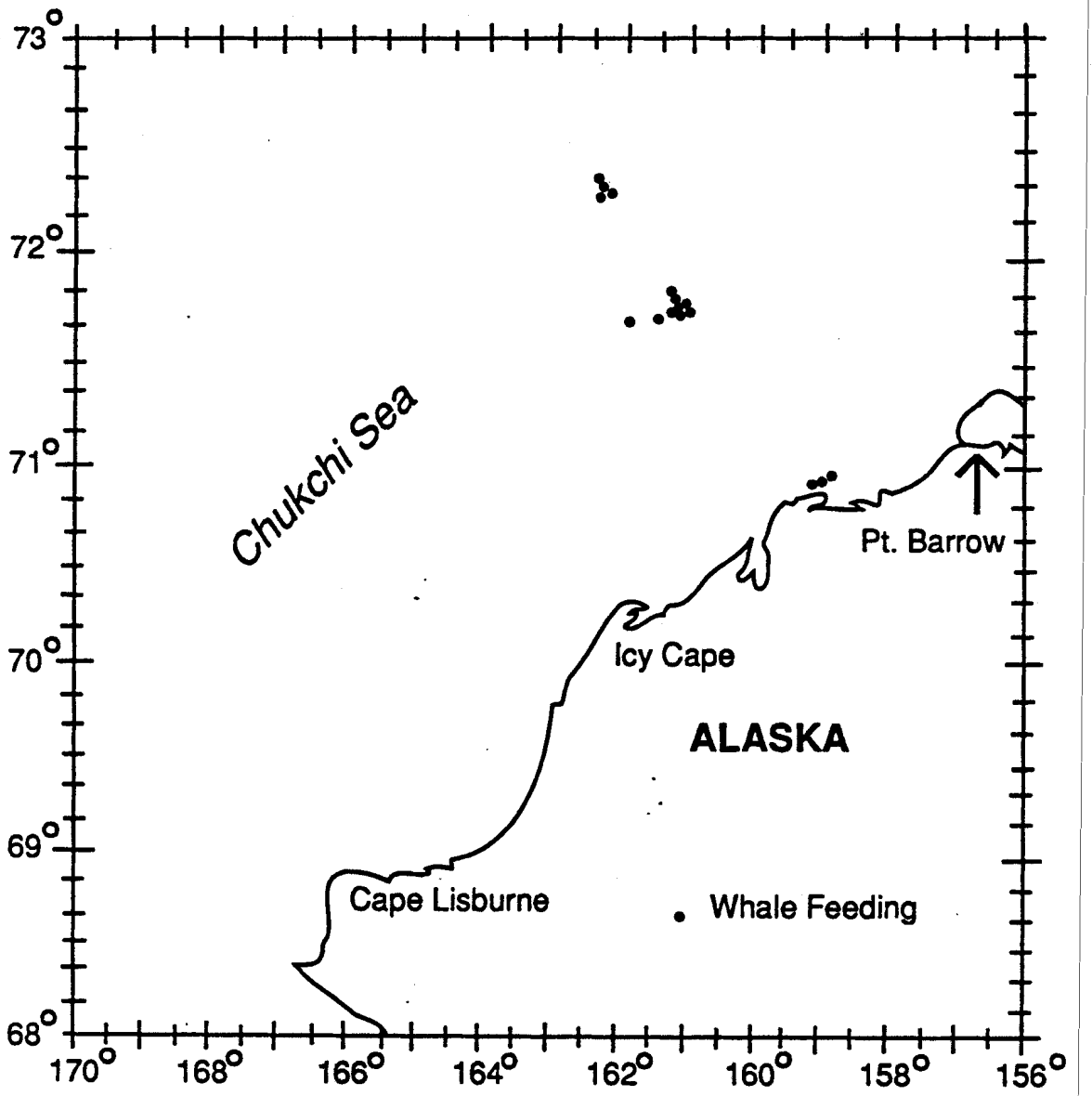

Figure 49. Distribution of gray whales observed feeding in the Chukchi Sea from September through October, 1989. Data from Moore and Clarke, 1990.

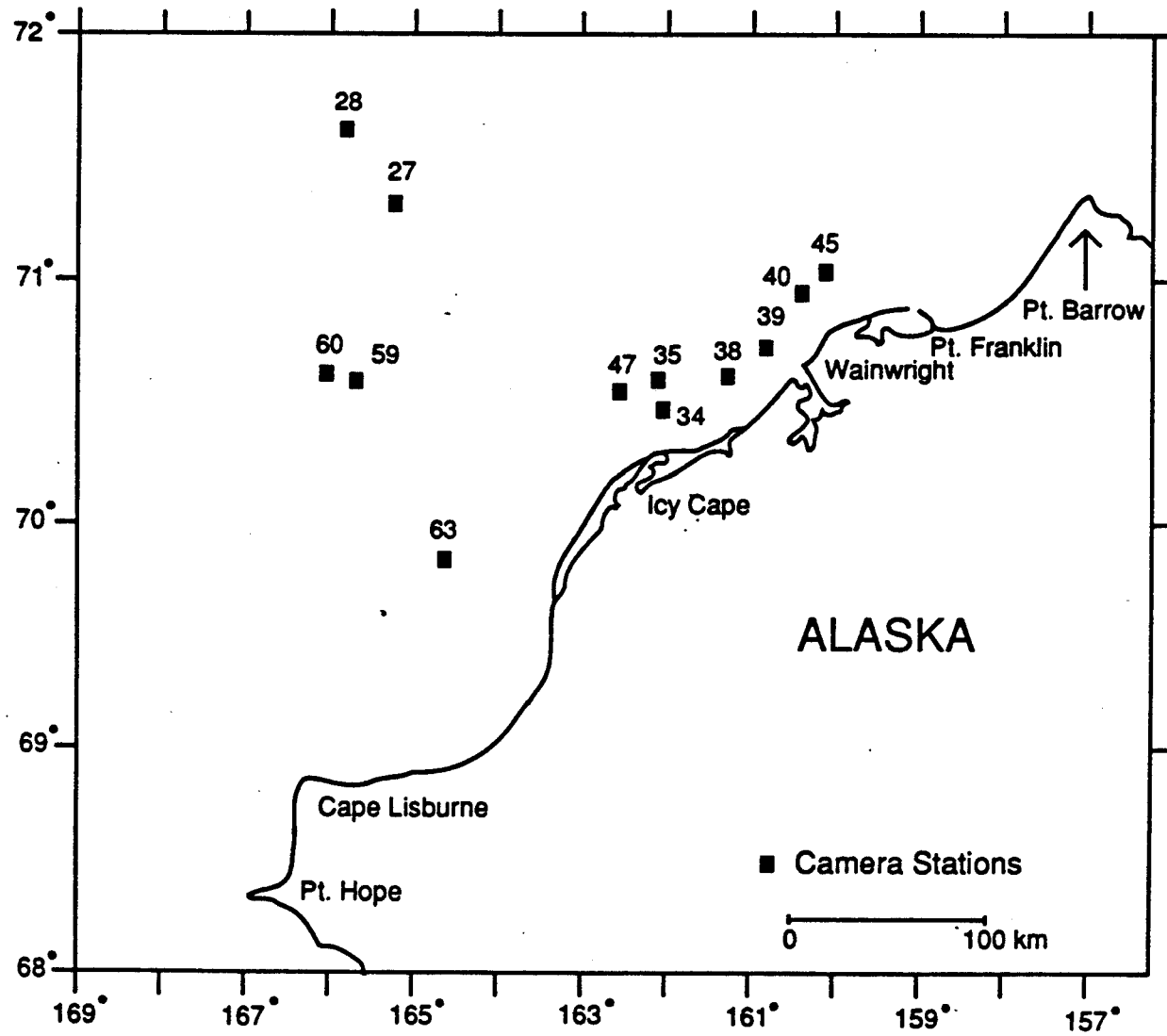

Figure 50. Camera stations taken in 1985 in the Chukchi Sea.

Figure 51. Station 63, 28 m depth

A. Sea floor photograph of sand facies containing abundant sand dollars (*Echinarachnius*) and brittle stars.

B. Photograph of small scale bedforms within the coastal sand facies. The scale bars are 5 cm.

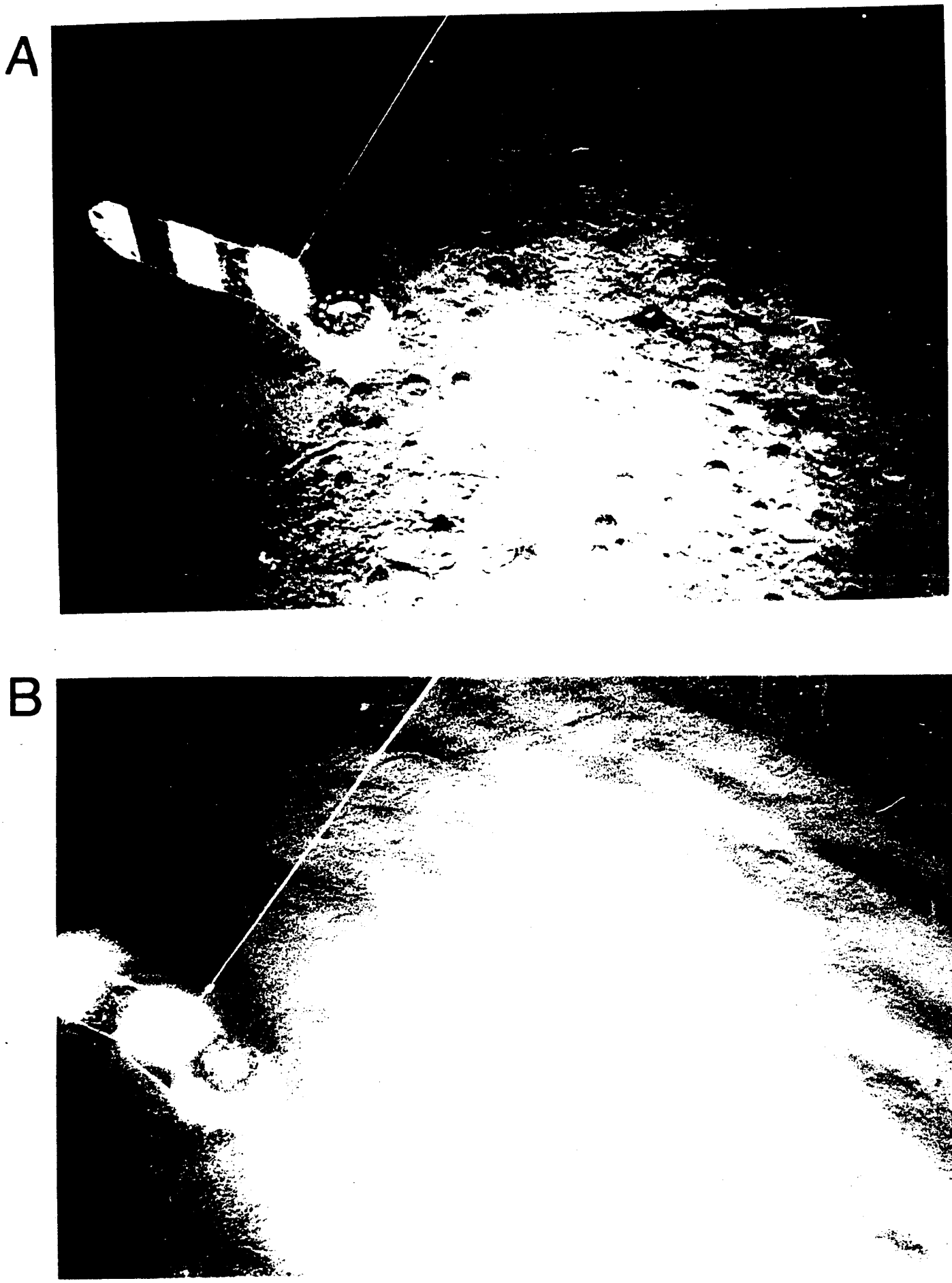
A
B

Figure 52.

A. Station 35, 41 m depth. Photograph of small scale sand waves containing abundant sand dollars, shell debris, and cobbles in the bedform trough regions.

B. Station 34, 26 m depth. Photograph of small scale sand waves and abundant sand dollars. Scale bars are 5 cm.

A

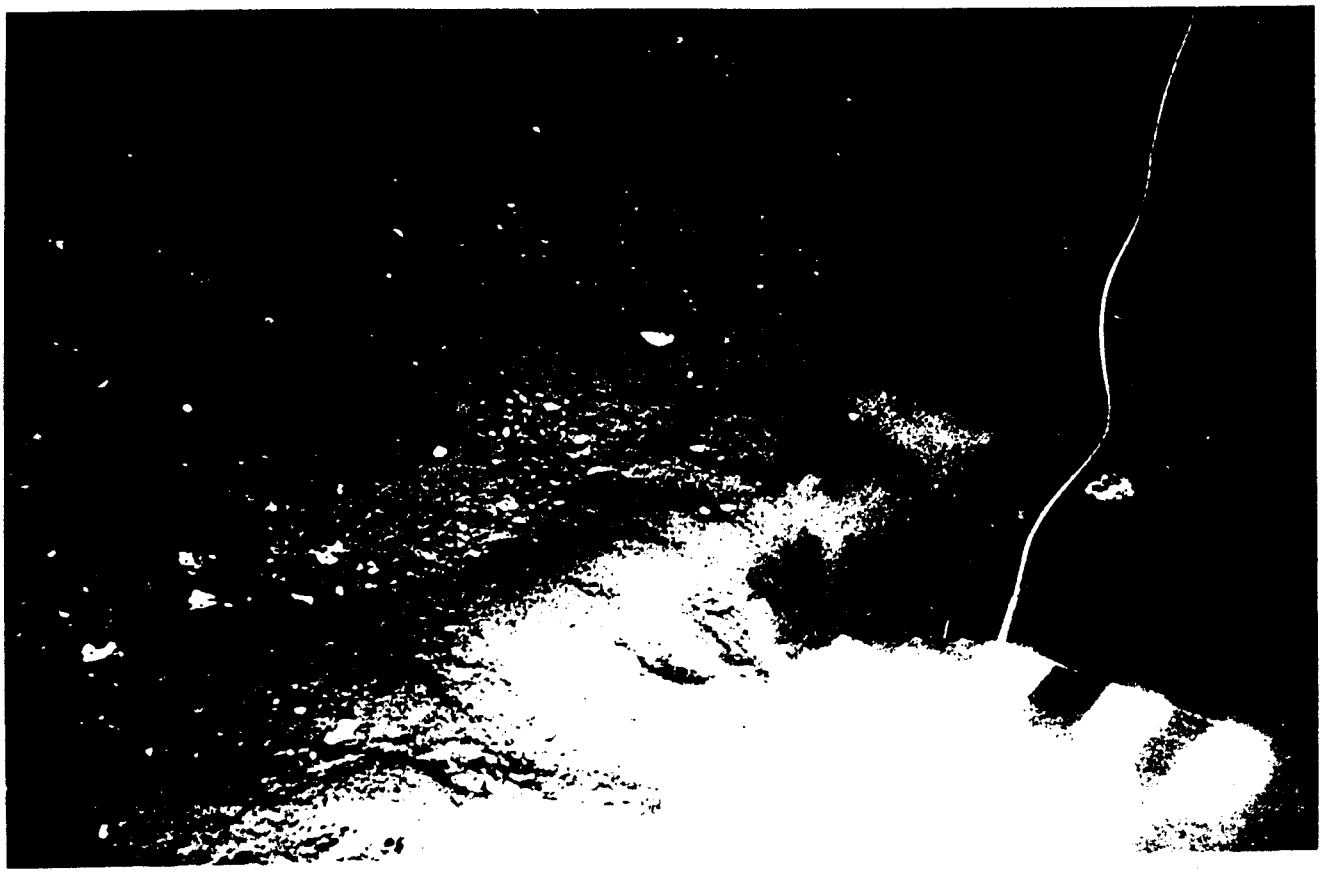

B

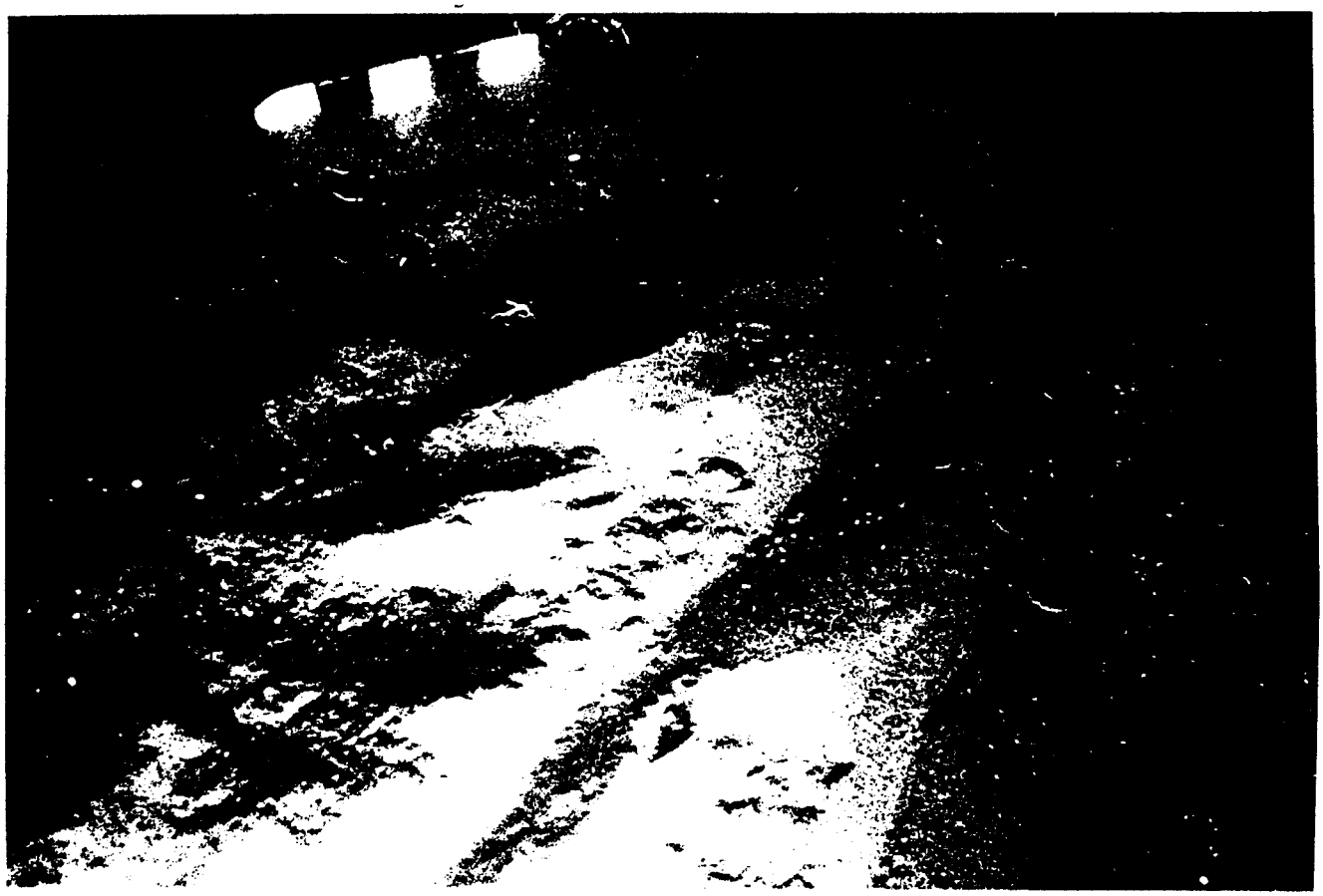

Figure 53.

A. Station 47, 40 m depth. Photograph of outer flank of coastal sand facies. The sea bed contains an irregular surface containing cobbles, shell debris, hermit crabs, and star fish.

B. Station 38, 39 m depth. Photograph of actively migrating ripples (moving from left to right) composed of medium sand. The thin stocks are bryozoans.

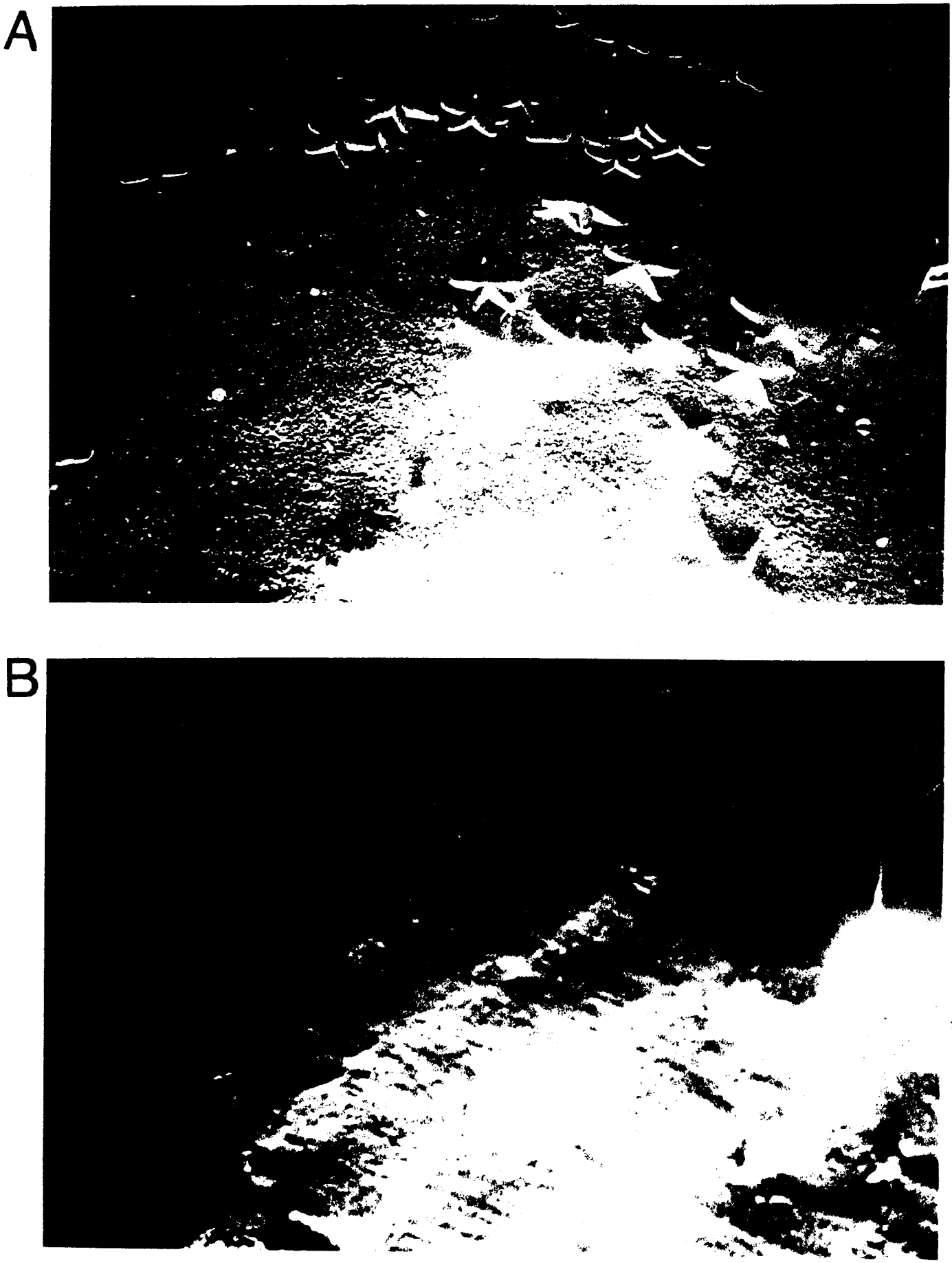
A
B

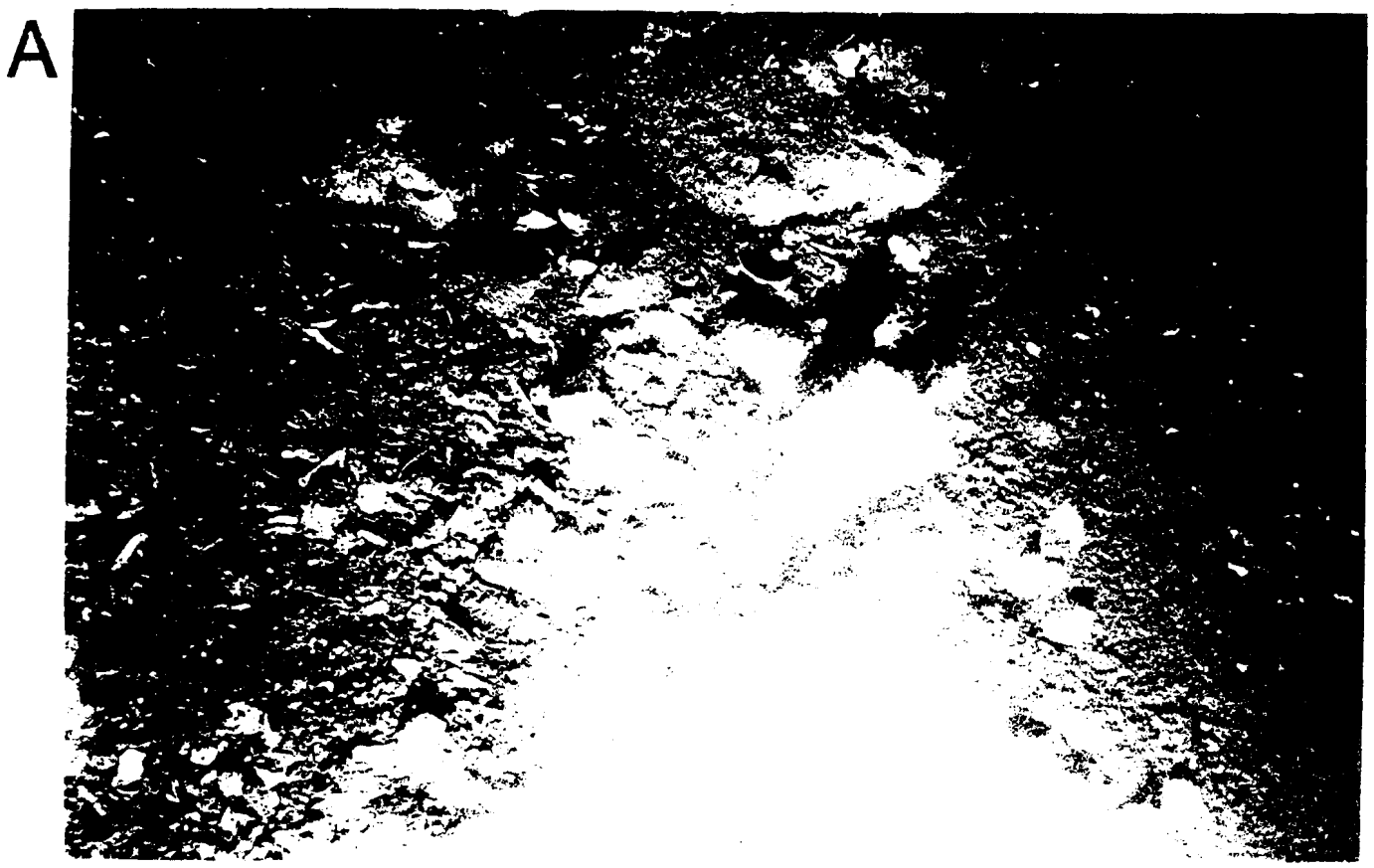

Figure 54.
Photograph of the southeastern flank of gravel field showing shell-cobble lag containing encrusting barnacles and bryozoans.

Figure 55 Station 39, 41 m depth.

A. Photograph of gravel covered sea floor west of Wainwright. Branching bryozoans, soft corals, and barnacles form the major fauna.

B. Photograph of cobble-boulder field. The large clast is covered with sponges and barnacles with bryozoans, soft corals, and tunicates common on the surrounding sea floor.

A

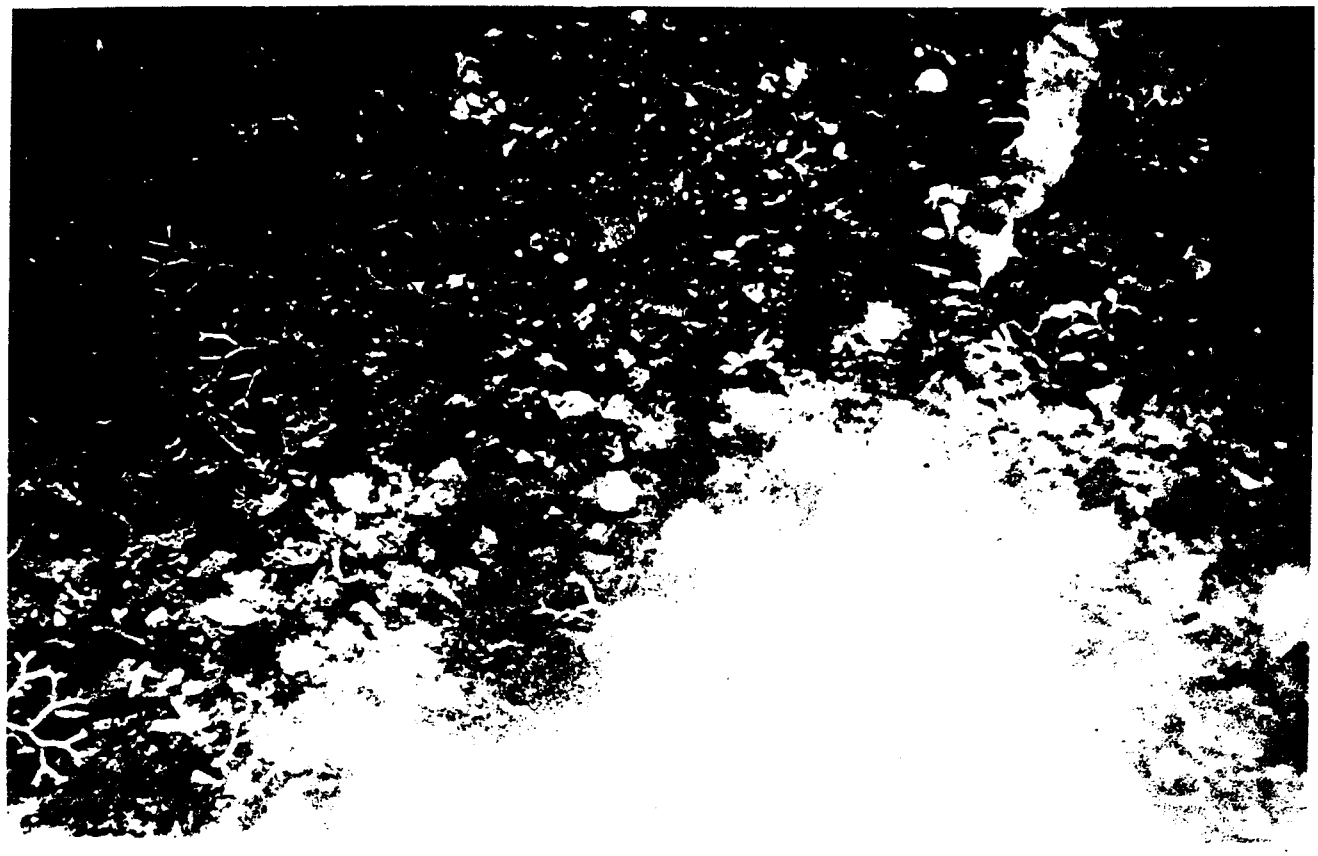

B

Figure 56. Station 40, 58 m depth.

A. Photograph of gravel covered sea bed. Soft corals, sponges, anemone, branching bryozoans and barnacles form the benthic community.

B. Photograph of gravel-boulder field. Sponges, soft corals, tunicates, branching bryozoans and anemones form the benthic communities.

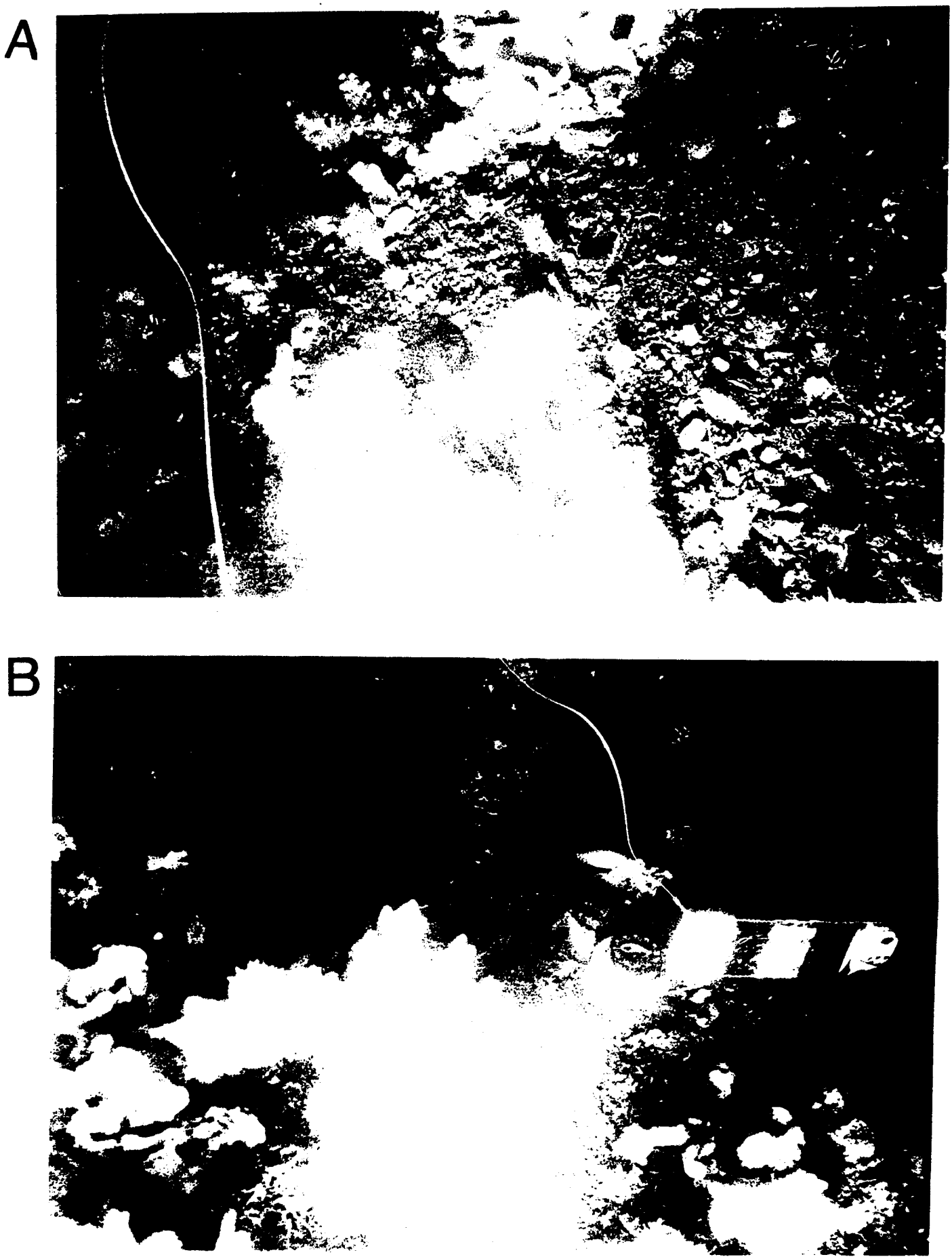
A
B

Figure 57 Station 45, 85 m depth.

A. Photograph of gravel-boulder community with barnacles, tunicates, and bryozoans encrusting cobbles.

B. Photograph of gravel-boulder field with anemones, sea pens, tunicates, barnacles, and branching bryozoans covering the clasts.

A

B

A

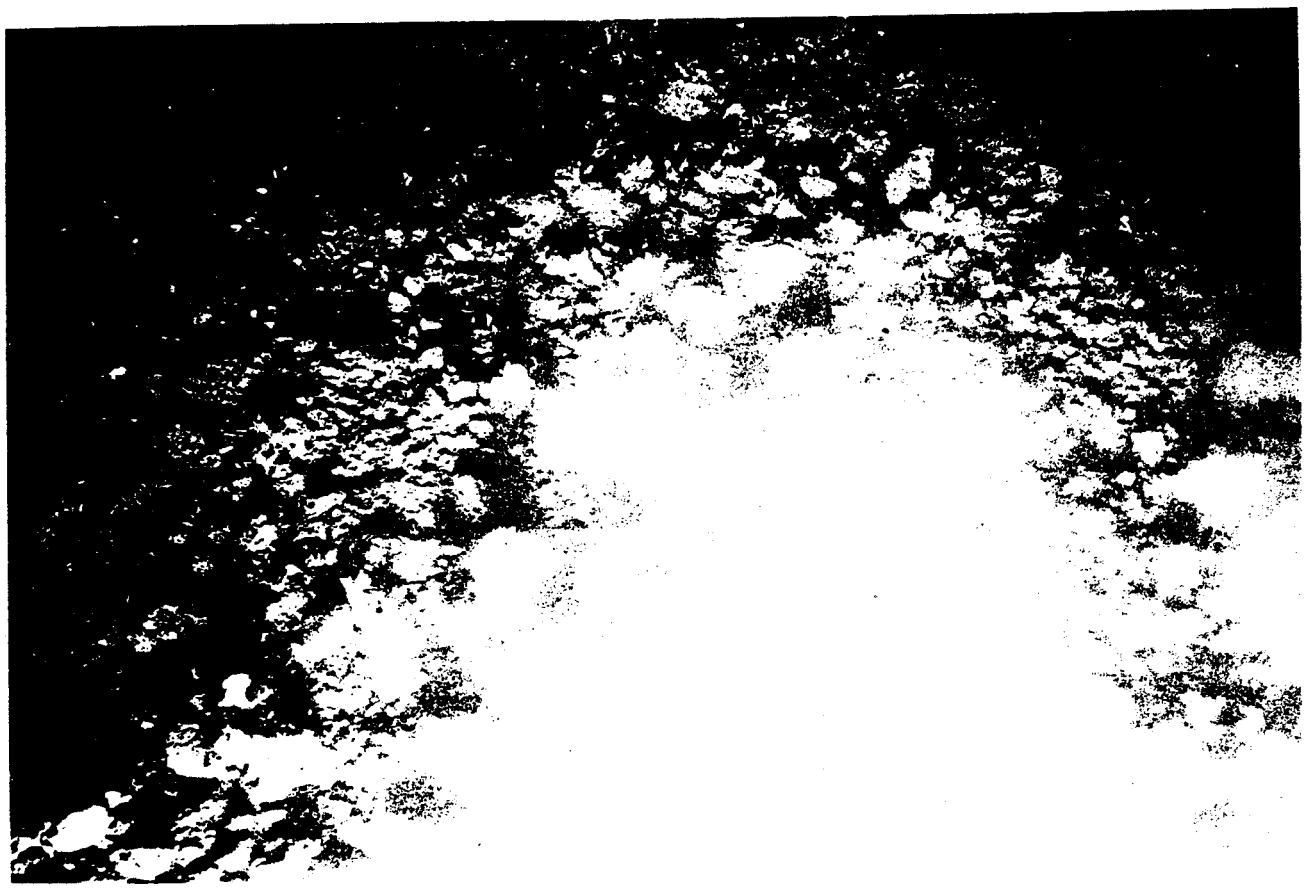

Figure 58. Station 60, 44 m depth.
Photograph of outer shelf gravel field. Barnacles, branching bryozoans, and sponge
are covering most of the cobbles.

Figure 59.

A. Station 59, 46 m depth. Photograph of tracks and trails in mud adjacent to the outer shelf gravel fields. The large tracks are formed by gastropods.

B. Station 28, 45 m depth. Photograph of outer shelf mud surface containing brittle stars.

A

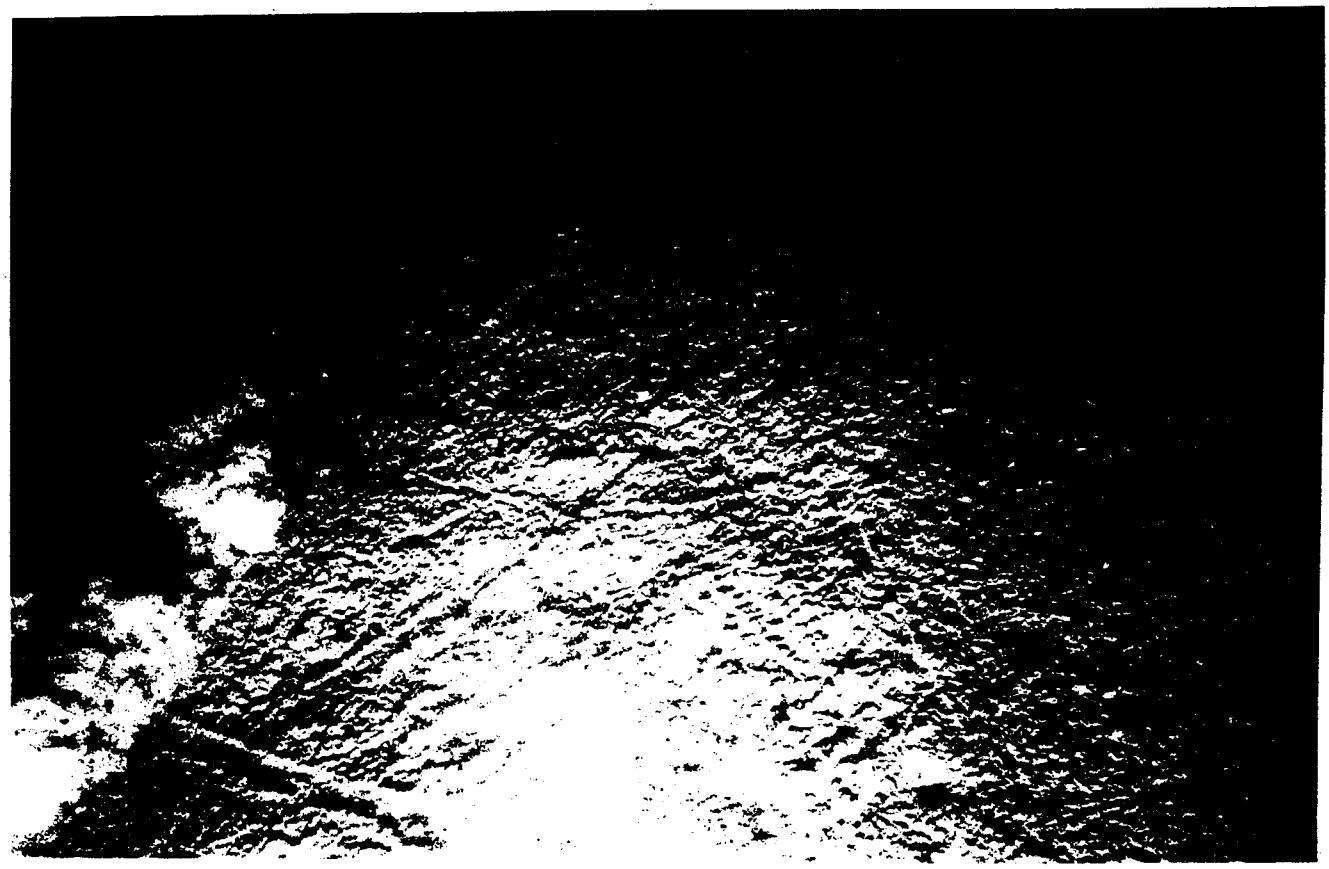

B

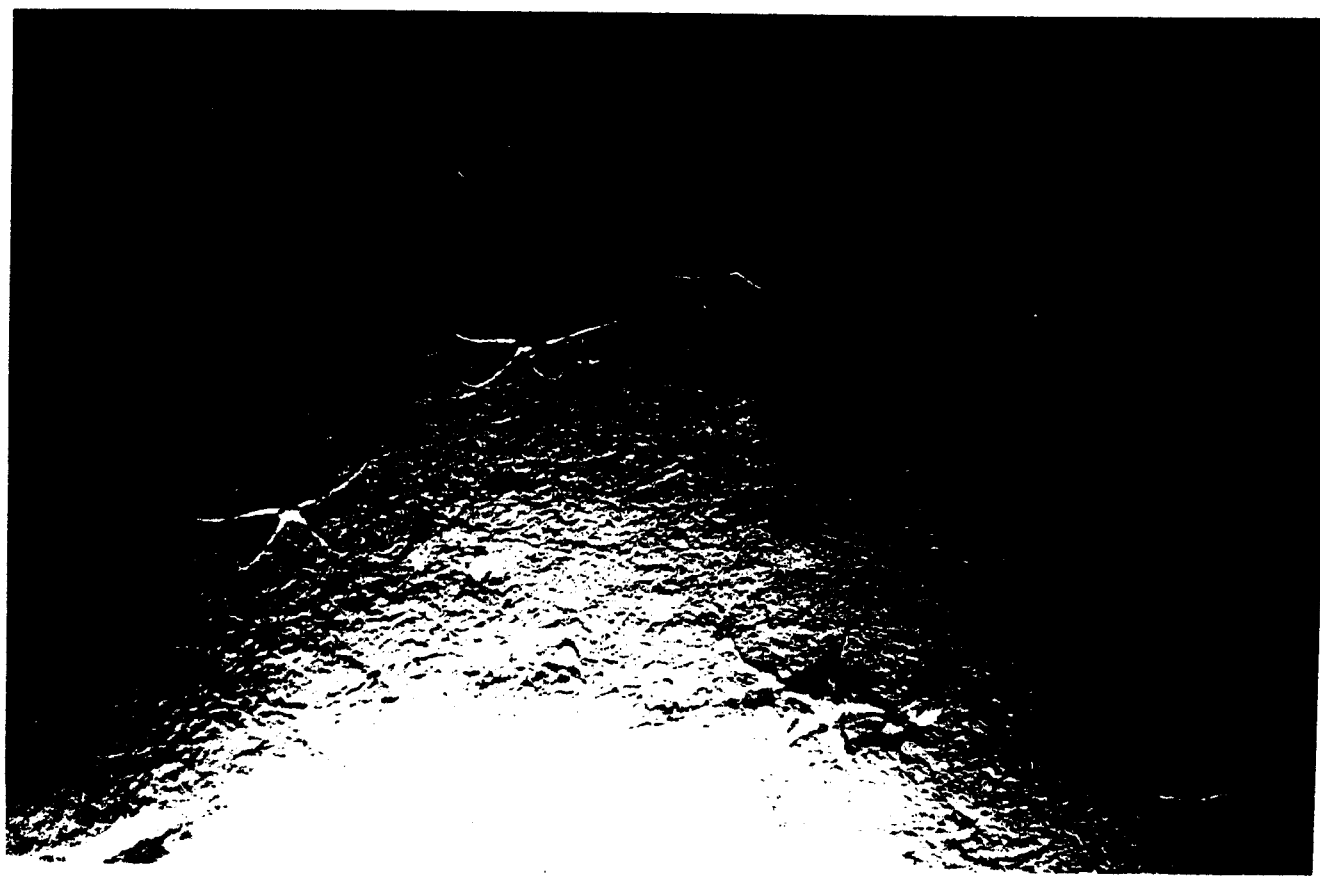

Figure 60. Station 27, 42 m depth.

A and B. Photograph of outer shelf mud with the sea floor containing brittle stars and anemones. The hummocky sea bed is apparently produced by feeding brittle stars.

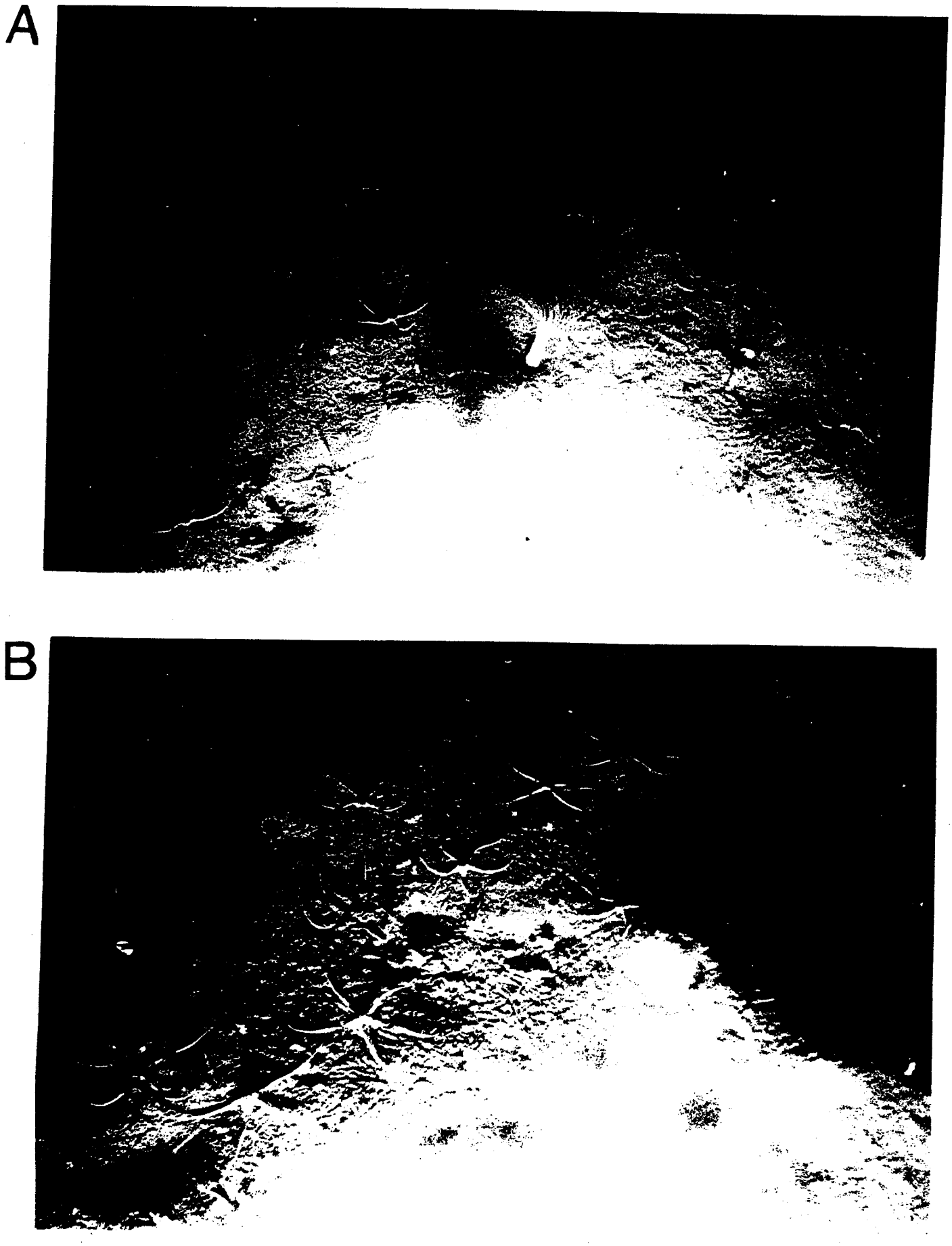
A
B

dominated by ampeliscid amphipods) in central Chirikov Basin. Nerini (1984) calculated a total biomass of 483 g/m^2 for the same area and found 34 percent was contributed by the amphipod community. Thomson (1984) indicates that in the areas of most intense gray whale feeding 50 to 75 percent of the biomass is composed of ampeliscid amphipods and the average amphipod biomass is 171 g/m^2. In contrast, the four stations in the northeast Chukchi Sea with high amphipod abundances contain a much lower average biomass of only 43 g/m^2 (Feder and others, 1989) although individual stations contain as much as 188 g or 4,319 +/- 1,987 individuals/m^2).

WHALE AND WALRUS FEEDING ECOLOGY

Gray Whales

Gray whales feed mostly during the summer. The stomachs of migrating whales are generally empty (Rice and Wolman, 1971), as are those of whales in the breeding lagoons of the Gulf of California (Scammon, 1874). Rice and Wolman (1971) reported that the southbound whales were 11 to 29 percent heavier than northbound whales. Nerini (1984) cites reports of whales actively feeding during migration. It is clear that they do feed sporadically and sometimes voraciously during migration to and from the southern waters, but the relative proportion of total yearly food intake this accounts for is unknown, although probably minor (Howell and Huey, 1930; Sund, 1975; Wellington and Anderson, 1978; Hudnall, 1981; Oliver and others, 1983a; Kvitek and Oliver, 1986). The majority of evidence suggests that gray whales feed only occasionally during migration, calving, and mating; they take most of their nourishment for the year during the summer on the Alaskan continental shelf.

The Bering and Chukchi seas are the main feeding areas of the gray whales. After migration from the breeding and calving lagoons of Baja California, the whales move into various feeding grounds north of the Aleutian Islands (Pike, 1962). The largest group feeds in central Chirikov Basin and nearshore areas of St. Lawrence Island (figs. 3, 61) (Braham and others, 1977; Consiglieri and others, 1980; Votrogov and Bogoslovskaya, 1980; Braham, 1984; Moore and Ljungblad, 1984). Of 299 gray whales sighted in Chirikov Basin in 1981 (Moore and Ljungblad, 1984), 85 percent were associated with sediment plumes which are reliable indicators of benthic feeding.

A smaller group of gray whales apparently stays near the Alaska Peninsula, where they are frequently observed feeding in the surf or very shallow water in Bristol Bay (Consiglieri and others, 1980; Braham and others, 1982). Their main prey species in these areas are unknown.

Soviet whalers reported taking gray whales from the nearshore western side of Chirikov Basin and in the Gulf of Anadyr at least as far south as Cape Navarin (Zenkovich, 1934, 1937, 1955; Zimushko and Lenskaya, 1970; Zimushko and Ivashin, 1980). Zenkovich (1937) reported that feeding whales were apparently segregated by age, and near Cape Navarin in the Gulf of Anadyr he

noted the presence of a feeding ground dominated by two-year old male gray whales. In the summer of 1991, intense gray whale feeding and sediment plumes containing amphipods were observed in Bering Strait and Russian scientists reported new whale feeding locations off Chukotka that previously had not been observed (Piatt, 1992). The latter observation may provide anecdotal information suggesting that the rapid increase in gray whale population from 16,000 in 1983 (Reilly, 1983) to approximately 21,000 individuals by 1992 (Loughlin, 1992) is taxing the present carrying capacity of the normal feeding grounds.

Another large group of feeding gray whales is found in the central Chukchi Sea, as well as along both the Alaskan and Siberian coasts (Bogoslovskaya and others, 1981; Coyle, 1981). Our sidescan studies cover only the Alaskan coast between Icy Cape and Point Franklin where several hundred whales are often observed feeding (Ljungblad, 1987). Gray whales have been spotted in the Beaufort Sea as far east as the MacKenzie River Delta of Canada (Maher, 1960; Rugh and Fraker, 1981).

A few small isolated groups of gray whales do not go far north to feed but spend the summer feeding at certain points along the migration route. One such group feeds in the outer Strait of Juan de Fuca and along the west coast of Vancouver Island, British Columbia (Hudnall, 1981; Oliver and others, 1984). Local ampeliscid amphipod mat communities exist in Pachena Bay and Port Renfrew Bay, Vancouver Island, and are being exploited by a small group of gray whales (Kvitek and Oliver, 1986). Thus, although Chirikov Basin has historically been regarded as the main feeding area (Rice and Wolman, 1971), other areas certainly receive substantial feeding pressure. This pressure may increase as the gray whale population continues to rebound.

Gray whales are omnivorous, feeding primarily by benthic suction, but also by engulfing and surface skimming (Nerini, 1984; Swartz and Jones, 1987). This provides a high diversity of prey and a good survival potential for the whales, making inaccurate the assessment of feeding resources by benthic means alone. The inaccuracy is very small, however as the vast majority of gray whale feeding is benthic in nature (Rice and Wolman, 1971; Nerini, 1984). Stomachs of gray whales taken in the feeding grounds contain mainly infaunal amphipods (Zenkovich, 1934; Pike, 1962; Rice and Wolman, 1971). Frequently they also contain sand, gravel, and cobbles (Zenkovich, 1937) .

There appear to be regional differences in main prey species. In Chirikov Basin, the ampeliscid amphipod *Ampelisca macrocephala* appears to be dominant (Zenkovich, 1934; Pike, 1962; Rice and Wolman, 1971; Coyle, 1981), but other ampeliscid amphipods such as *A. estrichii, A. birula, Byblis sp.*, and *Haploops sp.* are also heavily utilized by the whales. Closer to Siberia, the main prey species is the amphipod *Pontoporeia femorata* (Zimushko and Lenskaya, 1970; Zimushko and Ivashin, 1980; Bogoslovskaya and others, 1981). In the Chukchi Sea, within areas where gray whales were observed feeding off Wainwright, the amphipods consist of: *Ampelisca macrocephala, A. estrichti, Byblis gaimardi, Atylus bruggeni, Ischyrocerus, Protomedeia* spp. *Grandifoxus,* and *Erichthonius* (Group III, sandy assemblage of Feder and others, 1989) with the amphipods comprising 24 percent of the biomass (Feder and others, 1989). In the adjacent gravel-floored areas (Group 1, muddy sandy gravel assemblage of Feder and others, 1989)

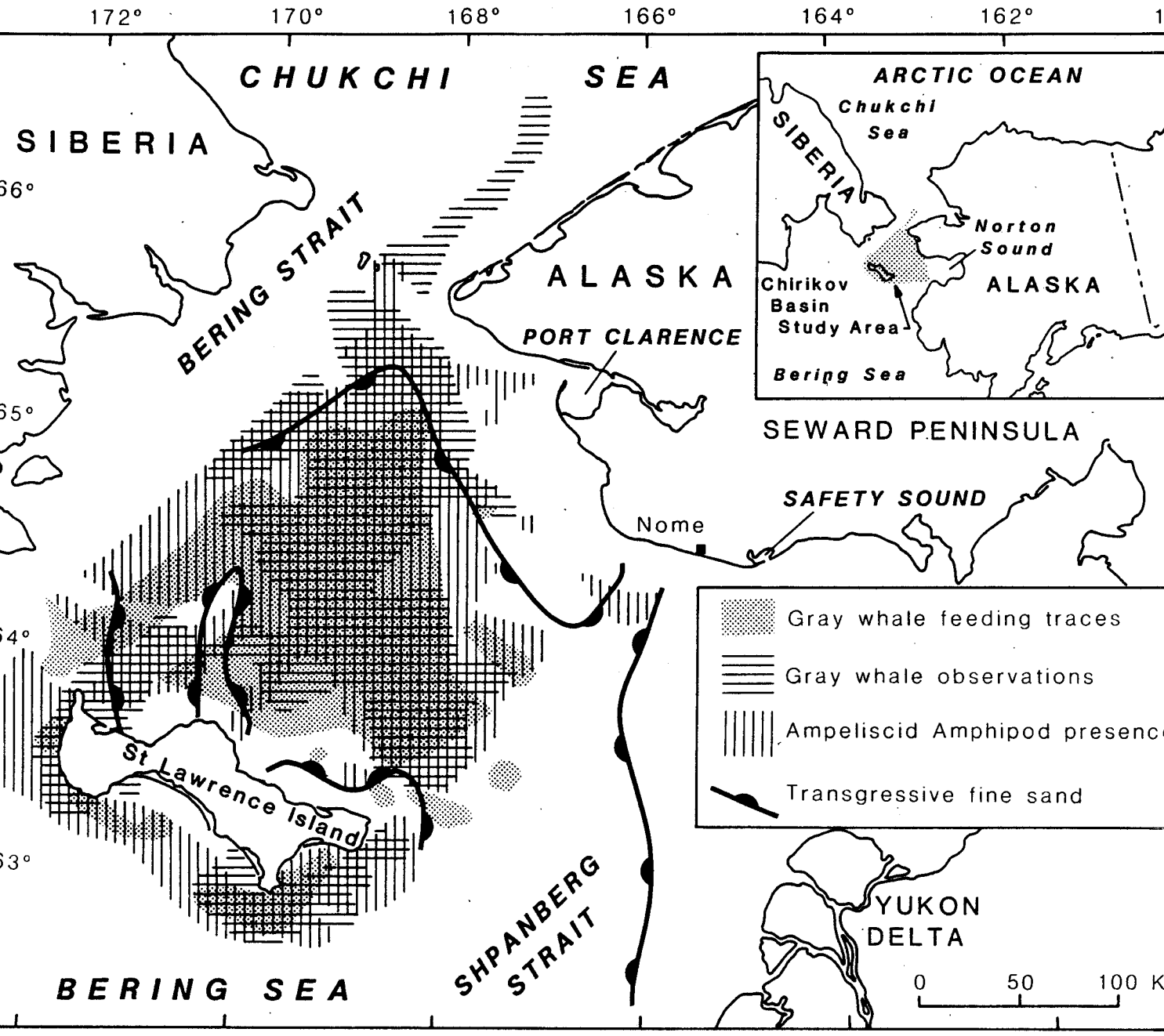

Figure 61. Distribution of gray whale feeding pits in the northeastern Bering Sea, mapped from side-scan sonar, sightings of feeding gray whales, distribution of Ampeliscid amphipods, and area of the transgressive sand sheet (from Johnson and Nelson, 1984).

Harpinia. In addition to *A. macrocephala*, *P. femorata*, and *Byblis gaimardi*, a number of other amphipods, polychaete worms, incidental infauna, and nektonic forms such as mysids and small fish are consumed (Nerini, 1984).

The manner in which the whales extract the amphipods from their sandy habitats has long been a subject of speculation. From diving and behavior observations by Norris and others (1977), Hudnall (1981, 1983), and Nerini (1984), it is theorized that gray whales roll to one side, mouth parallel to the bottom, and use suction formed by the retraction of the large muscular tongue in the mouth cavity to rip up patches of amphipod-rich sediment. The sediment is then expelled through the baleen on the opposite side of the mouth, and the amphipods are retained on the hairy inner side of the baleen plates to be swallowed at a later time. This hypothesis is supported by the observed feeding behavior of the captive gray whale, Gigi (Ray and Schevill, 1974).

The suction feeding process is difficult to observe directly in natural habitats, but this hypothesis is supported by observations of whale behavior in shallow water (Hudnall, 1981, 1983; Nerini and Oliver, 1983; Oliver and others, 1983a). In most cases, the whales are seen to roll on their sides with their mouth parallel to the bottom; however further observation was impaired by the ensuing sediment plume. Recently, in a natural habitat off western Vancouver Island, British Columbia, a single young whale was observed and photographed while exhibiting all the above described feeding behavior (Swartz and Jones, 1987). Good bottom photographs (Nelson and Johnson, 1987) (fig. 62) and sidescan sonographs (figs. 63, 64) also document the presence of freshly formed feeding pits from a number of gray whale habitats off western North America (Johnson and Nelson, 1984; Kvitek and Oliver, 1986; Cacchione and others, 1987).

No evidence shows that gray whales plough into the sea floor along the hundreds of kilometers necessary to filter sufficient amphipods to account for yearly and total gains of body weight. Kasuya and Rice (1970) studied uneven wear on the inner side of the baleen plates of 31 whales and showed that 27 of the whales fed predominantly with the right side of their heads. They also showed a greater frequency of healed or open wounds and fewer parasitic barnacles on the right side of the rostrum. These results suggest that more whales may be right-handed (or right-mouthed) and implies that the whales do occasionally come into contact with the abrasive sands of the sea floor.

Benthic feeding by gray whales produces a variety of pits in the sea floor. Sidescan sonar surveys show elongate furrows as long as 10 m in areas of heavy whale feeding in the Bering Sea (Nerini and others, 1980; Johnson and Nelson, 1984). In the northeastern Bering Sea, scuba divers measured pits ranging in length from 0.6 m to 3 m and attributed them to feeding gray whales (Nerini and Oliver, 1983). S.L. Swartz (University of California, Santa Cruz, oral communication, 1982) has observed whales making pits as long as their gape and as wide as 1 meter in the highly mobile sands of their breeding lagoons in Baja California, Mexico. These pits resemble feeding pits, but should be attributed to mock feeding, test feeding, or some other unexplained behavior, since cores taken near these pits contained few macroscopic fauna. Oliver and others (1984) have observed

pits as long as 1.5 m in ampeliscid-amphipod-bearing sediment associated with a juvenile gray whale that was actively feeding in Pachena Bay, Vancouver Island. The pits observed in these various locations often occur in groups, as multiple-suction feeding events (Johnson and others, 1983; Johnson and Nelson, 1984; Nerini, 1984; Oliver and Kvitek, 1984; Kvitek and Oliver, 1986).

In order to determine the shape and size of features likely to be made by a whale foraging on the benthos, a histogram of gray whale gape (mouth) lengths based mainly on data from Rice and Wolman (1971), has been compiled (fig. 65). Gape lengths were calculated by multiplying the head length by 0.75. The average gape length was 2.0 m for 131 males and 2.1 m for 105 females. The average gray whale head, when viewed from above, is triangular, and the line from the snout to the posterior end of the gape is straight. Most of the mouth is parallel to the bottom, and a large percentage of the gape may be utilized during feeding.

If a whale were swimming or drifting in the current while sucking up the sediment, the size of the resulting feature could be considerably larger than gape size. The length of a feature made by a moving whale would be controlled by the duration of the suction event, the speed of the whale, the effect of current movement on the whale, and percentage of mouth area used. By a combination of propulsion and suction, whales have the potential to make pits several meters long (fig. 4).

Observations of feeding whales show both stationary and mobile feeding modes. Records of dive times and positions of diving and surfacing of bottom-feeding whales near St. Lawrence Island show that whales often surface near where they dive, implying minimal movement on the bottom (Wursig and others, 1983). The juvenile gray whale observed by scuba divers at Pachena Bay, British Columbia, was moving along the sea floor while feeding. The resulting pits were as long as 1.5 meters, longer than the gape of the small whale (Oliver and others, 1984). Although the size of the pit left by a stationary whale generally may be expected to be approximately the size and shape of the gape, the pits could potentially be smaller (suction out of only a part of the mouth) or larger (suction while moving).

The average depth of the pits has been estimated in the northern Bering Sea to be about 10 cm for freshly excavated pits and as deep as 40 cm for older current-modified pits (Johnson and others, 1983; Thomson, 1984). Primary feeding excavations deeper than 15 cm appear unnecessary for harvesting amphipods and probably are difficult to accomplish by the normal suction method of whale feeding.

Pacific Walrus

The Pacific walrus (*Odobenus rosmarus divergens*) consumes a diet consisting mainly of clams (Frost and Lowry, 1981; Fay, 1982). The walrus also feeds mainly by excavating benthic infauna. Walrus forage for their infaunal prey by hydraulically creating pits and furrows to excavate the clams. They apparently excavate individual pits (as much as 47 cm in diameter) when foraging in water of good visibility or when hunting for large, isolated, deep-burrowing clams such as *Mya sp.* These small pits are only poorly resolved by even high resolution sidescan systems

Figure 62. Photograph of gray whale feeding pit , taken by Larry Martin of LGL Ecological Research Associates, Inc. Pit is approximately 2.5 m long, 1.5 m wide, and 10 cm deep. From Johnson and Nelson (1987).

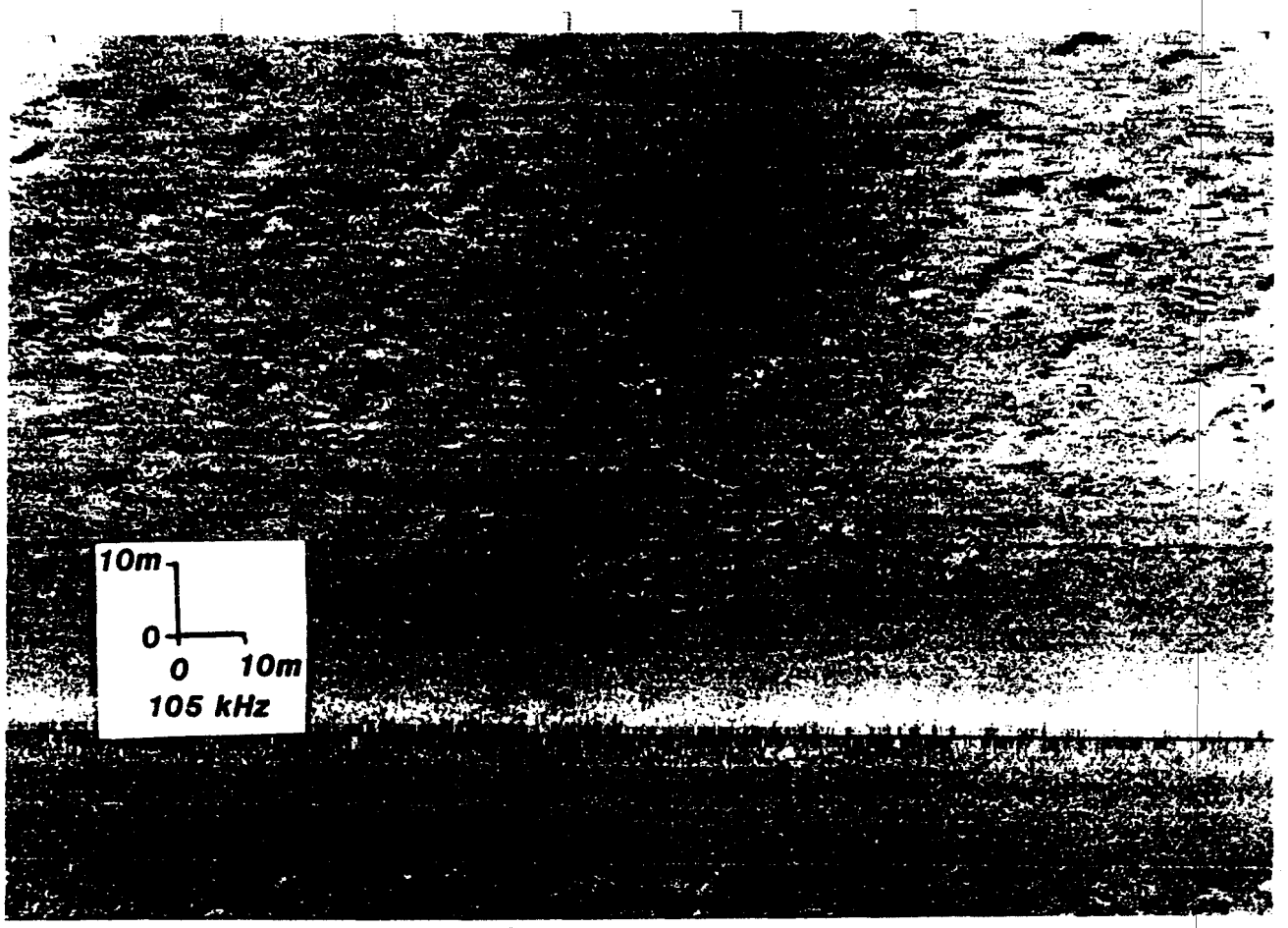

Figure 63. Sonograph showing fresh and current-modified gray whale feeding pits, Chirikov Basin, northeastern Bering Sea.

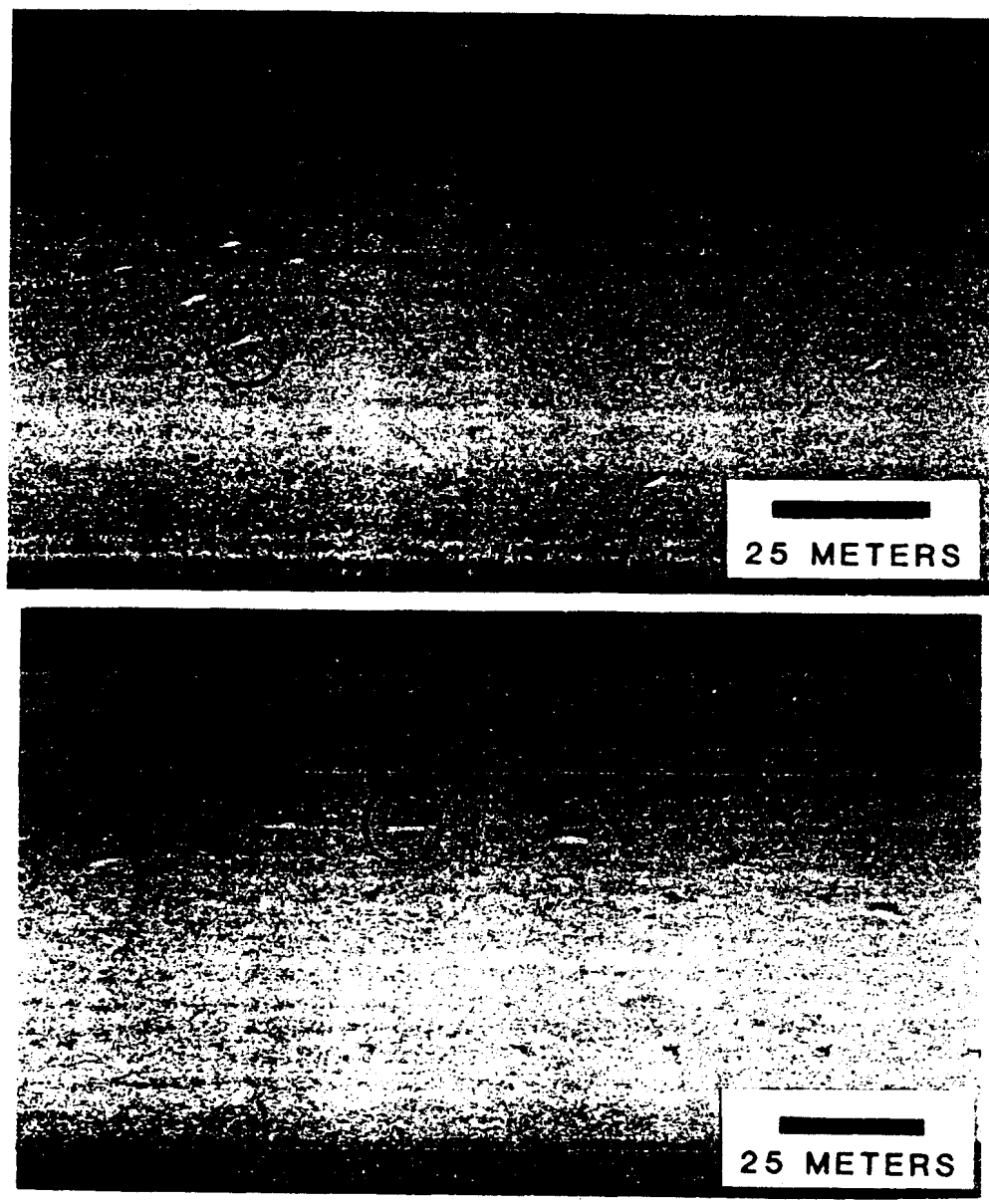

Figure 64. Sonographs of gray whale feeding pits, off Stewart's Point, central California, 60-70 m water depth. Examples of pits are circled (from Cacchione and others, 1987).

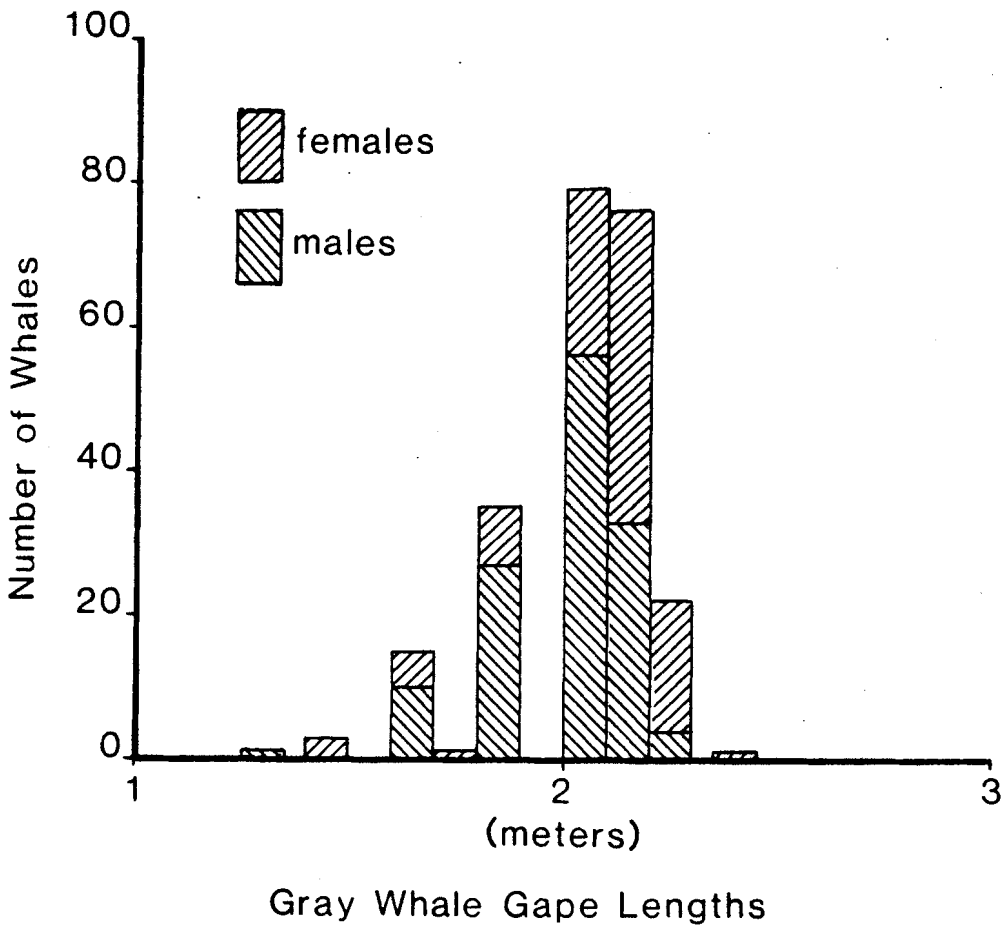

Figure 65. Histogram of gray whale gape lengths (from Nelson and others, 1983).

and they also are difficult to distinguish from other sidescan features and artifacts. When foraging in water of poor visibility or when searching for smaller, more numerous, near-surface clams such as *Spisula sp.* or *Macoma sp.*, they create very long, narrow furrows (Oliver and others, 1983b). These furrows which may reach several tens of meters in length, are distinguishable on the sidescan sonar record (fig. 5) (Nelson and others, 1987).

Generally, the whale and walrus consume different prey species, eliminating feeding competition between the two, but not necessarily implying different feeding grounds (Nelson and others, 1987). In the Chukchi Sea, the main whale feeding grounds are associated with the sandy areas dominated by amphipod assemblages. Whale feeding is not associated with muddy or gravelly areas characterized by walrus prey faunal assemblages. The walrus, however, migrate with the ice edge and feed on clams within and outside the sandy whale feeding regions. Thus walrus may compete very marginally for some of the same prey resources in whale feeding areas.

The bulk of the Pacific walrus population lives along the edge of the pack ice, and rides to new feeding grounds as they are uncovered by the receding ice. The Chukchi Sea south of 71° is uncovered by mid June, and by traveling with the migrating ice edge, walrus are able to traverse nearly the entire shelf (figs. 66-68) (Fay, 1982). Inspection of walrus stomachs shows the walrus to be an opportunistic omnivore. In 44 walrus stomachs inspected, 36 prey taxa were found, with ten bivalve and nine gastropod taxa being the most numerous (Feder and others, 1989). Walrus prey mainly on molluscs, but more than sixty genera from ten phyla have been identified as prey of the Pacific walrus (Fay, 1982). This ability to be omnivorous allows the walrus great freedom within the Chukchi Sea because there is a high average number of benthic and epibenthic prey taxa. Feeding pressure in the Chukchi also appears to be shifting slightly, forcing the walrus to diversify and feed more on nektonic forms. As much as 3.4 percent by weight of fish are included in the diet, holothurians and scyphozoa are detected in relatively large amounts, and a number of seal eating walrus were found (Fay and others, 1984).

The walrus furrows seen on the side scan sonar, actually are a series of interconnecting depressions (fig. 5). Like whales, the skin of a walrus is too tender to plow through the sediment. What appear to be furrows are actually a series of interconnected pits, created by the walrus blowing a strong stream of water out of its mouth (Oliver and others, 1983b). These pits are where the walrus has jetted sediment away in search of benthic fauna to eat. Diving observations show that furrows average 35-45 cm in width and pits vary from 11-32 cm in depth (Fay, 1982; Oliver and others, 1983b; Klaus and others, 1990).

The Pacific bearded seal (*Erignathus barbatus*) consumes primarily epifauna, but also is known to eat clams. Seal feeding excavations are likely to be much smaller than those of the walrus simply because of the relative size of the two animals. Competition between the walrus and seal, combined with a rapidly increasing walrus population, has caused the seals to rely more on epifaunal prey and less on clams (Lowry and others, 1980).

CHARACTERISTICS OF MAMMAL FEEDING TRACES AND DISTRIBUTION

Mammal Feeding Traces Compared to Other Physical and Biological Features

Study of several types of data from the Chukchi Sea and comparison of diving observations with sidescan sonographs in several whale and walrus feeding areas off western North America have established that whale and walrus feeding pits are present in the northeastern Chukchi Sea (Johnson and others, 1983; Nerini, 1984; Oliver and others, 1984; Kvitek and Oliver, 1986, Nelson and others, 1987). Compilations of the summer distribution of feeding gray whales (figs. 69-72) and walrus (fig. 68) (Fay, 1982), types and distribution of substrate (fig. 9) (Phillips and Colgan, 1987a and b), and distribution of benthic assemblages (fig. 8) (Feder and others, 1989) all indicate that conditions for gray whale and walrus feeding grounds exist in northeastern Chukchi Sea.

The sea floor in the Chukchi Sea is disturbed by the physical processes of ice gouging and migrating current-generated bedforms (fig. 6). Current-generated sandwave fields occur in nearshore areas associated with the coastal current (fig. 43) (Phillips and others, 1988). Ice gouges are found throughout the area, are arrayed in sub-parallel groups, typically extend for tens of meters, and may have occasional angular turns or crossings (fig. 6) (Toimil, 1978; Phillips, 1987). Mammal feeding traces which have irregular shapes can be distinguished from the distinct linear and angular features made by physical processes of ice and currents (Johnson and others, 1983; Phillips and Colgan, 1987a).

The seasonality of the physical processes and mammal feeding, however, can result in a bias in the representation of feeding traces. For example, if sidescan data were obtained several weeks after a main episode of mammal feeding, migrating sand waves might have obliterated or modified the fresh feeding traces to appear much smaller than they were originally. The importance of this interplay is shown by the progressive increase in the number of walrus furrows as one approaches the ice edge, where the main population of walrus is actively feeding (fig. 73). On the other hand, because ice gouging generally occurs during the winter season prior to the summer feeding season, it may disturb old traces, but it does not affect the fresh mammal feeding traces that we are examining in this study.

The bottom roughening caused by the feeding behavior of gray whales enhances subsequent current scour that modifies fresh feeding pits created by the whales (Nelson and others, 1987). Separation of the original fresh pits and the current-scour modified pits becomes an important task in the analysis of sidescan sonographs. Diver observations, and calibration of freshly formed whale feeding pits with high-resolution sidescan sonographs help distinguish the wide variety of feeding traces and modification by physical processes that exists (Johnson and others, 1983; Nerini, 1984; Oliver and Kvitek, 1984; Thomson, 1984).

Whale Pits

We collected detailed sidescan data along the coast from Pt. Hope north to Pt. Barrow. Our reconnaissance coverage of sidescan

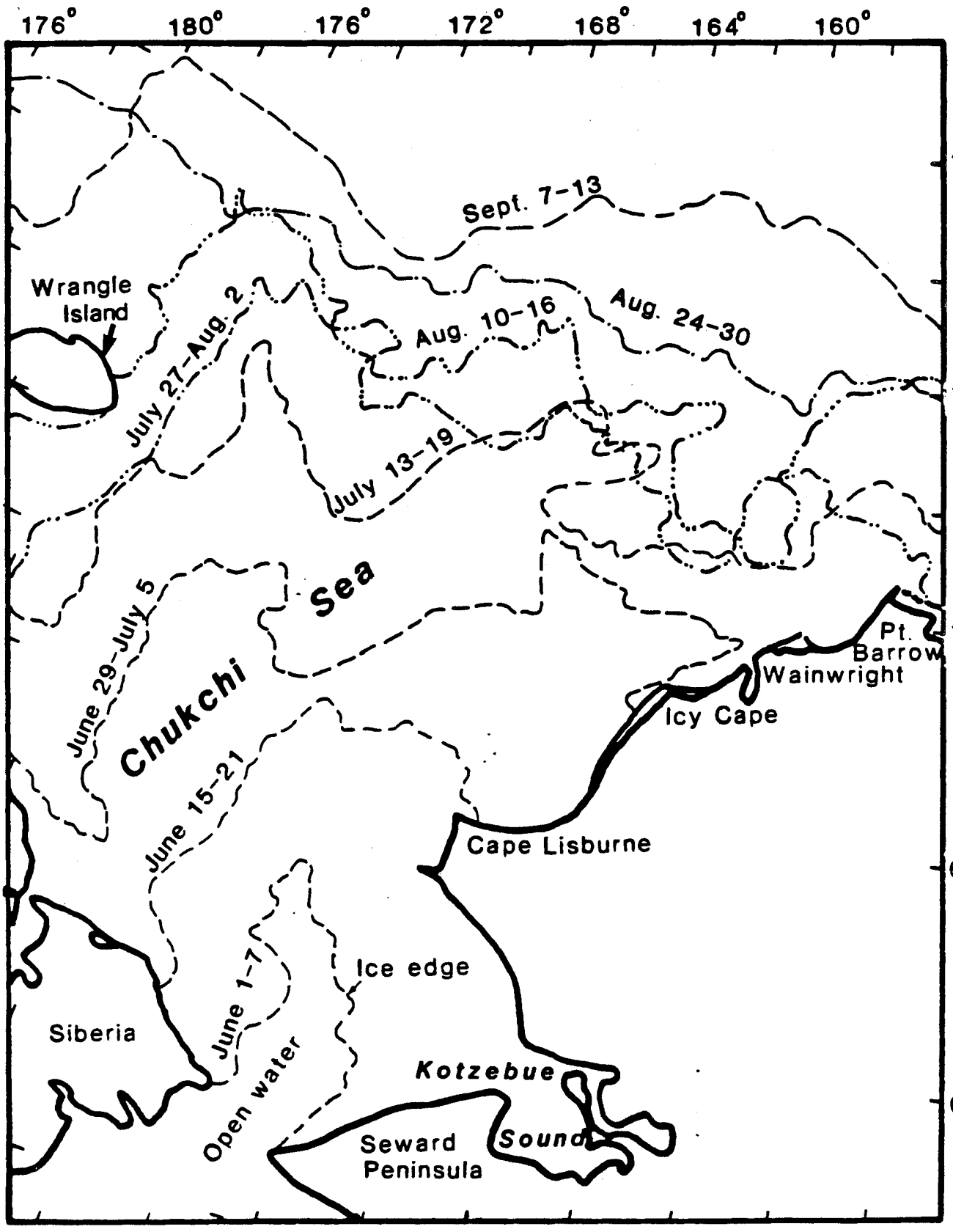

Figure 66. Maximum extent of ice from June to September 13. Data from Stringer and Groves (1987) summary of 1972-1983 maximum extent of summer time ice edge i the Chukchi Sea.

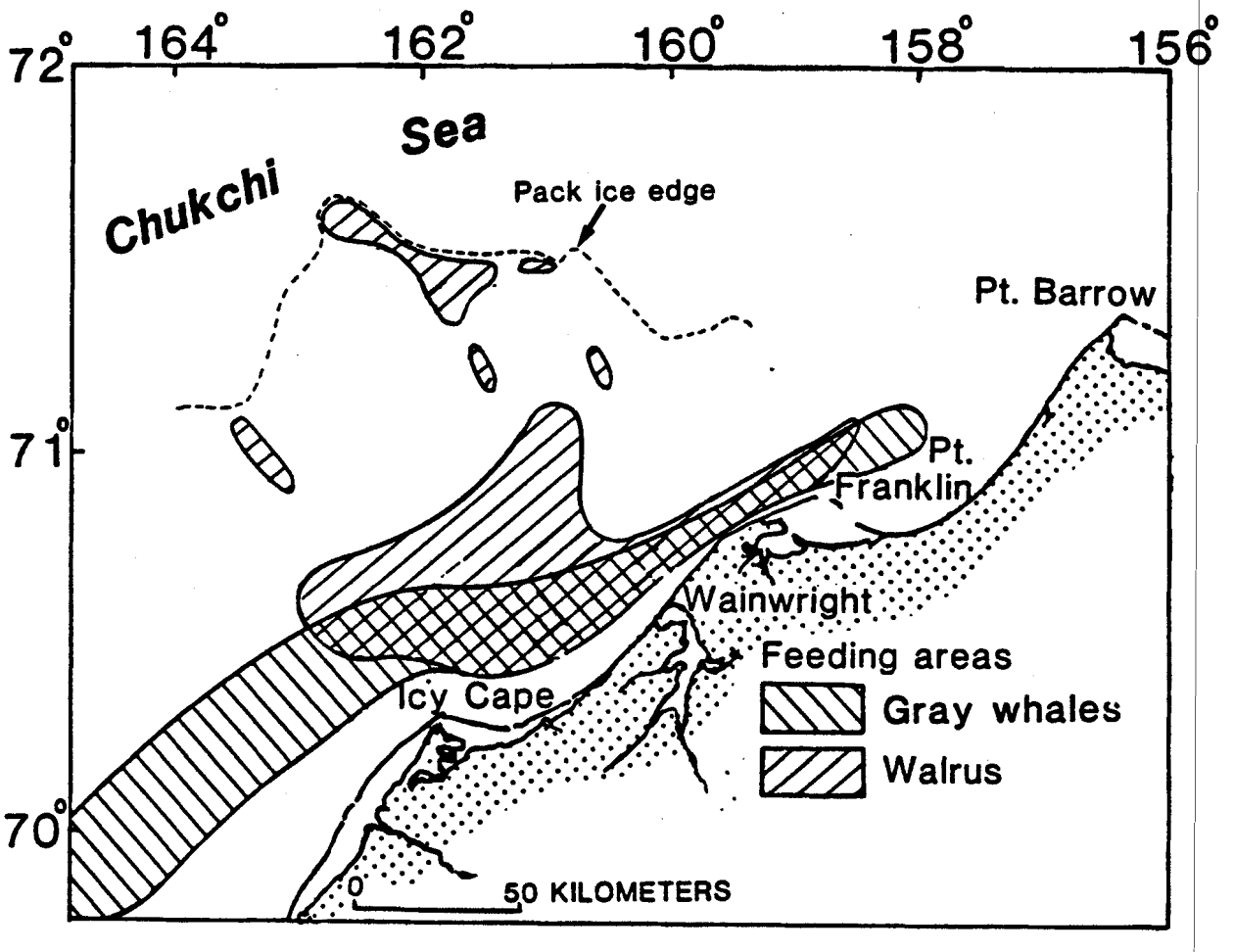

Figure 67. Areas of northeast Chukchi Sea containing benthic feeding traces of gray whales and walrus initially reported by Phillips and Colgan (1987c).

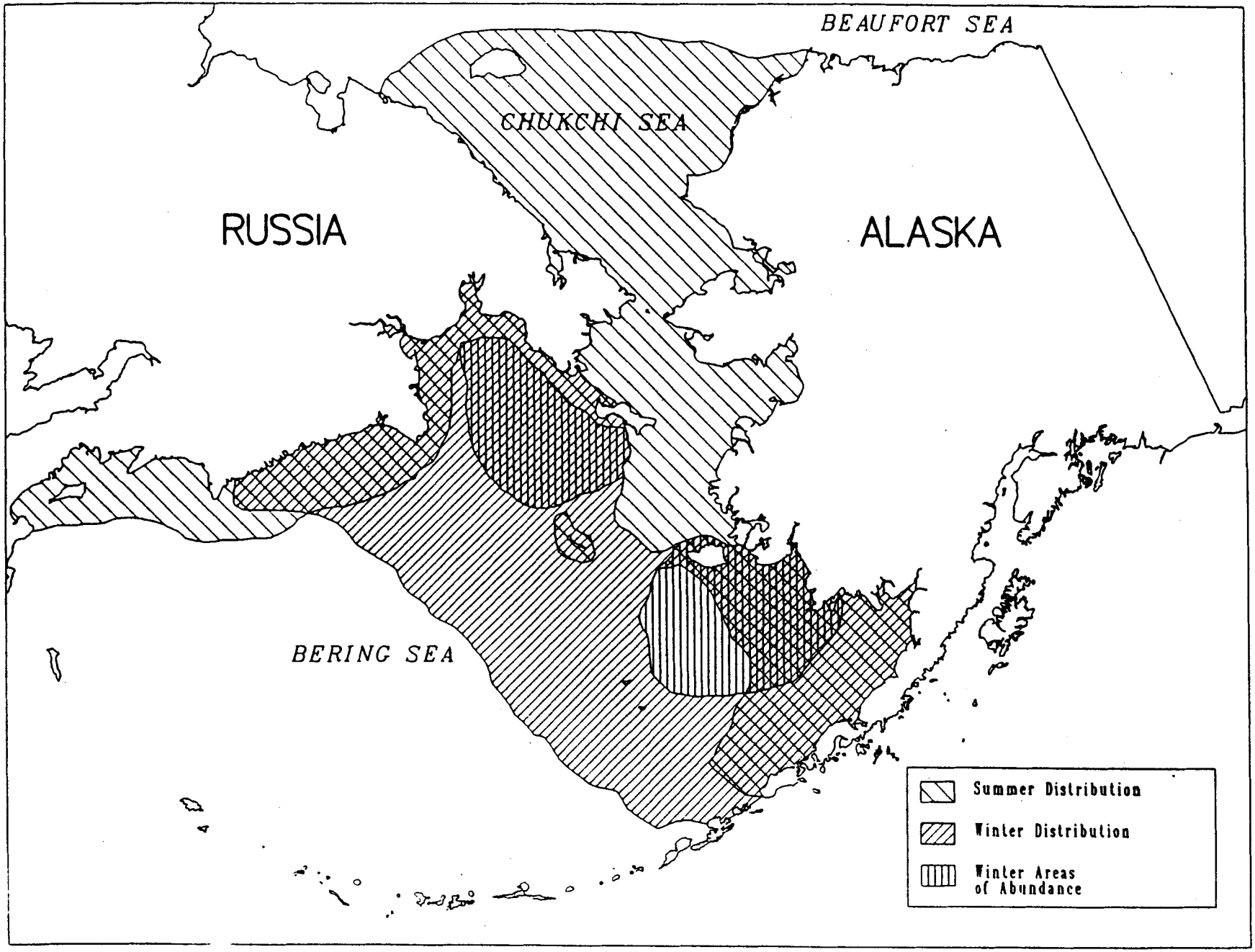

Figure 68. Generalized distribution of the Pacific walrus (*Odobenus rosmarus* divergens) (Jon Nickles, US Fish and Wildlife Service, Anchorage, AK, written communication, 1992).

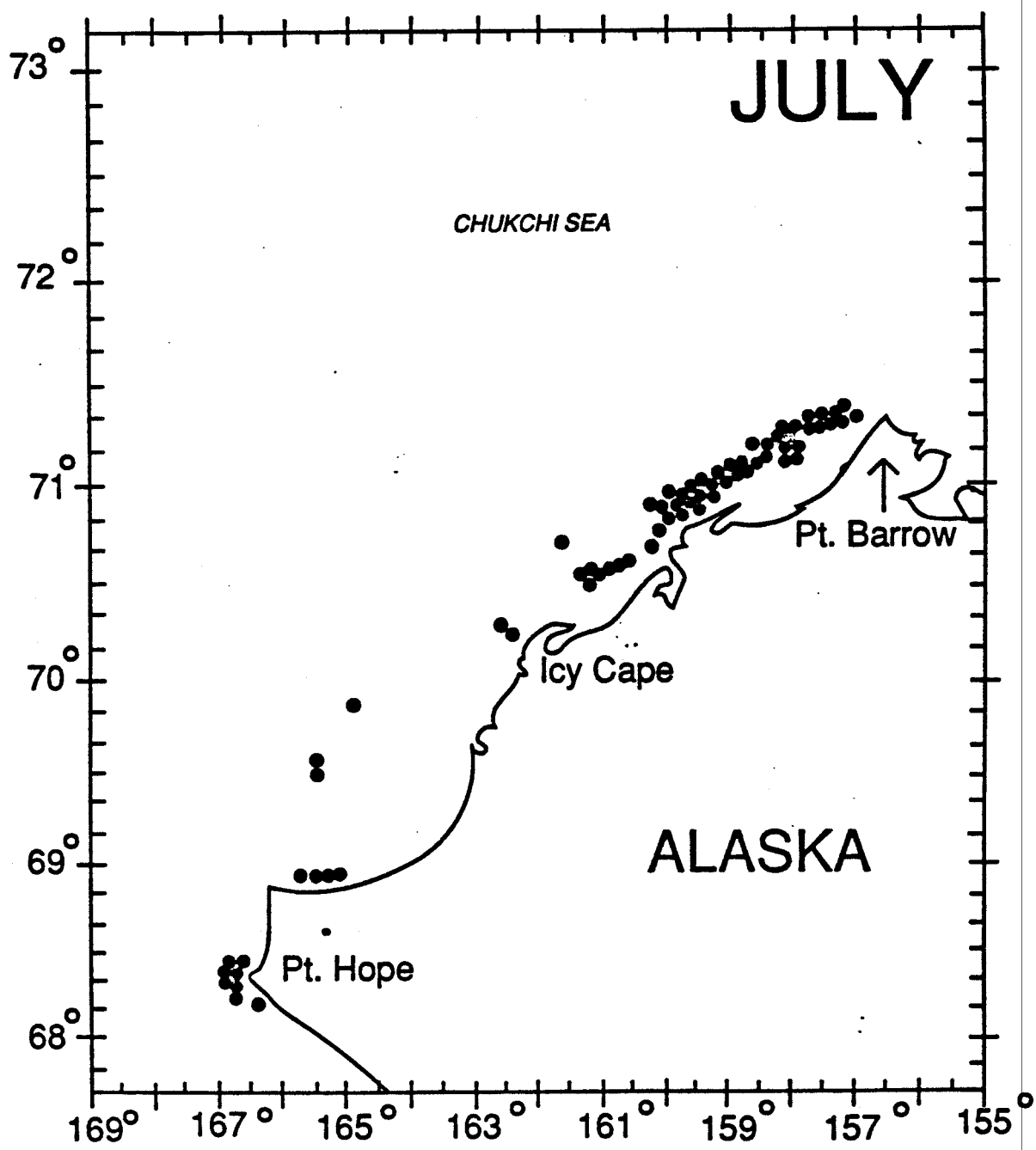

Figure 69. Distribution of 107 sightings of 380 gray whales in July, 1982 to 1987 in the Chukchi Sea. Data from Clarke and others, 1989.

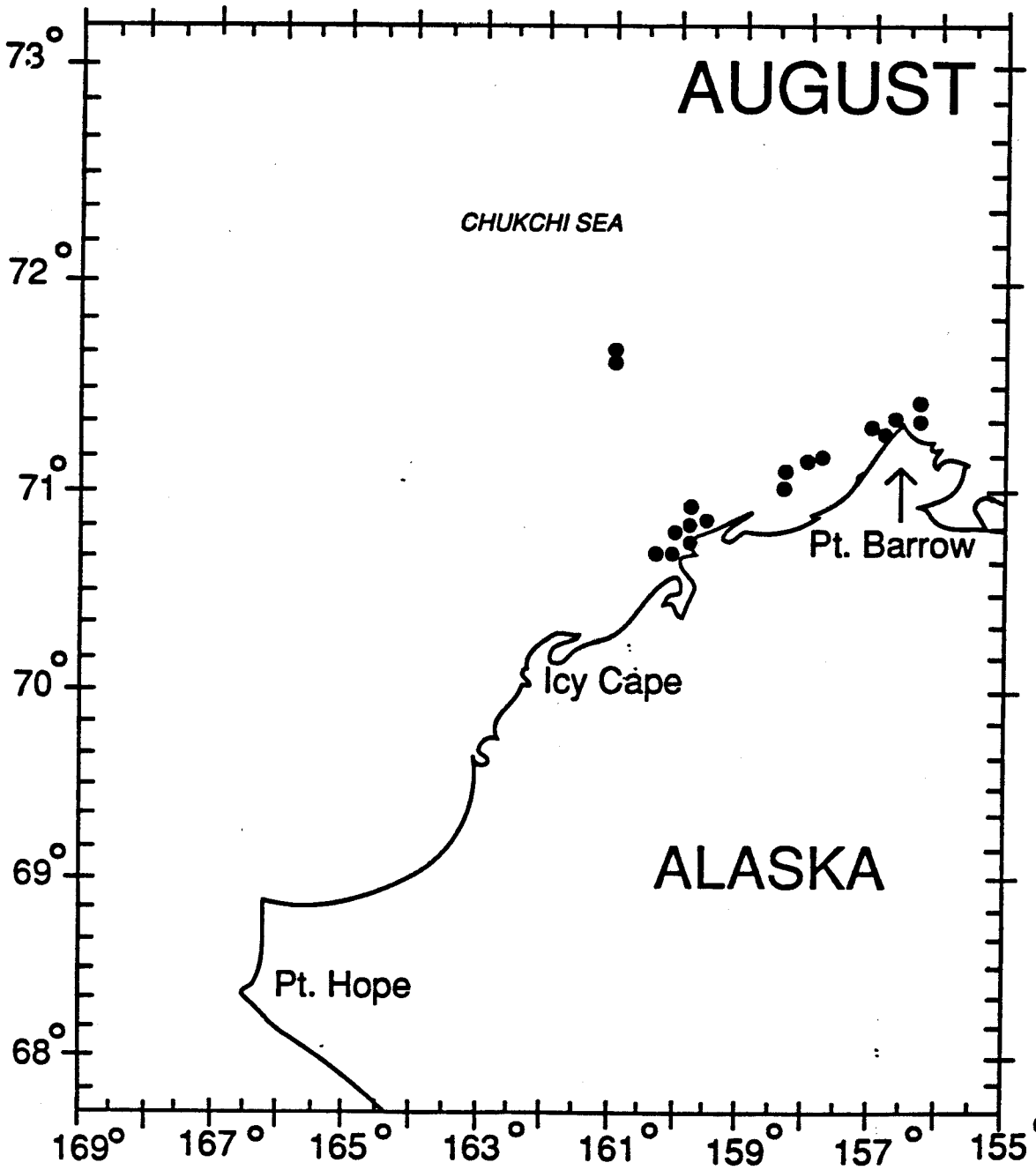

Figure 70. Distribution of 18 sightings of 47 gray whales in August, 1982 to 1987 in the Chukchi Sea. Data from Clarke and others, 1989.

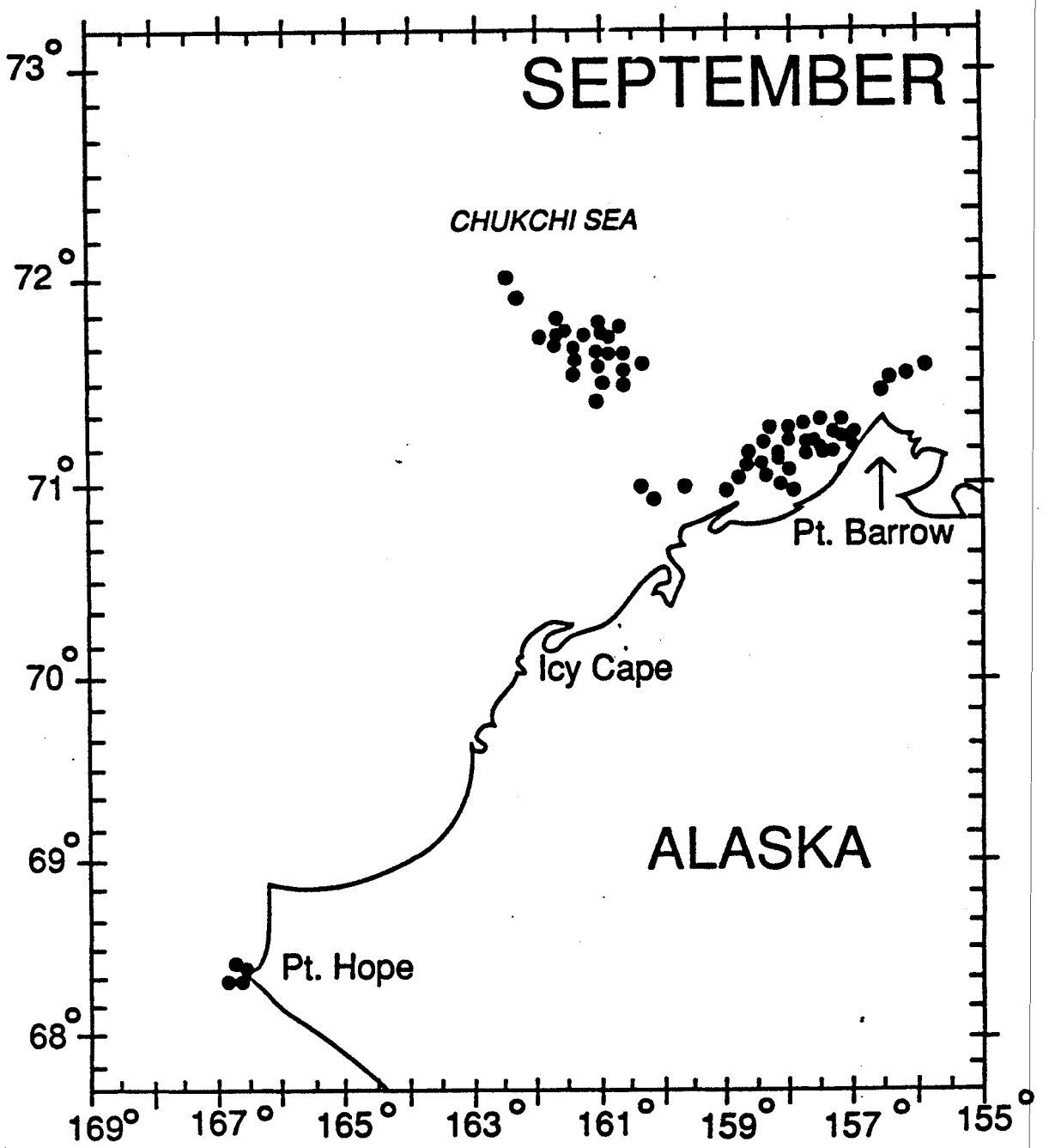

Figure 71. Distribution of 95 sightings of 312 gray whales in September, 1982 to 1987. Data from Clarke and others, 1989.

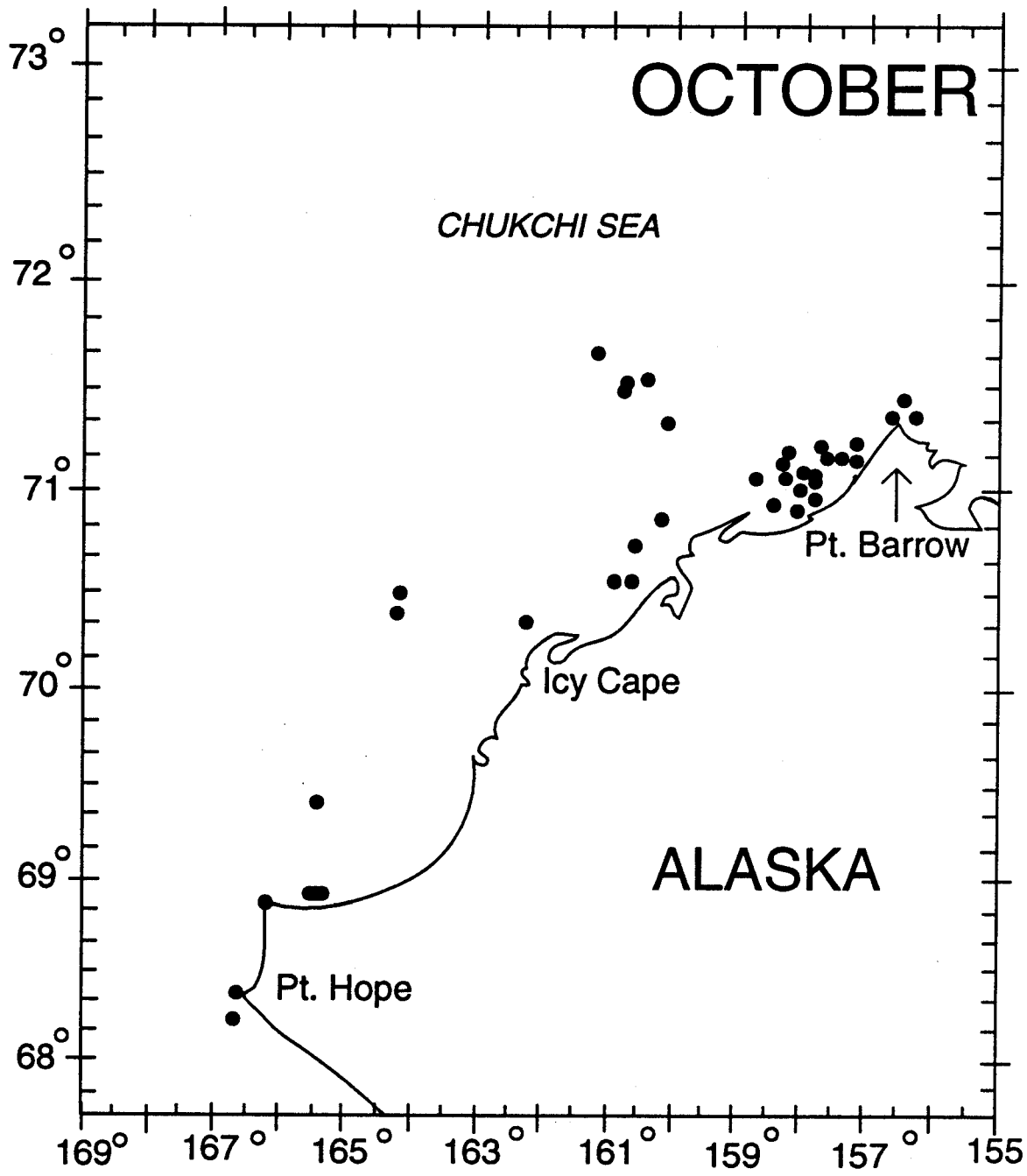

Figure 72. Distribution of 46 sightings of 82 gray whales in October, 1982 to 1987. Data from Clarke and others (1989).

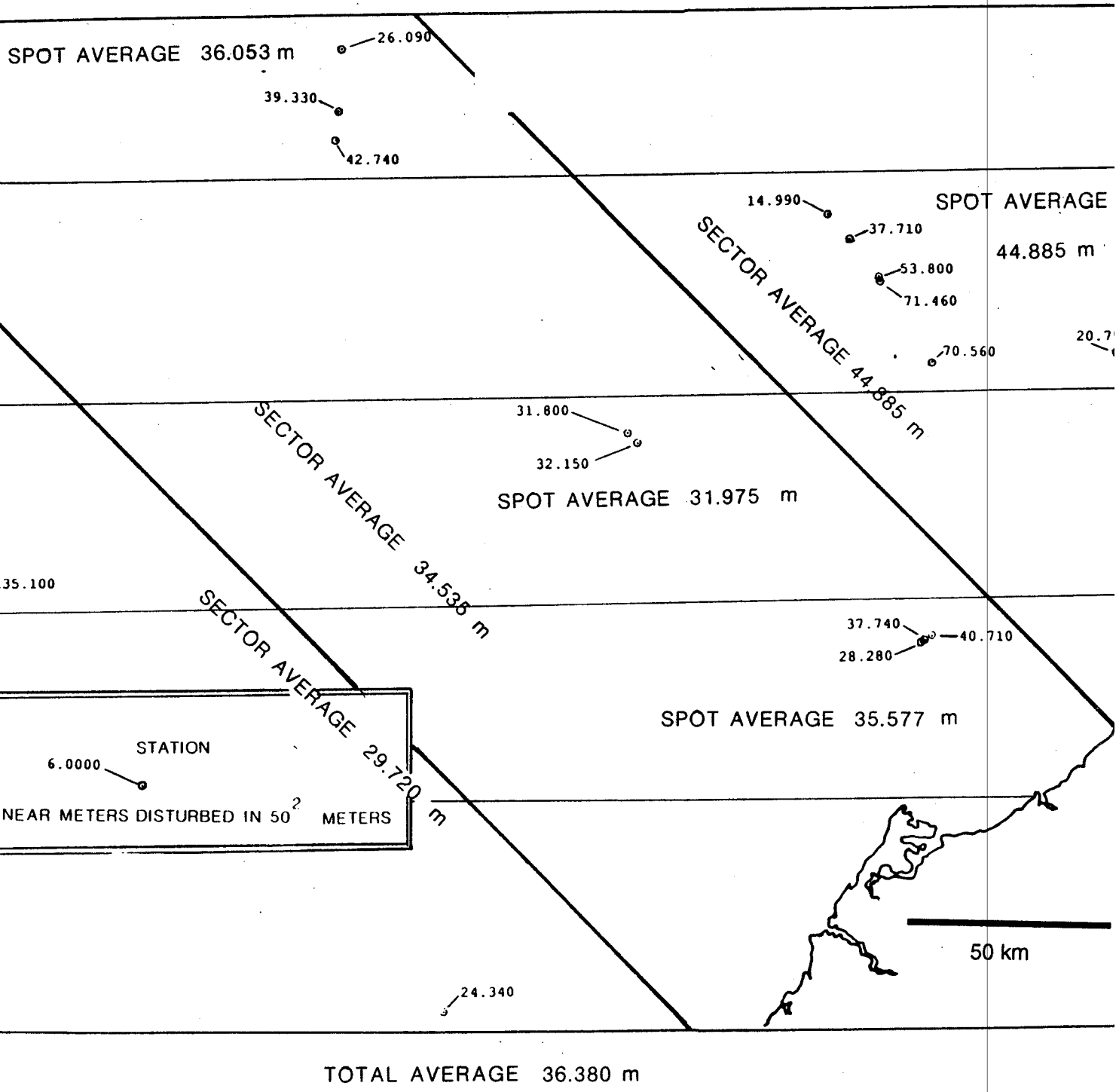

Figure 73. Map showing variations in total sediment disturbed by walrus at quantification stations in the Chukchi Sea. Values are total length of feeding furrows identified in a 50-m^2 block. Spot averages identify averages for data clusters. Sector averages identify trends parallel to the movement of the ice sheet. Overall average disturbance is indicated at the bottom of the figure.

sonar tracklines extends from this coastal area and west to 169 degrees west longitude (figs. 13-16). In this area, whale feeding pits were mainly observed within 50 km along the coast and westward for 300 km offshore from the coastal area between Icy Cape and Wainwright (fig. 17). The location of the feeding pit distribution coincides with the general distribution of whale sightings (figs. 69-72), sandy and gravelly substrate (fig. 9) and faunal assemblages III and IV that contain an abundance of amphipods (fig. 8). Whale sightings are common in the region of the sand-covered Hanna Shoal (figs. 2, 9), but we have no sidescan sonar coverage to show whale pit occurrence here because of ice cover during cruise times in this area. The highest abundance of whale sightings occurs along the coast from Pt. Franklin to Pt. Barrow, but the same problem prevented determination of pit occurrence in this area (figs. 69-72).

Feeding pits in Chukchi Sea generally are scattered across the sea floor, but in some cases they can be found in ordered groups as linear strings or clusters of pits that represent multiple suction events on a single feeding dive (fig. 4). The pits occur as four basic types (see figure 4): (1) those that are grouped, (2) elongate, (3) oval, and (4) scour enlarged that can be modified from types 1, 2 and 3. The Chukchi Sea area is dominated by types 1 and 3, with infrequent observations of types 2 and 4. Type 3 is more common in Chukchi Sea than in Bering Sea (Nelson and others, 1987), perhaps due to coarser grain size of the substrate that is typical in the whale feeding areas of Chukchi Sea. The most common configurations of type 1 grouped pits are parallel adjacent pits caused by a whale that feeds while moving laterally or drifting, strings of several pits caused by a whale that feeds while moving in a straight line, large U-shaped groups or complete circles of pits caused by a whale that feeds while turning on a larger radius, and radiating pits that result when a whale feeds while slowly turning (fig. 4).

Feeding-pit orientation and size parameters from the 18 quantitative stations in Chukchi Sea (fig. 19) are presented in Appendix 3. The orientation of whale feeding pits typically exhibits an organized pattern that is shown by orientation of long axes of the pits (fig. 74). Though the axes may vary, there is a preferred direction that appears to be related to the direction of the strongest currents in each area of quantification (figs. 11, 74). The pit orientations are either subparallel to the main coastal current and divergent eddies within the current, or they are perpendicular to currents. During cruises, whales within the strong currents also have been sighted feeding parallel or perpendicular with the currents, whereas in areas without strong currents feeding orientations were variable. The reason for the normal-to-current feeding patterns perhaps is related to a feeding behavior that utilizes the currents to efficiently push against the whale's body length like a sail as they browse for food, or it may be related to some other phenomena which we do not yet understand.

The whale feeding pits vary in size, but the statistical calculations of all the quantitative data give us some mean size numbers and standard deviations to provide a general description of pit morphology (Table 5). In Chukchi Sea, where feeding pits may be characterized as elliptical in shape, the aspect ratios average 2.8:1 (Table 5) (Appendix 3). The average length of the

feeding trace in the Chukchi is approximately 1 meter +/- 0.8 m, whereas a whale gape (mouth size) averages 2.05 m (fig. 65). The average pit length seems to be smaller here than in the Bering Sea where the average length is 3.5 m. In the Chukchi Sea, the mean pit width is 0.4 meters, +/- 0.2 m, and this pit width also is smaller than that observed in the Bering Sea, where pit width is 1.4 m.

In Bering Sea, whale feeding pits form two distinct statistical populations, termed "fresh" (i.e. approximate whale gape size), and "modified" (i.e. current-scour enlarged) (Johnson and Nelson, 1984). In the Chukchi Sea, however, only a single "fresh" (or one year class) population can be distinguished because all pits are smaller than the average whale gape size (figs. 4, 75-78) (Johnson and Nelson, 1984).

The area with the freshest and highest number of pits per square kilometer in the Chukchi Sea was located in the northeastern part of the field area where active whale feeding was observed while the data was being collected (fig. 9, Station 9). This area showed as much as 19 percent disturbance, compared to the average of 1.92 percent found in other areas. The relationship between the whale sightings and the high quantity of pit disturbance may be a key to understanding generally low disturbances in other areas. With the dominance of active bedform migration found in many whale feeding areas of the Chukchi Sea, preservation of feeding traces may be poor. The destruction of pits by bedform modification not only may help explain the paucity of whale feeding data recovered in some areas, it also suggests that our quantitative estimates of the whale feeding resource in Chukchi Sea are low.

Based on mapped presence of feeding pits, distribution of substrate suitable for amphipod prey species and on sightings of feeding whales, at least 29,782 km^2 of sea floor in the northeastern Chukchi Sea exhibits evidence of gray whale feeding activity (figs. 19, 49). Four distinct geographic areas within this region have been mapped based on the amount and kinds of amphipods available and the type of substrate (figs. 8,9) (Table 1). These four areas are; Pt. Barrow to Icy Cape (3,690 km^2), Hanna Shoal (11,952 km^2), Icy Cape to Cape Lisburne (12,160 km^2), and west of Icy Cape (1,980 km^2). Areas containing feeding pits can exhibit any of the following conditions: (1) fine sand, fairly well sorted, with some finer-grained fraction, (2) evidence of some migrating bedforms, as in the coastal sandwave fields, and (3) sea floor scouring by pack ice. Ice gouges generally occur in the relatively shallow shelf waters used as hunting grounds by gray whales.

Maps of whale sightings, (figs. 48, 49, 69-72) compiled by the University of Alaska, do not always show the highest density of sightings in the areas of highest prey density. The two coincide in some areas, including Hanna Shoal and the coastal sand sheet off Wainwright, Alaska. Where they do not coincide, the whales may be taking advantage of high planktonic productivity by feeding in the water column and not on the sea floor. Some of the areas which show the highest density of sightings, also coincide with known polynyas, where nutrient-rich upwelling can cause turbulent eddies that promote large planktonic blooms.

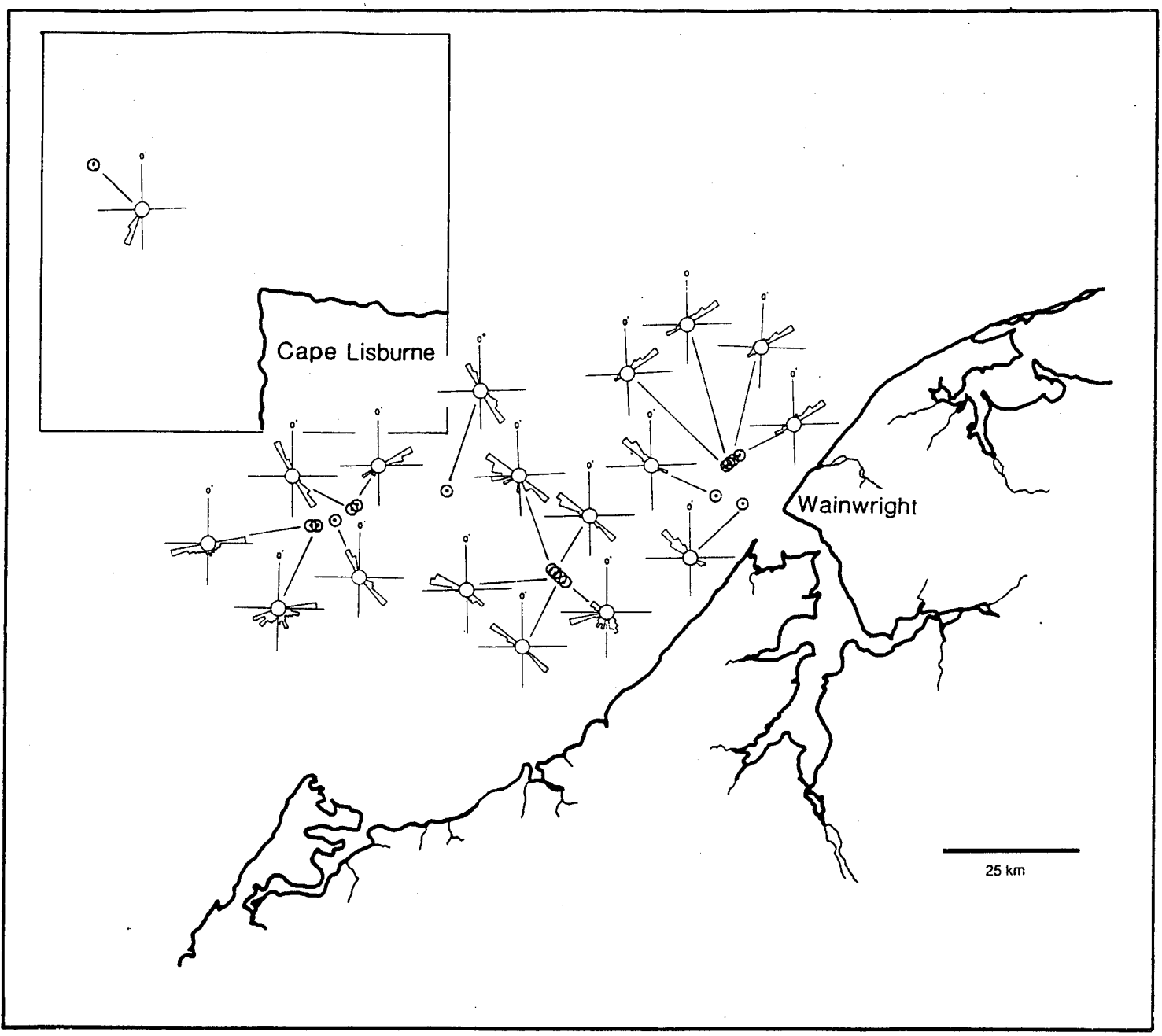

Figure 74. Map showing orientation of whale feeding traces in the Chukchi Sea. Each rose diagram summarizes pit orientation data at the indicated quantification station.

Table 5. Size parameters for gray whale feeding pits in the Chukchi Sea (n=1050).

	Average	Max	Min*
Length (m)	0.964	8.063	0.25
Width (m)	0.347	2.734	0.06
Area (m^2)	0.608	22.040	0.25

*mid-point of the smallest size class

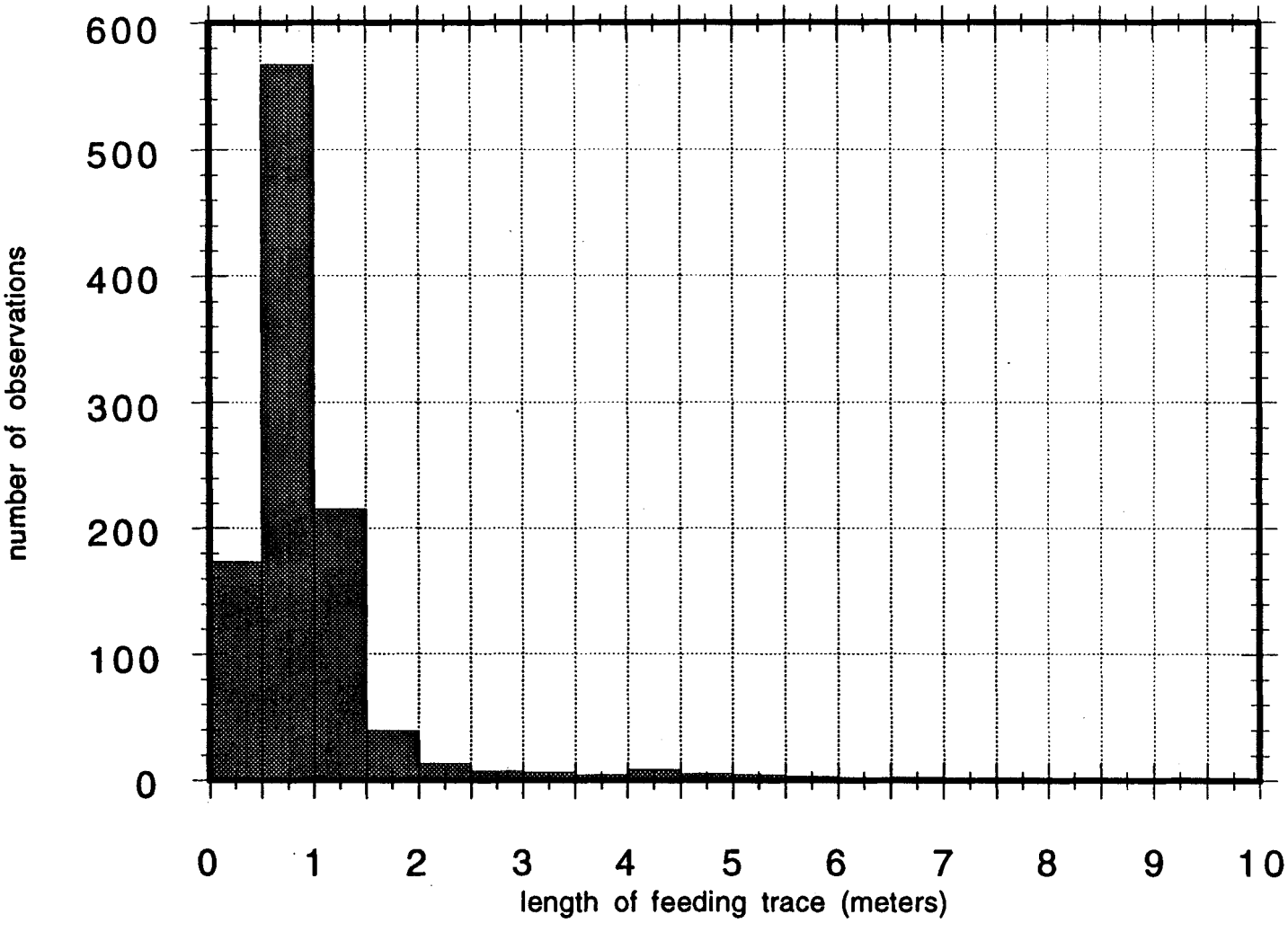

Figure 75. Histogram showing length (major axis) of Gray whale feeding pits in the Chukchi Sea. Summary of all whale quantification stations (n>1000).

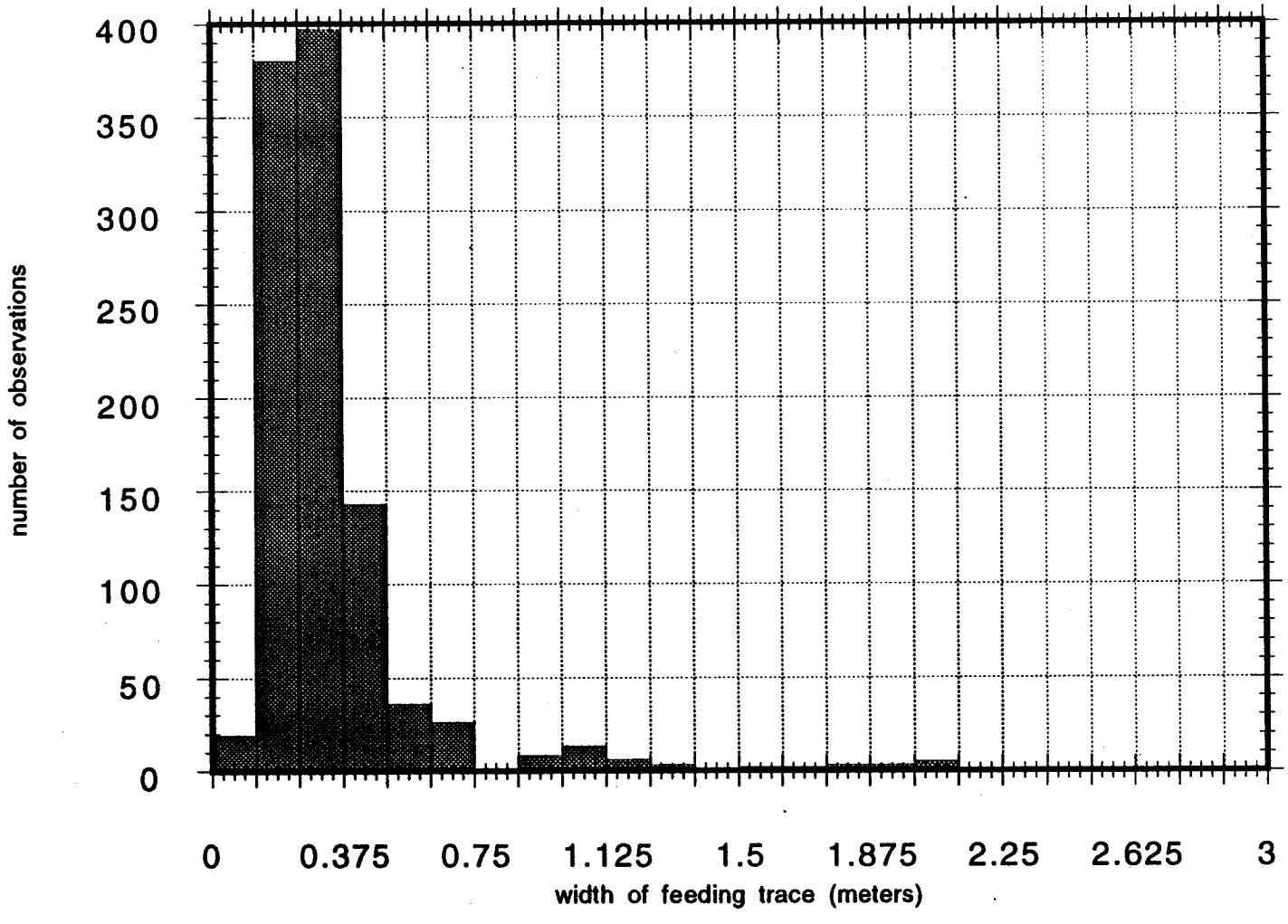

Figure 76. Histogram showing width (minor axis) of Gray whale feeding pits in the Chukchi Sea. Summary of all whale quantification stations (n>1000).

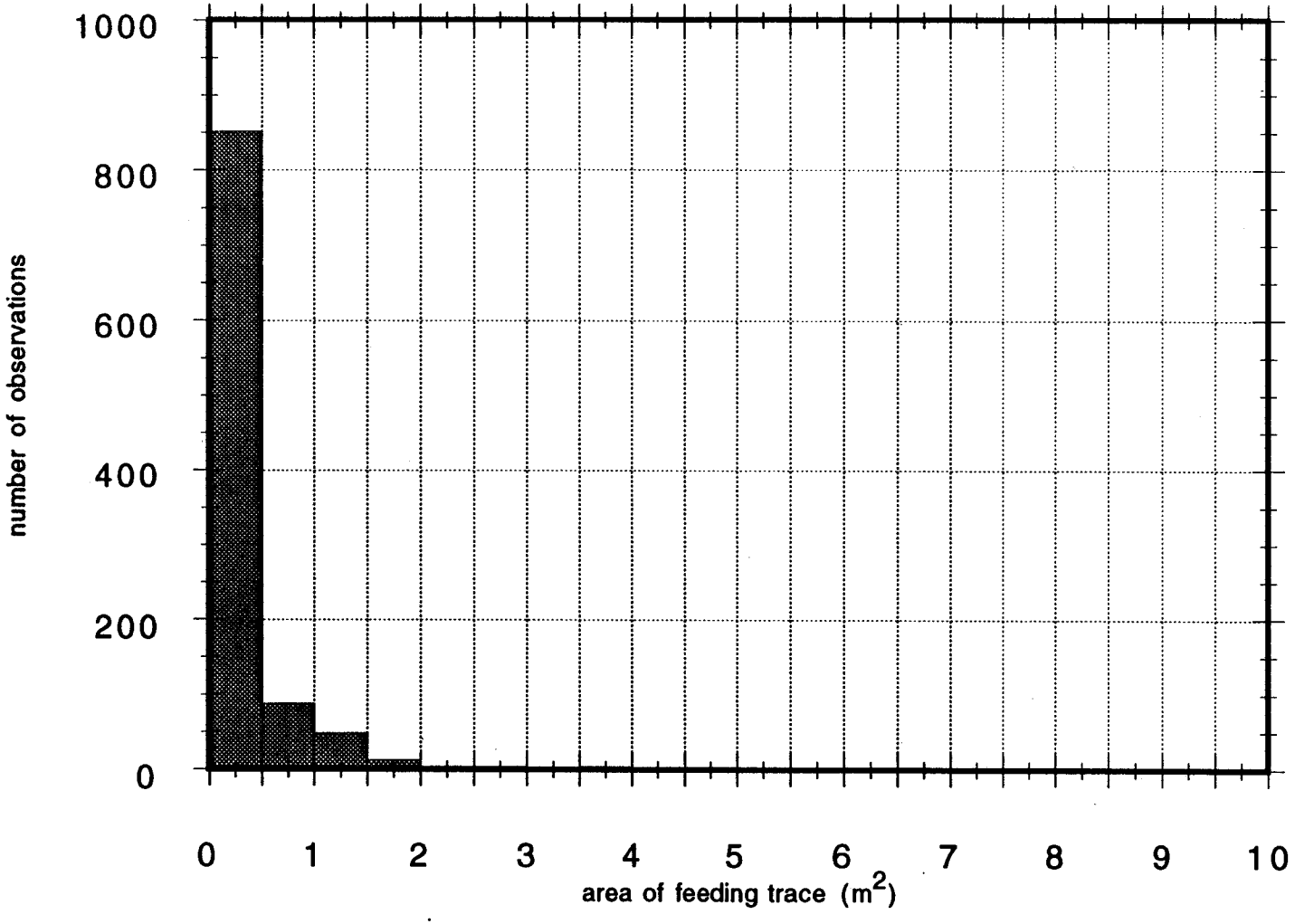

Figure 77. Histogram showing area of Gray whale feeding pits in the Chukchi Sea. Summary of all whale quantification stations (n>1000).

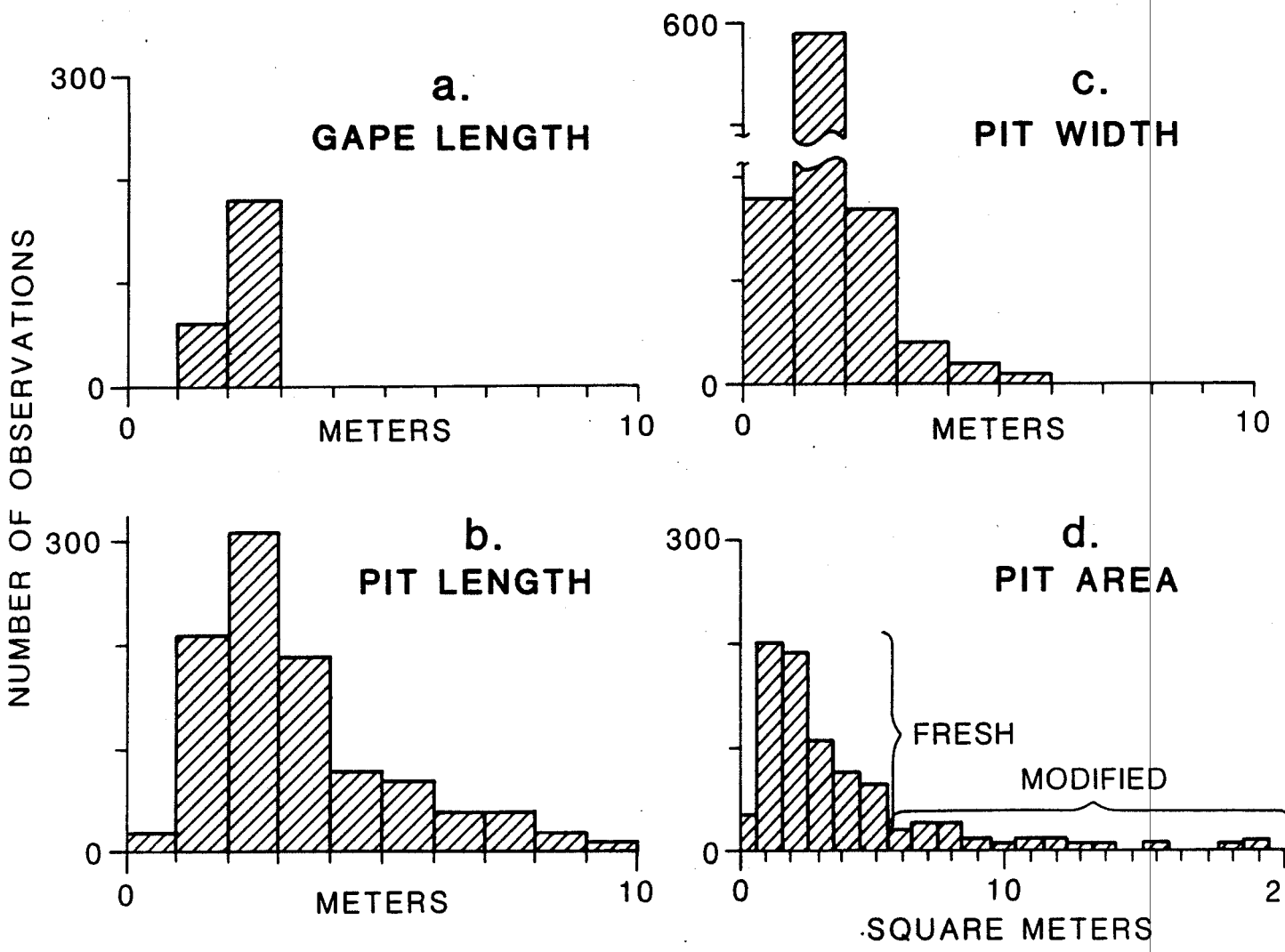

Figure 78. Histogram summarizing gape length (a) and whale-pit length (b), width (c), area (d) in the northeastern Bering Sea (from Nelson and others, 1987).

Because walrus are omnivorous, distributed throughout the Chukchi Sea during the summer season (fig. 68), and able to feed to 60 m water depth (Fay, 1982), the entire Chukchi Sea is a potential feeding ground and shows significant furrow development (fig. 18). The potential feeding area for the walrus north of Pt. Hope thus consists of a total of 180,222 km^2. In this area, 16 stations were examined in detail and the length of walrus feeding traces were measured in a 50 m^2 area (fig. 20).

The average length of individual furrow was 2.46 m, however the measured furrow length was seldom the entire length of a feeding trace, but rather was the length of a segment that had been cut by numerous other furrows. These cross-cutting relationships were not always clear to define single entire furrows and there was no way to ascertain which were fresh traces from old furrows of other years. In the Bering Sea, where there is a low density of walrus furrows and little or no cross cutting, individual traces up to 47 m in length have been reported (Nelson and others, 1987). No preferred orientation of walrus furrows could be determined because of the intense cross cutting of numerous furrows (fig. 27), difficulty distinguishing the individual furrows, and variable directions that individual furrows take when they can be traced (fig. 5).

Cumulative length of walrus furrows ranged from 15 m / (50 m^2 ≈ block) at Station 9, to 71m / block at Station 11 (fig. 73). The study area has been divided into three sectors, with the sector average disturbance computed from all the stations in each sector. The average cumulative furrow length as shown in figure 73 can be converted to percentage of seafloor disturbed, using an average furrow width of 0.40 m as determined by diving observations in the Bering Sea (Fay, 1982; Oliver and others, 1983b; Oliver and Kvitek, 1984) This calculation shows a trend from lower disturbance (29.72 m * 0.4 m / 50 m^2 = 24 percent) in the southwest sector to higher amounts of disturbance in the northeast sector (44.885 m * .04 m / 50 m^2 = 36 percent). This 12 percent increase in disturbance in the northeast sector is attributed to fresh feeding grounds being developed along the receding ice edge where feeding was most active at the time of sidescan data collection in September (figs. 15, 16, 66). At progressively greater distances from the ice edge at this time there apparently has been greater furrow destruction by wave and current reworking of the sea floor.

The average cumulative furrow length per block for the walrus quantitative stations is 36.38 m for the entire northeastern Chukchi Sea (fig. 73), or 36.38 m * 0.4 m / 50 m^2 = 29 percent. Since each block is 50 m^2, and assuming that the blocks are representative of the Chukchi Sea floor, we determine that 29 percent of the Chukchi sea floor observed in our sidescan records is disturbed by walrus feeding.

Our sidescan records do not show the total amount of walrus feeding during the year, since the records were collected in August and September, and ice does not close off the feeding grounds until November typically. We estimate that our records were taken when only 57% of the feeding season had taken place.

The remaining 43 percent of the feeding season should produce (.29/.57)*.43, or an additional 22 percent of sea-floor disturbance, indicating the the potential total disturbance of the seafloor by walrus furrows during the entire feeding season is 29+21=51 percent.

How much of this furrow disturbance occurred in the same season in which it was observed? Whale-pit feeding disturbance in the Bering Sea shows a clear differentiation between smaller pits which can be presumed to be produced in the current year, and larger, current-modified pits which have had at least one intervening storm season (Johnson and Nelson, 1984). Unlike these whale feeding pits, there are no criteria from sidescan images to assess how much of the 51 percent walrus furrow disturbance is due to fresh new-year-class walrus furrows. We did demonstrate, however, a 12 percent increase in disturbance from the southern open water to the northern ice edge in September when our sidescan sonar images were collected (figs. 15, 16, 66, 73). This suggests an additional 12 percent of new walrus furrow development occurs as the ice edge and associated feeding walrus population migrates southward during the fall. If this scenario is correct, than the northward and southward feeding passes together cause about 24 percent sea-floor disturbance from fresh furrow development each year and the other 27 percent of the observed 51 percent total disturbance is attributed to furrows from previous years.

IMPLICATIONS FOR WHALE FOOD RESOURCES

The distribution and density of the whale feeding pits can be used to create a whale food resource budget for the northeastern Chukchi Sea. The sea floor of the northeastern Chukchi Sea includes approximately 29,782 km^2 that have the correct substrate and prey types for gray whale feeding (figs. 8, 9) (Table 1). Because there is no significant evidence of scour enlargement, and storm reworking of the sea floor is extensive in the whale feeding area (fig. 43), we can assume that all the pits we quantified are recent pits from the years the data was collected. Thus, the average disturbance can be used to calculate the total disturbance and faunal intake in the Chukchi whale feeding regions. These areas for calculation include all inshore areas of fine sand substrate where whale prey fauna are found (fig. 9) (Feder and others, 1989).

Because fresh pits do not seem to accumulate significantly from year to year in the Chukchi Sea or the Bering Sea (Johnson and Nelson, 1984), they can be used to measure the minimum yearly feeding pressure. By using the percentage of area disturbed by fresh whale feeding at specific sample sites (Table 5), we can calculate the total area of recent pits in the northeastern Chukchi Sea feeding region. An average of 1.7 percent disturbance due to recent pits was observed in the 38,846 m^2 that was closely analyzed by computer methods (Tables 6, 7). Cruise data were collected mainly between Aug. 26 to Sept. 17, 1984 and Sept. 14 to Oct. 6, 1985 (23 days on each cruise). The gray whale feeding season in the northeastern Chukchi Sea lasts from July through October (Clarke and others, 1989), therefore approximately 65 percent of the yearly feeding record had accumulated by the time

Table 6. Summary of walrus feeding disturbance identified at 16 quantification stations in the Chukchi Sea.

Station #	Area examined (m^2)	Total furrow length (m)	Area disturbed (m^2)*
1	50	40.71	
2	50	37.74	
3	50	28.28	
4	50	42.74	
5	50	39.33	
6	50	26.09	
7	50	20.79	
8	50	37.71	
9	50	14.99	
10	50	53.80	
11	50	71.46	
12	50	70.56	
13	50	32.15	
14	50	31.80	
15	50	24.34	
16	50	35.10	
total	800	607.55	243.02

*Based on width of walrus feeding furrow = 0.4 m.

Table 7. Comparison of walrus and gray whale utilization of the Chukchi Sea floor.

	Gray whale	Pacific walrus
(1) Chukchi Sea feeding ground ground (km^2)	29,782	180,222
(2) Survey area (m^2)	38,846	800
(3) Survey area with feeding disturbance (m^2)	647.72	243.02[a]
(4) Percentage of survey area disturbedby feeding (observed)	1.7	30.4
(5) % of total disturbance (extrapolated to single full year)	2.62	24[b]
(6) total area disturbed by feeding (5)*(1) (km^2)	780	43,300
(7) total feeding area in Alaska (km^2)	10^6 (c)	10^6 (c)
(8) % of total feeding area (1)/(7) (km^2)	3	18
(9) minimum % of total food resource from Chukchi Sea.	0.8[d]	25 (?)[b,e]
(10) maximum % of total food resource from Chukchi Sea.	4.4[f]	126 (?)[g]

[a] From Table 6.
[b] based on 12% change from south to north feeding range in 1/2 feeding year.
[c] Frost and Lowry (1981) for whale area; walrus assumed approximately the same.
[d] see p. 25 for explanation.
[e] with the assumption that 1/5 of biomass is utilized.
[f] see p. 29-30 for explanation.
[g] see p. 26-28: note that this assumes that total biomass is consumed each year, whereas walrus are selective feeders of mainly clams that take several years to reach maturity, thus, maximum estimated total food resource may be closer to percentages shown in (4) and (5).

the data were collected. Therefore the percentage of sea floor disturbed by the end of the feeding season was (0.017/0.65) or 2.62 percent. The actual disturbance area probably was greater than this because of the strong bottom currents, mobility of the substrate, and complete or partial covering of some feeding traces before the sidescan data was obtained (fig. 79).

The area of fresh feeding pits combined with the ratio of biomass of the amphipod and other soft-bodied prey population per unit area may be used to approximate the total weight of biomass utilized for whale feeding in one season in the northeastern Chukchi Sea. In our calculations we assume uniform amphipod distribution and uniform whale foraging behavior in areas of the correct substrate and biomass for whale feeding. Feder and others (1989) show a mean amphipod biomass in the whale foraging area of 28.59 g/m^2 (28,590 kg/km^2). In addition, whales are known to consume other soft bodied worms (Klaus and others, 1990) in the foraging area which average 14.46 g/m^2 (14,460 kg/km^2) (Feder and others, 1989). The estimated total area disturbed by gray whales (29,782 km^2 * 2.62 percent, a total of 780 km^2) multiplied by average estimated prey species biomass (43,050 kg/km^2) yields the total biomass consumed by gray whales in the northeastern Chukchi Sea during an average feeding season (33,600,000 kg).

The amount of food that a mature gray whale consumes each day has been calculated by three groups of workers. Zimushko and Lenskaya (1970) calculated a feeding rate of 1,200 kg/day. Both Rice and Wolman (1971), and Brodie (1975) calculated rates of 1,000 kg/day. Averaging the reported whale feeding rate (1,100 kg/day) and the total estimated prey species biomass consumed in the northeastern Chukchi Sea (33,600,000 kg) we calculate that the number of whale feeding days (hereafter referred to as 'WFD') that the northeastern Chukchi Sea is estimated to provide is 30,545 WFD (33,600,000 kg of prey divided by 1,100 kg per day per whale). This is a minimum estimate because the sidescan sonar system does not detect feeding disturbance that is present at a site but smaller than the system is capable of resolving.

The relative importance of the northeastern Chukchi Sea as a gray whale feeding area is estimated by calculating the total number of WFD per season in Alaskan waters for the entire gray whale population for the duration of the feeding season. Assuming a population of 21,100 whales (Loughlin, 1992) that spends at least 180 days/year feeding in Alaskan waters (Clarke and others, 1989), this population accrues 3,800,000 WFD/season. Thus, northeastern Chukchi Sea, whose potential substrate area for whale feeding covers 29,782 km^2, or 3 percent of Alaskan feeding area (29,782/1,000,000), accounted for a minimum of 0.8 percent of the food resource (30,545 WFD / 3,800,000 WFD).

These are minimum estimates because areas with the highest numbers of whale sightings have not yet been surveyed with sidescan sonar surveys, and these areas may be regions where both filter feeding and benthic feeding occurs. Of the areas studied, it is important to note that sonographs slightly underrepresent features that are not parallel to the trackline (Oliver and Kvitek, 1984). Whale feeding is not accounted for along margins of large pits. Underestimation error results from modification by storms and ice destroying pits before sidescan analysis. If other whale feeding methods could be documented in the Chukchi Sea, such

as an epibenthic method for utilizing the more gravelly substrates where pits may not be observed on sidescan, or more dependence on planktonic blooms and nektonic lifeforms, the area may be able to contribute more to the total whale feeding days figure. These reasons and the dominance of smaller-sized female and juvenile populations observed in the Chukchi Sea may make the food resource several times the minimum estimated amount.

IMPLICATIONS FOR WALRUS FOOD RESOURCES

Through the process of jetting a furrow, a walrus will disturb a calculable amount of sediment. The width and depth of furrows are relatively constant, with length being the determinant factor in disturbance. Walrus generally feed on most benthic fauna, limited to a water depth of less than 60 meters. As in the whale food resource calculations, we will use the biomass of walrus prey species (Feder and others, 1989) over the area where walrus prey species occur (the entire Chukchi Sea to a depth of 60 m) and attempt to determine the relative importance of the Chukchi Sea as a walrus food resource.

The most recent census finds that the total walrus population in the Bering and Chukchi seas is about 234,000 and remaining stable or beginning a slight decline in numbers (Gilbert, 1989; Loughlin, 1992). It is estimated that each walrus eats an average of 85 kg of food each day (Fay, 1982). The total northeast Chukchi Sea area available to walrus for harvest of prey species is 180,222 km^2. Using an estimated new disturbance each year of 24 percent as determined from sidescan sonar images in this study, walrus then disturbed a total of 43,300 km^2. With an average prey biomass of 211.5 g/m^2 (211,500 kg/km^2), the total amount of prey consumed annually by the walrus in the Chukchi Sea could be as much as 9,148,000,000 kg. When the total number of kilograms consumed is divided by the number of kilograms (85) consumed by a walrus each day, we get the walrus feeding days (hereafter referred to as WalFD) provided by the Chukchi Sea, which would equal 107,600,000 WalFD. Walrus are assumed to feed every day, so the walrus population, multiplied times the number of days in a year, will give the total WalFD requirements for the entire walrus population each year (234,000 walrus * 365 days) which is 85,410,000 WalFD per year. The Chukchi Sea can thus support 1.26 times the walrus population each year according to these calculation estimates based on a total yearly sea floor disturbance of 24 percent.

<u>For the following reasons related to sidescan and biomass methodology as well as walrus feeding habits, it appears that the above calculation method does not give reliable walrus food resource results as it does for whale food resources</u> :

1. For whale pits we have methods to determine the fresh feeding pits from older pits of other year classes, but we cannot distinguish fresh and older walrus furrows. Because many of the substrate areas are gravel-rich (fig. 9), it is likely that we observe furrows from several years and this results in a significant overestimation of the yearly walrus feeding disturbance if, as the above calculations assume, they are all from one year.

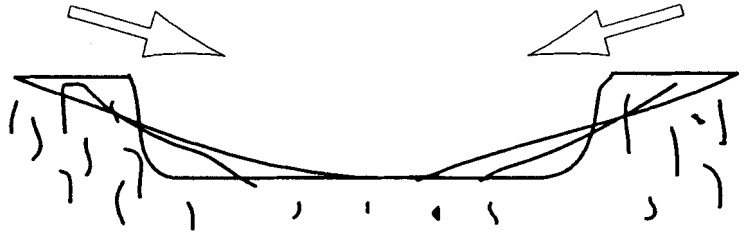

Bering Sea (Chirikov Basin)

Pervasive amphipod mat, finer sand size, higher, sediment cohesion, no superimposed bedforms = higher preservation potential

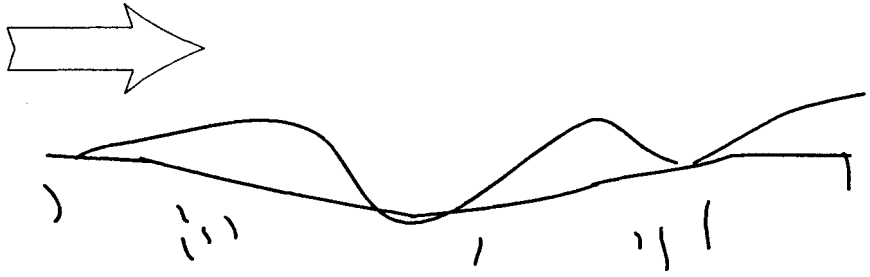

Chukchi Sea

Sparse amphipod mat, coarser sand size, lower sediment cohesion, superimposed bedforms, = lower preservation potential

Figure 79. Comparison of preservation potential of gray whale feeding pits on the Bering sea floor (Chirikov Basin) and the Chukchi sea floor, based on substrate characteristics.

2. Another important problem is that walrus furrows are at the limits of resolution for the sidescan images and thus the best examples had to be selected for analysis which leads to a possible bias toward images with higher furrow density than average. Furrow length and average disturbance numbers, however, are quite consistent from station to station (fig. 73).
3. Evaluation of biomass calculations and feeding habits are much more complicated for the walrus than the whale because whales are non-selectively eating mainly single year class amphipods and worms. In contrast, the main food source for the walrus are clam species that have a wide variation in year classes from perhaps 1-15 years. For example, if a mean age of the standing stock food source for walrus is 5 years in northeastern Chukchi Sea, then our estimate of the biomass utilized from the furrows should be one fifth that shown by the calculations above.
4. It is also known from stomach content analysis that walrus are selective feeders preferring mainly clams (Stoker, 1981). Consequently, walrus furrowing activities primarily may be a searching behavior in which a significant portion of sediment is disturbed, but much of the total biomass is not eaten. Our above calculation methods, however, had to assume utilization of all biomass because there is no way to predict this variable feeding behavior.

An independent calculation of walrus energetics confirms the problems of overestimation of the yearly food supply by the above methods. If the average walrus must consume 85 kg a day (Fay, 1982), and the northeastern Chukchi Sea substrate contains an average biomass of 211.5 g/m^2 (Feder and others, 1989), then a Pacific walrus must jet approximately 18.3 cubic meters or create a total of 403 linear meters of sea floor furrows each day (assuming a furrow depth of .10 cm and a width of .40 m). We can assume that the walrus population spends about half the year creating furrows in the northeastern Chukchi Sea because the main walrus population and associated ice edge are observed here for 4 months and in southern Chukchi Sea for only about 1 month (figs. 66,68) (Sease and Chapman, 1988; Nickles, 1992). If each walrus is consuming 85 kg and the entire biomass from the disturbed sediment each day, then only about 4 percent of the northeastern Chukchi sea floor would have to be disturbed by furrowing each year (234,000 walrus * 182.5 days * 403 m of furrows per day * 0.40 m furrow width/ 10^6 m^2 per km^2/ 180,000 km^2 area of Chukchi Sea).

The energetics estimates of 4 percent disturbance and all the aforementioned unquantifiable factors about feeding ecology lead to a considerable overestimation of the walrus food resource utilized and available in the Chukchi Sea. Actually, anecdotal evidence from recent studies has shown the walrus to be increasingly dependent on fish, seals, holothurians and other coelenterates that did not previously appear to be a normal part of their diet (Fay and others, 1989). The change in diet, the greater amount of smaller and younger clams in recent stomach contents, and other reproductive data suggests that the walrus population may be under stress because it is exceeding the carrying capacity of the substrate (Fay, 1982; Fay and others, 1989).

The selective feeding and the need to find sufficient food for the walrus population together with the observation that a total of 49 percent of the sea floor is disturbed by multi-year walrus furrowing indicate that considerably more than a minimal 4 percent yearly foraging disturbance occurs in the Chukchi Sea. We make this inference because there appears to be a minimum of 12 percent new furrow disturbance where active walrus feeding was occurring when the sidescan data were collected near the ice edge (fig. 73). The actual new disturbance per year may be approximately 24 percent because an additional 12 percent of walrus feeding could occur as the ice edge and associated feeding walrus population migrates southward during the fall. The entire Chukchi sea floor thus may be disturbed every three years which suggests that the standing stock with a possible greater average age than this may not provide sufficient carrying capacity. This observation of perhaps 24 percent yearly walrus furrow disturbance in northeastern Chukchi Sea contrasts with the low gray whale disturbance measured in both Bering (5.6 percent) and Chukchi (2.62 percent) for a mammal group that has seen a 25 percent population growth during the past decade (Reilly and others, 1980; Reilly, 1983; Nelson and others, 1987; Loughlin, 1992).

COMPARISON OF CHUKCHI AND BERING SEA MAMMAL FOOD RESOURCES

We cannot make an accurate numerical estimate for walrus feeding in northeastern Chukchi Sea like we can for gray whale feeding. From the above discussions on walrus food resources, however, this area appears to provide a significant portion of the total food resource for the walrus population (e.g. > 24 percent sea floor disturbance per year). In contrast to walrus feeding, the Chukchi Sea has only 1/6 of its area as benthic feeding grounds for gray whales and provides <1 percent of the food resource for them (Table 7). This is a minimum estimate of the potential whale food resource in the Chukchi Sea because the Pt. Franklin to Pt. Barrow area with the greatest number of whale sightings (figs. 70-72) does not have sidescan data and this and other areas may have significant water-column, as well as benthic, feeding.

The food resource relations for whales and walrus are opposite in the northeastern Bering Sea. Here the gray whale food resource greater (feeding pressure is 6.5 percent at a minimum, see Johnson and Nelson, 1984) and the food resource of the walrus, although without quantified estimates, is likely many times less than that of the Chukchi Sea (Table 7) (Johnson and Nelson, 1984; Nelson and others, 1987). The even sandy substrate throughout the main Chirikov Basin area of northeastern Bering Sea contains important amphipod assemblages that result in significant gray whale feeding with only the nearshore fringes as walrus feeding grounds (Nelson and others, 1987). The walrus feeding may be greater than is apparent from sidescan images, however, because the intense whale pitting of Chirikov Basin probably destroys walrus furrows that form earlier in the feeding season. In a few locations, early season sidescan images exhibited walrus furrowing. In contrast later season images, when nearly all of our data there were collected, showed only the intense whale pitting that had obliterated all earlier walrus furrow traces (Johnson and others, 1983). It is likely, in both the Chukchi and

the Bering Seas, that by late summer, when most of our observations have been made, whale feeding has obliterated feeding furrows produced by the walrus that are following the receding ice front at the onset of summer . We suspect, however, that this is a relatively marginal effect, since the prey habitats for walrus and gray whales do not overlap significantly.

To more completely assess the differences between mammal food resources of the Bering and Chukchi seas, more seasonal data needs to be collected and greater sidescan coverage is necessary. Seasonal monitoring with sidescan data is required to determine interplay of the whale and walrus feeding in places like Chirikov Basin and to assess the rate of modification of the feeding features, particularly walrus furrows in the Chukchi Sea. Such information will be required to make quantitative estimates of walrus feeding activity. Sidescan images need to be obtained to analyze mammal feeding resources on the Russian sides of the Bering and Chukchi seas. Significant portions of the whale and walrus populations have always been observed feeding off Russia, but this feeding activity of both mammal groups appears to have increased greatly off Russia in the past few years (Fay and others, 1984; Sease, 1985; Gilbert, 1989; Nickles, 1992; Piatt, 1992).

The whale food resource is significantly underestimated by our lack of sidescan sonar data for the Russian part of the Chukchi Sea. The combination of few reported whale sightings (figs. 70-72), the limited distribution of sandy substrate and the low quantity of prey species (Feder and others, 1989) suggest that the American side of the Chukchi Sea provides a relatively small amount of the total food resource for the gray whales. In contrast, high quantities of whale sightings have been reported off the Chukchi coast of Russia and summer populations of 2,000 to 10,000 have been estimated (Berzin, 1984; Blokhin, 1984).

Analysis of whale energetics shows that the northeastern Bering Sea, with its relative abundance of amphipod prey species and tremendous extent of fine sand, appears to support a much larger proportion of the gray whale population than the northeastern Chukchi Sea (Johnson and Nelson, 1984; Nelson and others, 1987). Analysis by Rice and Wolman (1971) show that a gray whale gains an average of 5,063 kg during a summer feeding season in Alaska. The weight gain was based on the difference in yield of rendered fat from whales hunted before and after the feeding season. Nerini (1984) calculated that to provide the lipid fraction for this amount of gain in fat (blubber) per whale, a gray whale must consume 36,821 kg/year of amphipods. This would require disturbing at least 3,556 km^2 of amphipod-rich substrate to feed the entire gray whale population for a year (Nerini, 1984). This figure suggests that the Chirikov Basin with 1200 km^2 of disturbed area, or one third of the year's food supply, is a major whale food resource (Johnson and others, 1983). In contrast, the 780 km^2 of disturbed area in northeastern Chukchi Sea on average contains only 25 percent of the amphipod biomass of Chirikov Basin (Nerini, 1984; Feder and others, 1989). Based on this energetics model, if the northeastern Bering Sea provides about 33 percent of the whale food resource by benthic feeding, the northeastern Chukchi comparatively provides about 5.4 percent based on a whale population of 16,000 in 1984 (Reilly, 1983).

With the present population at 21,000 (Loughlin, 1992) these comparative figures are reduced to 25 percent and 4.4 percent respectively for Bering Sea and Chukchi Sea.

One of the reasons for the lower food resources based on disturbance observed on sidescan images of the Chukchi Sea is that pit sizes there are significantly smaller than in Bering Sea. The average Chukchi whale feeding trace is 0.96 m long, 0.35 m wide, with an area of 0.6 m (Table 5) compared to average Bering Sea pit 3.5 m long by 1.4 m wide with an area 4.9 m^2 (Nelson and others, 1987). There are several potential explanations, and it is likely that a combination of factors is responsible for the differences that we see from the Bering Sea data. The causal factors may be divided into categories of geologic (e.g. grain size, currents, storms) and biologic processes (e.g., population demographics).

In the Bering Sea, whale pit size averaged 35 percent smaller in the coarser grain size of gravelly sand compared to fine sand with amphipod mats (Johnson and others, 1983; Nelson and others, 1987). In the Chukchi Sea, most of the substrate of whale feeding areas is gravelly, and this coarser sediment is less cohesive and more subject to slumping around the pit margins, thus reducing pit diameter and making them rounder (fig. 79).

This coarser and less cohesive sediment of the Chukchi Sea is also more easily eroded and thus under the shearing stress of the strong coastal current, migrating bedform fields are common in the main area where whale pits form (figs. 17, 43). Consequently, pits may be rapidly modified and partially covered by migrating bedforms which would further reduce the pit size before sidescan images were collected. Large unmodified whale feeding pits were common in the Bering Sea because the cohesive amphipod mats in most feeding areas resulted in good preservation of pits and the main storm modification of pits occurred in the winter storm season after the the summertime collection of sidescan data (Johnson and others, 1983; Nelson and others, 1987).

The storm season in the Chukchi Sea is not as seasonal as that in the Bering Sea and major events may occur several times a summer with consequent modification of pits (Phillips and Colgan, 1987a). As a result, any time during the ice free period when whales feed, there is also a strong potential for pit infilling and size reduction by storm-related, wind-forced currents and wave-surge effects on the sea floor. The physical processes of migrating bedforms during normal weather and storm modification combined with coarse grain size appear to have a strong impact on the preservation of feeding traces in the Chukchi Sea. The presence of maximum pit disturbance on sidescan images collected among actively feeding whales suggests that physical processes actrivley modify pits during the summer (figs. 17, 49). During the winter, ice gouging in the shallower shelf areas of whale feeding further modifies the feeding pits (fig. 38).

Small pit size in the Chukchi Sea also may result in part from selected distribution of more whale cows and and smaller-sized calves in the Chukchi Sea. Cow and calf pairs remain in the breeding grounds longer than the bulls, and consistently lag behind the bulls as they migrate north to the summer feeding grounds (Reilly, 1983). The delay in arrival appears to force cow and calf pairs to the Chukchi, because the prime areas in the Bering Sea may already be occupied by a high density of whales or

may even be stripped clean of prey by the earlier arriving bulls. The net result of more calves with small-sized mouths in the Chukchi Sea compared to more older bulls with the largest-sized mouths in the Bering Sea may help cause a larger proportion of small original whale feeding pit sizes in the Chukchi Sea.

The larger average pit size in the Bering Sea compared to the Chukchi Sea also results in part from inherent biological and physical processes that have been defined in the Bering Sea. Original smaller pits are observed to have been later enlarged by continued whale feeding along the margin of a pre-existing pit or by bottom-current scour (fig. 4) (Nelson and others, 1987). The enlargement of pits by edge feeding has been observed by divers and documented in sidescan profiles in local bays of western Vancouver Island (Kvitek and Oliver, 1986). In the Bering Sea, uniformly enlarged and oriented pits are observed to have formed from current scour (fig. 63). The shape and orientation of the whale-enlarged pits observed by Kvitek and Oliver (1986) are irregular compared to the shape of typical current-scour-modified pits. Because there is a regional orientation of the larger pits and the observed size distribution of pits was evenly skewed to the right at every station examined in the Bering Sea (fig. 78) (Johnson and others, 1983), the predominant enlargement process appears to be current scour.

If current scour modification of whale pits was taking place in Chukchi Sea, there should be a continuum of pit sizes ranging from fresh to greatly enlarged. Instead, pit size is limited from 0.5 m to 2.5 m in length, with few pits that lie significantly outside this population (figs. 75-77). This contrasts with the Bering Sea enlarged pits and may be explained by the substrate differences in the two areas and the different response to bottom current shear. Previous studies in the Bering Sea show that in sediment with a fine sand size (0.088 mm) or less, such as Chirikov Basin, current speeds greater than 18 cm/s will cause erosion and formation of scour depressions (Larsen and others, 1979). In the Bering Sea areas where grain size is greater than fine sand, and both substrate as well as current speeds are comparable to those of the coastal current in northeastern Chukchi Sea, mobile bedforms occur (Nelson and others, 1982). Consequently, current-scour-enlarged pits would be expected to characterize Chirikov Basin whale feeding areas and mobile bedform fields that cover and reduce pit size would be expected in northeastern Chukchi Sea.

IMPLICATIONS FOR GEOLOGIC PROCESSES

Gray whale feeding habits have a profound effect on the geology of feeding areas as a result of the cumulative effects of continuously reworking the sediment. Box cores from the central Chirikov Basin, the intense whale feeding area in the Bering Sea, show very few physical sedimentary structures (Thor and Nelson, 1979; Nelson and others, 1981). This may also be true in the Chukchi Sea, but at present a less detailed analysis of sediment disturbance has been completed (Appendix 1).

A much more significant geologic process is the introduction of suspended sediment into the water column by both whale and walrus benthic feeding processes. Based on sidescan sonar images,

a minimum of 780 km^2 of the Chukchi Sea appears to be disturbed by whale feeding each year (Table 8). With a minimum excavation depth in the feeding pits of 10 cm, it is possible to calculate the volume of sediment that is resuspended when it is engulfed by gray whales and expelled into the water column (Nelson and others, 1987). A minimum of 78 million m^3 (780 km^2 x 10 cm) or about 112 million metric tons[1] of bottom sediment is resuspended each year by whale feeding in the Chukchi Sea (Table 8). This amount is approximately 1.86 times the annual suspended sediment discharge (60 x 10^6 metric tons) of the Yukon River, the third largest in North America (Milliman and Meade, 1983). This sediment is tranported by the Alaskan Coastal Current through the northeastern Chukchi Sea (Nelson and Creager, 1977). The sediment resuspension by whale feeding in the Chukchi Sea is about two thirds that in the Bering Sea (Table 8) (Nelson and others, 1987).

Bioturbation by whales and walrus may winnow out fine silts improving the sorting of the fine sands, and providing the ideal habitat for amphipods. Whether the fine sediment ejected as a result of whale feeding remains as part of the suspended sediment load, or settles back to the sea floor, is a function of the local current regime and grain size. Most sand and coarse silt expelled by feeding whales does settle quickly to the bottom where it helps to fill in the whale feeding pits. Finer suspended silt and clay particles may be entrained in the strong Alaskan Coastal Current (Nelson and others, 1987) and be transported out of the northeastern Chukchi Sea to the Beaufort Sea.

To estimate the sediment resuspension amounts caused by walrus feeding activity each year is not as simple as whale sediment resuspension budgets because of problems defining fresh feeding furrows from older year furrows. Maximum and minimum amounts, however, can be constrained by two independent calculation methods. If the 24 percent total observed furrow disturbance on sidescan images is assumed to be from the same year, then over 6 billion tons of sediment at a maximum may be resuspended by walrus feeding (Table 8). To sustain the walrus population for the past decade at the numbers that have been maintained and with the population distribution that has been observed (figs. 68, 70-72) (Sease and Chapman, 1988; Gilbert, 1989), the walrus population has been feeding for at least half a year in northeastern Chukchi Sea. This requires that the average walrus must consume 85 kg of biomass a day (Fay, 1982) and assuming that the substrate contains an average biomass amount of 211.5 g/m^2, then each walrus must jet approximately 18.3 m^3 or disturb a total of 403 linear meters of sea floor each day assuming a furrow depth of 10 cm and a width of 0.40 m. Consequently, about 4 percent of the sea floor must be disturbed (234,000 walrus * 182.5 days * 403 m of furrows per day * 0.4 m furrow width/ 10^6 m^2 per km^2/ 180,000 km^2 area of northeastern Chukchi Sea). This results in about 1.18 billion tons of sediment that must be resuspended each year to meet these minimum feeding requirements (234,000 walrus * 182.5 days * 18.3 m^3 sediment * 1.43 t/m^3). Again, for a common reference point this is about

[1]One m^3 of sediment having a bulk density of 1.88 g/cm^3 (an average value for the sandy area of the northeastern Bering Sea contains 1.43 tons of sediment (Olsen and others, 1982).

Table 8. Sediment budget for marine mammal disturbance, northeastern Bering Sea and southeastern Chukchi Sea.

	Gray whale		Walrus
	Bering	Chukchi	Chukchi
(1) Area disturbed (km^2)	1200[a]	780[b]	$43.3*10^3$[(b)]
(2) depth of trace=10^{-4} km (10 cm)			
(3) volume disturbed (1)*(2) (km^3)	0.12	0.078	4.33
(4) Dry bulk density=$1.43*10^9$ t/km^3[(c)]			
(5) Weight of sediment resuspended (3)*(4) (t)	$172*10^6$	$112*10^6$	$6.19*10^9$

[a] from Nelson and others (1987).

[b] from Table 7, line 6: assumes 24% new walrus disturbance each year.

[c] dry bulk density derived using wet bulk density=1.88 g/cm^3, grain specific gravity=2.6 g/cm^3, and water content=45% by weight. t=metric ton=10^6 grams.

18.6 times the annual suspended sediment discharge of the Yukon River.

Analysis of the sidescan images shows that the walrus because of selective feeding habits (i.e. not capturing and consuming the total biomass per sediment volume) are disturbing much more than the estimated 4 percent amount of sea floor to satisfy their feeding requirements. As described previously, the actual disturbance per year appears to be approximately 24 percent. If about 24 percent of the northeastern Chukchi sea floor is disturbed each year, then based on present data, about 6.19 billion tons of sediment per year, over 100 times the Yukon sediment load, may be resuspended by walrus feeding activity (Table 8).

Current Transport of Sediment Resuspended by Marine Mammals

Fine sediment injected into the water column by benthic mammal feeding may be advected from the region by currents. Transport pathways for this sediment depend on the height the material is injected above the sea floor, the grain size of the material, and the current speeds. Sediment plumes from actively feeding whales are often observed reaching the water surface (Moore and Ljungblad, 1984). Because gray whales may make several pits on one dive before leaving the sea floor (fig. 4) and the majority of sediment is resuspended by walrus feeding at the sea floor, we estimate that most of the sediment is introduced into the water column at a height of 0.5 m above the sea floor. We assume that most of this sediment becomes entrained in the northward-flowing Alaskan Coastal Current (fig. 11).

Current speeds in the Alaskan Coastal Current area are sufficient to advect fine silt and clay-size particles from the Chukchi Sea or to transport larger particles some distance downcurrent, depending on their grain size (fig. 11) (Coachman and others, 1975; Hufford, 1977; Nelson and others, 1987). Because we do not know the variable net northward current speeds, we can calculate neither specific distances that coarser sediment travels with each resuspension episode from mammal feeding nor what proportion of time the fine silt and clay advects northward from the western part of the American Chukchi Sea to the Beaufort Sea. Because the western area has generally low current speeds and is dominated by walrus feeding at the bottom in a clay-rich substrate, the main result of feeding resuspension here probably is local sediment remobilization and infilling of mammal feeding traces (figs. 9, 11, 18).

In the eastern region with the strong Alaskan Coastal Current and most of the whale feeding, resuspension by mammal feeding probably results in loss of most of the fine grained sediment from the region (figs. 11, 17). We can estimate the effect of this advection from mammal feeding by utilizing the estimated amount of whale and walrus sediment suspension and calculating the proportion of fine silt and clay or mud in it to show that 252 million tons of fine-grained sediment are lost from the eastern Chukchi Sea (sandy whale feeding region of 30,000 km^2 and walrus feeding region of108,000 km^2) because of mammal feeding (112 * 10^6 t whale resuspension + 6.19 * 10^9 t walrus resuspension = 6.3 billion t total resuspended sediment) * 4 percent mud) (figs. 42-

47) (Table 8) (Phillips and others, 1985). Consequently, extensive reworking of the eastern coastal sand sheet in the Chukchi Sea (Phillips and others, 1987), may prevent most long-term deposition of modern mud in this area. This reworking by mammals may in part explain the presence of a relict, transgressive inner-shelf sand with a low clay content in the eastern Chukchi Sea (fig. 11).

Current Scour

Whales and walrus not only physically excavate the sediment on the sea floor, but they also indirectly cause further erosion of the pits and furrows that they excavate. They are a major force in initiating current scour of the sea floor by eliminating the biological binding of the sediment surface and causing large-scale roughness (e.g., fig. 63). In some areas of the Chukchi Sea, there may be an amphipod mat that is a binding force holding the sediment particles together in the manner that it does in the amphipod-rich substrate of Chirikov Basin (Johnson and Nelson, 1984; Nelson and Johnson, 1987). When a whale sucks up a patch of the amphipod mat, it exposes the underlying fine sand and current scour can then become effective because the biological sediment-binding force is reduced.

Both the whale and walrus feeding traces roughen the sea floor and this significantly increases the sediment erosion and transport (fig. 79). On a flat bottom, a current velocity of approximately 30 cm/s at 1 m above the bottom is necessary to mobilize a fine (0.125 mm diameter) sand (Miller and others, 1977). On a rough bottom, the threshold velocity of erosion becomes significantly less. The velocity needed to erode sediment having the increased roughness comparable to that due to whale feeding disturbance is estimated at 18 cm/s by Cacchione and Drake (1982) (Nelson and others, 1987). In areas where currents are of sufficient strength to move only unbound sediment, the mammal feeding activity is a catalyst for erosion and scour.

The whale and walrus feeding traces are themselves a type of megabioturbation and should be recognized as primary sedimentary structures. The whale pits are similar to sediment excavations made by rays. Ray pits have been described from modern and Cretaceous sediments (Howard and others, 1977). Whale pits and walrus furrows also provide a modern example of a feature that could be recognized in the rock record to establish the presence of prehistoric benthic-feeding mammals. Given the shallowness and breadth of the pits in uncompacted sediment, and the extensive linear extent of furrows for tens of meters, identification of such features may be difficult at outcrop scales.

POTENTIAL FUTURE STUDIES

Both the modification rates of whale and walrus feeding traces and the prey species regeneration rates are critical data needed to understand the implications of California gray whale and Pacific walrus interaction with the sea floor in northeastern Chukchi Sea. These studies are most critical for the walrus because there is no way at present to ascertain new furrows from previous-year furrows. Without this furrow age distinction and an analysis of the benthic standing stock average age in Chukchi

feeding areas, it is impossible to calculate walrus energetics and estimate benthic substrate utilization as can be done with the present data base for whale pits. To assess modification rates of both walrus and whale feeding traces will require monitoring work involving the reoccupation of several stations at different depths and in different current regimes in the Chukchi Sea.

Feeding-trace modification can be examined in more detail with replicate sidescan surveys. It is possible, using shore-based navigation systems, to accurately resurvey an area with sidescan sonar (Reimnitz and others, 1977; Barnes and others, 1978). It has not been possible to identify bottom-feature changes through time during this study because of the lack of precision navigation systems, the use of sidescan systems with different resolutions, and the temporal spacing of the different surveys. A thorough study should last at least two years and should have a minimum of 2 surveys a year, one as early in the feeding season as possible and one as late in the season as possible. Ideally, a third survey should be made in the middle of each feeding season. Consistent sidescan techniques and precision navigation should be used throughout the study. A digital 500-kHz system would provide the best detail and ease of comparison between records. These data could also be used to establish year-to-year fluctuations of the areal extent of the walrus and whale feeding grounds.

A second phase of the monitoring study, particularly for walrus food stocks, should be study of the benthic prey species. The age-class composition for different prey species needs to be known, the average age of benthic standing stock must be determined and any changes in ages and types of species need to be noted. This information pertaining to average age of standing stock of walrus prey species and known area of one-year class furrows will make possible a calculation of walrus food resources in the Chukchi Sea.

The establishment of long-term current meters in the Chukchi Sea is a third type of monitoring that is essential for understanding the modification rate of furrows and pits and determining the most accurate total area of new feeding traces each year. A long-term current study makes possible an examination of the time periods during which whale feeding features are modified by storm activity, and the determination of relative ages of the feeding features. Long-term current-meter data also is necessary to model oil-spill trajectories and nutrient-plume trajectories. Information should be obtained on the sources of productivity and the possible influence of oil spill trajectories on each region of the whale and walrus feeding grounds in the Chukchi Sea.

A study done during ice-free years that combines sidescan sonar surveys, substrate analyses, and sediment history, similar to this study, could be used to survey whale-feeding grounds north of Pt. Franklin and over Hanna Shoal. Other mammal feeding areas in the western Chukchi Sea, Beaufort Sea, Bristol Bay, Aleutian Arc, southern Gulf of Alaska, western Chirikov Basin, and Gulf of Anadyr are also worthy of study. With a thorough knowledge of the sediment type and prey distribution throughout the entire feeding range of the gray whale, much more accurate estimates of feeding ground utilization can be obtained. Such a program would require

the cooperation of Russian scientists and should be coordinated with on-going studies of gray whale distribution.

The question of where the gray whales fed during the Pleistocene might be addressed by deep-water sidescan surveys on the shelf break of the Bering continental shelf. When Beringia was emergent, this area contained the proper habitat depth ranges for the gray whales. Relict sedimentary features from the Pleistocene, namely large sediment waves, have been detected with sub-bottom profilers (Karl and Carlson, 1982), and the potential to detect relict whale feeding pits does exist.

CONCLUSIONS

1. Amphipod assemblages, the main prey species of the California gray whales, are associated with 30,000 km^2 of shelf transgressive sand that mainly underlies the nearshore Alaska Coastal Current. This sandy nearshore substrate together with the central muddy shelf substrate covers 180,000 km^2 of northeastern Chukchi Sea at water depths less than 60 m to provide a variety of benthic prey assemblages for the omniverous Pacific walrus.

2. Gray whales feed mainly on amphipods by means of benthic suction, a process that produces a variety of feeding feeding pits of about 1-2 m length and a half meter width on the sea floor. Walrus feed mainly on clams by water expulsion. This feeding behavior can create nearly half-meter-wide furrows up to tens of meters in length.

3. These benthic feeding traces of pits and furrows can be studied and quantified regionally by means of the sidescan sonar, a planographic sea-floor mapping device well suited to reconnaissance surveys. This study proves the validity of sidescan sonar as a biological mapping tool for benthic feeding by whales and walrus.

4. Gray whale feeding-pit distribution as determined from sidescan sonar matches the distribution of Alaskan Coastal Water, transgressive fine sand, high concentrations of ampeliscid amphipods, and the summer sighting of feeding gray whales. Because of ice cover during studies, sidescan data were not available over the central Chukchi Hanna Shoal nor for the Pt. Franklin to Pt. Barrow coastal areas where gray whale sightings have been numerous and additional important feeding grounds may exist.

5. The ubiquitous high density furrow disturbance of the sea floor throughout the northeastern Chukchi shelf coincides with the widespread distribution of walrus throughout the summer season as they usually migrate with the retreating and advancing ice edge. The average length of furrows is only about 2.5 m because they are cut by other furrows. Young, fresh furrows cannot be distinguished from older furrows of other years year classes of benthic biomass are unknown, so that walrus food resources cannot be estimated.

6. Nearly all whale pits are small in size (<1 m^2) compared to those in Bering Sea, indicating that the pits observed in the Chukchi Sea sidescan images are exclusively fresh, one-year class pits. This permits estimates of whale food resources. Possible explanations for these smaller feeding pits include: (1) activity of strong bottom currents with migrating sand bedforms that partially cover feeding traces, (2) a generally gravel-rich

substrate that results in smaller rounder pits, and (3) a high proportion of young whales with small mouths that feed in the Chukchi Sea.

7. Total sea-floor disturbance from fresh whale feeding pits ranges from less than 1 percent to 19 percent in various feeding areas of the northeastern Chukchi Sea. The estimated average disturbance of the northeastern Bering Sea floor at the end of the gray whale feeding season equals 2.62 percent or a total of 780 km^2 of sea floor disturbance. The maximum disturbance was found where sidescan images were collected within a feeding pod of whales, which again suggests rapid modification of pits.

8. Observed disturbance from walrus furrows on sidescan images varied from 24 percent in the southwest to 36 percent in the northeast at the ice edge where associated feeding walrus occurred. The estimated total disturbance of the northeastern Chukchi Sea floor at the end of the walrus feeding season equals 51 percent of the 108,000 km^2 of Chukchi sea floor including both new year and old year furrows. The 12 percent change from south to north may represent the new year fresh furrows generated as ice receded. Additionally, if 12 percent more furrowing is added as ice advances south, annual furrowing may average an estimated 24 percent, and a yearly disturbance of 43,3000 km^2.

9. If all the biomass from furrows was consumed, only 4 percent disturbance is required to support the walrus population for a year, however, selective feeding habits and a benthic standing stock several years old suggest that a much greater disturbance closer to 24 percent each year is required. Because the entire sea floor may be disturbed by feeding furrows every three years and the average age of standing stock probably is greater, the present stable or declining population of walrus may be at the limit of the substrate carrying capacity.

10. Calculations based on the area of the sea floor disturbed by fresh whale feeding pits in the Chukchi Sea, published biomass data, estimated whale biomass feeding intake per day, and counts of whale feeding days in Alaska indicate that the northeast Chukchi Sea accounted for a minimum average of 0.8 percent of the entire gray whale summer feeding resource in about 3 percent of the total feeding region of the Bering Sea and Arctic Ocean. If 4,464 km^2 of amphipod-rich substrate must be disturbed (Nerini, 1984) to add the approximately 5,000 kg weight gain per individual that is observed from summer feeding (Rice and Wolman, 1971), then the 780 km of observed disturbance in the low average amphipod biomass of the northeastern Chukchi Sea may be estimated to provide 4.4 percent of the food resource for the present whale population of 21,000.

11. The northeastern Chukchi Sea provides much less gray whale food resource (1-4 percent) compared to the northeastern Bering Sea (5-22 percent) which has about the same area of feeding grounds. With as much as 24 percent yearly sea floor disturbance by walrus feeding, however, the Chukchi Sea provides a major portion of the walrus food resource compared to the Bering Sea. In the Chukchi Sea, whale pits are small (1 m^2) because of rapid modification by the continual strong bottom currents over non-cohesive coarser sand, whereas in the Bering Sea, whale pits are large (2-5 m^2) because removal of the cohesive amphipod mat results in current-scour enlargement during the fall storm season.

12. The whales may be farming their feeding grounds by (a) selectively capturing adult-sized amphipods, (b) seeding the juvenile amphipods, a pioneer species, into areas of freshly created and current-modified disturbance, and (c) dispersing the nutrient-rich sediment into the water column, thus boosting productivity (Nelson and Johnson, 1987). The intense walrus furrowing activity must result in a much greater nutrient recycling process than whale feeding.

13. The whale feeding results in excavation and resuspension of 112 x 10^6 metric tons of sediment each year, equivalent to about two times the yearly sediment load of the Yukon River. This is dwarfed by the walrus feeding that disturbs a minimum (2.5 percent) of 4,500 km^2 of sea floor or resuspends 560 million tons to a possible maximum disturbance (24 percent) of 43,300 km^2 or 6.19 billion tons of resuspended sediment injected into the water column each feeding season. A large proportion (4.5 million tons) of fine mud resuspended by whales near the coast is transported out of the Chukchi Sea to the Beaufort Sea each year by the strong northerly Alaska Coastal Current. In addition, sand is gradually transported northward and fills old feeding pits, and modern mud does not accumulate in the sea floor region under the Alaska Coastal Current.

14. Future studies should include: (a) the application of similar sidescan sonar reconnaissance studies to other whale feeding regions of Hope Basin, Hanna Shoal, and the Pt. Franklin to Pt. Barrow coastal area in Chukchi Sea as well as to other walrus and whales feeding regions off southern Alaska and Siberia, (b) periodic sidescan monitoring of prime walrus and whale feeding grounds in the Chukchi Sea so fresh mammal feeding traces can be identified from different years and food resource estimates refined, and (c) the examination of existing sidescan records to outline walrus feeding grounds in the northeastern Bering Sea and ascertain their relation to gray whale feeding grounds.

15. Any development or drilling affecting Chukchi requires careful planning because (1) the northeastern Chukchi Sea supports a large proportion of the walrus food resource as well as providing 1-4 percent of the gray whale food resource and (2) because the benthic population is susceptible to both oil spills and any dredging or destruction of their thin, nonrenewable substrate.

ACKNOWLEDGMENTS

We thank Mary Nerini, John Oliver, Dennis Thomson, Larry Martin, Kate Frost, Lloyd Lowry, Sam Stoker, Bud Fay, Ken Coyle, Steve Swartz, Mary Lou Jones, Steve Leatherwood, Jody Derman, Sue Moore, Marilyn Dalheim, Bob Nelson, Dale Rice, Gary Mauseth, Howard Braham, and Nora Foster for their willingness to share their knowledge of whale and walrus ecology and their benthic biology. Discussions with Erk Reimnitz, Ralph Hunter, and Peter Barnes added great depth to our understanding of the interplay of ice and other physical sedimentary processes which aided our interpretations of the the sidescan sonographs. Interpretations of current-meter data, scour enhancement, and resuspension of sediment by whales were aided by David Cacchione and David Drake. Our computer analysis of the sonographs was ably assisted by discussions with Rex Sanders, David Rubin, Tom Clifton, Bill Weber and Carol Madison.

This study was funded by the Minerals Management Service through interagency agreement with the National Oceanic and Atmospheric Administration as part of the Outer Continental Shelf Environmental Assessment Program.

Aagaard, Knut, 1984, Current, CTD, and pressure measurements in possible dispersal regions of the Chukchi Sea: U.S. Dep. Commer., NOAA, OCSEAP Final Report 57, 255-333.

Barnes, P. W., 1972, Preliminary results of geological studies in the eastern central Chukchi Sea: U.S. Coast Guard Oceanogr. Rept. Srs., v. 50, p. 87-100.

Barnes, P. W., McDowell, D., and Reimnitz, Erk, 1978, Ice gouging characteristics: Their changing patterns from 1975-1977, Beaufort Sea, Alaska: U. S. Geological Survey Open-File Report 78-730, 42 p.

Barnes, P.W., Scholl, D.M., and Reimnitz, Erk, 1984, The Alaskan Beaufort Sea: Ecosystems and Environments: Orlando, FL, Academic Press, 466 p.

Berzin, A. A., 1984, Soviet studies on the distribution and numbers of the gray whale in the Bering and Chukchi Seas from 1968-1982, *in* Jones, M. L., Swartz, S. L., and Leatherwood, S., eds., The Gray Whale: *Eschrichtius robustus* : New York, Academic Press, p. 409-419.

Blokhin, S. A., 1984, Investigations of gray whales taken in the Chukchi coastal waters, U.S.S.R., *in* Jones, M. L., Swartz, S. L., and Leatherwood, S., eds., The Gray Whale: *Eschrichtius robustus* : New York, Academic Press, p.487-509.

Bogoslovskaya, L. S., Votrogov, L. M., and Semenova, T. N., 1981, Feeding habits of the gray whale off Chukotka: Report of the International Whaling Commission, v. 31, p. 507-510.

Braham, H. W., 1984, Distribution and migration of gray whales in Alaska, *in* Jones, M. L., Swartz, S. L., and Leatherwood, S., eds., The Gray Whale: *Eschrichtius robustus:* New York, Academic Press, p. 249-266.

Braham, H. W., Everitt, R. D., Krogman, B. D., Rugh, D. B., and Withrow, D. E., 1977, Marine Mammals of the Bering Sea: A Preliminary Report on Distribution and Abundance 1975-1976: NOAA, National Marine Fisheries Service, Northwest and Alaska Fisheries Center Processed Report.

Braham, H.W., Oliver, G.W., Fowler, C., Frost, K.J., Fay, F.H., Cowles, C., Costa, D., Schneider, K., and Calkins, D., 1982, Marine mammals, Chap. 4 *of* Hameedi, M.J., ed., Proceedings of the Synthesis Meeting: St. George Environment and Possible Consequences of Planned Offshore Oil and Gas Development, 28-30 April, 1981, Anchorage, Alaska, p. 55-81.

Brodie, P. F., 1975, Cetacean energetics, an overview of intraspecific size variation: Ecology, v. 56, p. 152-161.

Brower, W.A., Jr., Diaz, H.J., Prechtel, A.S., Searby, H.W. and Wise, J.L., 1977, Climate atlas of the outer continental shelf

waters and coastal regions of Alaska, Chukchi-Beaufort Sea, v.3: Arctic Environmental Information and Data Center, Univ. of Alaska, Anchorage, 409 p.

Brownell, R. L., 1977, Current status of the gray whale: Report of the International Whaling Commission, v. 27, p. 209-211.

Cacchione, D. A., and Drake, D. E., 1982, Measurements of storm-generated bottom stresses on the continental shelf: Journal of Geophysical Research, v. 87, no. C3, p. 1952-1960.

Cacchione, D. A., Drake, D. E., Field, M. E., and Tate, G. V., 1987. Seafloor gouges caused by migrating gray whales off northern California: Continental Shelf Res., v. 7, p. 553-560.

Clarke, J. T., Moore, S. E., and Ljungblad, D. K., 1989, Observations on gray whales (*Eschrichtius robustus)* utilization patterns in the northeastern Chukchi Sea, July-October 1982-87: Can. J. Zool., v. 67, p. 2647-2654.

Coachman, L. K., Aagaard, K., and Tripp, R. B., 1975, Bering Strait: The Regional Physical Oceanography: Seattle, University of Washington Press, 186 p.

Coachman, L. K., and Tripp, R. B., 1970, Currents north of Bering Strait in winter: Limnology and Oceanography, v. 15, p. 625-632.

Consiglieri, L. D., Braham, H. W., and Jones, M. L., 1980, Distribution and abundance of marine mammals in the Gulf of Alaska from the platform of opportunity programs, 1978-1979: Outer Continental Shelf Environmental Assessment Program Quarterly Report RU-68. 11 p.

Coyle, K. 0., 1981, The oceanographic results of the cooperative Soviet and American cruise to the Chukchi and East Siberian seas aboard the Soviet whale hunting ship Razyashchii September-October 1980: Institute for Marine Science, University of Alaska, Fairbanks, 107 p.

Creager, J. S., and McManus, D. A., 1967, Geology of the floor of the Bering and Chukchi Seas--American studies, in Hopkins, D. M., ed., The Bering Land Bridge: Stanford Univ. Press, Stanford, CA, p. 7-31.

Drake, D. E., Cacchione, D. A., Muench, R. D., and Nelson, C. H., 1980, Sediment transport in Norton Sound Alaska: Marine Geology, v. 36, p. 97-126.

EG & G, Inc., Environmental Equipment Division, 1982, SMS 960 Seafloor Mapping System, Technical Presentation: 151 Bear Hill Road, Waltham, Mass. 02154.

Fay, F. H., 1982, Ecology and Biology of the Pacific Walrus, *Odobenus rosmarus divergens* Illiger: U.S. Fish and Wildlife Service series, North American Fauna, no. 74, 179 p.

Fay, F.H., Kelly, B.P., Gehnrich, P.H., Sease, J.L., and Hoover, A.A., 1984, Modern populations, migrations, demography, trophics, and historical status of the Pacific walrus: U.S. Dep. Commer., NOAA, OCSEAP, Final Rep. 37, p. 231-376.

Fay, F.H., Kelly, B.P., and Sease, J.L., 1989, Managing the exploitation of Pacific walruses: a tragedy of delayed response and poor communication. Marine Mammal Science, v. 5, no. 1, p. 1-16.

Feder, H. M., and Jewett, S. C., 1981, Feeding interactions in the eastern Bering Sea with emphasis on the benthos, *in* Hood, D.W., and Calder, J.A., eds., The Eastern Bering Sea Shelf: Oceanography and Resources, v. 2: Seattle, University of Washington Press, p. 1229-1261.

Feder, H. M., Naidu, A.S., Hameedi, J.W., Jewett, S.C., and Johnson, W.R., 1989, The Chukchi Sea continental shelf: benthos-environmental interactions: U.S. Dep. Commer., NOAA, OCSEAP, Final Rep. 68, p. 25-311.

Fleming, R. H., and Heggarty, D., 1966, Oceanography of the southeastern Chukchi Sea, in Wilimovsky, N.J., and Wolfe, J.N., eds., Environment of the Cape Thompson region, Alaska: U.S. Atomic Energy Commission, p. 697-754.

Folk, R. L., 1980, Petrology of Sedimentary Rocks: Hemphill Publishing Co., Austin, Texas, 182 p.

Folk, R. L., and Ward, W. C., 1957, Brazos River Bar: A study in the significance of grain size parameters: Journal of Sed. Petrology, v. 27, p. 3-20.

Frost, K. J., and Lowry, L. F., 1981, Foods and trophic relationships of cetaceans in the Bering Sea, in Hood, D. W., and Calder, J. A., eds., The Eastern Bering Sea Shelf: Oceanography and Resources, v. 2: Seattle, University of Washington Press, p. 825-836.

Gilbert, James R., 1989, Aerial census of Pacific walruses in the Chukchi Sea: Marine Mammal Science, v. 5, no. 1, p.17-28.

Gilmore, R. M., 1955, The return of the Gray Whale: Scientific American, v. 192, no. 1, p. 62-67.

Grantz, A., Dinter, D. A., Hill, E. R., Hunter, R. E., May, S. D., McMullin, R. H., and Phillips, R. L., 1982, Geologic framework, hydrocarbon potential, and environmental conditions for exploration and development of proposed oil and gas lease sale 85 in the central Chukchi Sea: U. S. Geological Survey Open-File Report 82-1053, 84 p.

Groves, J. E., and Stringer, W. J., 1991, The use of AVHRR thermal infrared imagery to determine sea ice thickness within the Chukchi Polynya: Arctic, v. 44 (Supp. 1), p. 130-139.

Hachmeister, L. E., and Vinelli, J. B., 1985, Nearshore and coastal circulation in the Northeastern Chukchi Sea: U.S. Dep. Commer., NOAA, OCSEAP, Final Report 57 (1988), p. 1-104.

Herzing, D. L., and Mate, B. R., 1981, California gray whale migration along the Oregon coast [abs.]: Abstracts Volume of the 4th Biennial Conference on the Biology of Marine Mammals, 14-18 December 1981, San Francisco, p. 54.

Hickey, L. J., 1973, Classification of the architecture of dicotyledonous leaves: American Journal Bot., v. 60, no. 1, p. 17-33.

Hill, E. R., Grantz, A., May, S. D., and Smith, M., 1984, Bathymetric map of the Chukchi Sea: Map I-1182-D, Dept. of the Interior, U. S. Geological Survey.

Howard, J. D., Mayon, T. V., and Heard, R. W., 1977, Biogenic sedimentary structures formed by rays: Journal of Sedimentary Petrology, v. 47, no. 1, p. 339-346.

Howell, A. B., and Huey, L.M., 1930, Food of the California gray and other whales: Journal of Mammalogy, v. 2, p. 321-322.

Hudnall, J., 1981, Population estimate, feeding behavior and food source of the gray whales, *Eschrichtius robustus*, occupying the Straits of Juan de Fuca, British Columbia [abs.]: Abstracts Volume of the 4th Biennial Conference on the Biology of Marine Mammals, 14-18 December, 1981, San Francisco, p. 58.

Hudnall, J., 1983, Gray Whale feeding behavior along the Vancouver Island coast: Whale Watcher, Journal of the American Cetacean Society, v. 17, no. 3, p. 3-5.

Hufford, G. L., 1977, Northeast Chukchi Sea coastal currents: Geophys. Res. Letters, v. 4, no. 10, p. 457-460.

Hunkins, K., 1965, Tide and storm surge observations in the Chukchi Sea: Limnol. Oceanogr., v. 10, p. 29-39.

Johnson, K. R, and Nelson, C. H., 1984, Side-scan sonar assessment of gray whale feeding in the Bering Sea: Science, v. 225, p. 1150-1152.

Johnson, K. R., Nelson, C. H., and Barber, J. H., Jr., 1983, Assessment of gray whale feeding grounds and seafloor interaction in the northeastern Bering Sea: U.S. Geological Survey Open-File Report 83-727, 112 p.

Jones, M. L., Swartz, S. L., and Leatherwood, S., eds., 1984, The Gray Whale: *Eschrichtius robustus*: New York, Academic Press, 600 p.

Kalyasin, V. E., 1989, On the maximal waves in the Chukchi Sea: Trans. Arctic and Antarctic Research Institute, v. 417, p. 1-49.

Karl, H. A., and Carlson, P. R., 1982, Large sand waves in Navarinsky Canyon head, Bering Sea: Geo-Marine Letters, v. 2, p. 157-162.

Kasuya, T., and Rice, D. W., 1970, Notes on baleen plates and on arrangement of parasitic barnacles of gray whale: Sci. Rep. Whales Res. Inst., no. 22, p. 39-43.

Klaus, A.D., Oliver, J.S., and Kvitek, R.G., 1990, The effects of gray whale, walrus, and ice gouging disturbance on benthic communities in the Bering Sea and Chukchi Sea, Alaska: National Geographic Research, v. 6, no. 4, p. 470-484.

Klein Associates, Inc., 1982, Hydroscan, Klein Side Scan Sonar and Sub-bottom Profiling Systems: Klein Associates, Klein Drive, Salem, NH 03079-1296, 47 p.

Kvitek, R. G., and Oliver, J. S., 1986, Side-scan sonar estimates of the utilization of gray whale feeding grounds along Vancouver Island, Canada: Continental Shelf Research, v. 6, p. 639-654.

Larsen, M. L., Nelson, C. H., and Thor, D. R., 1979, Geologic implications and potential hazards of scour depression on Bering shelf, Alaska: Environmental Geology, v. 3, p. 49-47.

Lewbel, G.S., 1984, Environmental hazards to petroleum industry development, Chapter 3 *of* Truett, J.C., ed., The Barrow Arch - Environment and Planned Offshore Oil and Gas Development: NOAA, OCSEAP, p. 31-46.

Lewbel, G.S., and Gallaway, B.J., 1984, Transport and fate of spilled oil, Chapter 2 *of* Truett, J.C., ed., The Barrow Arch - Environment and Planned Offshore Oil and Gas Development: NOAA, OCSEAP, p. 7-29.

Ljungblad, D.K., 1987, Gray whale distribution in the Chukchi and Bering Seas, *in* Hale, D.A., *ed.*, Chukchi Sea Information Update, June, 1987: NOAA, OCSEAP (MMS 86-0097), p. 101-106.

Loughlin, T.R., 1992, Status of Gulf of Alaska and Bering Sea pinnipeds and cetaceans: 1992 Information Transfer Meeting Conference Proceedings, Anchorage, AK, Minerals Management Service, Alaska OCS Region, p. 77-80.

Lowry, L. F., Frost, K. J., and Burns, J. J., 1980, Feeding of bearded seals in the Bering and Chukchi seas and trophic interaction with Pacific walruses: Arctic, v. 33, p. 330-342.

Maher, W. J., 1960, Recent records of the California gray whale (*Eschrichtius glaucus*) along the north coast of Alaska: Arctic, v. 13, p. 257- 265.

Mead, J. G., and Mitchell, E. D., 1984, Atlantic Gray Whales, *in* Jones, M. L., Swartz, S. L., and Leatherwood, S., eds., The

Gray Whale: *Eschrichtius robustus:* New York, Academic Press, p. 33-56.

Miley, J.M., and Barnes, P.W., eds., 1986, 1985 Field Studies, Beaufort and Chukchi Seas, Conducted from the NOAA Ship Discoverer: U. S. Geological Survey, Open-File Report 86-202, p. 1-57.

Miller, M. C., McCave, I. N., and Komar, P. D., 1977, Threshold of sediment motion under unidirectional currents: Sedimentology, v. 24, p. 507-527.

Milliman, J. D., and Meade, R. H., 1983, Worldwide delivery of river sediment to the oceans: Journal of Geology, v. 91, p. 1-21.

Moore, S. E., and Clarke, J. T., 1990, Distribution, abundance and behavior of endangered whales in the Alaskan Chukchi and western Beaufort Sea, 1989: Minerals Management Service, Anchorage, Alaska, 224 p.

Moore, S.E., and Ljungblad, D. K., 1984, The Gray Whales (*Eschrichtius robustus*) in the Beaufort, Chukchi, and Bering Seas: distribution and sound production, *in* Jones, M.L., Swartz, S.L., and Leatherwood, S., eds., The Gray Whale: *Eschrichtius robustus*: New York, Academic Press, p. 543-560.

Mountain, D. G., Coachman, L. K., and Aagaard, K., 1976, On the flow through Barrow Canyon: Journal Phys. Oceanography, v. 6, p. 461-470.

Naidu, A. S., 1988, Marine surficial sediments, Section 1.4., in Bering, Chukchi and Beaufort Seas, Coastal and Ocean Zones Strategic Assessment: Data Atlas: NOAA/SAB, Dept. Commerce, Rockville, Maryland.

Nelson, C. H., and Creager, J. S., 1977, Displacement of Yukon derived sediment from Bering Sea to Chukchi Sea during the Holocene: Geology, v. 5, p. 141-146.

Nelson, C. H., Dupre, W. R., Field, M. E., and Howard, J. D., 1982, Linear sand bodies on the Bering epicontinental shelf, *in* Nelson, C. H., and Nio, S. D., eds., The Northeastern Bering Shelf: New Perspectives of Epicontinental Shelf Processes and Depositional Products, Geologie en Mijnbouw, v. 61, p. 37-48.

Nelson, C. H., and Johnson, K. R., 1987, Whales and walruses as tillers of the sea floor: Scientific American, v. 255, p. 112-117.

Nelson, C. H., Johnson, K. R., and Barber, J. H., Jr., 1987, Gray whale and walrus feeding excavation on the Bering Shelf, Alaska: Jour. of Sed. Petrol., v. 57, no. 3, p. 419-430.

Nelson, C. H., Rowland, R. W., Stoker, S., and Larsen, B. R., 1981, Interplay of physical and biological sedimentary

structures of the Bering Sea epicontinental shelf, *in* Hood, D.W., and Calder, J. A., eds., The Eastern Bering Sea Shelf: Oceanography and Resources, v. 2: Seattle, University of Washington Press, p. 1265-1296.

Nerini, M. K., 1984, A review of Gray Whale feeding ecology, *in* Jones, M.L, Swartz, S.L., and Leatherwood S., eds., The Gray Whale: *Eschrichtius robustus:* New York, Academic Press, 441 p.

Nerini, M. K., Jones, M. L., and Braham, H. W., 1980, Gray whale feeding ecology: First Year Final Report to NOAA-OCSEAP [for March-December, 1980], Research Unit 593, contract no. R7120828.

Nerini, M. K., and Oliver, J. S., 1983, Gray whales and the structure of the Bering Sea benthos: Oecologia, v. 59, p. 224-225.

Nickles, J.R., 1992, Status of polar bear, walrus, and sea otters in the Gulf of Alaska/Lower Cook Inlet-Shelikof Strait/Bering Sea, 1992 Information Transfer Meeting Conference Proceedings, Anchorage, AK, Minerals Management Service, Alaska OCS Region, p. 81-85.

Norris, K. S., Goodman, R. M., Villa-Ramirez, B., and Hobbs, L., 1977, Behavior of the California Gray Whale, *Eschrichtius robustus*, In southern Baja California, Mexico: Fishery Bulletin, v. 75, no. 1, p. 159-172.

Oliver, J. S., and Kvitek, R. G., 1984, Side-scan sonar records and diver observations of the Gray Whale (*Eschrichtius robustus*) feeding grounds: Biology Bulletin, v. 167, p. 264-269.

Oliver, J. S., Slattery, P. N., O'Connor, E. F. and Lowry, L. F., 1983b, Walrus, *Odobenus rosmarus*, feeding in the Bering Sea: a benthic perspective: Fishery Bulletin, v. 81, p. 501-512.

Oliver, J. S., Slattery, P. N., Silberstein, M. A., and O'Connor, E. F., 1983a, A comparison of gray whale, *Eschrichtius robustus*, feeding in the Bering Sea and Baja California: Fishery Bulletin, v. 81, p. 513-522.

Oliver, J. S., Slattery, P. N., Silberstein, M. A., and O'Connor, E. F., 1984, Gray whale feeding on dense Ampeliscid amphipod communities near Bamfield, British Columbia: Canadian Journal of Zoology, v. 64, p. 41-49.

Olsen, H. W., Clukey, E. C., and Nelson, C. H., 1982, Geotechnical characteristics of bottom sediment in northern Bering Sea, *in* Nelson, C. H., and Nio, S. D., eds., The Northeastern Bering Sea Shelf: New Perspectives of Epicontinental Shelf Processes and Depositional Products: Geologie en Mijnbouw, v. 61, p. 91-103.

Paquette, R. G., and Bourke, R. H., 1974, Observations on the coastal current of Arctic Alaska: J. Marine Res., v. 32, p. 195-207.

Paquette, R. G., and Bourke, R. H., 1981, Ocean circulation and fronts as related to ice melt-back in the Chukchi Sea: J. Geophys. Res., v.86, p. 4215-4230.

Phillips, R. L., 1983, Chukchi Sea surficial geology and processes: OCSEAP Synthesis Meeting Report for Lease Sale 85, the Barrow Arch, Nov., 1983, 16 p.

Phillips, R. L., 1987, Summary of geology, processes, and potential geohazards in the northeastern Chukchi Sea, Chapter 4 *of* Hale, D. A., ed., Chukchi Sea: Information Update, June, 1987: NOAA, OCSEAP, p. 21-31.

Phillips, R. L., Barnes, P., Hunter, R. E., Rearic, D., Reiss, T., Kempema, E., Chin, J., Graves, S., and Scott, T., 1988, Geologic investigations in the Chukchi Sea, 1984, NOAA Ship Surveyor cruise: U. S. Geologic Survey, Open-File Report 88-25, 82 p.

Phillips, R. L., and Colgan, M. W., 1987a, Sea-floor feeding traces of gray whales and walrus in the northeast Chukchi Sea, *in* Galloway, J. P., and Hamilton, T. D., eds., Geologic Studies in Alaska by the U. S. Geological Survey during 1987. U. S. Geological Survey Circular 1016, p. 183-186.

Phillips, R. L., and Colgan, M. W., 1987b, Vibracore stratigraphy of the northeastern Chukchi Sea, *in* Hamilton, T. D., and Galloway, J. P., eds., Geologic studies in Alaska by the U. S. Geological Survey during 1986: U. S. Geological Survey Circular 998, p. 157-160.

Phillips, R. L., and Colgan, M. W., 1989, Gravel fields, bedforms, and episodic storm events on the shallow epicontinental Chukchi Sea, 28th International Geologic Congress, Washington, D. C., v.2, p. 604.

Phillips, R. L., Pickthorn, L. G., and Rearic, D. M., 1987, Late Cretaceous sediments from the northeast Chukchi Sea, *in* Galloway, J. P., and Hamilton, T. D., eds., Geologic Studies in Alaska by the U. S. Geological Survey during 1987: U. S. Geological Survey Circular 1016, p. 187-189.

Phillips, R. L., and Reiss, T. E., 1985a, Nearshore marine geological investigations, Icy Cape to Wainwright, northeast Chukchi Sea: U. S. Geological Survey Open File Report 84-828, 27 p.

Phillips, R. L., and Reiss, T. E., 1985b, Nearshore marine geological investigations, Point Barrow to Skull Cliff, Northeast Chukchi Sea: U. S. Geologic Survey Open-File Report 84-50, 22 p.

Phillips, R. L., Reiss, T. E., Kempema, E., and Reimnitz, E., 1982, Marine geologic investigations, Wainwright to Skull Cliff, northeast Chukchi Sea: U. S. Geological Survey Open-File Report 84-108, 33 p.

Piatt, J.F., 1992, Mapping pelagic seabird distributions in Alaska, 1992 Information Transfer Meeting Abstracts- Anchorage, AK, Mineral Management Service Alaska OCS Region, p.13.

Pike, G.C., 1962, Migration and feeding of the gray whale: Journal of Fishery Research Board Canada, v. 19, no. 5, p. 815-838.

Ray, G. C., and Schevill, W.E., 1974, Feeding of a captive gray whale: Mar. Fish. Rev., v. 36, p. 31-37.

Reilly, S. B., 1983, Projected future trends in Gray Whale population size [abs.]: Abstracts Volume of the 5th Biennial Conference on the Biology of Marine Mammals, 27 November-1 December, 1983, Boston, p. 85-86.

Reilly, S. B., Rice, D. W., and Wolman, A. A., 1980, Preliminary population estimate for the California Gray Whale based upon Monterey shore censuses, 1967/68 to 1978/79: Report of the International Whaling Commission, v. 30, p. 359-368.

Reimnitz, E., Barnes, P.W., and Phillips, R.L., 1984, Geologic evidence for 60 m deep pressure-ridge keels in the Arctic Ocean, *in* IAHR Ice Symposium (August 27-31, 1984, Hamburg), Proceedings, v. 2, p. 189-206.

Reimnitz, E., Barnes, P. W., Toimil, L. J., and Melchios, John, 1977, Ice gouge recurrence and rates of sediment reworking, Beaufort Sea, Alaska: Geology, v. 5, p. 405-408.

Rice, D. W., and Wolman, A. A., 1971, The life history and ecology of the gray whale (*Eschrichtius robustus*): American Society of Mammalogy Special Publication No. 3, 142 p.

Rugh, D. J., 1981, Fall gray whale census at Unimak Pass, Alaska 1977-79, [abs.]: Abstracts Volume of the 4th Biennial Conference on the Biology of Marine Mammals, 14-18 December 1981, San Francisco, p. 100.

Rugh, D. J., and Fraker, M. A., 1981, Gray whale (*Eschrichtius robustus*) sightings in the eastern Beaufort Sea: Arctic, v. 34, p. 186-187.

Scammon, C. M., 1874, The Marine Mammals of the Northwestern Coast of North America: New York, Dover Publications, Inc., 319 p.

Schumacher, J. D., and Tripp, R. B., 1979, Response of northeast Bering Sea shelf water to storms: EOS, Transactions of the American Geophysical Union, v. 60, p. 856.

Sease, J.L., 1985, Historical Status and Population Dynamics of the Pacific Walrus (unpublished M.S. Thesis): Univ. Alaska, Fairbanks, 213 p.

Sease, J.L., and Chapman, D.G., 1988, Pacific walrus (*Odobenus rosmarus divergens*), *in* Lentfer, J.W., ed., Selected Marine Mammals of Alaska: Species Accounts with Research and Management Recommendations: Marine Mammal Commission, Washington, D.C., p. 17-38.

Sharma, G. D., 1979, The Alaska shelf: hydrographic, sedimentary and geochemical environment: Springer-Verlag, New York, 487 p.

Stoker, S. W., 1978, Benthic invertebrate macrofauna of the eastern continental shelf of the Bering and Chukchi Seas (unpublished Ph.D. Dissertation): Fairbanks, University of Alaska, 259 p.

Stoker, S. W., 1981, Benthic invertebrate macrofauna of the eastern Bering/Chukchi continental shelf, in Hood, D.W., and Calder, J.A. eds., The Eastern Bering Sea Shelf: Oceanography and Resources, v. 2: Seattle, University of Washington Press, p. 1069-1090.

Stringer, W. J., 1978, Morphology of Beaufort, Chukchi, and Bering Seas nearshore ice conditions by means of satellite and aerial remote sensing: Geophy. Inst. Univ. of Alaska, Fairbanks, v.1, 34 p.

Stringer, W. J., 1982, Width and persistence of the Chukchi polynya: Univ. of Alaska Fairbanks report to NOAA/OCSEAP, 17 p.

Stringer, W. J., and Groves, J. E., 1991, Local and areal extent of polynyas in the Bering and Chukchi Seas: Arctic, v. 44 (Supp.1), p. 164-171.

Sund, P. N., 1975, Evidence of feeding during migration and of an early birth of the California Gray Whale (*Eschrichtius robustus*): Journal of Mammalogy, v. 56, p. 265-266.

Swartz, S. L., and Jones, M. L., 1987, Gray whales at play in Baja's San Ignacio Lagoon: National Geographic, v. 171, no. 6, p. 754-771.

Thomson, D. B., ed., 1984, Feeding ecology of Gray Whales (*Eschrichtius robustus*) In the Chirikof Basin, summer, 1982: U.S. Dep. Commer., NOAA, OCSEAP Final Rep. 43 (1986), p. 209-460.

Thor, D. R., and Nelson, C. H., 1979, A summary of interacting surficial geologic processes and potential geologic hazards in the Norton Basin, northern Bering Sea: Proceedings of the Offshore Technical Conference, Paper No. 3400, p. 377-381.

Thorndike, A. S. and Colony, R., 1982, Sea ice motion in response to geostrophic winds: Jour. Geophy. Res., v.87, no. C8, p. 5845-5852.

Toimil, L. J., 1978, Ice gouge microrelief on the floor of the eastern Chukchi Sea, Alaska: A reconnaissance survey: U. S. Geological Survey Open-File Report 78-693, 94 p.

Truett, J. C., 1984, Lower trophic levels, Chapter 7 *of* Truett, J. C., ed., The Barrow Arch Environment and Possible Consequences of Planned Offshore Oil and Gas Development: NOAA, OCSEAP, p. 133-151.

Votrogov, L. M., and Bogoslovskaya, L. S., 1980, Gray whales off the Chukotka Peninsula: International Whaling Commission, Report, v. 30, p. 435-437.

Wellington, G. M. and Anderson, S., 1978, Surface feeding by a juvenile gray whale, *Eschrichtius robustus:* Fishery Bulletin, v. 76, p. 290-293.

Wilson, D. E., Pace, S. D., Carpenter, P. D., Teas, H., Goddard, T., Wilde, P., and Kinney, P.J., 1982, Nearshore coastal currents, Chukchi Sea, summer 1981: U. S. Dep. Commer., NOAA, OSCEAP Final Report 41 (1986), p. 209-519.

Wiseman, W. J., Jr., and Rouse, L. J., Jr., 1980, A coastal jet in the Chukchi Sea: Arctic, v.33, no.1, p. 21-29.

Wursig, B., Croll, D. A., and Wells, R. S., 1983, Behavior of summering gray whales, in Thomson, D. H., ed., Feeding ecology of the gray whales (*Eschrichtius robustus*) in the Chirikof Basin, Summer 1982: U.S. Department of Commerce, NOAA/OCSEAP Final Reports, No. 43 (1986), p. 335-376.

Zenkovich, B. A., 1934, [Research data on cetacea of far eastern seas: Bulletin of the Far East Academy of Science, USSR, No. 10, [in Russian, transl. by F. Essapian, Miami, Fl.], 34 p.

Zenkovich, B. A., 1937 [More on the gray California whale (*Rhachianectes glaucus* Cope, 1864]: Bulletin of the Far East Academy of Science, USSR, no. 23, [in Russian], transl. by the Bureau of Commercial Fisheries, Office of Foreign Fisheries Translations, Washington, D. C., 19 p.

Zenkovich, B. A., 1955, O migratsiiakh kitov, promyslove raiony v dal'nevostochnyk vodakh (The migration of whales, whale fishing in the waters of the Soviet Far East), in Kleinenberg, S.E., and Makarova, T.I., eds., Kitoiony Promysel Sovetskogo Soyuza, VNIRO, Part I, (in Russian], transl. by Israel Program Sci. Transl. for U.S. Department of the Interior and National Science Foundation, 1968, 14 p.

Zimushko, V. V., and Ivashin, M.V., 1980, Some results of Soviet investigations and whaling of gray whales (*Eschrichtius robustus* Lilljeborg, 1961): Report of the International Whaling Commission, v. 31, p. 237-246.

Zimushko, V. V., and Lenskaya, S.A., 1970, Feeding of the gray whale (*Eschrichtius gibbosus* Erx.) at foraging grounds (in Russian): Ekologiya, v. 1, p. 26-35, transl. by Consultant's Bureau, 1971, New York, Plenum, 8 p.

APPENDIX 1
Boxcore descriptions

STATION 24-34BS

1. Latitude: 70° 37.9'
2. Longitude: 161° 33.1'
3. Water depth: 40.5 m
4. Core length: 30 cm

A. Length: 30 cm.
B. Sediment texture: Well sorted, subrounded medium grain sand. Scattered 1-5 cm diameter gravel of mixed lithologies. Shell and gravel lags common.
C. Sedimentary surface features: Bioturbated, burrows and animal tracks.
D. Sedimentary structures: Gravel/shell lag in bottom 7 cm of the core, clasts to 5.4 cm. Horizontal bed in center of core is defined by increases in granules and shells.
E. Most abundant living fauna: Brittle stars, isopods, amphipods, *Yoldia*, *Macoma calcarea*, and polychaete worms. Bivalve shells were concave down. Surface covered with isopods.

STATION 28-38BS

1. Latitude: 71° 36.1'
2. Longitude: 165° 48.7'
3. Water depth: 45 m
4. Core length: 56 cm

Description of the surface layer

A. Thickness: 6 cm
B. Sediment texture: Silty muddy ooze
C. Sedimentary surface features: Bioturbated with randomly distributed pebbles.
D. Most abundant living fauna: Amphipods, small clear sea cucumber, *Pectinaria*, *A. borealis*, *Nuculana*, *Nucula*, and the tube anemone *Pachycerianthus*.

Description of Depositional Interval from 6 cm to 56 cm

A. Color of unit: Olive grey and light olive grey
B. Sediment texture: Mud with dark organic silt.
C. Sedimentary structures: Bioturbated mud with a few scattered pebbles.
D. Bedding features: None - pebbles and shells randomly distributed.
E. Paleontologic observation: worm traces, simple and complex; *Macoma* shells, many in growth position; *Clinocardium* fragment; and other bivalve fragments.

STATION 29-39BS

1. Latitude: 71° 35.9'
2. Longitude: 166° 14.7'

3. Water depth: 46.5 m 4. Core length: 44 cm

Description of the surface layer

A. Thickness: 4 cm
B. Sediment texture: Yellowish grey clayey muddy ooze.
C. Sedimentary surface features: Bioturbated.
D. Most abundant living fauna: Amphipods, tunicates, hermit crab in *Neptunea* shell carrying platy bryozoan, polychaete worms (3 kinds). Dead fauna; Complete shell of *Macoma calcarea, Nuculana, Nucula pernula,* and a fragment of *Yoldia.*

Description of Interval from 4 cm to 44 cm

A. Color of unit: Light olive grey to olive black.
B. Sediment texture: Semi-consolidated mud to consolidated mud with a few scattered pebbles.
C. Sedimentary structures: Bioturbated mud with bivalves in upper 5 cm.
D. Bedding features: Shells in growth position
E. Paleontologic observation: Diversity of burrows open and closed; relict and modern burrowing. Few scattered shells; *Nucula* and *Macoma* (live), in growth position. Near bottom of the core, *Macoma* in growth position, shells intact, but brittle. Also, fragments of *Nuculana* and *Serripes* were found with their shells concave down.

STATION 29-40BS

1. Latitude: 71° 35.8' 2. Longitude: 166° 14.8'
3. Water depth: 46.5 m 4. Core Length: 53.5 cm

Description of the surface layer

A. Thickness: 8.5 cm
B. Sediment texture: Yellowish grey silty mud with abundant quartz pebbles.
C. Sedimentary surface features: Burrows, worms tubes.
D. Most abundant living fauna: Brittle star, sea cucumbers, *Nuculana pernula, Macoma calcarea* and *Serripes groenlandicus.*

Description of Interval from 8.5 cm to 53.5 cm

A. Color of unit: Light olive grey, olive grey to olive black.
B. Sediment texture: Semi-consolidated to consolidated silty mud with black quartzite pebbles.
C. Sedimentary structures: Bioturbated mud, with horizontal to disrupted bedding defined by sand and scattered pebbles. Some thin discontinuous horizontal laminations.
D. Bedding features: Pebbles and shells randomly placed.
E. Paleontologic observation: Live worm to 33.5 cm, tube anemone, vertical,

horizontal and U-shaped burrows; *Golfinga* burrow. Many open and closed burrows. Shells scattered throughout, *Astarte*, *Nucula*, and *Natica* with *Macoma* in growth position.

STATION 29-41BS

1. Latitude: 71° 35.8'
2. Longitude: 166° 15.3'
3. Water depth: 46.5 m
4. Core length 55 cm

Description of the Surface layer

A. Thickness: 8 cm
B. Sediment texture: Yellowish grey clayey mud.
C. Sedimentary surface features: Bioturbated.
D. Most abundant living fauna: Polychaete worms, *Nucula*, *Macoma* and *Nuculana*.

Description of Interval from 8 cm to 55 cm

A. Color of unit: Light olive grey to olive grey.
B. Sediment texture: Semi consolidated mud.
C. Sedimentary structures: bioturbated with scattered pebbles and shells.
D. Bedding features: None.
E. Paleontologic observation: Live worms, reinforced burrows, diverse worm traces, both active and closed. *Serripes* and other shell fragments scattered throughout unit. *Macoma* in growth position.

STATION 30-42BS

1. Latitude: 71° 38.6'
2. Longitude: 167° 4.5'
3. Water depth: 49 m
4. Core length 50 cm

Description of surface layer

A. Thickness: 5 cm
B. Sediment texture: Yellowish grey silty mud ooze.
C. Sedimentary surface features: Bioturbated.
D. Most abundant living fauna: *Golfinga*, tube to 34 cm. Polychaete worm.
E. Paleontologic observation: *Nucula* dead but whole. *Yoldia* fragment. Reinforced worm burrow. *Macoma* shell.

Description of Depositional Interval from 6 cm to 50 cm

A. Color of unit: Light olive grey to olive black.
B. Sediment texture: Semiconsolidated mud to consolidated mud.
C. Sedimentary structures: Bioturbated, scattered bivalves to 28 cm depth: some in growth position.
D. Bedding features: None.
F. Paleontologic observation: Active bioturbation, live worms and with a diverse assortment of burrowing styles. *Golfinga* burrows found

throughout the core. *Macoma* fragments. Lots of organic material.

STATION 31-43BS

1. Latitude: 71° 30.7'
2. Longitude: 167 40.7'
3. Water depth: 51 m
4. Core length: 51 cm

Description of the Surface

A. Surface thickness: 8 cm
B. Sediment texture: Silty muddy ooze with gravel.
C. Sedimentary surface features: Bioturbated.
D. Most abundant living fauna: Many worm burrows, reinforced burrows, small amphipods, *Nuculana*, *Buccinium*, and *Nucula*.

Description of Interval from 9 cm to 14 cm

A. Color of unit: Light olive grey to olive black.
B. Sediment texture: Semiconsolidated mud to consolidated clayey mud (more dense at bottom of core), few scattered granules.
C. Sedimentary structures: Bioturbated. Shell lag between 8 to 10 cm.
D. Bedding features: None.
F. Paleontologic observation: *Macoma calcarea* in growth position, along with scattered shell fragments. Diverse assortment of burrowing styles.

STATION 41-52BS

1. Latitude: 71° 26.2'
2. Longitude: 161° 21.6'
3. Water depth: 49 m
4. Core length: 56 cm

Description of the Surface

A. Surface thickness: 5 cm
B. Sediment texture: Fine sandy ooze.
C. Sedimentary surface features: Bioturbated.
D. Most abundant living fauna: amphipods, brittle stars, tube worms, and *Macoma*.

Description of Depositional Interval from 5 cm to 56 cm

A. Color of unit: Light olive grey to olive black.
B. Sediment texture: Semi-consolidated silty mud to consolidated mud with pebbles.
C. Sedimentary structures: Bioturbated sand and mud with shells and pebbles in upper 10 cm, few scattered pebbles and shell fragments in the rest of the core.
D. Bedding features: None.
E. Paleontologic observation: Live: *Macoma, Pectinaria, Golfinga,* and tube

worms. **Dead**: *Macoma, Yoldia,* and shell fragments. Diverse assortment of burrowing styles. Below 43 cm, *Macoma* found in growth position along with an assortment of barnacles, *Clinocardium, Yoldia, Astarte,* and many shell fragments.

STATION 41-53BS

1. Latitude: 71° 26.2'
2. Longitude: 161° 21.6'
3. Water depth: 49 m
4. Core length: 57 cm

Description of the Surface

A. Surface thickness: 6 cm
B. Sediment texture: Fine oozy mud.
C. Sedimentary surface features: Bioturbated with tube worms 3-5 cm above the surface.
D. Most abundant living fauna: Amphipods, shrimp, *Macoma* sp., many worm traces (none with reinforced tubes).

Description of Depositional Interval from 6 cm to 57 cm

A. Color of unit: Olive grey to black.
B. Sediment texture: Semi-consolidated silty mud to consolidated mud.
C. Sedimentary structures: Bioturbated mud with a few scattered granules.
D. Bedding features: None.
F. Paleontologic observation: Active bioturbation, reinforced sand tubes open and filled worm burrows, tube anemone *Pachycerianthus*. Scattered shell fragments with *Retus* and *Macoma*. A single *Macoma* was found in place.

STATION 41-54BS

1. Latitude: 71° 26.2'
2. Longitude: 161° 21.5'
3. Water depth: 49 m
4. Core length: 60 cm

Description of the Surface

A. Surface thickness: 6 cm.
B. Sediment texture: Fine sandy mud-ooze, light brown, green grey.
C. Sedimentary surface features: Bioturbated, only relief is worm and anemone tubes.
D. Most abundant living fauna: 3 species of amphipods, brittle stars, *Macoma, Yoldia,* sea anemone tube on surface, and many reinforced worm tubes.
E. Paleontologic observation: Fragments of *Yoldia, Macoma,* and of a few other shells.

Description of Depositional Interval from 5 cm to 60 cm

A. Color of unit: Light olive grey to olive black.
B. Sediment texture: Semi-consolidated mud with pebbles and shells to consolidated mud with scattered shell fragments.
C. Sedimentary structures: Bioturbated, at 11 cm abundant shells in growth position, shell lag at 48 to 50 cm.
D. Bedding features: None
F. Paleontologic observation: **Live:** Polychaete worm, many *Macoma*. **Dead:** *Yoldia, Macoma, Mya, Astarte,* and *Cyclocardia*. Active and relict burrowing with a diverse assortment of burrowing styles.

STATION 43-56BS

1. Latitude: 71° 31.0' 2. Longitude: 162° 28.2'
3. Water depth: 45.5 m 4. Core length: 57 cm

Description of the Surface

A. Surface thickness: 7 cm
B. Sediment texture: Coarse to medium sandy mud ooze. Gravel to 2 cm.
C. Sedimentary surface features: Bioturbated.
D. Most abundant living fauna: Brittle star, amphipods, clear sea cucumber, large and small worm tubes, *Macoma calcarea,* and *Astarte borealis*. **Dead:** *Nuculana pernula* in growth position.
E. Paleontologic observation: Bivalve shells were concave down.

Description of Depositional Interval from 7 cm to 57 cm

A. Color of unit: Light olive grey.
B. Sediment texture: Pebbly fine sandy semi-consolidated mud to medium coarse sandy mud with pebbles. Pebbles of mixed lithologies.
C. Sedimentary structures: Bioturbated.
D. Bedding features: A 10 cm thick gravel/shell lag starting at 10 cm from the surface. Disrupted gravel bed at 47 to 49 cm.
F. Paleontologic observation: **Live:** *Macoma*, and polychaete worms. Complex and simple burrows, anemone burrow, one *Macoma*, and *Mya* found in growth position between 21-28 cm. Scattered shell fragments concentrated in bottom of unit. An anemone burrow (4.5 X 23 cm) is filled with shells and gravel.

STATION 44-58BS

1. Latitude: 71° 05.3' 2. Longitude: 160° 48.9'
3. Water depth: 54 m 4. Core length: 26 cm

Description of the Surface

A. Surface thickness: 4 cm
B. Sediment texture: Muddy coarse to medium, poorly sorted gravel. Gravel clasts are angular up to 4 cm in diameter and of mixed lithology (quartzite and sandstone).

C. Sedimentary surface features: Bioturbation and tube worm.
D. Most abundant living fauna: Tube worms, sand-reinforced burrows, brittle star *Ophiophis*, brittle star *Ophiura*, *Pectinaria*, *Macoma*.

Description of Depositional Interval from 4 cm to 26 cm

A. Color of unit: Olive grey to black.
B. Sediment texture: Coarse sand with 2-6 cm clast, gabbro. Sand in muddy matrix - gravelly sandy mud.
C. Sedimentary structures: Surface gravel lag to 7 cm thick; bioturbated sandy mud with bioturbated planar laminations in the middle of the core. Gravel clast 6.5 cm in diameter at the base of the core.
D. Paleontologic observation: Abundant worm reinforced tube burrows.
Live; *Macoma*, *Nucula*, fish, worm burrows throughout, and sea cucumber.
Dead; *Astarte montagui* and *Pectinaria* fragments, brachiopod, limpets and other shell fragments. Shell concave up.

STATION 44-59BS

1. Latitude: 71° 05.4'
2. Longitude: 160° 48.9'
3. Water depth: 52 m
4. Core length: 27 cm
5. Additional comments: Second of three box cores at this station. Biology was the only sample collected.

A. Most abundant living fauna: Brittle stars, long legged sea spider, small amphipods, *Macoma*, bryozoan, polychaete cluster, tube sponge, sea cucumber *Psolus*.
B. Paleontologic observation: Piece of barnacle, dead *Macoma*.

STATION 44-60BS

1. Latitude: 71° 06.1'
2. Longitude: 160° 49.4'
3. Water depth: 51 m
4. Core length: 21 cm

Description of the Surface

A. Surface thickness: 2.5 cm
B. Sediment texture: Pebbly, coarse sandy mud. Surface clasts: 4 cm dolomite, angular; black chert 1 cm subrounded.
C. Sedimentary surface features: Bioturbated, surface gravel lag.
D. Most abundant living fauna: Amphipod, tube burrows, bivalve shells brittle star, sponge *Mya pseudoarenaria*, *Serripes groenlandicus*, *Astarte montagui*, *Astarte borealis*, *Yoldia scissurata*, *Boreotrophon*, and *Natica*.
E. Paleontologic observation: Bivalve shells were concave down.

Description of Depositional Interval from 2.5 cm to 21 cm

A. Color of unit: Olive grey to olive black.

B. Sediment texture: Semi-consolidated coarse sandy mud with some gravel.
C. Sedimentary structures: Bioturbated, with mud-filled burrows.
D. Bedding features: None.
F. Paleontologic observation: Live worms, brittle star, *Macoma, Golfinga* burrow, and some thin reinforced burrows. *Macoma* valve concave up.

STATION 46-61BS

1. Latitude: 71° 06.2' 2. Longitude: 158° 29.0'
3. Water depth: 35 m 4. Core length: 29 cm
5. Description of location: In sand waves north of TV/camera drop.

Description of the Surface

A. Surface thickness: 29 cm.
B. Sediment texture: Coarse well sorted sand with a few pebbles.
C. Sedimentary surface features: Rippled. Top 17 cm of the core contains small-scale crossbeds, some with heavy mineral laminations.
D. Most abundant living fauna: An amphipod, worm, *Lysonsia arenosa.*
E. Paleontologic observation: Hydrozoa, fragments of barnacles, *Yoldia, Astarte, M. subgracilis*
F. Additional comments: Very few barnacles. This is the largest of the 3 samples, and it had the lowest diversity, smallest pebbles and the least shell fragments.

STATION 46-62BS

1. Latitude: 71° 06.5' 2. Longitude: 158° 28.9'
3. Water depth: 37 m 4. Core length: 22 cm

Description of the Surface

A. Surface thickness: 22 cm
B. Sediment texture: Medium coarse sand with pebbles (.5 cm diameter). Coal layers, coarser than sand. Possible cross bedding.
C. Sedimentary surface features: Ripples. Small-scale crossbeds with heavy mineral lamination at the top of the core. The rest of the core is bioturbated with scattered shells and pebbles.
D. Most abundant living fauna: Sand dollars, amphipods, *Cyclocardia crebricosta,* and *Natica.*
E. Paleontologic observation: Barnacles, sand dollars, brachiopods, *Cyclocardia, Astarte borealis, Tachyrhynchus, Astarte montagui, Mya.* Shell fragments more rounded than 46-63BS. Bivalve shells were concave down.
F. Additional comments: Barnacles not as common as in 46-63BS. Fewer and smaller pebbles than in 46-63.

STATION 46-63BS

1. Latitude: 71° 07.1'
2. Longitude: 158° 28.9'
3. Water depth: 38 m
4. Core length: 11 cm

Description of the Surface

A. Surface thickness: 11 cm
B. Sediment texture: Muddy medium sand with gravel and lots of shells.
C. Sedimentary surface features: Ripples, bioturbated with amphipod tube on surface. Small-scale crossbeds at top of core.
D. Most abundant living fauna: *Liocyma, Serripes, Macoma,* and *Retus.* Tube-amphipods, a few thin worms, and mysids.
E. Paleontologic observation: *Hiatella, Retus, Cyclocardia, Serripes, Solanaria, Velutina, Macoma, Tachyrhynchus,* sand dollar, hydrozoa, and bryozoa.
F. Bivalve shells were concave down.
H. Additional comments: Concentration of shells at bottom of core. Shell fragments irregular - many whole. Barnacles comprise the largest fraction.

STATION 47-64BS

1. Latitude: 70° 35.4'
2. Longitude: 162° 17.0'
3. Water depth: 40 m
4. Core length: 14 cm

Description of the Surface

A. Surface thickness: 14 cm
B. Sediment texture: Medium sand, well sorted. Small pebbles, rounded.
C. Sedimentary surface features: Some small-scale crossbeds.
D. Most abundant living fauna: Sand dollars, worms, small amphipods, *Astarte montagui, Liocyma, Neptunea, Cyclocardia, Serripes, Astarte borealis.*
E. Paleontologic observation: Large sand dollar fragments, barnacle fragments, *Thracia* sp., reinforced worms, shell fragment majority rounded sand dollar pieces, and *Thracia adamsi*(?).
F. Additional comments: Fragments (sand dollar), *Astarte montagui* in growth position, *Liocyma.*

STATION 47-65BS

1. Latitude: 70° 35.8'
2. Longitude: 162° 17.2'
3. Water depth: 40 m
4. Core length: 24 cm

Description of the Surface

A. Surface thickness: 24 cm.
B. Sediment texture: Medium sand, well sorted. Few pebbles. Mud fraction in surface layer.

C. Sedimentary surface features: Flat.
D. Sedimentary Structures: Erosional surface 8 cm down with gravel/shell lag. Large "U-shaped" burrow filled with gravel and shells in the center of the core. Pebbles and shell fragments increase to the base of the core.
E. Most abundant living fauna: *Buccinum* (surface), small sand dollars, 2 species small. amphipods, *Macoma*, worms, polychaete worm (*Nepthys), Mya t., Astarte, Tachyrhynchus.*
F. Paleontologic observation: Sand dollar, *Clinocardium* (upper), reinforced burrows, large predator gastropod, larger sand dollar fragments, *Mya pseudoarenaria.* Shells in burrows, shell fragments (half and whole).
G. Bivalve shells were concave down.
H. Additional comments: Top slice: low mud content, living small sand dollars, *Clinocardium, Solanaria, Retus, Astarte* fragments: *Serripes, Cyclocardia, Macoma*, Dead sm. Sand dollars, few scattered gravels in upper section (subrounded, small). Upper middle: *Mya* concave down, almost no mud, draw down shell fragments, angular pebbles 1 cm in size, reinforced worm burrows, barnacle fragment, fewer shell fragments. Lower middle: *Macoma* concave down, low mud content, few tube worms, pebbles slightly larger (2 cm), unknown clam, *Macoma* fragments, fossil crab claw. Upper bottom: Shells concave down, *Cyclocardia* concave down, shell fragment concentration high, shells are small size and more fragmented, *Cyclocardia, Mya, Tachyrchynchus, Buccinum,* unknown species from above, sand dollar fragments (larger than surface), brachiopod fragment, *Pectinaria,* pebbles (more darker rounded, up to 13 cm). Lower bottom: darker color, *Cyclocardia* fragments, *Clinocardium* fragments, highest concentration of shell fragments, *Boreotrophon,* sand dollar (larger than at surface).

STATION 60-77BS

1. Latitude: 70° 37.6'
2. Longitude: 165° 50.5'
3. Water depth: 44 m
4. Core length: 34 cm

Description of the Surface

A. Surface thickness: 4 cm
B. Sediment texture: Muddy fine sandy gravels. Gravels rounded quartzite. Subangular sandstone and mudstones.
C. Sedimentary surface features: gravel with barnacles and bryozoa
D. Sedimentary structures: Surface gravel/shell lag to 7 cm thick. Bioturbated gravelly mud to 21 cm depth. Bottom 13 cm bioturbated muddy gravel.
E. Most abundant living fauna: Hydrozoans, *Pachyegeyis priceps*, foliate bryozoa, barnacles, reinforced worm tubes.
F. Paleontologic observation: limpet, barnacles, shell fragments.

Description of Depositional Interval from 4 cm to 15 cm

A. Color of unit: olive gray
B. Sediment texture: Scattered white and black quartzite gravels in mud.
C. Sedimentary structures: Bioturbated.
D. Bedding features: none
F. Paleontologic observation: *Macoma* fragments. Active bioturbation.

Description of Depositional Interval from 15 cm to 34 cm

A. Color of unit: Olive gray
B. Sediment texture: Muddy sandy gravel. Subangular to rounded quartzite clasts.
C. Sedimentary structures: Coarsen downward. At the bottom there is a thin (<1 cm) thick mud.
D. Bedding features: overall gravel-mud-gravel.
F. Paleontologic observation: Mainly barnacles, *Cyclocardia, Macoma, Clinocardium, Boreotrophon*, abundant shell fragments.

STATION 60-78BS

1. Latitude: 70° 37.8' 2. Longitude: 165° 49.6'
3. Water depth: 44.5 m 4. Core length: 41 cm

Description of the Surface

A. Surface thickness: 7 cm
B. Sediment texture: Fine sandy muddy ooze
C. Sedimentary surface features: Bioturbated.
D. Sedimentary structures: Surface gravel/shell lag truncates a gravel filled burrow 8 cm from the surface. An anemone burrow [7 X 31 cm (to base of core)] is filled with "clean" gravel. Lined vertical burrows to 0.8 cm wide in upper 10 cm. Middle of the core is bioturbated gravelly mud; bottom 17 cm, increased gravel content.
E. Most abundant living fauna: worms, amphipods

Description of Depositional Interval from 7 cm to 10 cm

A. Color of unit: Olive gray.
B. Sediment texture: muddy pebbly gravel
C. Sedimentary structures: lag deposit
D. Bedding features: Bioturbated.
F. Paleontologic observation: abundant barnacle and bivalve fragments.

Description of Depositional Interval from 10 cm to 22 cm

A. Color of unit: Olive gray.
B. Sediment texture: Silty clayey mud with scattered gravel.
C. Sedimentary structures: Bioturbated.

D. Paleontologic observation: organic rich, tube worms, a *Macoma* fragment.

Description of Depositional Interval from 22 cm to 41 cm

A. Color of unit: Olive gray.
B. Sediment texture: Muddy coarse sandy gravel.
C. Sedimentary structures: Bioturbated.
D. Bedding features: overall mud-gravel-mud-gravel
E. Paleontologic observation: small shell fragments and worm tubes.

STATION 60-79BS

1. Latitude: 70° 37.1'
2. Longitude: 165° 50.1'
3. Water depth: 44.5 m
4. Core length: 31 m

Description of the Surface

A. Surface thickness: 8 cm
B. Sediment texture: silty muddy ooze
C. Sedimentary surface features: gastropod traces
D. Sedimentary structures: Surface gravel/shell lag to 15 cm thick overlying a gravelly mud. Bioturbated muddy gravel at bottom of core.
E. Most abundant living fauna: amphipods, *Tachyrhynchus*, and soft tube worms.

Description of Depositional Interval from 8 cm to 15 cm

A. Color of unit: Olive gray.
B. Sediment texture: Organic rich clayey muddy gravel. Clasts are rounded.
C. Sedimentary structures: Bioturbated.
D. Bedding features: none
E. Percent of bioturbation: 100%
F. Paleontologic observation: *Pecten, Macoma, Yoldia, Astarte, Costazia, Boreotrophon*, and hydrozoa, brachiopods.

Description of Depositional Interval from 15 cm to 26 cm

A. Color of unit: Olive gray.
B. Sediment texture: Sandy clayey mud moderately consolidated.
C. Sedimentary structures: Bioturbated
D. Bedding features: none
E. Percent of bioturbation: 100 %
F. Paleontologic observation: Worm burrows

Description of Depositional Interval from 26 cm to 31 cm

A. Color of unit: Olive gray
B. Sediment texture: Sandy organic rich muddy gravel.
C. Sedimentary structures: Bioturbated.

D. Bedding features: Overall mud-gravel-mud-gravel
F. Paleontologic observation: branching bryozoa, barnacles fragments and bases. Many shell fragments.

STATION 60-80BS

1. Latitude: 70° 37.2' 2. Longitude: 165° 51.8'
3. Water depth: 44 m 4. Core length: 41 cm

Description of the Surface

A. Surface thickness: 3 cm.
B. Sediment texture: Muddy sandy pebbly gravel.
C. Sedimentary surface features: gravel with barnacles.
D. Most abundant living fauna: sponge, barnacles, *Cyclocardia, Eunephthya rubiform, Carbasea carbacea, Costazia ventricosa, Boreotrophon,* shrimp, reinforced tubes, encrusting bryozoa, *Chelyosoma macleayanum; Astarte montagui, Musculus, Astartes borealis,* Brachiopod, and tube anemone.
E. Paleontologic observation: Brachiopods, Barnacles, *Colus, Macoma, Yoldia.*
F. Sedimentary structure: Gravel/shell lag to 8.5 cm at surface overlying 9 cm of bioturbated gravelly mud. Bottom 22 cm bioturbated muddy gravel.
G. Additional comments: gravels and cobble clasts, up to 3 cm; quartzite, dolomite, chert, mudstone, subangular to rounded, poorly sorted, cherty arkosic angular sandstone.

Description of Depositional Interval from 4 cm to 24 cm

A. Color of unit: Olive gray.
B. Sediment texture: Organic rich clayey mud with scattered pebbles, much of the coarse material is in burrows.
C. Sedimentary structures: Bioturbated.
D. Bedding features: none
E. Percent of bioturbation: 100 %
F. Paleontologic observation: active burrowing, burrows, reinforced burrows

Description of Depositional Interval from 24 cm to 41 cm

A. Color of unit: Olive gray.
B. Sediment texture: Gravelly sandy mud.
C. Sedimentary structures: the unit is somewhat graded with coarser sand and large gravel at the bottom
D. Bedding features: overall 3 beds gravel, mud, gravel
F. Paleontologic observation: Barnacles, *Astarte, Macoma,* many shell fragments, and live tube sea anemone.

STATION 68-88BS

1. Latitude: 69 54.1
2. Longitude: 164 47.5
3. Water depth: 38 m
4. Core length: 18 cm

Description of the Surface

A. Surface thickness: 18 cm
B. Sediment texture: Muddy fine sand grading downward to silty mud. Scattered pebbles of coal and black quartzite.
C. Sedimentary surface features: ripples
D. Most abundant living fauna: *Nucula, Macoma,* reinforced worm tubes, smaller worms
E. Paleontologic observation: *Macoma, Nucula.*
F. Sedimentary structure: Small-scale crossbeds at the top of the core, rest is bioturbated. Pebbles increase in abundance to base of core.

STATION 68-89BS

1. Latitude: 69° 54.0'
2. Longitude: 164° 46.7'
3. Water depth: 38 m
4. Core length: 19 cm

Description of the Surface

A. Surface thickness: 19 cm
B. Sediment texture: muddy medium to fine sand on surface grading downward to a pebbly silty mud
C. Sedimentary surface features: Ripples
D. Most abundant living fauna: *Astarte,* thin reinforced burrows, *Nepthys,* and *Nucula.*
E. Paleontologic observation: Barnacle, *Tachyrhychus, Neptunea, Astartes,* and *Nucula.*
F. Sedimentary structure: Bioturbated, with small-scale crossbeds at the top of the core. Gravel and shell fragments increases to base of core.

STATION 68-90BS

1. Latitude: 69° 54.0'
2. Longitude: 164° 46.4'
3. Water depth: 38 m
4. Core length: 20 cm

Description of the Surface

A. Surface thickness: 20 cm.
B. Sediment texture: Muddy medium to fine sand on surface grading downward to a pebbly silty mud.
C. Sedimentary surface features: Ripples.
D. Most abundant living fauna: amphipod, reinforced tube worms, *Nucula, Macoma, Mya* siphon, worms.
E. Paleontologic observation: *Serripes, Macoma,* and *Nucula.*

F. Sedimentary structure: Bioturbated, with small-scale crossbeds at the top of the core. Gravel and shell fragments increases to base of core.

Appendix 2

Description of image analysis software

Analysis of gray whale and Pacific walrus feeding features for this study was done using NIH *Image* , version 1.31. The following pages provide a summary of the capabilities and availability of this program. This information has been taken from the online users manual of NIH *Image*, version 1.51, the most current version as of August, 1993.

Introduction

NIH *Image* is a public domain image processing and analysis program for the Macintosh. It can acquire, display, edit, enhance, analyze, print and animate images. It reads and writes TIFF, PICT, PICS and MacPaint files, providing compatibility with many other applications, including programs for scanning, processing, editing, publishing and analyzing images. It supports many standard image processing functions, including contrast enhancement, density profiling, smoothing, sharpening, edge detection, median filtering, and spatial convolution with user defined kernels up to 63x63. *Image* also incorporates a Pascal-like macro programming language, providing the ability to automate complex, and frequently repetitive, processing tasks.

Image can be used to measure area, average gray value, center and angle of orientation of a user defined regions of interest. It also performs automated particle analysis and can be used to measure path lengths and angles. Measurement results can be printed, exported to text files, or copied to the Clipboard.

Spatial calibration is supported to provide real world area and length measurements. Density calibration can be done against radiation or optical density standards using user specified units. The user can select from any of eight different curve fitting methods for generating calibration curves.

Image provides MacPaint-like editing of color and gray scale images, including the ability to draw lines, rectangles, ovals and text. It can flip, rotate, invert and scale selections. It supports multiple windows and 8 levels of magnification. All editing, filtering, and measurement functions operate at any level of magnification and are undoable.

Image supports Data Translation and Scion frame grabber cards for capturing images or movie sequences using a TV camera. Acquired gray scale images can be shading corrected and frame averaged.

Image is written using Think Pascal from Symantec Corporation, and the complete source code is freely available.

System Requirements

Image requires a Macintosh with at least 4MB of memory, but 8MB or more are recommended for working with 3D images, 24-bit color or animation sequences. It requires a monitor with the ability to display 256 colors or shades of gray. *Image* directly supports, or is compatible with, large monitors, flatbed scanners, film recorders, graphics tablets, PostScript laser printers, photo typesetters and color printers.

Acknowledgments

The author wishes to thank the following individuals for their help, encouragement, and contributions: Peter Ahrens, Joseph Ayers, Greg Brown, Mike Castle, Rick Chapman, Dennis Chesters, Ted Collburn, Andras Eke, Chuck Fiori, Garth Fletcher, Tom Ford-Holevinski, Keith Gorlen, Joseph Hennessey, Greg Hook, Marshal Housekeeper, Edward J. Huff, Werner Klee, Cary Mariash, Kelly Martin, Reuben Mezrich, Ranney Mize, Steve Pequigney, David Powell, Ira Rampil, Arlo Reeves, Robert Rimmer, Bob Rodieck, Christian Russ, John Russ, Matthew Russotto, Bruce Smith, Seth Snyder, Roy Standing, Cliff Stoll, Steve Ruzin, and Mark Vivino.

I. Updated Versions and Bug Reports

Updates to *Image* are available to Internet users via anonymous ftp from zippy.nimh.nih.gov. Those without Internet access can get updates from many Macintosh bulletin boards and user group libraries. A reasonably current version, including Pascal source code and example images, is available from any of the following sources:

1) From a friend. The *Image* program, including source code and documentation, is public domain and may be freely copied, distributed and modified. However, if you modify *Image*, please update the about box before distributing your version of the program.

2) Via anonymous FTP from zippy.nimh.nih.gov[128.231.98.32]. Enter "anonymous" as the user name and your e-mail address as the password. The /pub/nih-image directory contains the latest version of *Image*(nih-image152.hqx), documentation in Word format(nih-image152_docs.hqx), and complete Think Pascal source code(nih-image152_source.hqx). The directory /pub/image/images contains sample TIFF and PICT images. The directory /pub/image/image_spinoffs contains versions of *Image* extended to do FFTs(ImageFFT), fractal analysis(ImageFractal), and to support quantitative evaluation of cerebral blood flow, glucose metabolism, and protein synthesis(Image/MG). There is a README file(0README.txt) with information on the file formats used.

3) Library 9(Graphics Tools) of the MACAPP forum on CompuServe. Source code is in Library 6 of the MACDEV forum.

4) Twilight Clone BBS in Silver Spring, MD. The Clone has 16 lines on sequential rollover, starting with 301-946-8677. To guarantee a V.32 connection, call 946-5034. *Image* is currently available at no charge from the Twilight Clone.

5) Subscribe to the NIH *Image* mailing list by sending a message containing the line "subscribe nih-image <your name>" to listserv@soils.umn.edu. Next obtain a list of the available NIH *Image* archive files by sending an "index nih-image" command to listserv@soils.umn.edu. These files can then be retrieved by means of a "get nih-image filename" command. The files are Binhexed and broken into chunks less than 32K in size. The NIH mailing is maintained by a group in the Soil Science Department at the University of Minnesota.

6) NTIS(National Technical Information Service), 5285 Port Royal Road, Springfield, VA 22161, phone 703-487-4650, order number PB93-504868 ($100 check, VISA, or Mastercard). Both the zippy.nimh.nih.gov FTP site and the Twilight Clone BBS are likely to have newer versions of *Image* than NTIS.

Bug reports and suggestions are welcome, as are corrections or additions to this manual. The author (Wayne Rasband) can be reached at the following electronic mail addresses:

Internet, BitNet:	wayne@helix.nih.gov
AppleLink:	wayne@helix.nih.gov@internet#
CompuServe:	>INTERNET: wayne@helix.nih.gov

APPENDIX 3
Whale pit measurements and plots

This appendix contains all measurements made at each whale pit quantitative station. For each whale feeding pit identified there are values associated with pit area in m^2 (area), pit width in m (minor), pit length in m (major), the angle the pit's major axis makes with the trackline (angle), and the azimuth of the pit's major axis (compass). Pit azimuths at each station are also displayed in histograms.

	area	minor	major	angle	compass
1	0.26100	0.25900	0.86500	0.0000	115.02
2	0.26100	0.33500	0.75300	5.0510	116.43
3	0.19800	0.22400	0.60700	6.4230	117.02
4	0.27000	0.22100	0.94100	7.8570	117.14
5	0.33300	0.37100	0.95300	7.9800	118.58
6	0.22100	0.14300	0.81300	8.5740	119.95
7	0.19800	0.29500	0.57300	9.9820	125.00
8	0.14400	0.18700	0.40000	132.41	307.81
9	0.74300	0.72700	0.85200	139.79	309.04
10	0.22100	0.22700	0.70600	147.76	310.33
11	0.18900	0.22200	0.52400	148.99	310.92
12	0.35100	0.36100	1.1890	153.05	311.35
13	0.18900	0.17700	0.57600	155.85	311.70
14	0.30600	0.29200	0.91400	158.72	312.79
15	0.28400	0.24800	0.86600	159.02	313.00
16	0.29300	0.34300	0.80700	159.73	313.27
17	0.25700	0.32900	0.73100	161.29	313.43
18	0.47300	0.35800	1.2840	161.66	313.66
19	0.22500	0.29800	0.70600	162.63	313.82
20	0.33800	0.43100	1.0450	162.79	313.85
21	0.23900	0.21900	0.73900	162.98	315.22
22	0.21600	0.33300	0.66200	163.43	316.79
23	0.17100	0.22900	0.57700	164.81	316.80
24	0.26100	0.17800	0.46700	164.84	317.78
25	0.22100	0.24400	0.78600	164.93	318.71
26	0.23000	0.27600	0.75300	165.45	319.02
27	0.34200	0.30500	1.0810	165.98	319.55
28	0.30600	0.35200	0.81800	166.29	320.07
29	0.27500	0.44200	0.84700	167.22	320.16
30	0.24300	0.36200	0.74500	168.20	320.19
31	0.22500	0.22200	0.75500	168.21	321.57
32	0.28400	0.43800	0.73300	169.78	322.02
33	0.19400	0.30100	0.44300	171.15	322.21
34	0.30200	0.42200	0.87500	171.18	322.37
35	0.16700	0.27600	0.46200	171.34	323.34
36	0.25700	0.39500	0.66700	171.57	323.71
37	0.25200	0.39900	0.75800	171.73	325.27
38	0.25200	0.37400	0.62500	172.00	325.98
39	0.23400	0.33800	0.69600	172.21	326.28
40	0.24300	0.29900	0.75700	173.30	329.15
41	0.29300	0.39600	0.83300	173.65	331.95
42	0.29700	0.36100	0.87000	174.07	336.01
43	0.22100	0.31200	0.71700	174.67	337.24
44	0.23000	0.17600	0.41600	175.96	345.21
45	0.25700	0.19700	0.41500	177.19	352.59

	area	minor	major	angle	compass
1	0.27621	0.38640	0.71484	0.042000	111.63
2	0.20646	0.24150	0.85491	1.5220	113.28
3	0.18994	0.28497	0.66654	3.1310	115.71
4	0.20508	0.28497	0.71967	8.8810	116.12
5	0.24187	0.30912	0.78246	9.2910	121.87
6	0.15397	0.26565	0.57960	11.717	123.48
7	0.23949	0.28497	0.84042	13.375	124.96
8	0.20249	0.33810	0.59892	150.26	305.15
9	0.19155	0.33327	0.57477	152.26	307.68
10	0.38703	0.50715	0.76314	154.64	307.76
11	0.14760	0.27531	0.53613	158.94	308.50
12	0.19466	0.27048	0.71967	159.15	309.21
13	0.26203	0.37674	0.69552	160.86	309.47
14	0.24789	0.31878	0.77763	161.74	309.49
15	0.18061	0.23667	0.76314	162.33	310.18
16	0.21747	0.28497	0.76314	162.84	311.98
17	0.23621	0.36225	0.65205	163.90	312.74
18	0.22956	0.38640	0.59409	165.27	314.15
19	0.20408	0.26082	0.78246	165.34	314.19
20	0.16445	0.25599	0.64239	165.63	314.93
21	0.14396	0.24633	0.58443	167.21	315.24
22	0.20063	0.24150	0.83076	167.97	316.78
23	0.27304	0.37191	0.73416	168.22	317.03
24	0.22993	0.30912	0.74382	169.76	317.79
25	0.040312	0.15456	0.26082	170.07	319.37
26	0.13596	0.29946	0.45402	170.81	319.66
27	0.19148	0.27531	0.69552	170.85	319.73
28	0.12609	0.22701	0.55545	172.26	321.10
29	0.14921	0.25116	0.59409	173.02	322.16
30	0.10974	0.20286	0.54096	174.82	322.67
31	0.26723	0.38157	0.70035	175.51	323.26
32	0.23672	0.35259	0.67137	175.53	324.14
33	0.067327	0.18837	0.35742	175.79	325.85
34	0.19708	0.31878	0.61824	176.50	326.06
35	0.19545	0.34293	0.56994	177.24	330.36
36	0.19960	0.29946	0.66654	177.32	332.74
37	0.16321	0.31878	0.51198	179.85	334.74

	area	minor	major	angle	compasss
1	0.20400	0.22500	0.28900	52.794	130.70
2	0.11600	0.16500	0.22300	51.388	141.04
3	0.10200	0.17100	0.19100	142.37	149.16
4	0.17800	0.18700	0.30300	160.84	152.22
5	0.12400	0.17900	0.22100	23.380	155.10
6	0.13800	0.19300	0.22800	150.37	159.63
7	0.067000	0.13900	0.15300	154.90	164.75
8	0.093000	0.16400	0.18100	168.96	167.63
9	0.17800	0.21600	0.26200	57.354	194.33
10	0.049000	0.081000	0.19300	97.079	195.80
11	0.062000	0.10300	0.19200	105.64	204.36
12	0.20400	0.20400	0.32000	157.78	212.92
13	0.044000	0.11100	0.12800	115.67	220.00
14	0.098000	0.12800	0.24300	56.578	223.33
15	0.062000	0.12300	0.16100	57.073	240.59
16	0.14700	0.19700	0.23700	57.601	252.40
17	0.14200	0.14100	0.32000	114.20	252.65
18	0.20000	0.18500	0.34500	8.7720	252.93
19	0.18700	0.14900	0.39800	1.8630	253.42
20	0.68400	0.29800	0.73200	179.30	257.21
21	0.12900	0.16300	0.25200	69.410	258.61
22	0.18200	0.17300	0.33600	10.609	286.62
23	0.098000	0.15500	0.20100	145.25	298.63
24	0.22200	0.21000	0.33700	11.368	299.39
25	0.044000	0.057000	0.24900	86.673	301.23
26	0.044000	0.038000	0.40000	90.000	308.14

	area	minor	major	angle	compass
1	0.26000	0.17200	0.96400	174.63	130.37
2	0.13200	0.17900	0.41600	18.314	130.48
3	0.16700	0.19000	0.58400	0.22000	130.73
4	0.15000	0.13200	0.56200	2.8740	130.79
5	0.17600	0.20400	0.53500	4.7470	130.93
6	0.27300	0.21000	0.95500	176.33	131.32
7	0.13700	0.16700	0.46300	4.9950	131.64
8	0.16300	0.18200	0.54000	8.0800	131.87
9	0.19400	0.13400	0.74400	4.8100	132.14
10	0.23800	0.23200	0.77900	172.82	132.38
11	0.14500	0.15600	0.51300	179.21	133.18
12	0.24700	0.28700	0.75800	176.82	133.25
13	0.21100	0.22300	0.75600	14.278	133.65
14	0.15400	0.20300	0.51700	178.68	133.66
15	0.20300	0.19700	0.69000	179.07	133.67
16	0.19800	0.26400	0.60600	173.67	134.26
17	0.19800	0.26200	0.65900	172.45	134.42
18	0.18900	0.24800	0.61200	5.5930	134.44
19	0.21600	0.26700	0.62600	6.3800	134.68
20	0.25100	0.27800	0.78700	178.13	134.71
21	0.19400	0.22500	0.56800	9.2870	134.75
22	0.15900	0.18400	0.54900	4.1930	135.37
23	0.18100	0.28000	0.51100	178.36	136.33
24	0.17200	0.17700	0.59500	4.4670	137.18
25	0.18900	0.21600	0.61100	175.32	137.34
26	0.17200	0.20900	0.58300	10.876	137.55
27	0.19800	0.23200	0.61000	175.56	138.48
28	0.15900	0.19500	0.57500	7.7810	139.47
29	0.15000	0.21900	0.46800	15.113	143.14
30	0.18900	0.13900	0.68600	10.667	145.38
31	0.16700	0.20800	0.47200	19.722	274.85
32	0.17600	0.18400	0.57800	171.52	283.56
33	0.19800	0.15100	0.72500	175.58	288.26
34	0.21600	0.23600	0.63500	170.53	290.28
35	0.16700	0.26700	0.48900	35.151	291.12
36	0.20700	0.17900	0.70500	6.1360	291.69
37	0.34800	0.23800	1.0470	18.881	294.69
38	0.17200	0.22400	0.57500	10.544	294.89
39	0.15000	0.20200	0.45200	179.63	295.72
40	0.15400	0.19800	0.51700	1.3920	298.42
41	0.23300	0.24200	0.82800	4.4350	299.12
42	0.13200	0.17200	0.44800	175.29	299.33
43	0.15900	0.20800	0.50500	26.444	299.46
44	0.14500	0.17900	0.51800	11.579	300.71
45	0.19800	0.27500	0.52000	15.314	301.26
46	0.16300	0.17700	0.57200	2.0820	301.33
47	0.16300	0.25000	0.52100	175.25	301.64

	area	minor	major	angle	compass
48	0.21600	0.22400	0.73700	8.1220	301.84
49	0.22500	0.22200	0.78200	8.3580	301.88
50	0.18900	0.27300	0.62600	175.74	301.92
51	0.16700	0.23400	0.60000	179.52	302.22
52	0.18500	0.20400	0.63300	176.34	303.62
53	0.20700	0.23100	0.65600	177.62	303.71
54	0.24700	0.24000	0.59600	1.9060	303.86
55	0.19400	0.18700	0.65900	176.35	304.41
56	0.21100	0.22300	0.72300	172.66	305.01
57	0.18900	0.25700	0.64900	6.2910	305.19
58	0.22500	0.14900	0.75200	8.1570	305.25
59	0.20700	0.30000	0.56900	3.7940	305.53
60	0.17200	0.22600	0.56400	8.7420	305.57
61	0.19800	0.17800	0.65300	177.86	305.81
62	0.13700	0.15400	0.46400	179.27	305.84
63	0.14500	0.21300	0.45500	3.1990	306.21
64	0.20300	0.31000	0.59200	176.75	306.80
65	0.11000	0.12000	0.38600	0.97200	307.13
66	0.14100	0.13500	0.49800	1.1930	307.86
67	0.14500	0.14600	0.53900	0.93700	307.92
68	0.16300	0.19600	0.58600	0.97500	308.09
69	0.18100	0.20500	0.58200	4.1600	308.61
70	0.14500	0.19900	0.50000	2.1400	308.81
71	0.18500	0.29600	0.57900	164.62	309.02
72	0.14500	0.17500	0.50600	166.86	309.03
73	0.20300	0.31300	0.59100	21.740	309.06
74	0.18100	0.23800	0.58300	8.6750	309.78

	area	minor	major	angle	compass
1	0.14600	0.22100	0.44900	3.9180	133.13
2	0.25100	0.25500	0.69100	170.86	137.26
3	0.22100	0.32700	0.57700	10.378	139.07
4	0.23100	0.26100	0.65800	6.6190	139.14
5	0.22600	0.30700	0.64600	166.46	143.54
6	0.33700	0.33900	0.76000	11.442	147.35
7	0.33700	0.39400	0.93500	20.033	151.17
8	0.23100	0.30500	0.58300	142.52	152.63
9	0.28700	0.38200	0.77600	157.37	167.48
10	0.28200	0.32600	0.85000	12.700	276.83
11	0.20600	0.18600	0.59400	5.7550	287.46
12	0.23600	0.20200	0.75900	170.93	289.97
13	0.17100	0.22700	0.46600	12.132	293.66
14	0.23100	0.24100	0.75000	33.166	296.37
15	0.26700	0.32600	0.66200	10.539	297.30
16	0.27700	0.28900	0.88800	1.8830	297.87
17	0.23100	0.22100	0.68100	172.74	298.41
18	0.19600	0.26800	0.49000	16.339	298.56
19	0.20100	0.22300	0.59500	13.632	299.46
20	0.13100	0.21600	0.36300	176.87	299.62
21	0.27700	0.26600	0.77600	162.65	302.18
22	0.18600	0.21700	0.56200	22.541	303.08
23	0.31200	0.33300	0.97600	158.83	303.38
24	0.22100	0.25200	0.68000	6.9220	304.24
25	0.22600	0.23600	0.66600	3.2270	306.08
26	0.19100	0.24400	0.53900	7.8150	306.77
27	0.17100	0.26900	0.48100	11.587	308.12

	Area	Minor	Major	Angle	Compass
1	0.16400	0.15700	0.62000	5.9380	130.38
2	0.14100	0.16300	0.48400	177.32	130.40
3	0.19700	0.20900	0.60700	176.27	130.67
4	0.16400	0.20600	0.53500	179.62	131.17
5	0.16400	0.14800	0.63700	1.4240	131.45
6	0.16000	0.12800	0.58200	2.2380	131.75
7	0.21100	0.13400	0.76900	8.4680	132.13
8	0.22000	0.19900	0.76600	1.1350	132.15
9	0.18300	0.16000	0.62400	177.85	132.52
10	0.21600	0.21400	0.74700	162.87	132.53
11	0.16000	0.20800	0.55300	10.778	132.67
12	0.16400	0.18400	0.54400	12.106	132.68
13	0.11700	0.17300	0.44100	12.671	133.04
14	0.22500	0.30600	0.62100	4.4580	133.73
15	0.23500	0.30300	0.74400	3.5390	133.76
16	0.17800	0.16100	0.64000	17.605	134.40
17	0.19200	0.22100	0.58100	168.52	135.01
18	0.18300	0.17800	0.64500	176.24	135.69
19	0.17400	0.26100	0.52100	178.25	135.93
20	0.14500	0.16900	0.45200	177.33	136.65
21	0.18300	0.20100	0.58000	10.501	140.75
22	0.16400	0.25100	0.51700	178.55	141.48
23	0.12200	0.11100	0.46900	12.807	141.68
24	0.23500	0.26200	0.74600	14.695	141.73
25	0.16000	0.17700	0.52200	179.60	147.13
26	0.20200	0.21900	0.62100	174.07	260.16
27	0.16900	0.15400	0.58200	13.066	268.59
28	0.21100	0.34600	0.60900	0.50800	281.22
29	0.22500	0.17900	0.74100	11.070	281.28
30	0.20200	0.21400	0.67800	2.5670	285.47
31	0.19200	0.24900	0.57600	168.27	292.39
32	0.18800	0.17100	0.66200	0.0000	293.22
33	0.15000	0.18700	0.44800	28.778	293.86
34	0.17400	0.16700	0.63400	10.096	294.01
35	0.11700	0.16100	0.41800	9.3610	295.30
36	0.21600	0.14800	0.73900	168.32	296.93
37	0.15500	0.19100	0.51700	12.337	297.19
38	0.16400	0.23600	0.49300	10.846	297.33
39	0.23500	0.25200	0.74800	177.47	297.66
40	0.23500	0.27800	0.75300	6.9280	297.89
41	0.20200	0.20700	0.62600	10.053	298.72
42	0.18300	0.24000	0.59100	169.25	298.93
43	0.19200	0.25300	0.54900	177.48	299.08
44	0.21100	0.18900	0.72800	0.29700	299.15
45	0.15500	0.19600	0.44900	2.2180	299.22
46	0.16900	0.17300	0.53500	3.1510	299.50
47	0.20600	0.25000	0.65000	5.6090	299.62

	Area	Minor	Major	Angle	Compass
48	0.13600	0.17200	0.47000	7.2180	299.90
49	0.16900	0.19500	0.55900	176.96	299.95
50	0.19200	0.20200	0.65700	177.87	300.64
51	0.23000	0.32800	0.75200	174.99	301.53
52	0.25800	0.25500	0.83200	179.33	302.41
53	0.16900	0.15400	0.56300	3.1980	302.78
54	0.22000	0.29100	0.65700	178.83	302.99
55	0.20200	0.25700	0.55100	10.381	303.07
56	0.15000	0.24900	0.45000	173.35	303.61
57	0.21600	0.25500	0.65500	16.139	304.06
58	0.17400	0.27500	0.49400	11.283	304.39
59	0.21600	0.27100	0.59500	7.0130	305.54
60	0.15000	0.21400	0.44700	24.526	306.46
61	0.18300	0.23500	0.55900	174.31	306.80
62	0.16000	0.21400	0.50200	6.3900	306.82
63	0.16900	0.23200	0.51600	41.414	306.85
64	0.18800	0.20500	0.63300	2.0330	307.43
65	0.20200	0.22800	0.62900	49.839	307.76
66	0.13100	0.17400	0.48900	3.1850	307.78
67	0.14100	0.17500	0.48700	175.60	307.97
68	0.25800	0.13900	0.92600	10.915	308.58
69	0.15500	0.26700	0.45300	16.776	308.86
70	0.18300	0.19300	0.55600	28.720	309.49
71	0.14500	0.23200	0.40600	7.5920	309.70
72	0.18300	0.29000	0.53000	15.986	310.00

	area	minor	major	angle	compass
1	0.32000	0.43200	0.49800	65.163	134.04
2	0.17300	0.21000	0.61400	168.63	135.94
3	0.40400	0.47700	1.2360	23.102	136.18
4	0.20000	0.24800	0.62800	5.6500	141.37
5	0.18700	0.30300	0.48500	156.37	153.63
6	0.16400	0.23200	0.50600	173.82	185.89
7	0.16900	0.30600	0.44400	124.11	244.84
8	0.16900	0.22800	0.47200	3.4040	266.49
9	0.13300	0.21100	0.42900	4.7410	268.60
10	0.14700	0.21500	0.50700	175.96	278.26
11	0.12000	0.16600	0.42500	174.06	285.19
12	0.40000	0.47100	1.1560	31.745	286.90
13	0.33300	0.28300	1.0850	16.683	293.32
14	0.41300	0.45600	1.3690	24.813	295.19
15	0.42700	0.62900	1.2730	14.810	304.35
16	0.38200	0.55400	1.0680	41.403	305.26
17	0.45800	0.57200	1.4500	43.510	306.60

	area	minor	major	angle	compass
1	0.046000	0.038000	0.40500	0.0000	11.221
2	0.26000	0.31300	0.75600	4.2230	11.298
3	0.16400	0.21300	0.56000	169.83	12.039
4	0.29700	0.37000	0.89500	18.503	18.357
5	0.17300	0.21700	0.57600	9.5630	23.128
6	0.18700	0.20000	0.54500	0.88800	31.864
7	0.20100	0.27900	0.65100	179.12	32.451
8	0.26900	0.27000	0.87200	6.1910	36.500
9	0.27400	0.24800	0.87900	177.14	36.793
10	0.23300	0.20400	0.71200	160.98	41.288
11	0.15500	0.16300	0.56300	162.03	41.497
12	0.15500	0.20900	0.49300	7.6690	42.752
13	0.21000	0.28300	0.67700	178.60	43.232
14	0.26000	0.24200	0.89500	27.549	45.000
15	0.35200	0.27000	1.0230	18.712	45.085
16	0.25600	0.34000	0.70100	36.872	45.314
17	0.29200	0.29500	0.93000	48.779	45.554
18	0.18700	0.21600	0.55900	172.12	46.244
19	0.26900	0.35900	0.71700	41.643	47.271
20	0.27400	0.30900	0.83300	48.702	48.026
21	0.29200	0.27800	0.95200	23.500	48.346
22	0.17300	0.20300	0.42300	11.654	48.859
23	0.19600	0.29100	0.63300	2.2800	49.165
24	0.21000	0.25100	0.62600	23.207	49.274
25	0.26500	0.29800	0.82300	0.76700	49.341
26	0.41500	0.36500	1.3620	179.94	49.663
27	0.17300	0.20700	0.58200	10.041	49.959
28	0.32000	0.27200	1.0850	14.686	50.175
29	0.16000	0.19600	0.43800	11.141	50.421
30	0.30600	0.38900	0.88800	2.0260	50.437
31	0.21900	0.22200	0.56300	169.17	50.595
32	0.15100	0.17400	0.46800	178.54	51.106
33	0.23300	0.28200	0.80800	9.8250	51.496
34	0.22800	0.26200	0.70900	1.2780	52.200
35	0.16000	0.19100	0.52500	8.8940	52.331
36	0.12300	0.16800	0.38900	11.974	53.271
37	0.30100	0.31200	0.97700	10.835	53.298
38	0.11400	0.18200	0.40000	1.3590	53.494
39	0.21000	0.18400	0.72700	178.01	53.809
40	0.35600	0.38200	1.2220	28.136	54.924
41	0.34200	0.36500	1.1630	16.768	55.155
42	0.14200	0.17300	0.47900	0.63300	55.456
43	0.24200	0.22600	0.82400	4.5440	55.480
44	0.24200	0.28900	0.72000	179.83	55.777
45	0.16000	0.16800	0.51800	176.20	56.108
46	0.16000	0.18400	0.49600	169.65	56.187
47	0.17800	0.24300	0.52700	157.80	57.220

	area	minor	major	angle	compass
48	0.27400	0.33600	0.85300	2.7800	57.519
49	0.29700	0.38000	0.79100	47.961	57.720
50	0.15500	0.16400	0.51300	179.08	57.974
51	0.26000	0.30800	0.81500	4.8450	58.049
52	0.29200	0.32800	0.95300	10.726	58.641
53	0.13200	0.16400	0.39900	177.54	58.722
54	0.23300	0.16800	0.81500	174.95	58.798
55	0.12800	0.19400	0.38200	9.5790	58.865
56	0.22400	0.23500	0.72800	4.5200	59.112
57	0.14600	0.18300	0.44400	15.000	59.233
58	0.17800	0.23400	0.55900	6.5060	59.367
59	0.21900	0.18300	0.79400	174.70	60.000
60	0.26500	0.28300	0.81300	10.659	240.06
61	0.24200	0.21100	0.81200	177.26	240.17
62	0.35600	0.37300	1.1910	3.8920	240.88
63	0.26900	0.22200	0.91500	13.756	240.92
64	0.26000	0.20700	0.85700	6.7290	241.40
65	0.31000	0.35300	0.98800	10.337	241.46
66	0.19600	0.19400	0.66800	5.0760	241.99
67	0.32400	0.36700	1.0180	8.5040	242.46
68	0.30100	0.21300	1.0180	12.729	242.74
69	0.22800	0.19200	0.71000	3.8130	242.86
70	0.24700	0.18200	0.90100	1.2020	243.80
71	0.16400	0.18600	0.57700	1.9510	245.05
72	0.29700	0.32100	1.0400	14.446	245.30
73	0.27800	0.35700	0.79800	7.8000	247.88
74	0.17300	0.18900	0.60000	14.915	250.17
75	0.38800	0.34700	1.2890	6.7020	250.35
76	0.23700	0.26600	0.82400	2.4810	250.83
77	0.18300	0.19300	0.61600	158.49	257.97
78	0.18300	0.17900	0.60900	9.4050	259.02
79	0.41500	0.49700	1.4660	17.248	261.52
80	0.19600	0.19600	0.63200	1.1350	262.20

	area	minor	major	angle	compass
1	0.034787	0.13750	0.25300	56.764	3.2360
2	0.11011	0.22000	0.50050	179.48	43.404
3	0.26620	0.27500	0.96800	5.4870	45.543
4	0.60222	0.43450	1.3860	3.0340	46.711
5	0.42078	0.35750	1.1770	2.5280	47.804
6	0.31136	0.25850	1.2045	167.33	49.474
7	0.23958	0.24200	0.99000	4.1170	51.432
8	0.034485	0.10450	0.33000	83.823	52.002
9	0.13637	0.25300	0.53900	5.0190	54.513
10	0.025410	0.11000	0.23100	90.000	54.981
11	0.11011	0.19250	0.57200	8.5680	55.450
12	0.28232	0.28050	1.0065	1.9680	55.883
13	0.10264	0.15950	0.64350	179.78	56.326
14	0.074536	0.15400	0.48400	1.3120	56.966
15	0.18132	0.29700	0.61050	13.289	57.221
16	0.066429	0.19800	0.33550	79.750	57.340
17	0.092565	0.18700	0.49500	178.39	57.472
18	0.10969	0.20350	0.53900	16.596	58.032
19	0.29830	0.31350	0.95150	0.078000	58.688
20	0.026620	0.11000	0.24200	85.219	58.920
21	0.078075	0.15950	0.48950	168.37	59.922
22	0.069696	0.19800	0.35200	101.98	240.22
23	0.14217	0.27500	0.51700	179.17	240.52
24	0.098010	0.24750	0.39600	101.53	240.83
25	0.14054	0.25300	0.55550	2.7790	241.04
26	1.3909	0.72050	1.9305	3.6740	241.61
27	0.094864	0.15400	0.61600	1.0800	251.63
28	0.031037	0.10450	0.29700	103.20	252.67
29	0.072418	0.11550	0.62700	4.5500	316.80
30	0.11888	0.16500	0.72050	2.6600	318.02
31	1.0505	0.53350	1.9690	10.526	318.47
32	0.63752	0.41250	1.5455	178.96	330.00
33	1.2632	0.52800	2.3925	14.457	334.78
34	0.55212	0.42900	1,2870	7.9980	336.18
35	0.96491	0.45100	2.1395	12.196	340.25
36	1.9769	0.92400	2.1395	11.974	50.421
37	9.2209	1.7160	5.3735	10.835	50.437
38	2.2022	1.0010	2.2000	1.3590	50.595
39	4.0465	1.0120	3.9985	178.01	51.106
40	14.121	2.1010	6.7210	28.136	51.250
41	12.841	2.0075	6.3965	16.768	51.496
42	2.5067	0.95150	2.6345	0.63300	51.575
43	5.6333	1.2430	4.5320	4.5440	52.200
44	6.2944	1.5895	3.9600	179.83	52.331
45	2.6325	0.92400	2.8490	176.20	52.951
46	2.7607	1.0120	2.7280	169.65	53.271
47	3.8738	1.3365	2.8985	157.80	53.298

	area	minor	major	angle	compass
48	8.6699	1.8480	4.6915	2.7800	53.494
49	9.0925	2.0900	4.3505	47.961	53.733
50	2.5450	0.90200	2.8215	179.08	53.809
51	7.5934	1.6940	4.4825	4.8450	54.924
52	9.4557	1.8040	5.2415	10.726	55.155
53	1.9794	0.90200	2.1945	177.54	55.456
54	4.1418	0.92400	4.4825	174.95	55.480
55	2.2418	1.0670	2.1010	9.5790	55.777
56	5.1752	1.2925	4.0040	4.5200	56.108
57	2.4579	1.0065	2.4420	15.000	56.187
58	3.9569	1.2870	3.0745	6.5060	56.326
59	4.3954	1.0065	4.3670	174.70	56.969
60	6.9599	1.5565	4.4715	10.659	56.981
61	5.1828	1.1605	4.4660	177.26	57.218
62	13.438	2.0515	6.5505	3.8920	57.220
63	6.1447	1.2210	5.0325	13.756	57.519
64	5.3663	1.1385	4.7135	6.7290	57.720
65	10.550	1.9415	5.4340	10.337	57.728
66	3.9202	1.0670	3.6740	5.0760	57.974
67	11.302	2.0185	5.5990	8.5040	58.049
68	6.5592	1.1715	5.5990	12.729	58.641
69	4.1237	1.0560	3.9050	3.8130	58.722
70	4.9605	1.0010	4.9555	1.2020	58.798
71	3.2465	1.0230	3.1735	1.9510	58.865
72	10.099	1.7655	5.7200	14.446	58.893
73	8.6178	1.9635	4.3890	7.8000	59.112
74	3.4304	1.0395	3.3000	14.915	59.233
75	13.530	1.9085	7.0895	6.7020	59.367
76	6.6303	1.4630	4.5320	2.4810	59.664
77	3.5964	1.0615	3.3880	158.49	60.000
78	3.2976	0.98450	3.3495	9.4050	240.00
79	22.040	2.7335	8.0630	17.248	240.06
80	3.7471	1.0780	3.4760	1.1350	240.17
81	0.33732	0.34650	0.97350	150.85	240.88
82	0.46509	0.41250	1.1275	6.2670	240.92
83	0.84700	0.55000	1.5400	2.7820	241.04
84	0.66958	0.52250	1.2815	2.2720	241.40
85	0.52514	0.38500	1.3640	166.99	241.46
86	0.45932	0.40150	1.1440	3.0190	241.99
87	0.41930	0.45650	0.91850	159.49	242.46
88	0.32050	0.35750	0.89650	167.55	242.74
89	0.49495	0.44550	1.1110	3.0310	242.86
90	0.27769	0.33000	0.84150	1.1070	243.80
91	0.24584	0.34650	0.70950	7.0490	245.05
92	0.40922	0.48950	0.83600	8.7500	245.30
93	0.35072	0.34100	1.0285	18.323	246.07
94	0.32089	0.42900	0.74800	11.819	247.88

	area	minor	major	angle	compass
95	0.49078	0.42900	1.1440	0.33600	250.17
96	0.27679	0.33550	0.82500	12.062	250.35
97	0.42035	0.39600	1.0615	27.080	250.83
98	0.42498	0.34650	1.2265	165.31	252.45
99	1.3909	0.72050	1.9305	3.6740	252.87
100	0.35172	0.42350	0.83050	173.93	253.01
101	0.39304	0.33550	1.1715	167.13	254.69
102	0.32461	0.40150	0.80850	180.00	257.97
103	1.0390	0.58850	1.7655	178.96	259.02
104	1.5094	0.69300	2.1780	9.8860	260.51
105	1.5245	0.58850	2.5905	14.480	261.52
106	0.91149	0.59400	1.5345	8.4250	262.20
107	1.2735	0.53350	2.3870	12.128	269.15
108	0.034787	0.13750	0.25300	56.764	3.2360
109	0.11011	0.22000	0.50050	179.48	43.404
110	0.26620	0.27500	0.96800	5.4870	45.543
111	0.60222	0.43450	1.3860	3.0340	46.711
112	0.42078	0.35750	1.1770	2.5280	47.804
113	0.31136	0.25850	1.2045	167.33	49.474
114	0.23958	0.24200	0.99000	4.1170	51.432
115	0.034485	0.10450	0.33000	83.823	52.002
116	0.13637	0.25300	0.53900	5.0190	54.513
117	0.025410	0.11000	0.23100	90.000	54.981
118	0.11011	0.19250	0.57200	8.5680	55.450
119	0.28232	0.28050	1.0065	1.9680	55.883
120	0.10264	0.15950	0.64350	179.78	56.326
121	0.074536	0.15400	0.48400	1.3120	56.966
122	0.18132	0.29700	0.61050	13.289	57.221
123	0.066429	0.19800	0.33550	79.750	57.340
124	0.092565	0.18700	0.49500	178.39	57.472
125	0.10969	0.20350	0.53900	16.596	58.032
126	0.29830	0.31350	0.95150	0.078000	58.688
127	0.026620	0.11000	0.24200	85.219	58.920
128	0.078075	0.15950	0.48950	168.37	59.922
129	0.069696	0.19800	0.35200	101.98	240.22
130	0.14217	0.27500	0.51700	179.17	240.52
131	0.098010	0.24750	0.39600	101.53	240.83
132	0.14054	0.25300	0.55550	2.7790	241.04
133	1.3909	0.72050	1.9305	3.6740	241.61
134	0.094864	0.15400	0.61600	1.0800	251.63
135	0.031037	0.10450	0.29700	103.20	252.67
136	0.072418	0.11550	0.62700	4.5500	316.80
137	0.11888	0.16500	0.72050	2.6600	318.02
138	1.0505	0.53350	1.9690	10.526	318.47
139	0.63752	0.41250	1.5455	178.96	330.00
140	1.2632	0.52800	2.3925	14.457	334.78
141	0.55212	0.42900	1.2870	7.9980	336.18

	area	minor	major	angle	compass
142	0.96491	0.45100	2.1395	12.196	340.25

	area	minor	major	angle	compass
1	0.26000	0.30800	0.87600	12.522	3.6900
2	0.30600	0.39400	0.82300	22.475	27.380
3	0.26900	0.34600	0.87400	178.36	28.551
4	0.35600	0.34200	1.1630	7.6800	29.287
5	0.23300	0.23400	0.78400	1.3950	33.975
6	0.23300	0.24700	0.80500	4.9390	34.803
7	0.50200	0.52900	1.6550	12.344	35.618
8	0.21500	0.30300	0.59600	56.310	37.525
9	0.41500	0.43800	1.3220	179.42	38.584
10	0.32900	0.36300	1.1290	178.14	38.760
11	0.39300	0.46000	1.2970	169.66	38.838
12	0.48400	0.45000	1.6940	178.88	40.040
13	0.23300	0.24400	0.82300	178.15	41.589
14	0.28300	0.26400	0.97300	2.5410	42.727
15	0.37400	0.32600	1.1010	12.210	42.753
16	0.40600	0.53600	1.2740	21.240	43.167
17	0.33300	0.29100	1.1370	17.273	43.859
18	0.35200	0.37100	1.1490	2.7440	44.817
19	0.21900	0.27200	0.69400	177.87	45.206
20	0.32400	0.38700	1.0540	7.3750	45.635
21	0.33300	0.35300	1.1070	4.8710	46.301
22	0.42900	0.46200	1.1440	167.19	47.001
23	0.32400	0.36600	1.0370	14.794	47.478
24	0.28800	0.26900	0.85300	178.52	47.656
25	0.31000	0.43100	0.92000	13.699	47.790
26	0.34700	0.40500	1.0040	4.7860	48.066
27	0.35600	0.38400	1.2410	4.8270	48.340
28	0.41500	0.49400	1.3360	10.383	49.283
29	0.36500	0.41200	1.2230	6.3930	49.617
30	0.26500	0.32200	0.90300	0.85200	49.649
31	0.49300	0.46100	1.7340	14.365	50.315
32	0.32900	0.37600	1.0790	4.1040	50.965
33	0.45700	0.44600	1.4610	3.0260	51.312
34	0.45200	0.49800	1.4900	12.999	51.366
35	0.38300	0.33700	1.1990	178.51	52.320
36	0.30100	0.35600	0.90100	5.5480	52.455
37	0.56600	0.49300	1.9860	169.25	52.625
38	0.25100	0.30100	0.78200	31.449	53.041
39	0.22400	0.24400	0.74900	19.960	53.193
40	0.56600	0.60000	1.8180	4.6510	53.307
41	0.30600	0.31800	0.93200	10.717	53.607
42	0.68000	0.39100	1.9540	3.5000	53.637
43	0.28300	0.29000	0.95200	4.9970	53.964
44	0.32900	0.43600	0.88300	174.68	54.345
45	0.30100	0.34500	0.92800	26.025	54.452
46	0.38800	0.39300	1.1890	5.6550	54.454
47	0.35600	0.44500	1.0720	9.0350	54.809

	area	minor	major	angle	compass
48	0.32000	0.40200	1.0400	179.75	54.819
49	0.27400	0.31900	0.91600	15.183	55.003
50	0.28800	0.36400	0.81000	24.382	55.061
51	0.31000	0.31900	1.0560	3.3280	55.129
52	0.30100	0.32000	0.90400	6.0360	55.173
53	0.43800	0.41900	1.5620	6.6930	55.214
54	0.42500	0.34100	1.2630	1.9650	55.349
55	0.37900	0.36400	1.1410	179.61	55.459
56	0.44700	0.49800	1.4690	5.1910	55.896
57	0.42000	0.41300	1.1430	6.3630	56.340
58	0.32900	0.33000	1.0600	170.74	56.500
59	0.33300	0.37800	1.1000	21.416	56.672
60	0.39300	0.60500	1.0470	166.15	56.734
61	0.36100	0.38300	1.1610	179.51	56.974
62	0.39300	0.33800	1.2840	3.6600	57.256
63	0.34200	0.37400	1.0340	179.12	57.459
64	0.27800	0.26300	0.98300	3.2660	57.719
65	0.20500	0.24200	0.67800	9.6850	58.035
66	0.32900	0.39600	1.0340	11.934	58.605
67	0.49800	0.49900	1.6500	170.20	59.148
68	0.28800	0.38600	0.88200	10.351	240.25
69	0.30100	0.38400	0.85800	18.411	240.39
70	0.42000	0.37100	1.4500	16.833	240.49
71	0.25600	0.28600	0.92400	5.5460	240.58
72	0.40600	0.43700	1.4200	25.197	240.88
73	0.29700	0.43700	1.0140	139.46	241.12
74	0.40600	0.48500	1.3420	7.5450	241.22
75	0.37000	0.42500	1.1350	17.247	241.48
76	0.29200	0.34400	0.93800	5.1810	241.49
77	0.36500	0.33400	1.1540	8.6340	241.64
78	0.21500	0.28800	0.60500	32.620	241.85
79	0.36100	0.35500	1.2240	8.6880	241.86
80	0.27400	0.22700	0.97900	176.66	242.13
81	0.25100	0.28500	0.83800	11.660	242.83
82	0.34200	0.36700	0.81500	176.14	243.34
83	0.37400	0.41200	1.2490	6.8070	243.86
84	0.36500	0.39200	1.2540	178.78	245.32
85	0.26000	0.38000	0.81000	30.713	249.26
86	0.22400	0.25700	0.74700	16.141	249.80
87	0.32400	0.30700	1.1210	4.5410	250.34
88	0.27800	0.32500	0.90900	21.162	250.75
89	0.23300	0.28900	0.76800	168.52	251.48
90	0.25100	0.29200	0.85200	6.9590	252.81
91	0.25600	0.31300	0.81600	2.2810	253.85
92	0.24700	0.22900	0.73700	177.17	280.54

	Area	minor	major	angle	compass
1	0.25190	0.34136	0.73794	165.43	18.933
2	0.19616	0.28112	0.69778	163.07	30.601
3	0.11819	0.17570	0.67268	7.1090	32.307
4	0.17865	0.25602	0.69778	5.0310	34.525
5	0.18595	0.23594	0.78814	20.468	36.144
6	0.43660	0.38654	1.1295	8.9360	36.942
7	0.41732	0.46184	0.90360	12.500	37.468
8	0.27521	0.33634	0.81826	177.85	39.532
9	0.39464	0.43674	0.90360	20.136	39.604
10	0.45688	0.37148	1.2299	17.926	39.864
11	0.45905	0.34638	1.3253	10.248	41.892
12	0.24903	0.27108	0.91866	2.5430	42.074
13	0.21909	0.31626	0.69276	147.15	43.971
14	0.39837	0.32128	1.2399	176.17	45.825
15	0.12678	0.21586	0.58734	23.058	45.973
16	0.57311	0.41666	1.3755	1.0390	46.366
17	0.25402	0.35140	0.72288	22.532	46.729
18	0.13427	0.24096	0.55722	3.3380	47.215
19	0.42276	0.36144	1.1697	3.0300	47.500
20	0.47901	0.44176	1.0843	1.5410	47.604
21	0.22902	0.32128	0.71284	179.17	48.149
22	0.30823	0.40662	0.75802	154.70	48.792
23	0.22363	0.29116	0.76806	155.21	49.065
24	0.35986	0.34136	1.0542	4.7260	49.752
25	0.24999	0.32128	0.77810	12.785	50.258
26	0.37627	0.39658	0.94878	7.7160	51.064
27	0.21262	0.29618	0.71786	164.67	51.737
28	0.30845	0.36144	0.85340	25.475	51.903
29	0.13437	0.21586	0.62248	7.7230	52.173
30	0.32561	0.36646	0.88854	29.399	52.277
31	0.46691	0.48192	0.96886	14.175	52.284
32	0.31412	0.22590	1.3905	177.45	52.803
33	0.26831	0.31626	0.84838	41.067	52.891
34	0.30271	0.33132	0.91364	12.396	52.970
35	0.47780	0.39658	1.2048	1.5020	54.008
36	0.20322	0.32128	0.63252	23.856	54.579
37	0.23285	0.28112	0.82830	14.027	54.838
38	0.36964	0.38152	0.96886	2.8100	54.969
39	0.45018	0.38654	1.1646	8.2630	54.981
40	0.43960	0.44678	0.98392	2.3220	55.274
41	0.40623	0.32630	1.2450	18.108	56.497
42	0.28154	0.28614	0.98392	11.851	56.662
43	0.17686	0.29116	0.60742	16.029	56.970
44	0.27065	0.30120	0.89858	2.7500	57.190
45	0.13981	0.19076	0.73292	1.7140	57.250
46	0.25712	0.28614	0.89858	2.2440	57.457
47	0.31611	0.28112	1.1245	7.0300	57.649

	Area	minor	major	angle	compass
48	0.31208	0.36144	0.86344	177.82	57.678
49	0.28703	0.33634	0.85340	9.7420	57.756
50	0.54201	0.38152	1.4207	13.271	58.001
51	0.27761	0.36144	0.76806	5.4210	58.286
52	0.33597	0.33132	1.0140	0.18100	58.459
53	0.33643	0.37650	0.89356	11.208	58.498
54	0.33517	0.38152	0.87850	5.1620	58.948
55	0.18739	0.26104	0.71786	8.0970	58.961
56	0.54909	0.40662	1.3504	7.1970	59.485
57	0.59236	0.36646	1.6164	1.0520	59.819
58	0.50645	0.38654	1.3102	2.3510	240.83
59	0.19898	0.28112	0.70782	20.396	242.15
60	0.31223	0.29618	1.0542	177.13	242.18
61	0.36490	0.40160	0.90862	176.91	242.55
62	0.23638	0.35140	0.67268	10.935	242.87
63	0.15423	0.22590	0.68272	7.8270	243.09
64	0.34217	0.36646	0.93372	13.634	243.83
65	0.20160	0.25100	0.80320	1.9990	254.57
66	0.46434	0.37148	1.2500	5.9920	255.33
67	0.30437	0.30622	0.99396	5.0190	256.93
68	0.13608	0.22590	0.60240	0.51500	264.79
69	0.25281	0.33132	0.76304	3.5030	265.30
70	0.17781	0.28112	0.63252	27.693	272.85

	area	minor	major	angle	compass
1	1.6330	0.38600	1.3750	1.0020	61.285
2	1.6880	0.40400	1.3310	1.5200	63.110
3	1.3140	0.32600	1.2830	2.4290	63.961
4	1.2000	0.31300	1.2220	3.0770	64.506
5	0.68000	0.27500	0.78700	6.1700	64.567
6	1.3280	0.32100	1.3170	6.4770	64.966
7	1.8610	0.39300	1.5060	22.150	65.820
8	1.4100	0.40800	1.1000	28.348	66.818
9	1.7560	0.44300	1.2620	35.120	67.711
10	0.97200	0.35000	0.88300	35.899	67.847
11	1.2550	0.33900	1.1780	153.63	68.095
12	1.3370	0.33500	1.2720	157.15	68.876
13	1.4460	0.47300	0.97300	160.68	68.903
14	1.0400	0.31200	1.0600	165.22	69.298
15	1.3730	0.32100	1.3630	165.34	69.984
16	1.1540	0.33100	1.1110	166.14	70.921
17	1.9020	0.43600	1.3900	168.24	70.950
18	1.2730	0.31300	1.2930	169.05	71.757
19	1.0170	0.34600	0.93900	169.08	73.856
20	1.2770	0.34000	1.1960	170.02	74.664
21	0.87100	0.33500	0.82800	170.70	74.778
22	1.0770	0.25700	1.3340	171.10	79.324
23	1.7520	0.63400	0.88400	171.12	82.848
24	1.1680	0.32000	1.1600	171.90	86.368
25	1.4100	0.37200	1.2050	172.15	204.10
26	0.86700	0.33100	0.83400	172.29	204.88
27	1.0540	0.32100	1.0460	173.18	211.65
28	1.2270	0.36700	1.0650	174.18	217.85
29	0.73400	0.30100	0.77700	175.03	233.52
30	0.72100	0.23400	0.97900	175.43	233.83
31	1.1500	0.29100	1.2570	175.49	236.92
32	1.0310	0.30800	1.0740	176.04	237.57
33	0.70700	0.31600	0.71200	176.89	238.48
34	0.99900	0.39700	0.80000	178.71	239.00

	area	minor	major	angle	compass
1	0.14000	0.17800	0.46300	3.5670	122.82
2	0.21500	0.22500	0.67700	166.53	129.91
3	0.16200	0.19700	0.56800	174.19	131.62
4	0.13200	0.14100	0.46700	179.44	133.13
5	0.30300	0.30500	1.0200	16.873	133.75
6	0.30300	0.24400	1.0540	169.15	134.05
7	0.29400	0.26800	0.92700	168.82	134.36
8	0.32500	0.31700	1.0340	8.3680	135.50
9	0.13600	0.18300	0.42800	169.84	135.33
10	0.27600	0.31200	0.93900	15.504	135.53
11	0.17500	0.23800	0.55800	177.13	136.06
12	0.37700	0.35100	1.2810	0.28400	137.63
13	0.40800	0.33400	1.3530	11.784	138.22
14	0.21500	0.22400	0.68700	173.89	140.93
15	0.32900	0.36300	1.0660	15.950	142.63
16	0.15800	0.21700	0.55500	6.5950	142.71
17	0.20200	0.24000	0.65800	173.53	143.40
18	0.32500	0.30900	1.0130	27.177	144.09
19	0.36400	0.37400	1.1450	5.2610	144.49
20	0.32500	0.34600	1.0930	175.43	144.70
21	0.35100	0.30000	0.94900	13.944	144.74
22	0.38600	0.37500	1.2480	175.19	145.36
23	0.34200	0.31500	1.1580	4.3450	145.65
24	0.32500	0.35000	0.96900	4.2560	145.74
25	0.40800	0.42200	1.3820	14.672	145.75
26	0.25000	0.27400	0.81000	20.086	146.43
27	0.31600	0.29400	1.1170	3.4340	146.57
28	0.34200	0.24800	1.2460	1.0720	147.04
29	0.23200	0.21900	0.80200	5.5060	148.70
30	0.32900	0.30800	1.0620	170.50	148.93
31	0.25400	0.34600	0.72600	156.42	149.17
32	0.20600	0.18200	0.71400	0.34000	149.66
33	0.12700	0.12800	0.47900	5.3000	149.72
34	0.30700	0.24800	1.0450	0.044000	149.96
35	0.14500	0.19900	0.48500	158.40	330.56
36	0.17100	0.18100	0.56300	2.9620	331.50
37	0.27200	0.30600	0.88000	15.637	332.38
38	0.32000	0.38400	1.0290	174.79	332.86
39	0.19300	0.20800	0.67300	12.366	333.87
40	0.30700	0.28000	1.0460	0.83400	334.48
41	0.22800	0.28200	0.74700	175.11	334.57
42	0.28100	0.36200	0.88600	178.50	334.81
43	0.29400	0.27900	1.0250	175.52	334.89
44	0.28100	0.26400	1.0040	171.91	335.18
45	0.27200	0.31900	0.84600	5.9120	335.21
46	0.26300	0.25900	0.88500	166.66	335.81
47	0.18400	0.30800	0.55800	9.0750	335.89

	area	minor	major	angle	compass
48	0.36400	0.42000	1.1630	171.80	336.11
49	0.17500	0.19900	0.61800	16.249	336.47
50	0.36000	0.34400	1.0280	14.468	338.09
51	0.30700	0.34400	0.92600	177.62	338.20
52	0.14500	0.22900	0.48100	4.6440	338.61
53	0.34600	0.30700	1.1900	7.2880	338.83
54	0.28900	0.29300	1.0110	171.38	339.50
55	0.32900	0.33900	1.0620	176.13	339.58
56	0.29400	0.29700	0.98200	174.12	340.16
57	0.27600	0.23500	1.0040	18.382	340.30
58	0.32900	0.32200	1.0650	174.82	340.85
59	0.19700	0.18700	0.65600	4.2540	341.18
60	0.28500	0.25200	0.91400	171.17	343.34
61	0.17500	0.32800	0.52300	170.42	343.47
62	0.18900	0.21100	0.59500	162.88	347.12
63	0.27200	0.26200	0.96400	1.2990	351.60
64	0.23200	0.27600	0.75300	156.50	353.50
65	0.21900	0.29800	0.69400	169.70	353.58

	area	minor	major	angle	compass
1	0.27000	0.34900	0.90000	0.80300	123.17
2	0.27400	0.33600	0.93900	1.0720	124.73
3	0.30400	0.26600	1.0990	1.2430	126.95
4	0.23600	0.24600	0.81300	1.7520	129.85
5	0.30800	0.26300	1.0550	1.9560	129.96
6	0.58200	0.58600	0.97600	3.0080	132.99
7	0.20700	0.18800	0.77100	3.2050	133.11
8	0.27800	0.32400	0.84900	4.0890	133.36
9	0.29500	0.29600	1.0650	4.7280	133.42
10	0.26100	0.32900	0.80300	4.7310	138.41
11	0.26600	0.32100	0.93200	6.2830	139.64
12	0.28300	0.40100	0.91000	6.9280	140.24
13	0.33700	0.35400	1.1520	7.1830	140.50
14	0.31200	0.34200	1.0550	7.3980	141.02
15	0.20700	0.24300	0.69000	7.6860	141.30
16	0.28700	0.29400	0.86200	8.6970	142.31
17	0.29100	0.38900	0.98100	8.9760	142.60
18	0.23200	0.24200	0.85300	9.4970	142.82
19	0.28700	0.27400	1.0180	9.7580	143.07
20	0.24500	0.21400	0.90200	10.357	143.72
21	0.32000	0.28900	1.1640	11.585	145.27
22	0.36300	0.29500	1.1940	16.585	145.27
23	0.22800	0.27400	0.72100	16.644	145.91
24	0.29900	0.25000	1.0320	16.887	146.79
25	0.28300	0.30700	0.94000	17.011	146.99
26	0.20200	0.20000	0.74400	20.038	148.04
27	0.28300	0.25000	0.97800	20.145	148.25
28	0.27400	0.33300	0.92800	23.051	148.76
29	0.25300	0.33200	0.84000	25.266	148.93
30	0.20200	0.19800	0.64600	26.828	149.20
31	0.25300	0.24700	0.84300	163.98	330.74
32	0.18600	0.21300	0.61100	164.65	331.22
33	0.24900	0.23400	0.85500	164.75	331.61
34	0.31200	0.32500	1.1080	166.24	332.43
35	0.30400	0.36600	1.0240	166.78	333.42
36	0.23600	0.23500	0.77800	166.84	333.94
37	0.35000	0.31800	1.1600	167.28	334.06
38	0.29100	0.28400	1.0410	167.38	335.27
39	0.24500	0.21900	0.83900	167.40	335.91
40	0.24900	0.29400	0.89100	170.18	337.25
41	0.29100	0.28400	1.0630	170.43	338.04
42	0.30400	0.25700	1.0490	170.99	339.01
43	0.23600	0.30100	0.79900	171.96	339.57
44	0.15600	0.14700	0.33900	172.75	339.82
45	0.29900	0.33600	1.0030	174.09	342.60
46	0.25700	0.35600	0.81900	174.73	342.62
47	0.28300	0.32400	0.90700	175.94	342.72

	area	minor	major	angle	compass
48	0.23600	0.30200	0.78700	176.06	343.16
49	0.26100	0.23600	0.97200	176.58	343.22
50	0.24500	0.29500	0.76000	177.57	343.76
51	0.20700	0.30400	0.63500	178.39	345.25
52	0.25300	0.29100	0.85000	178.78	345.35
53	0.26600	0.38800	0.77800	179.26	346.02

	area	minor	major	angle	compass
1	0.31900	0.24700	0.41100	114.52	81.479
2	0.46900	0.28700	0.52100	45.000	82.470
3	0.22500	0.20200	0.35500	107.14	82.673
4	0.24400	0.25900	0.30000	76.224	82.848
5	0.82600	0.25700	1.0240	158.20	85.823
6	0.30000	0.24200	0.39600	39.972	85.849
7	0.45000	0.31500	0.45400	177.33	88.130
8	0.30000	0.24300	0.39300	25.248	88.197
9	0.28100	0.20400	0.44000	149.50	88.462
10	3.0780	0.53600	1.8270	6.0250	88.693
11	0.71300	0.43500	0.52200	100.77	89.339
12	0.65700	0.25500	0.81900	13.048	91.316
13	0.54400	0.30900	0.56000	143.00	94.120
14	0.54400	0.33900	0.51000	50.304	101.80
15	0.56300	0.27500	0.65200	171.87	102.04
16	0.20600	0.17400	0.37800	139.25	103.48
17	0.86300	0.27200	1.0110	171.80	103.87
18	0.56300	0.23800	0.75300	156.13	105.48
19	0.30000	0.23200	0.41200	77.751	110.50
20	0.39400	0.30300	0.41300	39.230	113.93
21	0.41300	0.28800	0.45700	177.53	117.00
22	0.52500	0.35300	0.47400	111.11	120.75
23	0.91900	0.31700	0.92300	18.579	121.52
24	0.26300	0.22000	0.38100	97.161	133.12
25	0.30000	0.17100	0.56000	174.15	143.43
26	0.33800	0.13000	0.82700	174.18	145.48
27	0.31900	0.20100	0.50500	38.253	148.89
28	0.20600	0.18200	0.36000	116.57	152.86
29	0.67600	0.40900	0.52600	126.88	159.23
30	0.76900	0.30000	0.81500	21.146	162.82
31	1.3700	0.35400	1.2310	6.7430	162.84
32	0.61900	0.21700	0.91000	165.88	165.27
33	0.45000	0.22400	0.63900	22.663	167.69
34	0.30000	0.22800	0.41900	79.838	170.00
35	0.56300	0.35200	0.51000	84.221	175.78
36	1.2570	0.46500	0.86100	156.52	176.22
37	0.58200	0.20300	0.91400	3.4640	180.16
38	0.48800	0.25100	0.61900	178.52	182.25
39	0.63800	0.44200	0.45900	59.136	183.78
40	1.1070	0.36100	0.97700	170.66	192.73
41	1.0320	0.44200	0.74300	171.31	200.86
42	1.6700	0.38900	1.3680	177.15	209.70
43	1.3320	0.30500	1.3910	1.6110	210.51
44	0.33800	0.23200	0.46400	94.731	213.86
45	0.18800	0.20900	0.28600	90.000	215.00
46	0.28100	0.13700	0.65300	171.54	220.03
47	0.39400	0.25300	0.49500	46.143	220.77

	area	minor	major	angle	compass
48	0.24400	0.23400	0.33200	83.780	221.75
49	0.28100	0.18600	0.48200	49.489	231.33
50	0.24400	0.18600	0.41700	67.269	232.98
51	0.48800	0.23000	0.67400	154.52	234.75
52	0.54400	0.26600	0.65200	157.96	237.34
53	1.1070	0.30000	1.1760	4.0880	238.47
54	0.20600	0.17300	0.38000	92.310	238.85
55	0.22500	0.16700	0.43000	97.177	241.42
56	2.1580	0.45000	1.5260	10.838	246.95
57	0.37500	0.23700	0.50300	146.07	249.16
58	0.33800	0.28800	0.37400	28.672	252.67
59	0.43200	0.27000	0.50800	138.48	253.26
60	0.88200	0.31900	0.88000	21.526	253.98
61	1.1070	0.33200	1.0600	168.68	254.19
62	1.0510	0.31000	1.0800	5.8120	255.91
63	2.1020	0.43600	1.5330	7.3260	256.54
64	0.43200	0.27200	0.50400	27.019	258.39

	area	minor	major	angle	compass
1	0.10152	0.24700	0.41100	114.52	80.889
2	0.14953	0.28700	0.52100	45.000	81.113
3	0.071710	0.20200	0.35500	107.14	81.465
4	0.077700	0.25900	0.30000	76.224	81.479
5	0.26317	0.25700	1.0240	158.20	82.321
6	0.095832	0.24200	0.39600	39.972	82.404
7	0.14301	0.31500	0.45400	177.33	82.470
8	0.095499	0.24300	0.39300	25.248	82.673
9	0.089760	0.20400	0.44000	149.50	82.711
10	0.97927	0.53600	1.8270	6.0250	82.848
11	0.22707	0.43500	0.52200	100.77	83.735
12	0.20885	0.25500	0.81900	13.048	84.836
13	0.17304	0.30900	0.56000	143.00	85.099
14	0.17289	0.33900	0.51000	50.304	85.312
15	0.17930	0.27500	0.65200	171.87	85.789
16	0.065772	0.17400	0.37800	139.25	85.823
17	0.27499	0.27200	1.0110	171.80	85.849
18	0.17921	0.23800	0.75300	156.13	86.506
19	0.095584	0.23200	0.41200	77.751	86.959
20	0.12514	0.30300	0.41300	39.230	87.423
21	0.13162	0.28800	0.45700	177.53	88.130
22	0.16732	0.35300	0.47400	111.11	88.197
23	0.29259	0.31700	0.92300	18.579	88.265
24	0.083820	0.22000	0.38100	97.161	88.462
25	0.095760	0.17100	0.56000	174.15	88.693
26	0.10751	0.13000	0.82700	174.18	89.202
27	0.10151	0.20100	0.50500	38.253	89.339
28	0.065520	0.18200	0.36000	116.57	89.357
29	0.21513	0.40900	0.52600	126.88	91.316
30	0.24450	0.30000	0.81500	21.146	91.440
31	0.43577	0.35400	1.2310	6.7430	94.120
32	0.19747	0.21700	0.91000	165.88	95.249
33	0.14314	0.22400	0.63900	22.663	98.765
34	0.095532	0.22800	0.41900	79.838	101.80
35	0.17952	0.35200	0.51000	84.221	102.04
36	0.40036	0.46500	0.86100	156.52	103.48
37	0.18554	0.20300	0.91400	3.4640	103.87
38	0.15537	0.25100	0.61900	178.52	105.48
39	0.20288	0.44200	0.45900	59.136	110.50
40	0.35270	0.36100	0.97700	170.66	113.93
41	0.32841	0.44200	0.74300	171.31	117.00
42	0.53215	0.38900	1.3680	177.15	120.75
43	0.42426	0.30500	1.3910	1.6110	121.52
44	0.10765	0.23200	0.46400	94.731	123.25
45	0.059774	0.20900	0.28600	90.000	133.12
46	0.089461	0.13700	0.65300	171.54	143.43
47	0.12523	0.25300	0.49500	46.143	145.48

	area	minor	major	angle	compass
48	0.077688	0.23400	0.33200	83.780	148.89
49	0.089652	0.18600	0.48200	49.489	152.86
50	0.077562	0.18600	0.41700	67.269	159.23
51	0.15502	0.23000	0.67400	154.52	162.82
52	0.17343	0.26600	0.65200	157.96	162.84
53	0.35280	0.30000	1.1760	4.0880	165.27
54	0.065740	0.17300	0.38000	92.310	167.69
55	0.071810	0.16700	0.43000	97.177	170.00
56	0.68670	0.45000	1.5260	10.838	175.78
57	0.11921	0.23700	0.50300	146.07	176.22
58	0.10771	0.28800	0.37400	28.672	180.16
59	0.13716	0.27000	0.50800	138.48	182.25
60	0.28072	0.31900	0.88000	21.526	183.78
61	0.35192	0.33200	1.0600	168.68	192.73
62	0.33480	0.31000	1.0800	5.8120	200.86
63	0.66839	0.43600	1.5330	7.3260	209.70
64	0.13709	0.27200	0.50400	27.019	210.51
65	0.43183	0.39800	1.0850	4.8550	213.86
66	0.57584	0.47200	1.2200	175.16	215.00
67	0.58781	0.48300	1.2170	161.24	220.03
68	0.82634	0.49900	1.6560	4.8300	220.77
69	0.53737	0.50600	1.0620	174.21	221.75
70	0.53158	0.39700	1.3390	176.26	224.75
71	0.51927	0.55300	0.93900	3.8840	226.74
72	0.86267	0.61400	1.4050	3.4280	229.62
73	0.50690	0.44700	1.1340	5.7690	231.33
74	1.2253	0.48700	2.5160	178.89	231.78
75	0.41936	0.47600	0.88100	3.6140	232.98
76	0.98909	0.43400	2.2790	0.23400	233.23
77	1.3253	0.74000	1.7910	17.973	234.75
78	0.54996	0.48200	1.1410	14.734	237.34
79	0.28800	0.36000	0.80000	11.325	238.47
80	0.39420	0.45000	0.87600	177.29	238.85
81	0.50715	0.48300	1.0500	9.8930	241.09
82	0.91359	0.63400	1.4410	28.222	241.42
83	0.98829	0.64300	1.5370	171.74	241.52
84	1.2076	0.69600	1.7350	35.253	241.56
85	0.62560	0.54400	1.1500	177.68	242.03
86	0.47515	0.44200	1.0750	8.5910	244.92
87	0.82529	0.52300	1.5780	170.64	245.27
88	1.6077	1.1410	1.4090	5.6140	246.73
89	0.63167	0.56500	1.1180	164.75	246.95
90	0.76982	0.61000	1.2620	170.80	248.68
91	0.56341	0.54700	1.0300	174.69	249.14
92	1.0138	0.53500	1.8950	13.273	249.16
93	0.48800	0.37800	1.2910	173.49	249.24
94	0.73872	0.57000	1.2960	10.762	250.11

	area	minor	major	angle	compass
95	1.0381	0.74200	1.3990	174.90	250.39
96	0.77616	0.48000	1.6170	1.3490	251.41
97	1.0821	0.65500	1.6520	26.769	252.00
98	1.3500	0.66900	2.0180	30.382	252.67
99	0.83166	0.66800	1.2450	179.11	253.26
100	0.96965	0.72200	1.3430	3.5270	253.98
101	0.90740	0.65000	1.3960	2.7210	254.19
102	0.91279	0.45800	1.9930	0.51500	254.23
103	0.80631	0.71800	1.1230	136.75	254.39
104	0.25013	0.38600	0.64800	0.47000	255.15
105	0.95771	0.69500	1.3780	173.04	255.17
106	0.68887	0.50100	1.3750	178.54	255.91
107	0.61951	0.49800	1.2440	3.1010	256.12
108	1.1446	0.77600	1.4750	1.4950	256.39
109	1.2579	0.90300	1.3930	10.859	256.47
110	0.72576	0.57600	1.2600	8.0020	256.54
111	1.0081	0.74400	1.3550	9.6060	256.57
112	0.30061	0.42700	0.70400	15.081	256.81
113	0.98850	0.65900	1.5000	177.60	256.90
114	0.86278	0.57100	1.5110	18.484	257.28
115	1.1814	0.74300	1.5900	168.56	258.39
116	0.74434	0.66400	1.1210	172.58	258.51
117	0.70708	0.57300	1.2340	0.75500	258.65
118	0.94466	0.63400	1.4900	18.914	259.24
119	0.78210	0.66000	1.1850	3.1880	259.48
120	0.85654	0.56800	1.5080	18.440	259.53
121	0.29372	0.41900	0.70100	33.255	259.77

	area	minor	major	angle	compass
1	0.36500	0.64500	0.93700	13.216	330.12
2	0.23000	0.24100	0.73200	179.88	330.35
3	0.15300	0.23100	0.46000	5.4660	332.12
4	0.26600	0.41100	0.78900	25.544	332.47
5	0.16200	0.26700	0.52000	167.25	333.04
6	0.27000	0.31800	0.77100	162.95	333.19
7	0.18900	0.23600	0.61400	13.508	334.19
8	0.17600	0.19500	0.61100	172.64	337.36
9	0.34200	0.44900	0.80400	27.698	337.96
10	0.19800	0.28600	0.61100	0.14500	341.63
11	0.15800	0.18500	0.55000	172.04	342.25
12	0.18900	0.22100	0.59700	7.6960	342.75
13	0.17600	0.24000	0.59200	1.6990	343.81
14	0.16200	0.24000	0.58500	34.168	347.05
15	0.16700	0.17600	0.54500	177.53	115.83
16	0.20300	0.22100	0.66200	26.692	122.30
17	0.18000	0.23900	0.61800	179.65	123.31
18	0.14000	0.15000	0.48700	13.880	124.46
19	0.16200	0.22400	0.53700	7.0870	126.86
20	0.25700	0.18900	0.90300	6.8990	128.40
21	0.25200	0.18200	0.90500	176.81	130.86
22	0.10400	0.16900	0.37400	6.0930	131.36
23	0.15800	0.21100	0.50900	175.81	132.96
24	0.19800	0.19200	0.60600	5.2900	136.12
25	0.18500	0.19600	0.55700	23.143	136.49
26	0.22500	0.28400	0.67100	176.96	136.78
27	0.22500	0.30800	0.66900	17.042	142.30
28	0.23900	0.29400	0.66900	21.602	142.91
29	0.15800	0.17000	0.55700	0.49900	143.10
30	0.31500	0.33200	0.95900	19.142	143.91
31	0.23400	0.24000	0.65600	18.642	144.53
32	0.15300	0.32800	0.45000	166.19	144.71
33	0.22500	0.26300	0.66400	167.75	147.64
34	0.23400	0.32400	0.70300	1.6700	147.93
35	0.17100	0.22800	0.56700	168.37	148.30
36	0.23400	0.35600	0.73300	2.3600	148.33
37	0.28400	0.38400	0.89300	2.0690	149.50
38	0.34200	0.41000	1.0530	177.88	149.85

	area	minor	major	angle	compass
1	1.6890	0.46600	1.1540	11.648	208.35
2	1.3110	0.45200	0.92300	9.2280	210.77
3	2.5820	0.54500	1.5080	15.432	204.57

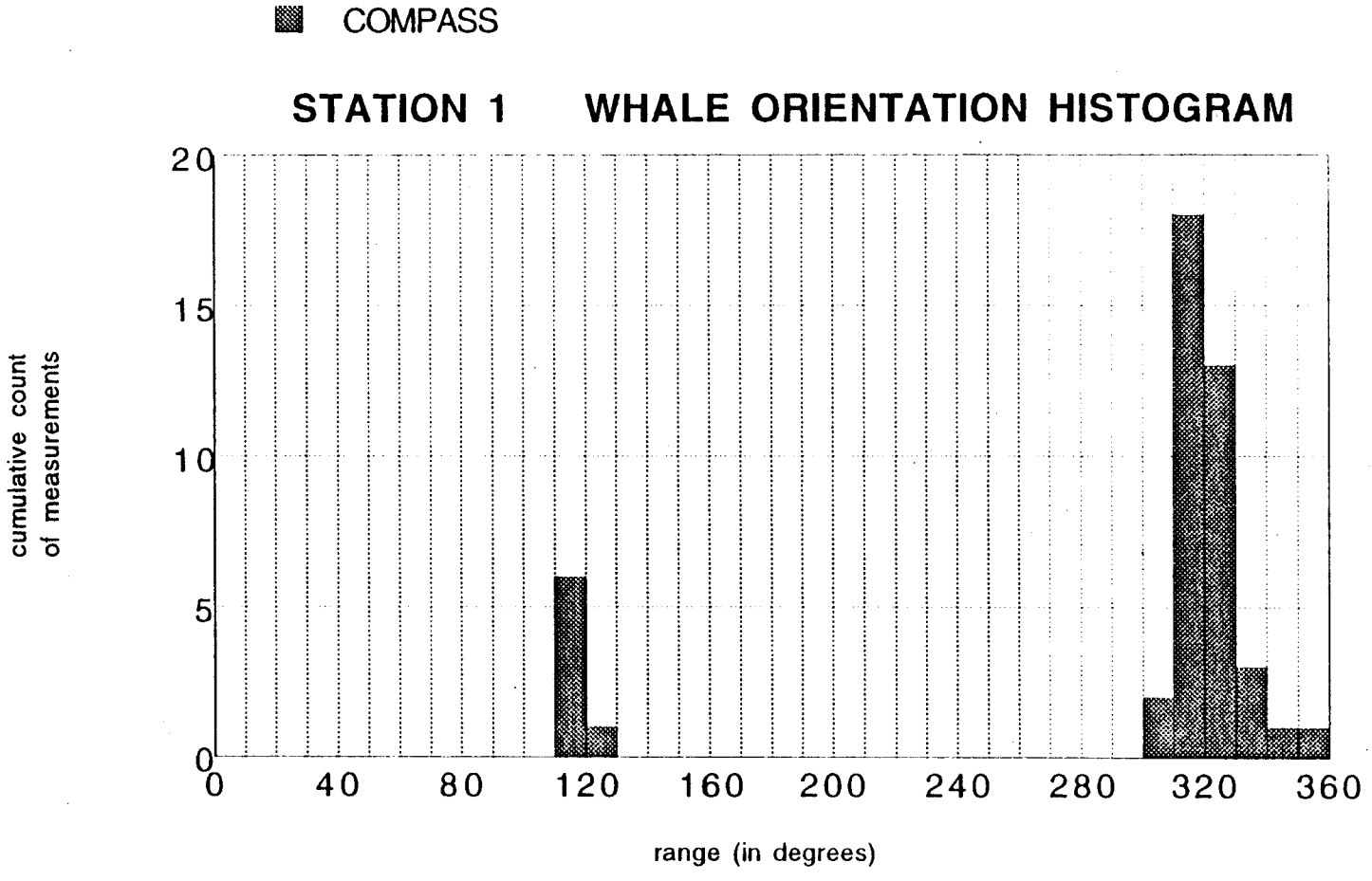
COMPASS
STATION 1 WHALE ORIENTATION HISTOGRAM
cumulative count of measurements
20
15
10
5
0
0
40
80
120
160
200
240
280
320
360
range (in degrees)

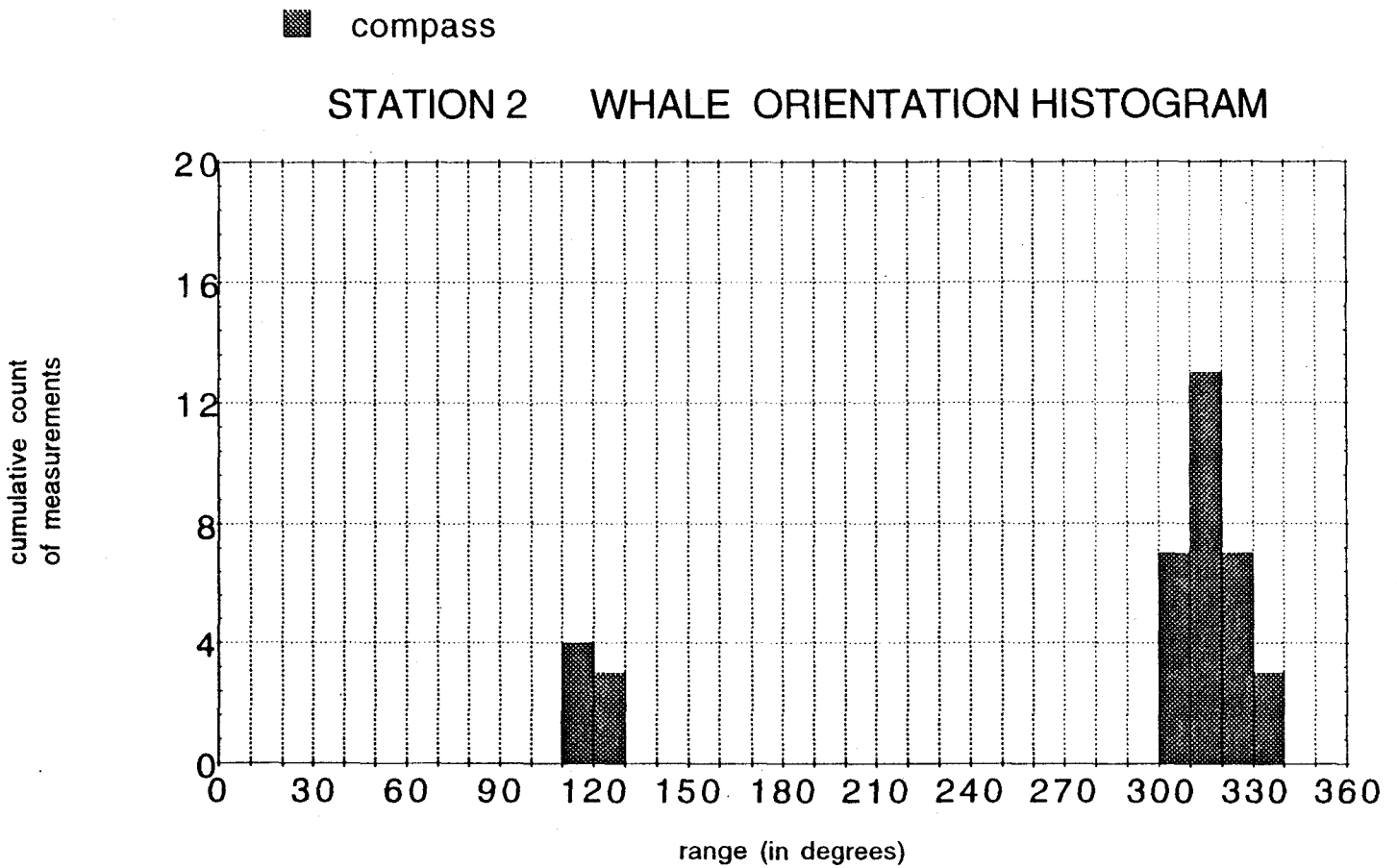
compass
STATION 2 WHALE ORIENTATION HISTOGRAM
cumulative count of measurements
20
16
12
8
4
0
0 30 60 90 120 150 180 210 240 270 300 330 360
range (in degrees)

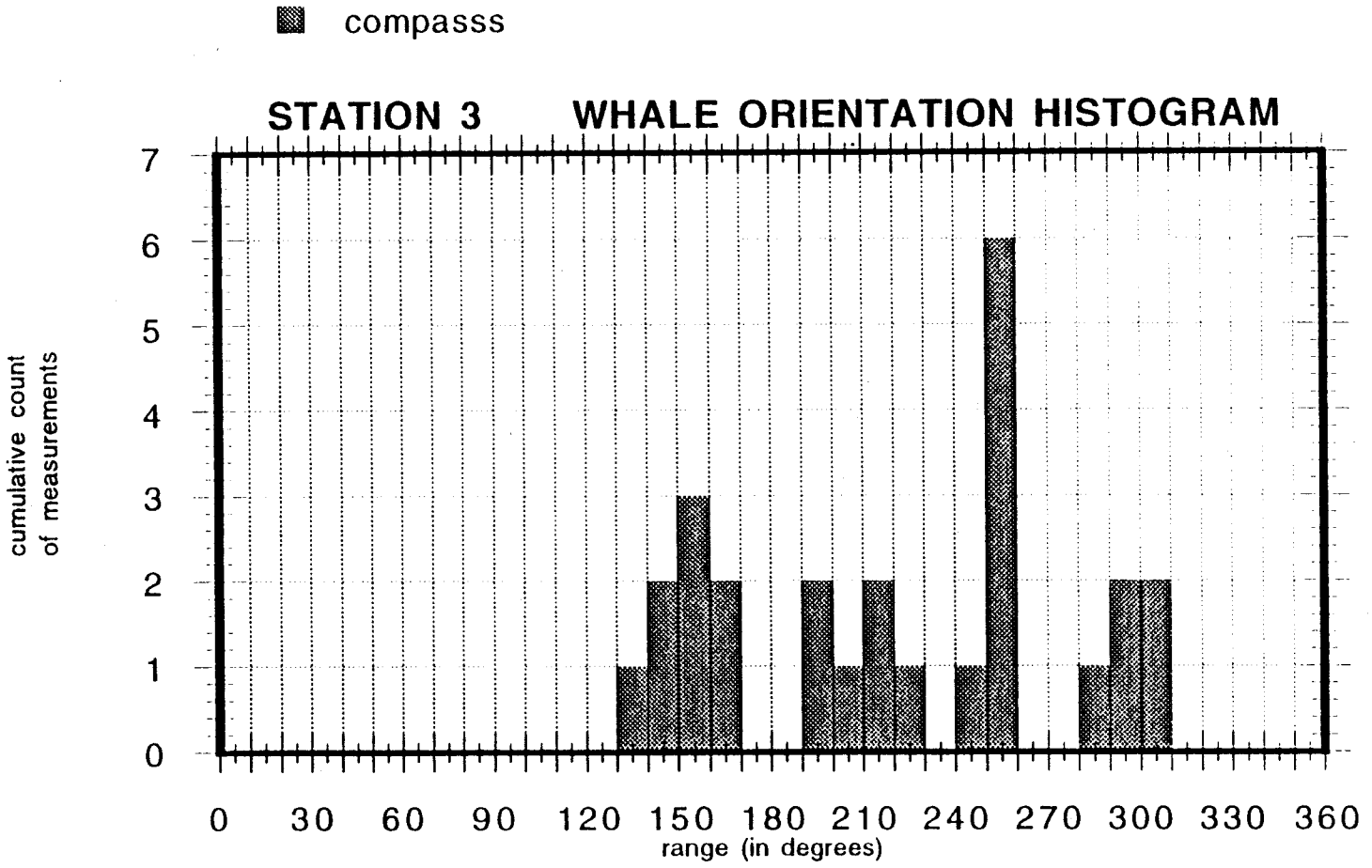
compasss
STATION 3 WHALE ORIENTATION HISTOGRAM
cumulative count
of measurements
0
1
2
3
4
5
6
7
0 30 60 90 120 150 180 210 240 270 300 330 360
range (in degrees)

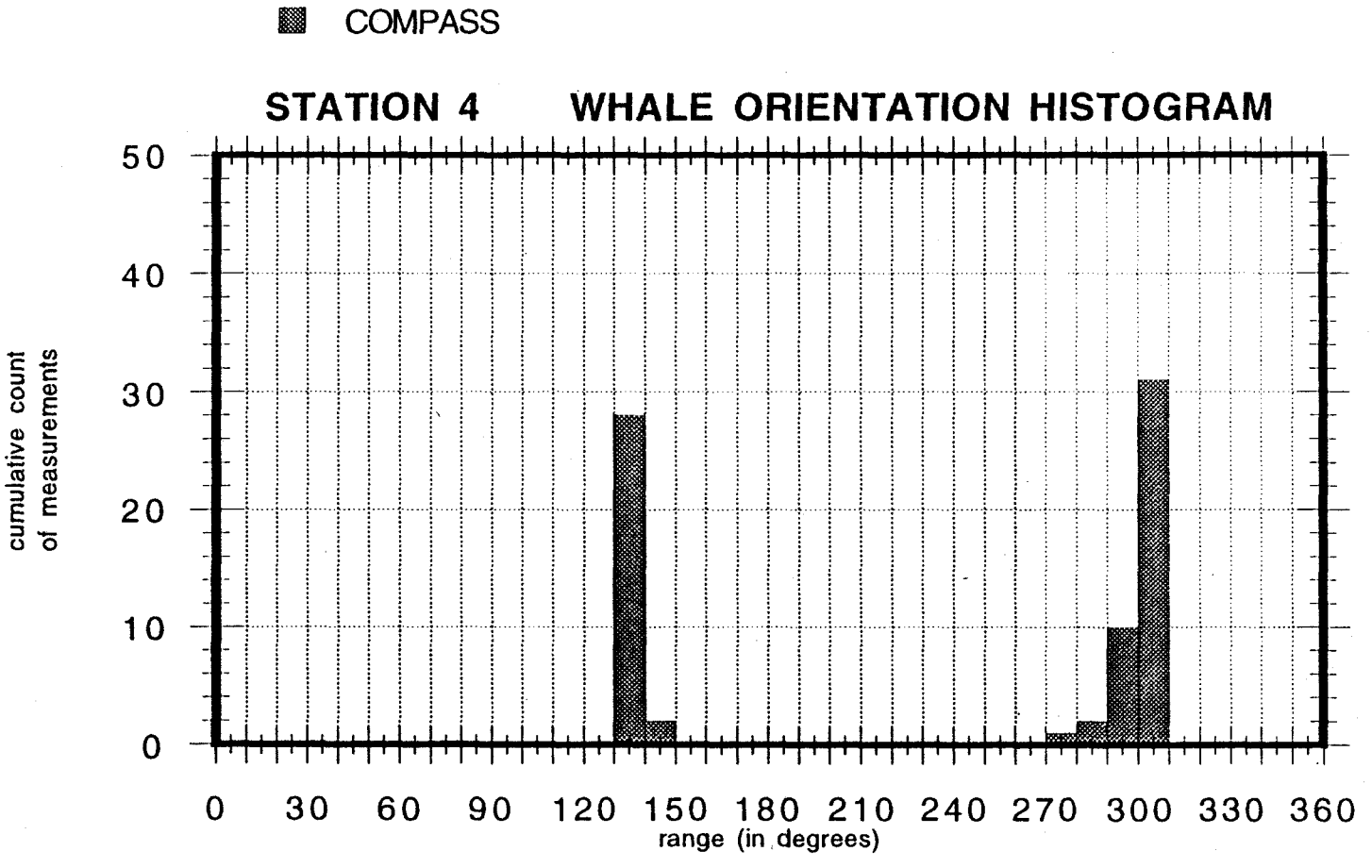
COMPASS
STATION 4 WHALE ORIENTATION HISTOGRAM
cumulative count of measurements
50
40
30
20
10
0
0 30 60 90 120 150 180 210 240 270 300 330 360
range (in degrees)

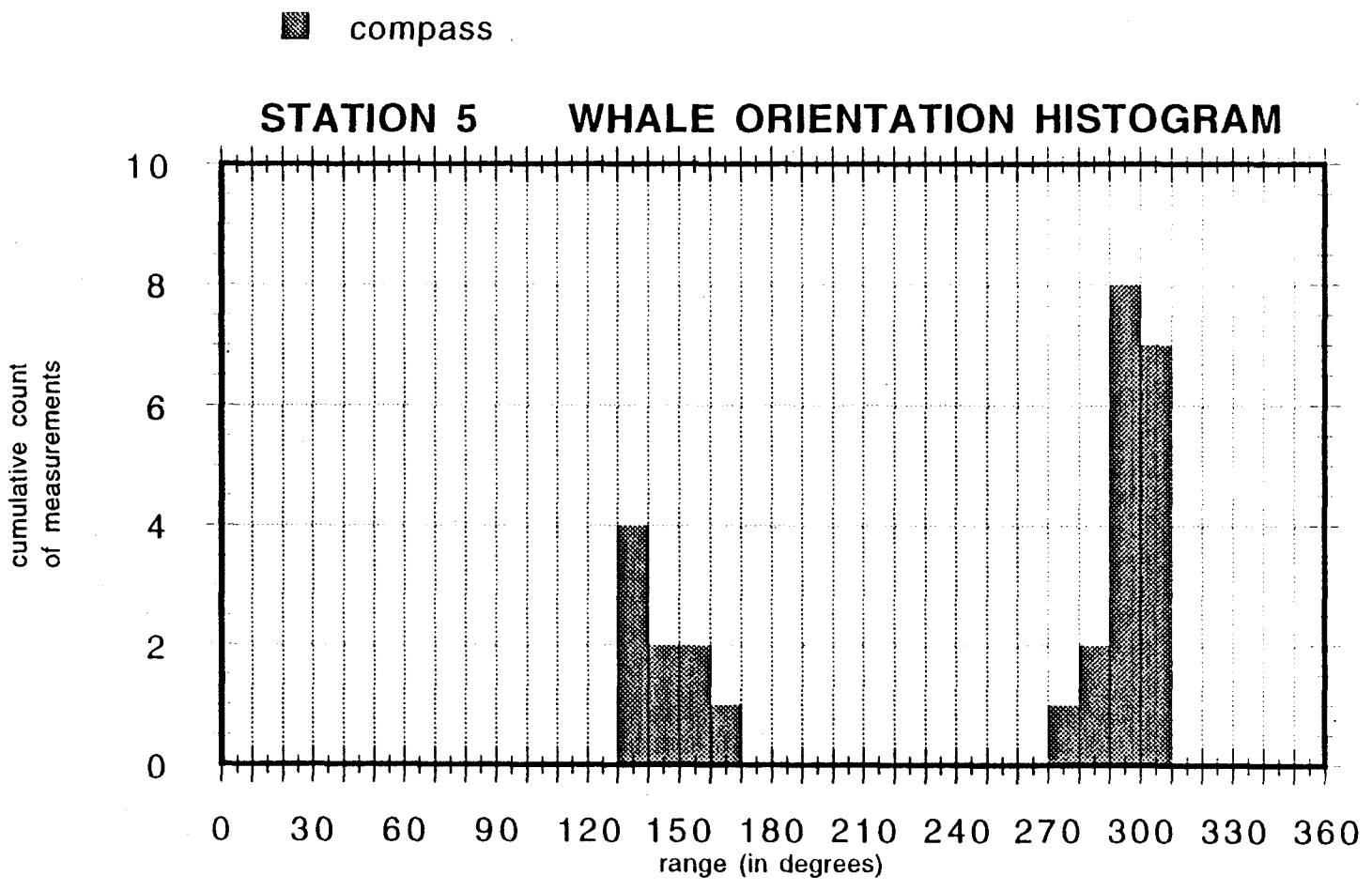
compass
STATION 5 WHALE ORIENTATION HISTOGRAM
cumulative count of measurements
10
8
6
4
2
0
0 30 60 90 120 150 180 210 240 270 300 330 360
range (in degrees)

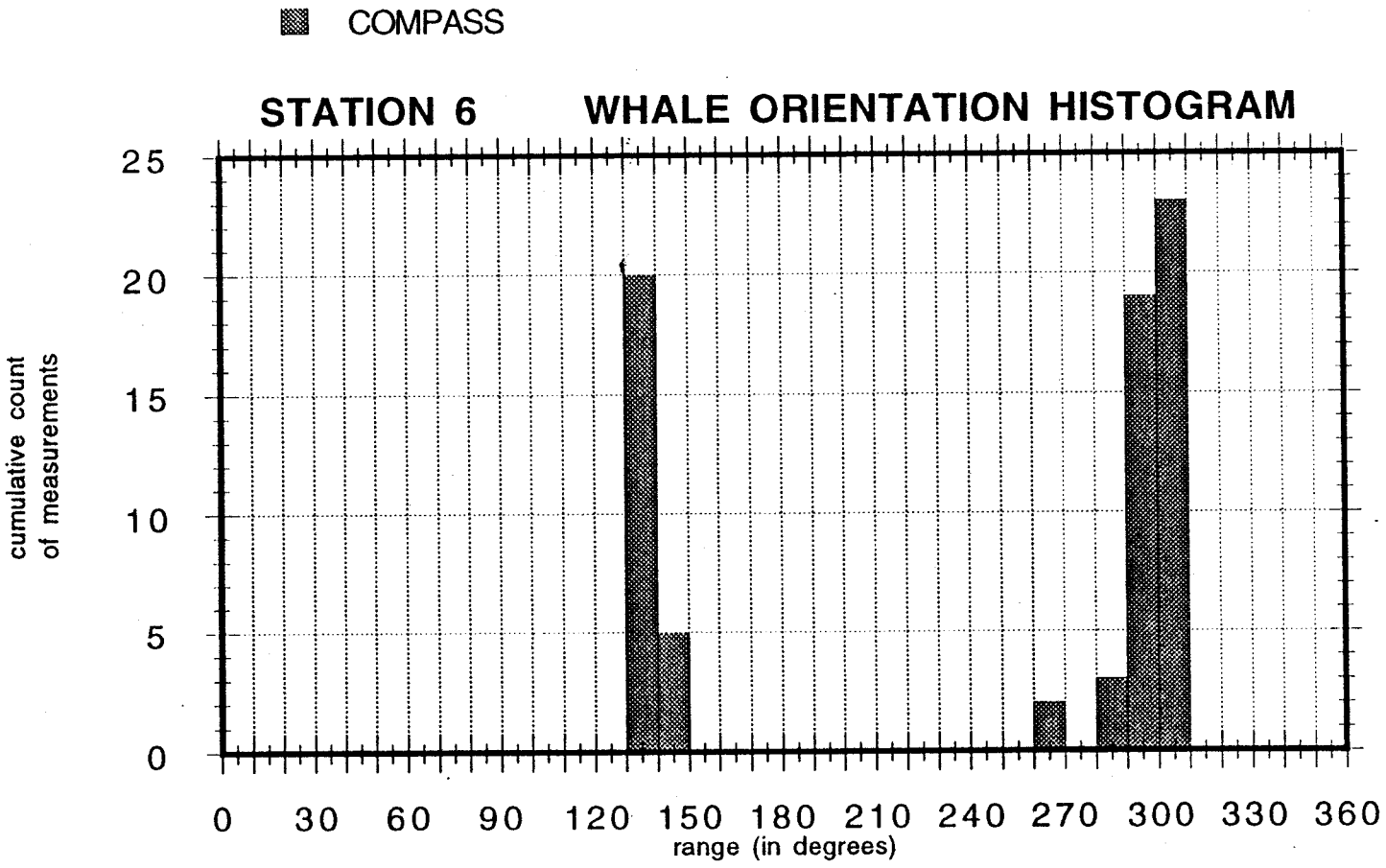
COMPASS
STATION 6
WHALE ORIENTATION HISTOGRAM
cumulative count
of measurements
25
20
15
10
5
0
0
30
60
90
120
150
180
210
240
270
300
330
360
range (in degrees)

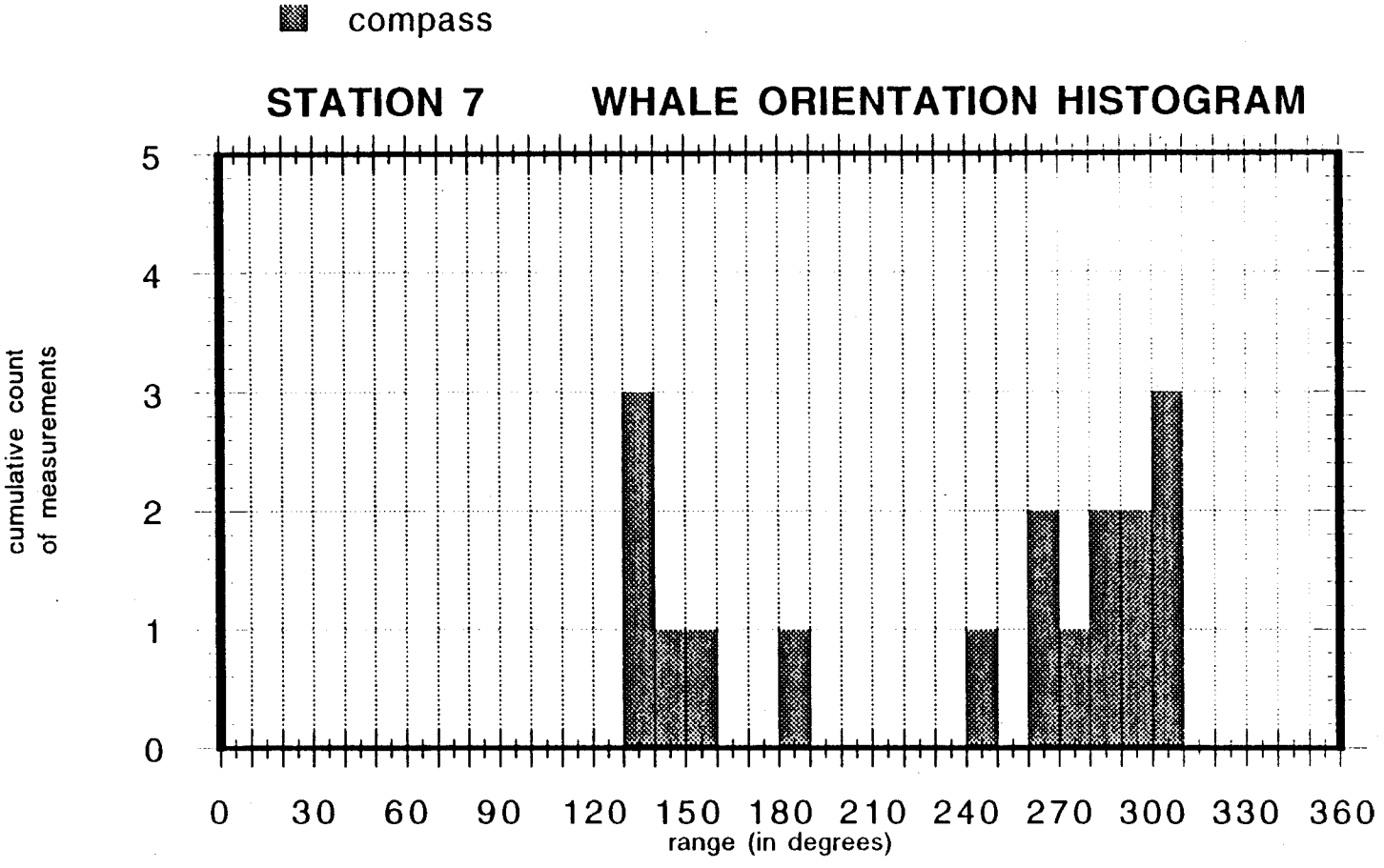
compass
STATION 7
WHALE ORIENTATION HISTOGRAM
cumulative count
of measurements
5
4
3
2
1
0
0
30
60
90
120
150
180
210
240
270
300
330
360
range (in degrees)

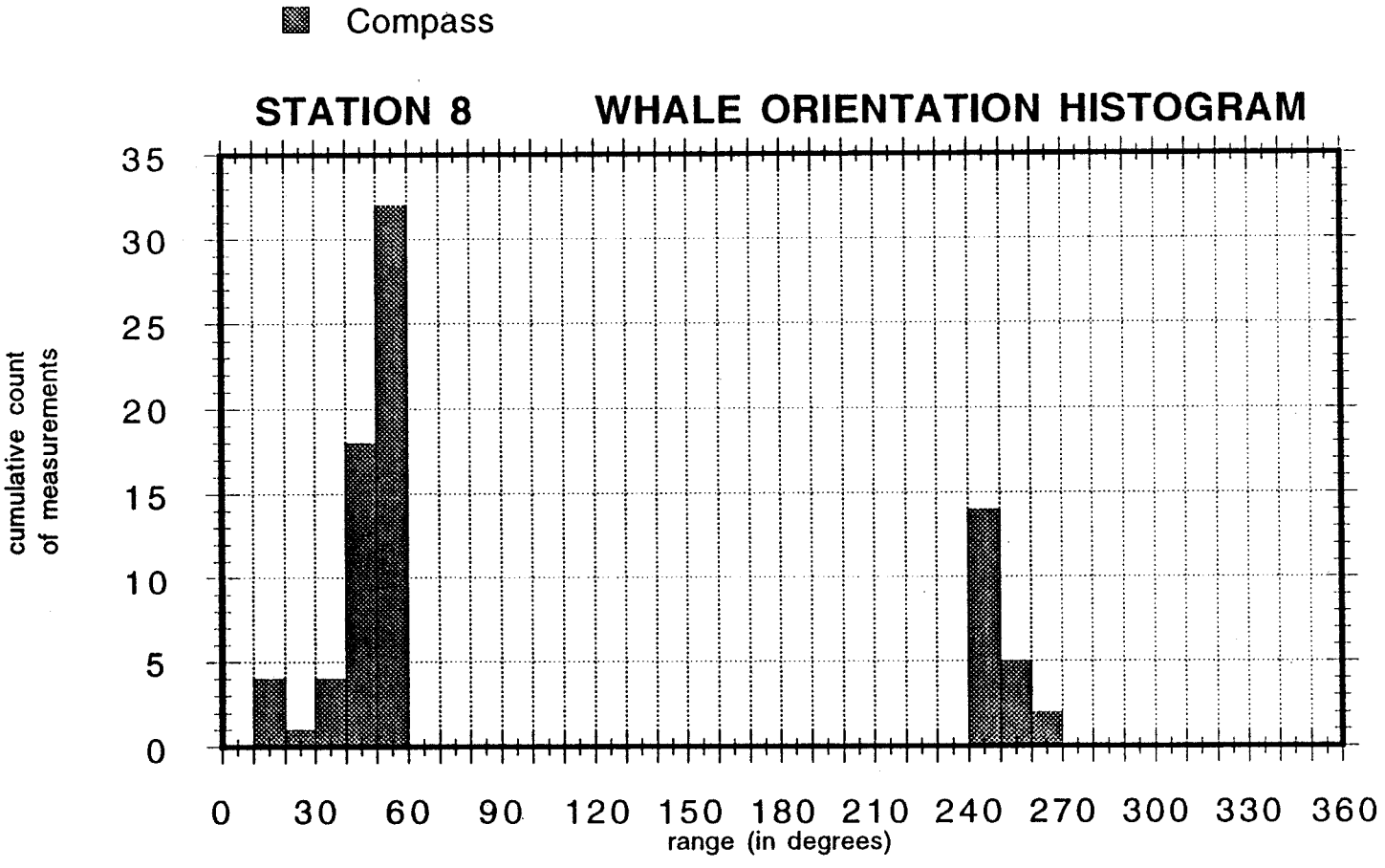
Compass
STATION 8
WHALE ORIENTATION HISTOGRAM
cumulative count
of measurements
35
30
25
20
15
10
5
0
0
30
60
90
120
150
180
210
240
270
300
330
360
range (in degrees)

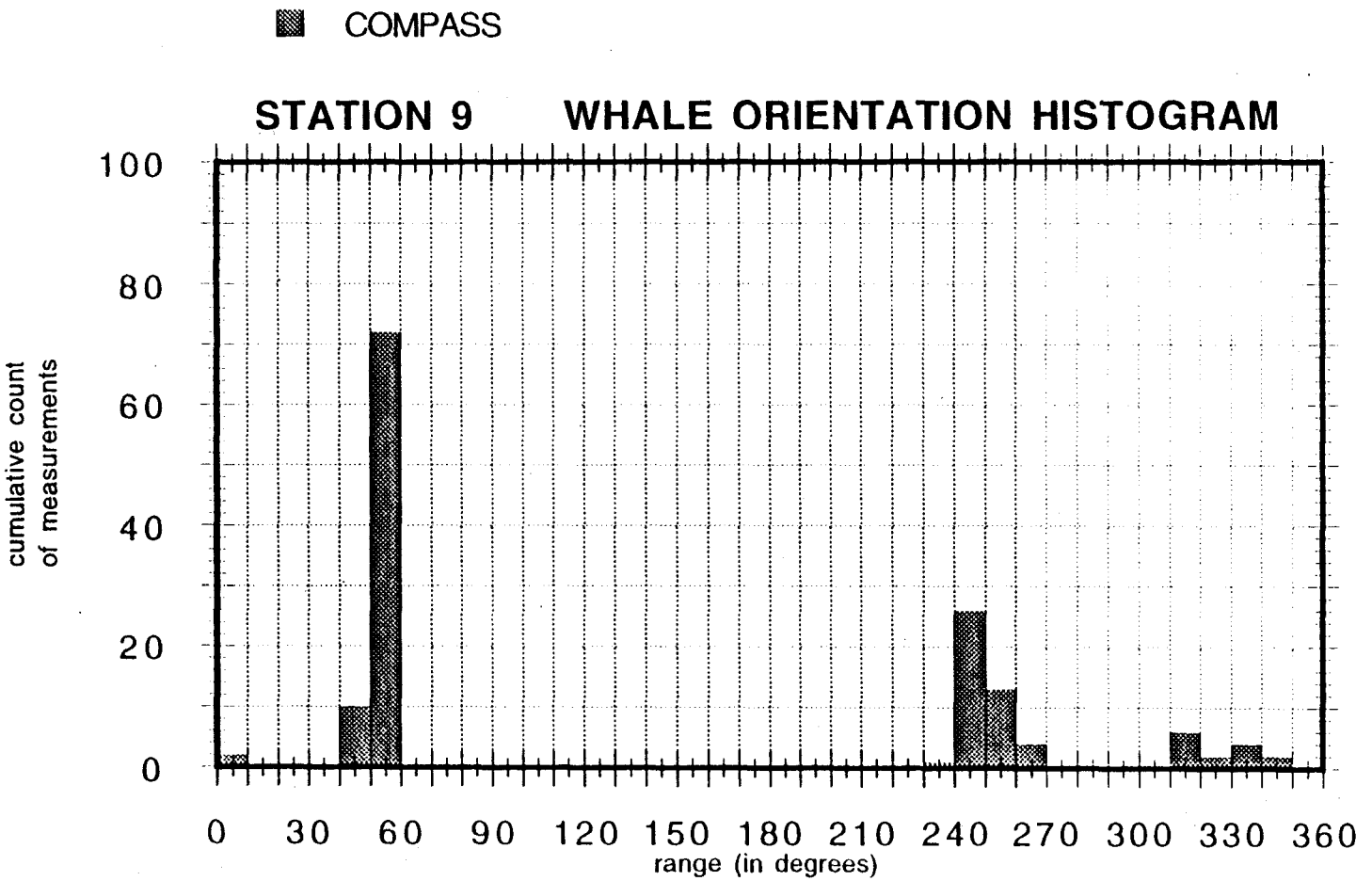
COMPASS
STATION 9 WHALE ORIENTATION HISTOGRAM
cumulative count of measurements
100
80
60
40
20
0
0 30 60 90 120 150 180 210 240 270 300 330 360
range (in degrees)

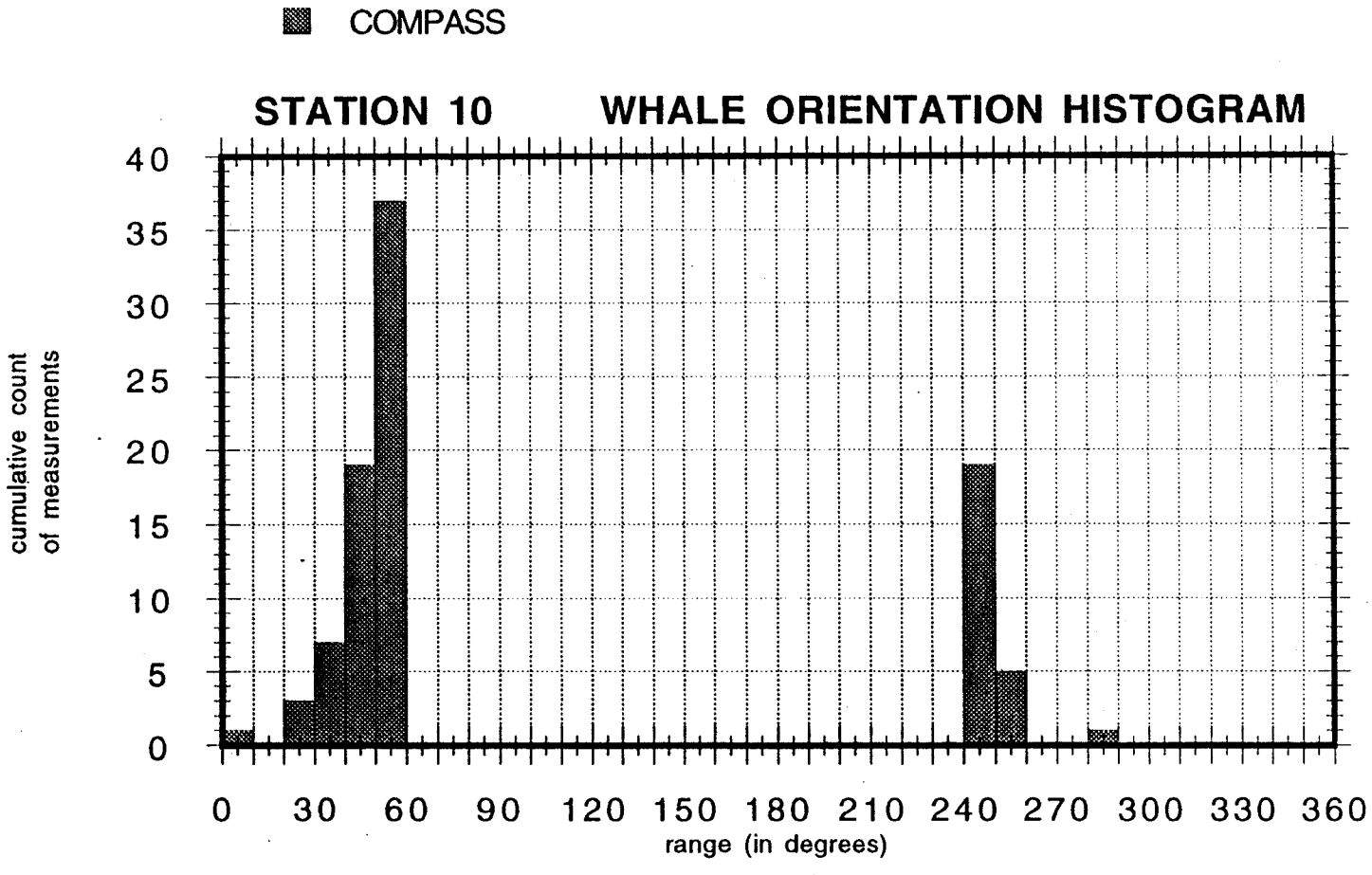
COMPASS
STATION 10 WHALE ORIENTATION HISTOGRAM
cumulative count of measurements
40
35
30
25
20
15
10
5
0
0 30 60 90 120 150 180 210 240 270 300 330 360
range (in degrees)

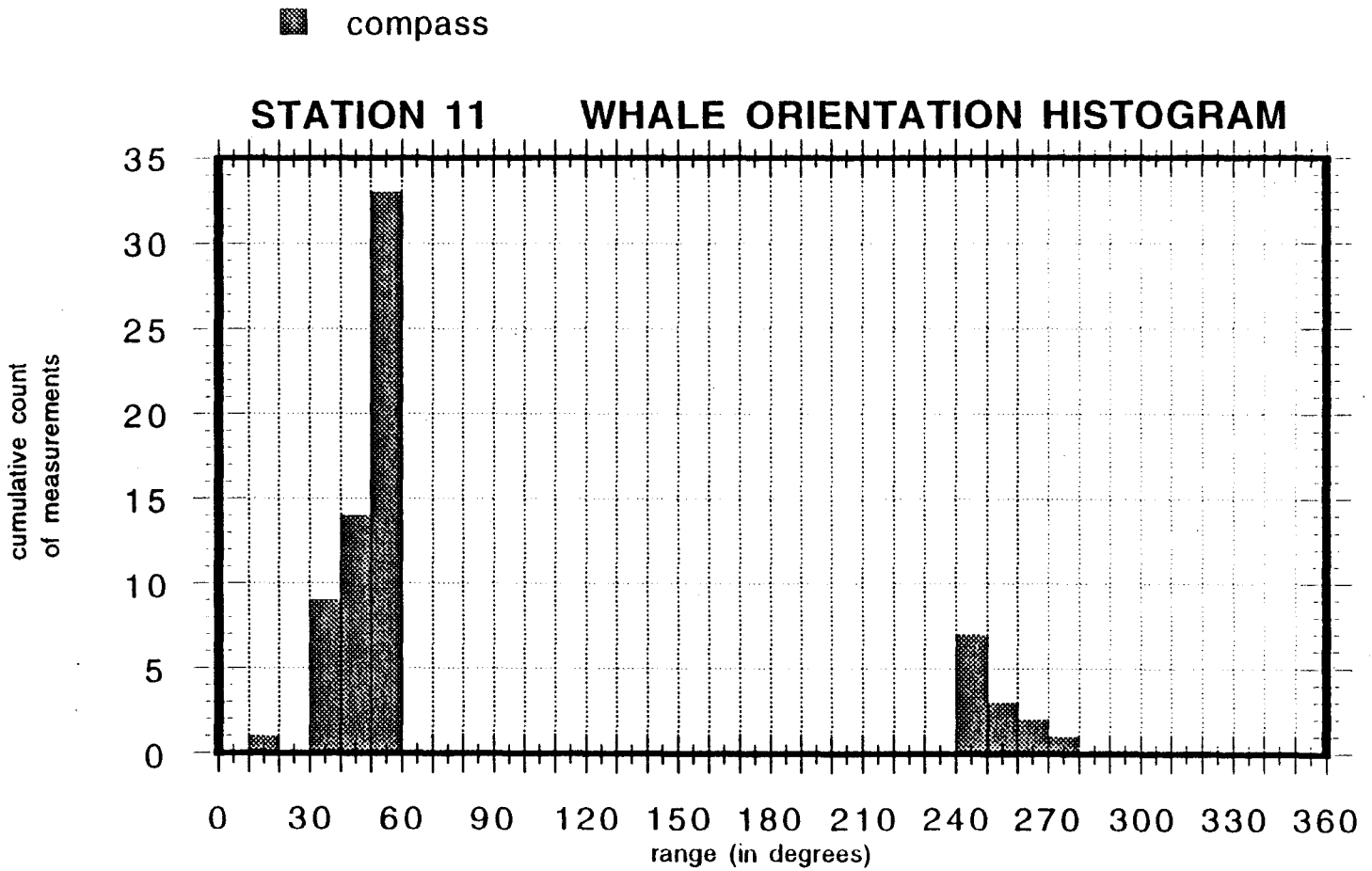
compass
STATION 11 WHALE ORIENTATION HISTOGRAM
cumulative count of measurements
35
30
25
20
15
10
5
0
0 30 60 90 120 150 180 210 240 270 300 330 360
range (in degrees)

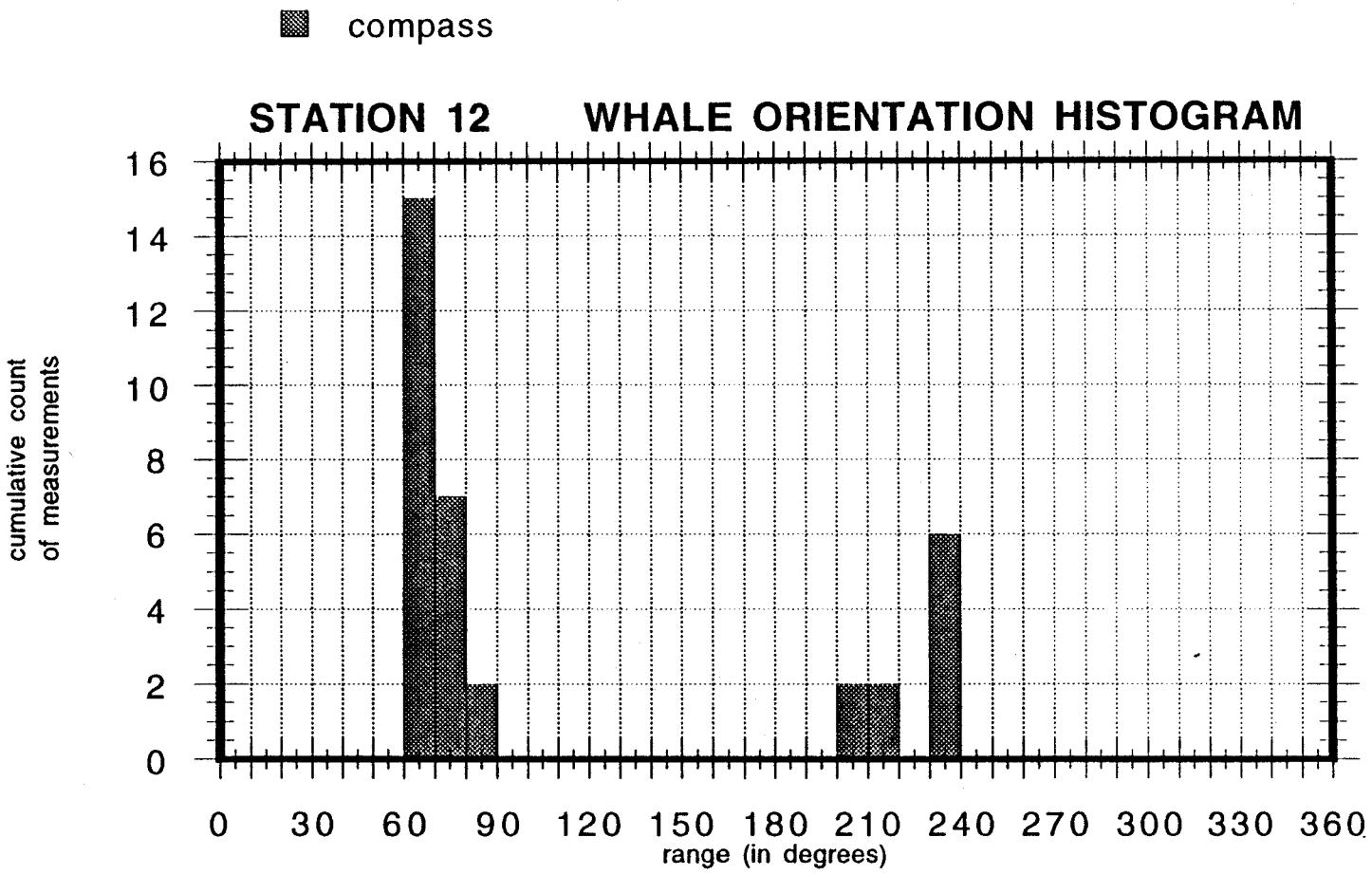
compass
STATION 12 WHALE ORIENTATION HISTOGRAM
cumulative count of measurements
16
14
12
10
8
6
4
2
0
0 30 60 90 120 150 180 210 240 270 300 330 360
range (in degrees)

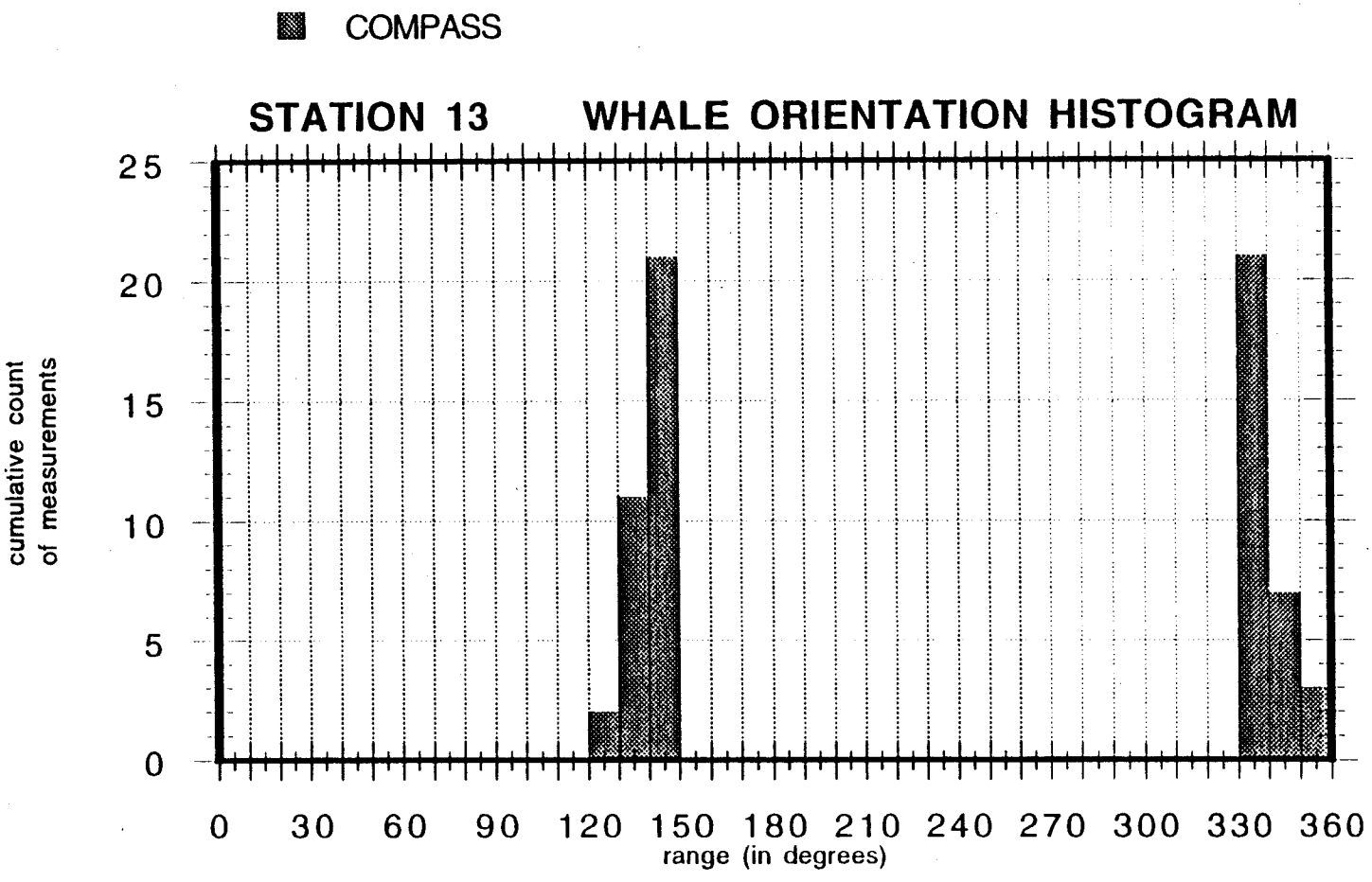
COMPASS
STATION 13 WHALE ORIENTATION HISTOGRAM
cumulative count of measurements
25
20
15
10
5
0
0 30 60 90 120 150 180 210 240 270 300 330 360
range (in degrees)

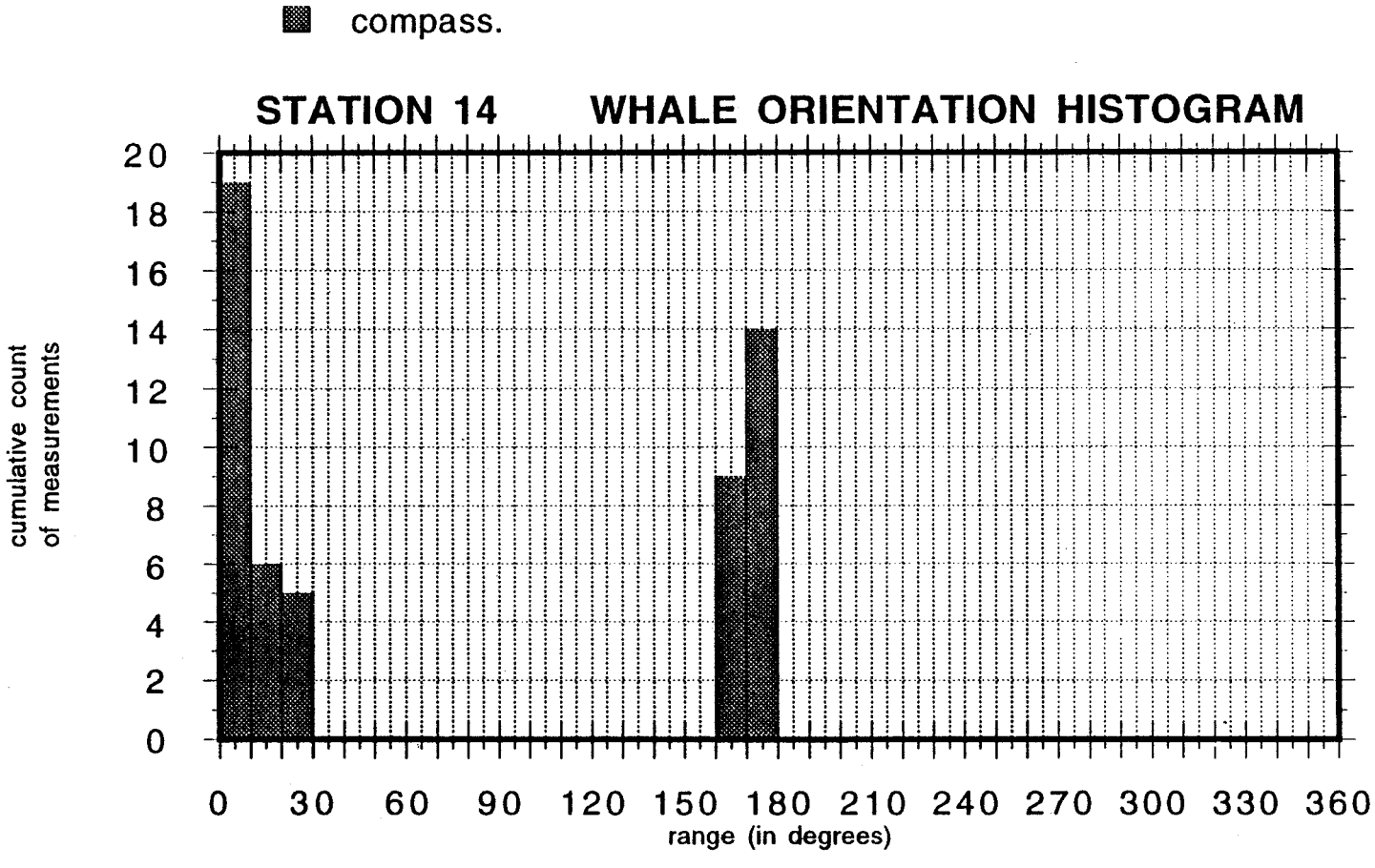
compass.
STATION 14 WHALE ORIENTATION HISTOGRAM
cumulative count of measurements
20
18
16
14
12
10
8
6
4
2
0
0 30 60 90 120 150 180 210 240 270 300 330 360
range (in degrees)

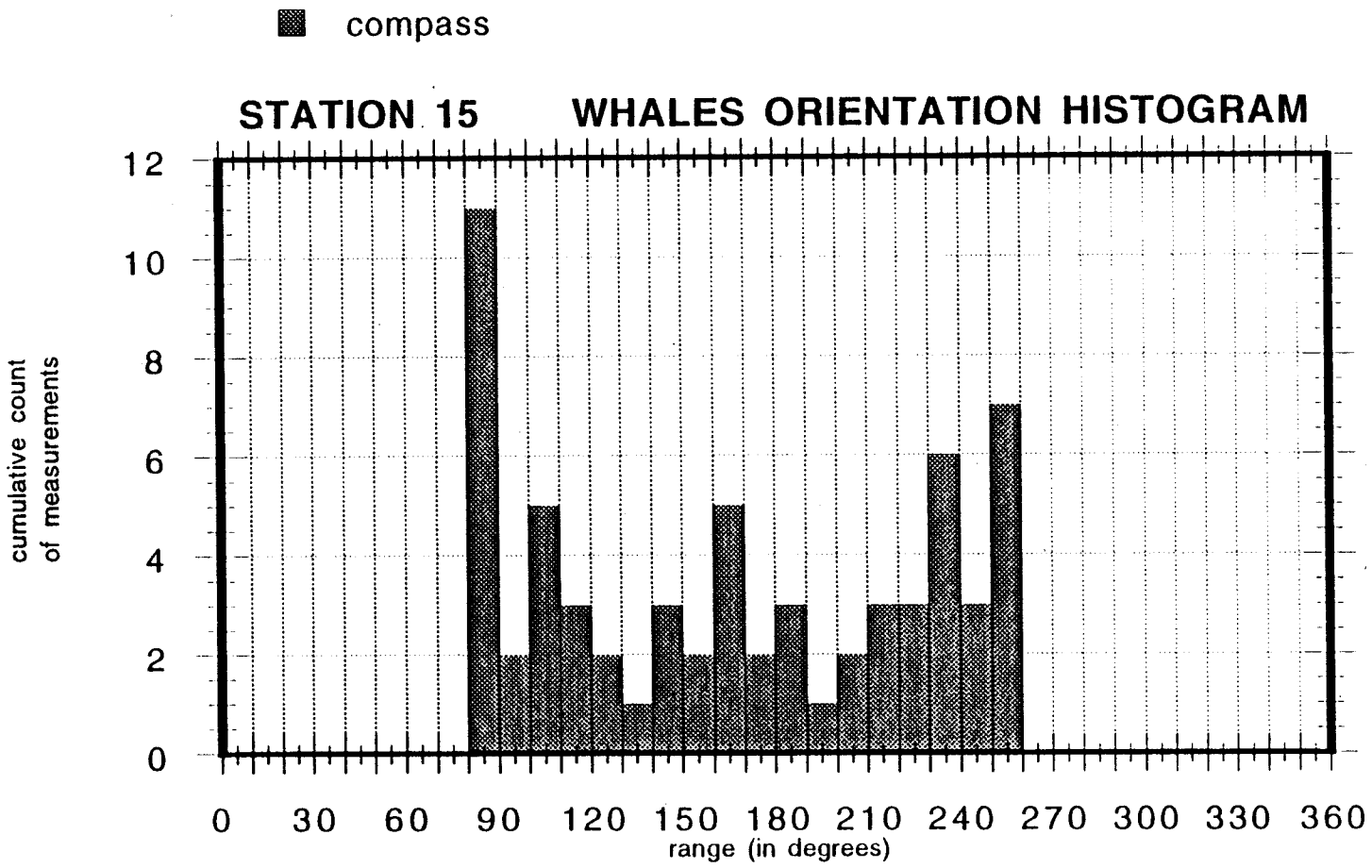
compass
STATION 15 WHALES ORIENTATION HISTOGRAM
cumulative count of measurements
12
10
8
6
4
2
0
0 30 60 90 120 150 180 210 240 270 300 330 360
range (in degrees)

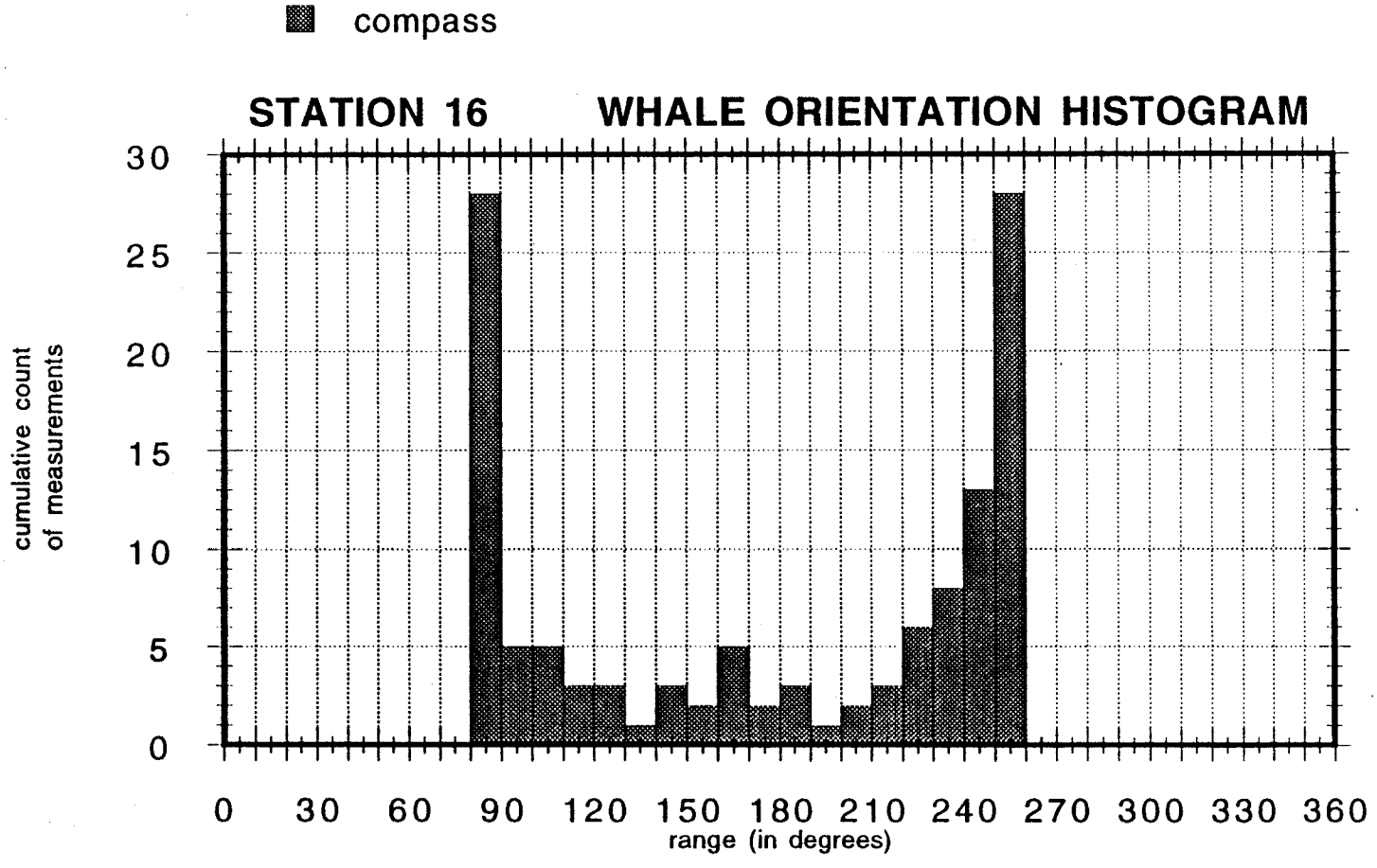
compass
STATION 16
WHALE ORIENTATION HISTOGRAM
cumulative count
of measurements
30
25
20
15
10
5
0
0
30
60
90
120
150
180
210
240
270
300
330
360
range (in degrees)

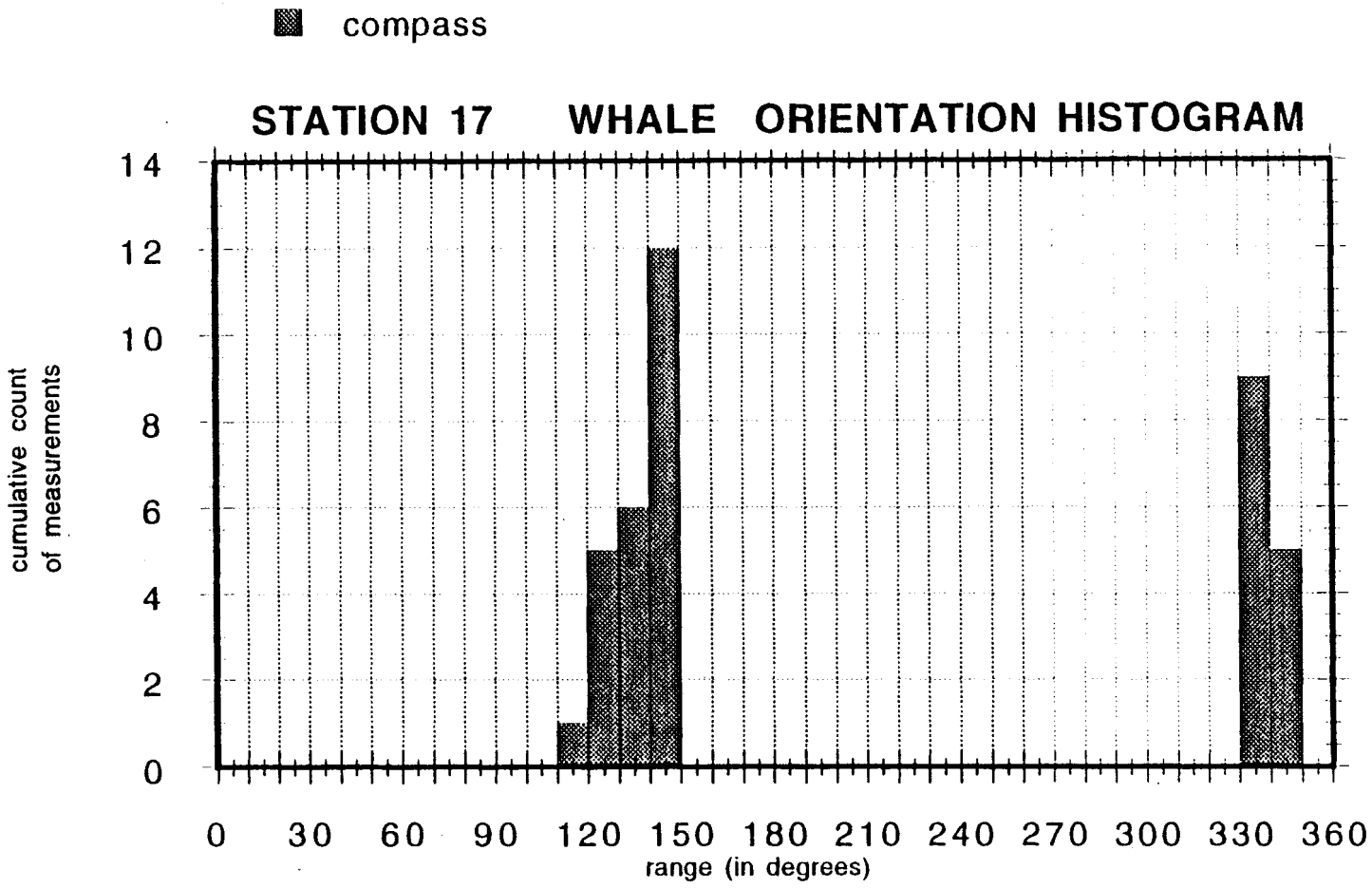
compass
STATION 17 WHALE ORIENTATION HISTOGRAM
cumulative count of measurements
14
12
10
8
6
4
2
0
0 30 60 90 120 150 180 210 240 270 300 330 360
range (in degrees)

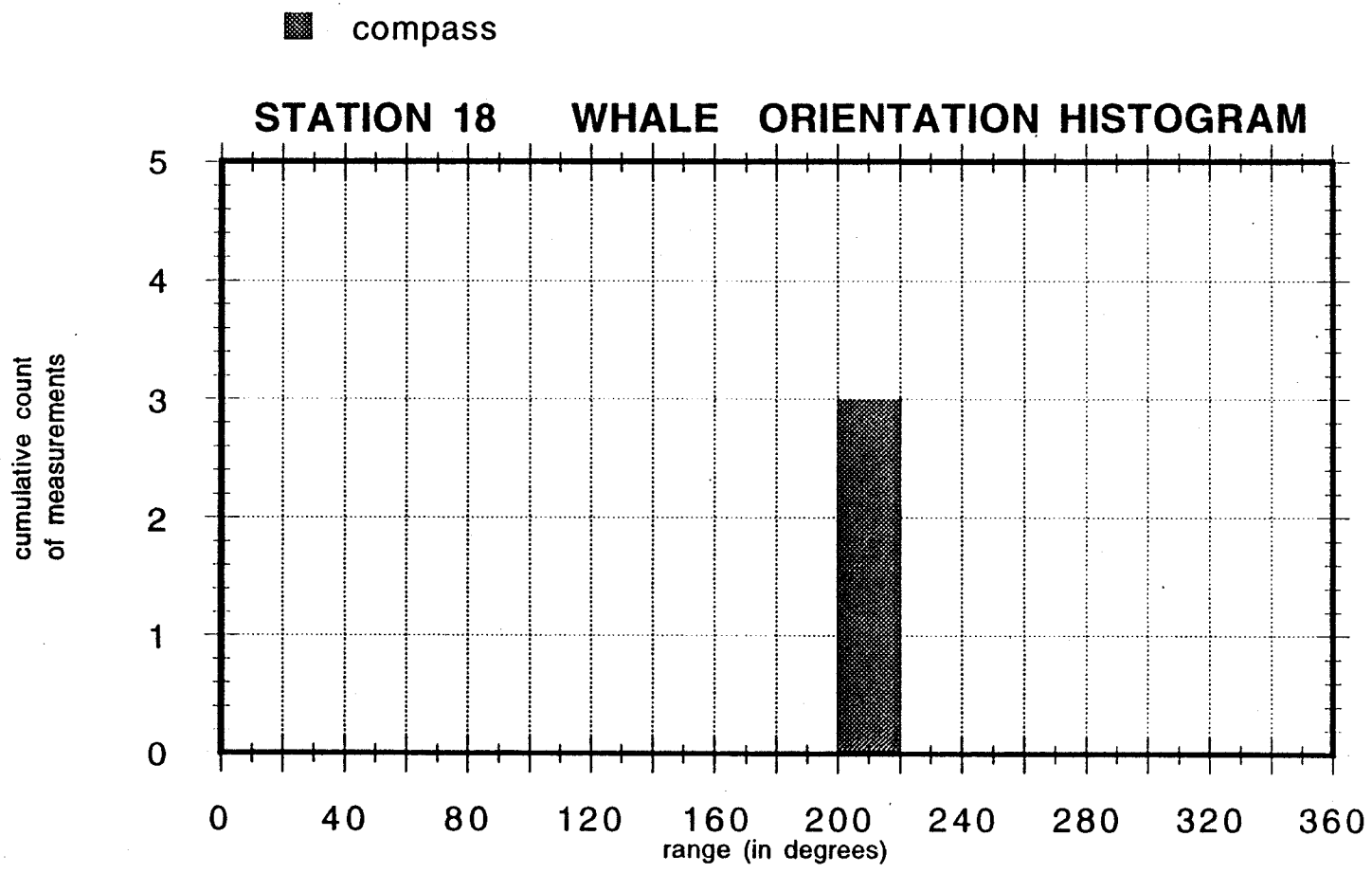
compass
STATION 18 WHALE ORIENTATION HISTOGRAM
cumulative count of measurements
5
4
3
2
1
0
0
40
80
120
160
200
240
280
320
360
range (in degrees)